NUREG/CR-3711
EPRI NP-3602
GEAP-30496

BWR Full Integral Simulation Test (FIST) Phase I Test Results

Prepared by W. S. Hwang, Md. Alamgir, W. A. Sutherland

Nuclear Fuel and Special Projects Division
General Electric Company

Prepared for
U.S. Nuclear Regulatory Commission

and
Electric Power Research Institute

and
General Electric Company

GPO Printed copy price: $7.00

NUREG/CR-3711
EPRI NP-3602
GEAP-30496
R2

BWR Full Integral Simulation Test (FIST) Phase I Test Results

Manuscript Completed: November 1983
Date Published: September 1984

Prepared by
W. S. Hwang, Md. Alamgir, W. A. Sutherland

Nuclear Fuel and Special Projects Division
General Electric Company
San Jose, CA 95125

Prepared for
Division of Accident Evaluation
Office of Nuclear Regulatory Research
U.S. Nuclear Regulatory Commission
Washington, D.C. 20555
NRC FIN No. B3014

and
Electric Power Research Institute
3412 Hillview Avenue
Palo Alto, CA 94303

and
Nuclear Fuel and Special Projects Division
General Electric Company
San Jose, CA 95125

PREVIOUS REPORTS IN BWR FIST SERIES

BWR Full Integral Simulation Test (FIST) Program Test Plan, J. E. Thompson, General Company, NUREG/CR-2575, September 1983.

BWR Full Integral Simulation Test (FIST) Facility Description Report, A. G. Stephens, General Electric Company, NUREG/CR-2576, May 1984.

NUREG/CR-3711
EPRI NP-3602
GEAP-30496
November 1983

BWR FULL INTEGRAL SIMULATION TEST (FIST) PROGRAM

CONTRACT NRC-04-76-215

BWR FULL INTEGRAL SIMULATION TEST (FIST)

PHASE I TEST RESULTS

W. S. Hwang

Md. Alamgir

W. A. Sutherland

Approved: W. A. Sutherland
W. A. Sutherland, Manager
LOCA System Technology

Approved: Larry L. Myers
L. L. Myers, Program Manager
External Programs

Approved: G. E. Dix
G. E. Dix, Manager
Core Methods

Approved: J. E. Wood
J. E. Wood, Manager
Core and Fuel Technology

NUCLEAR FUEL AND SPECIAL PROJECTS DIVISION • GENERAL ELECTRIC COMPANY
SAN JOSE, CALIFORNIA 95125

GENERAL ELECTRIC

LEGAL NOTICE

This report was prepared by the General Electric Company as an account of work sponsored by the Nuclear Regulatory Commission, the Electric Power Research Institute, and the General Electric Company. No person acting on behalf of the NRC, the Institute, or members of the Institute, or General Electric Company:

A. Makes any warranty or representation, express or implied, with respect to the accuracy, completeness, or usefulness of the information contained in this report, or that information, apparatus, method of process disclosed in this report may not infringe privately owned rights, or

B. Assumes any liabilities with respect to the use of, or for damages resulting from the use of any information, apparatus, method or process disclosed in this report.

ABSTRACT

A new full height BWR system simulator has been built under the Full-Integral-Simulation-Test (FIST) program to investigate the system responses to various transients. The test program consists of two test phases. This report provides a summary, discussions, highlights and conclusions of the FIST Phase I tests.

Eight matrix tests were conducted in the FIST Phase I. These tests have investigated the large break, small break and steamline break LOCA's, as well as natural circulation and power transients. Results and governing phenomena of each test have been evaluated and discussed in detail in this report.

Two of these tests tieback to tests conducted with the earlier TLTA facility. Comparisons between the FIST and TLTA tests have been made. The similarities and differences between the counterpart tests are identified. Effects of the facility scaling compromises on the test results are identified.

One of the FIST program objectives is to assess the TRAC code by comparisons with test data. Two pretest predictions made with TRACB02 are presented and compared with test data in this report. These predictions agree very well with the test results. TRAC's capability to correctly predict the system responses during the transient is demonstrated.

TABLE OF CONTENTS

TABLE OF CONTENTS (Continued)

TABLE OF CONTENTS (Continued)

LIST OF FIGURES

LIST OF FIGURES (Continued)

LIST OF FIGURES (Continued)

LIST OF FIGURES (Continued)

LIST OF FIGURES (Continued)

LIST OF FIGURES (Continued)

LIST OF FIGURES (Continued)

LIST OF FIGURES (Continued)

LIST OF FIGURES (Continued)

LIST OF FIGURES (Continued)

LIST OF TABLES

LIST OF ACRONYMS

Acronym	Meaning
ADS	Automatic Depressurization System
BD/ECC	BWR Blowdown/Emergency Core Cooling
BDHT	Blowdown Heat Transfer
BHL	Bottom of Heated Length
BWR	Boiling Water Reactor
CCFL	Counter Current Flow Limiting
ECCS	Emergency Core Cooling System
HPCS	High Pressure Core Spray
LOCA	Loss of Coolant Accident
LPCI	Low Pressure Coolant Injection
LPCS	Low Pressure Core Spray
MSIV	Main Steam Isolation Valve
PCV	Pressure Control Valve
RCIC	Reactor Core Isolation Cooling
SEO	Side Entry Orifice
SRV	Safety Relief Valve
TC	Thermocouple
THL	Top of Heated Length
TLTA	Two Loop Test Apparatus
UTP	Upper Tie Plate

ACKNOWLEDGEMENTS

The FIST test program has been carried out as a team effort. The authors would like to acknowledge the contributions of all those who were involved in the successful execution of the FIST Phase I tests and participated in the reduction and interpretation of test results. Thanks are due particularly to Dr. G. E. Dix for his guidance and direction provided throughout the test program, to D. W. Danielson, D. A. Wilhelmson, H. Ngo and A. G. Stephens (EG&G) for conducting the tests and reducing the data, to S. A. Allison for preparing the TRAC model and inputs used for the pretest predictions and to S. D. Stevens for preparing the figures.

The FIST test program has been carried out under the joint sponsorship of the U.S. Nuclear Regulatory Commission (USNRC), Electric Power Research Institute (EPRI), and General Electric Company (GE). This program has been benefited from the leadership provided by the Program Management Group (PMG) Members, Dr. W. D. Beckner (NRC), Dr. S. P. Kalra (EPRI) and J. C. Black (GE).

SUMMARY

A new full height BWR system simulator, FIST, built under the Full-Integral-Simulation-Test program, has been used to experimentally investigate the system responses to various transients. The test program consists of two test phases; phase 1 was completed in 1983 and phase 2 is to be performed in 1984. Test results and governing phenomena observed in FIST phase 1 tests are discussed in this report. In addition, two pretest predictions were carried out using the TRAC code for two FIST phase 1 tests. This effort is to assess the TRAC capability in analyzing the system responses during the transients. Comparisons of the pretest predictions with test data are also presented.

FIST phase 1 test series include the large break, small break and steamline break LOCA's as well as natural circulation and power transients. Test results have demonstrated the adequacy of BWR designs and responses to various transients. Test results, governing phenomena and hightlights observed in the tests are briefly summarized below.

(A) LOCA Tests

Three LOCA tests were conducted to investigate system responses to various break sizes and locations. The large break simulates a double ended break and the small break simulates a BWR break of 0.20 ft^2 in the recirculation loop. The main steamline break test investigates a double ended break upstream of the flow limiter in one of the four main steamlines.

Test results indicate that the bundle is uncovered in the large break and small break, but is always covered in the steamline break. Effectiveness of ECC cooling in limiting the fuel rod heatup is clearly demonstrated in these tests. A peak cladding temperature of 710°F and 925°F is measured in the large break and small break, respectively. No heatup is seen in the steamline break.

Comparisons of FIST tests with the counterpart tests conducted in the Two-Loop-Test-Apparatus (TLTA) have shown effects of the jet pump height on the system inventory responses. The full height jet pumps in the FIST facility reduce the core inventory depletion during the blowdown and refilling as compared to the TLTA. The system inventory is recovered with ECC injection and the bundle is completely reflooded.

The counter-current-flow-limiting (CCFL) observed in many LOCA tests performed in other test facilities is also seen in the FIST tests. CCFL is again shown to be an important factor affecting the system behavior. CCFL occurs at various locations in the FIST tests and CCFL effects on the system responses during the transient are discussed.

The stored heat, particularly in the vessel wall, is a common scaling compromise in a small scale test facility. It is found that local thermal hydraulic responses in the bypass and guide tube regions are affected strongly by the stored heat in that region, particularly during the reflood period. Flow oscillation is seen in the refilling/reflood phase in the large break test. However, the peak cladding temperature is measured long before the stored heat effect begins to take place. The observed stored heat effect on the system performance is attributed to the FIST design and is a FIST system characteristic. The stored heat effect in a BWR is expected to be negligible.

(B) Natural Circulation Tests

A series of seven tests with bundle powers of 0.5 to 3.0 MW were performed to investigate the natural circulation in FIST. Test results generally agree with the natural circulation analysis results of a BWR. The natural circulation is a function of water level and bundle power. These tests provide an excellent set of natural circulation data which can be used for code assessment.

(C) Power Transients

Three power transient tests were conducted to investigate BWR system responses to the Main Steamline Isolation Valve (MSIV) closure without the control rod insertion, plus with or without High Pressure Core Spray (HPCS) for a BWR/6 and a BWR/4.

As FIST uses electrically heated rods in the bundle, the kinetics feedback in a BWR during power transients is not simulated. These tests were conducted based on simulating the BWR core average power expected in the event. The FIST bundle power was programmed to simulate the calculated core average rod surface heat flux in a BWR.

Test results have shown that the system responses are very similar to the code analysis. The bundle was always covered and no rod heatup was seen in these tests.

(D) Code Assessment

Two pretest predictions were performed using the TRAC code for the FIST large break and small break tests. Comparisons of the pretest predictions with test data are presented. TRAC predictions agree very well with test results and TRAC's capability in correctly predicting the system responses during the transients has been clearly demonstrated.

1. INTRODUCTION

1.1 BACKGROUND

A major objective in power reactor design is to provide sufficient cooling capability to keep fuel cladding temperature below specified safety values for a wide range of postulated events. These events are loss-of-coolant accidents (LOCA's), with various break sizes, operational transients involving loss-of-inventory, multiple system failures and power transients.

Since 1974 a series of test programs have been carried out to investigate system thermal-hydraulic and bundle heat transfer responses over a wide range of the simulated BWR conditions. A BWR system simulator, Two-Loop-Test Apparatus (TLTA), was first built under the Blowdown Heat Transfer (BDHT) program to conduct LOCA system blowdown tests. The TLTA was modified, under the BWR Blowdown/Emergency Core Cooling (BD/ECC) program to reflect changes in BWR designs and to extend the investigations into the ECCS injection period of a LOCA. Results of the above tests identified many TLTA scaling compromises. Consequently, a new test facility was built under the Full-Integral-Simulation-Test (FIST) program. The FIST facility provides a more realistic simulation of LOCA's, from break initiation through refill/reflood, as well as simulations of transient events. All of these test programs have been funded jointly by the U.S. Nuclear Regulatory Commission (USNRC), Electric Power Research Institute (EPRI), and General Electric Company (GE).

The FIST test program consists of two test phases. Phase I tests were completed in June 1983. This report presents the test results of Phase I matrix tests. Detailed descriptions of the FIST facility and test plan of the entire test program are given elsewhere[1],[2].

1.2 REPORT OBJECTIVE AND CONTENT

The first objective of this report is to provide a summary, discussion, highlights, and conclusions of the FIST phase I tests, based on interpretations and evaluations of the observed phenomena in the tests.

Two TLTA tie-back tests, a large break and a small break, were conducted in Phase I. The second objective of this report is to provide comparisons of these two tests with their TLTA counterpart tests.

One of the test program objectives is the assessment of the TRAC code with test data. Two pretest predictions of Phase I tests were performed using the TRAC code. The third objective of this report is to provide comparisons of the pretest predictions with test data.

2. FIST PHASE I MATRIX TESTS

The FIST test program consists of two test phases to investigate the system responses to various transients. Detailed discussions of the matrix tests of the entire test program are given in reference 2.

Table 2-1 lists eight matrix tests and two additional tests conducted in Phase I. There are four BWR/6 LOCA Simulation tests, including one large break (6DBA1B), two small breaks (6SB2C and 6SB1), and one main steamline break (6MSB1). Tests 6DBA1B and 6SB2C are the TLTA tieback tests to 6425/R2 and 6432/R1, respectively (References 3 and 4). These two tests were conducted with test conditions of their TLTA counterpart tests, which simulated a central average power of 5.05 MW. Other tests simulate a core average of 4.64 MW.

The natural circulation test 6PNC1 includes 7 runs with bundle power of 0.5 to 3.0 MW. In these tests, data were collected as the system was maintained at a constant pressure of 1040 PSIA and a constant bundle power. The test 6PNC1-7A was conducted with subcooled feedwater injecting into the downcomer.

Three tests were performed to investigate the power transient responses to a main steamline isolation valve (MSIV) closure. As the FIST uses an electrically heated bundle, kinetics feedback is not simulated in this facility. Therefore, these tests were conducted with preprogrammed transient power based on BWR calculations.

Tests 6PMC2 and 6SB2B are additional tests performed during the program. Test 6PMC2 was to simulate the power transient response to MSIV closure without HPCS, but the high power of test 6PMC1 (with HPCS) was used. Test 6SB2 was a small break test with an underscaled ADS size. Data of all FIST tests are in the INEL data bank.

Table 2-1
FIST TESTS (PHASE 1)

Test Number	Description	Initial Power	Available ECCS	Highlights
6DBA1B	BWR/6 DBA	5.05	HPCS, LPCS LPCI (1)	core inventory depletion reduced due to full height jet pump, CCFL, PCT=710°F, reflood affected by stored heat.
6SB2C	SB, W/O HPCS	5.05	LPCS, LPCI (3)	PCT = 925°F
6SB1	SB, STUCK SRV	4.64	LPCS, LPCI (3)	Responses similar to 6SB2C, PCT = 720°F.
6MSB1	MS LINE BREAK	4.64	HPCS, LPCS, LPCI (1)	CCFL, no core uncovery, no heatup
6PNC1-1A 1-2B 1-3 1-4 1-5 1-6 1-7A	Natural Circ.	0.5 1.0 1.5 2.0 2.5 3.0 2.0+SUB	N/A	Natural circulation flow affected by power and water level. Internal circulation flow observed. Responses similar to BWR analysis.
6PMC1	BWR/6 MSIV Clos.	4.64	All	Responses similar to BWR analysis, no core uncovery, no heatup.
6PMC2A	BWR/6 MSIV Clos. (w/o HPCS)	4.64	RCIC, LPCS, LPCI (3)	Responses similar to BWR analysis, no core uncovery, no heatup.
4PMC1	BWR/4 MSIV Clos.	4.35	All	Responses similar to BWR analysis, no core uncovery, no heatup.
*6PMC2	Separate Effect BWR/6 MSIV Clos. (w/o HPCS, 6PMC1 power)	4.64	RCIC, LPCS, LPCI (3)	Upper bundle uncovered and heatup due to high power, test terminated by bundle protection.
*6SB2B	SB, w/o HPCS	5.05	LPCS, LPCI (3)	Small ADS size, power off by bundle protection at 340 sec., PCT = 950°F.

*Not matrix tests. Data are available in INEL data bank.

3. FIST FACILITY DESCRIPTION

3.1 FIST TEST FACILITY

The FIST Facility is scaled to a BWR/6-218 standard plant. A full size bundle with electrically heated rods is used to simulate the reactor core. A scaling ratio of 1/624 is applied in the design of the system components. A schematic of the FIST facility is shown in Figure 3-1.

Major improvements over the TLTA, and key features of the FIST facility, include:

(1) Full height test vessel and internals

(2) Correctly scaled fluid volume distribution

(3) Simulation of Emergency Core Cooling System (ECCS), Safety Relief Valves (S/RV), and Automatic Depressurization System (ADS)

(4) Level trip capability

(5) Heated feedwater supply system, which provides the capability for steady state operation.

Detailed descriptions of the FIST system are given in Reference 1.

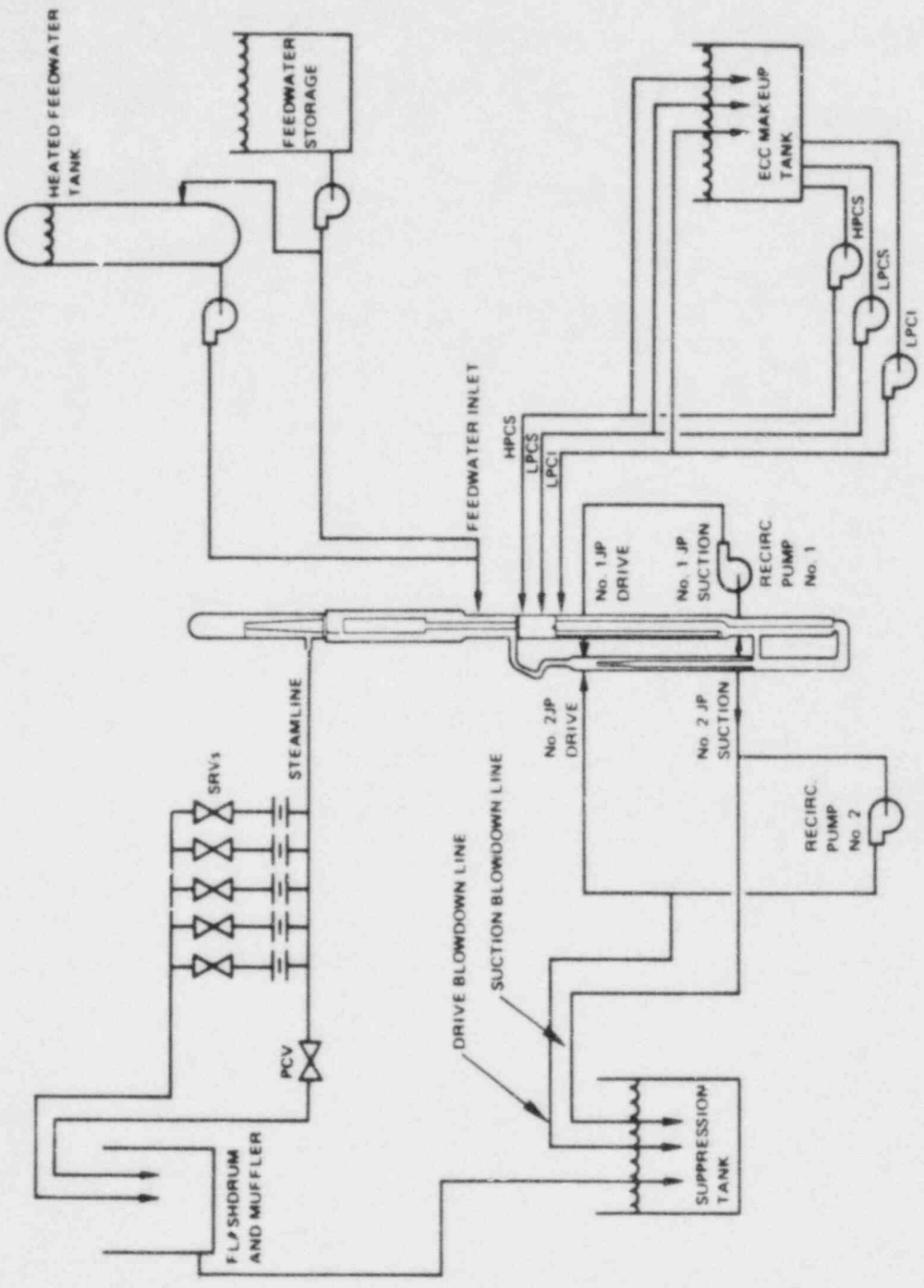

Figure 3-1. BWR FIST Test Facility Schematic

4. TEST SIMULATION STUDY

An extensive scaling study was carried out during the FIST design to identify and minimize the scaling compromises in the facility. Results of this study are discussed in Reference 1. Some scaling compromises and facility capability limitations could not be completely eliminated in FIST and may affect the system performance, depending upon the tests. Areas of concern include excess fluid mass in the recirculation loops, S/RV and ADS sizes, MSIV closure, feedwater supply control, and power transient test simulation.

4.1 RECIRCULATION LOOP ISOLATION

FIST has two external recirculation loops for simulating the normal and coastdown performance of the drive pump flow. Due to design constraints, the FIST loops are overscaled in size and length and thus contain excess fluid. In a depressurization transient the fluid in the loops will flash and interact with the fluid in the pressure vessel. To improve the system post-flashing response, valves are installed in the suction and drive lines to isolate each loop before flashing starts.

In most cases these valves are closed, and excess mass in the loops is isolated from the pressure vessel, after the jet pump coastdown is completed at about 20 seconds. However, in a rapid depressurization transient, such as the large break or steamline break, the loop fluid may begin to flash before the jet pump coastdown is completed. In such cases, these valves are closed just before the occurrence of flashing. Once the system begins to flash, the jet pump performance will be dominated by the flashing effect and the coastdown simulation is no longer important. Table 4-1 lists the loop isolation timings for the Phase I tests.

Table 4-1
LOOP ISOLATION TIMES

- Large Break Test (6DBA1)
  - Based on TRAC Analysis, Loop Flashing at ∿14 Sec.
    - (A) Broken Loop: 0 sec
    - (B) Intact Loop: 13 sec

- Small Break Tests (6SB1 and 6SB2)
  - No Loop Flashing before SRV/ADS
    - (A) Broken Loop: 0 sec
    - (B) Intact Loop: 20 sec

- Power Transient Tests (6PMC1, 6PMC2 and 4PMC1)
  - No Loop Flashing
    - (A) Both Loops: 20 sec

- Steamline Break Test (6MSB1)
  - Based on Pretest Data, Loop Flashing at ∿8 Sec
    - (A) Both Loops: 7 sec

4.2 S/RV AND ADS SIZES

Five S/RV valves with properly sized orifices (Table 4.2-1) are used in the FIST to simulate the S/RV functional groups in a BWR. The normal and low/low set operations of these groups in a BWR are simulated (Tables 4.2-2 and 3). One of these valves is also used to simulate the ADS operation. S/RV orifices are sized to simulate the scaled S/RV flows. Two sets of S/RV orifices are used for the BWR/6 and BWR/4 simulations (cases I and III of Table 4.2-1).

ADS is activated in a small break test, resulting a rapid system depressurization, flashing, and mass redistribution. Major interest of the small break test is to investigate these phenomena, and the interactions of ECC injections with the system performance in the post ADS period. Therefore, it is necessary to correctly simulate the post-ADS depressurization. As discussed in Reference 1, the FIST vessel contains overscaled metal mass and stored heat, resulting in extra steam generation during the system depressurization. An oversized ADS orifice (Case II of Table 4.2-1) is used to discharge excess steam and to achieve the simulation of the calculated BWR depressurization (Figure 4.2-1). In the power transient tests, the system is maintained at high pressure and the vessel wall stored heat has a small effect on the system performance.

4.3 MSIV CLOSURE

The Main Steamline Isolation Valve (MSIV) in a BWR takes about 4 seconds to complete the closing operation upon receiving the trip signal. The FIST MSIV control cannot simulate this gradual closing operation and a step closing is employed at 2 seconds after the trip signal. This gives a correct simulation of the total steam discharge during the MSIV closure.

Table 4.2-1
FIST S/RV AND ADS SIZES

	S/RV Size, Dia. In.		
S/RV No.	BWR/6 Case 1	BWR/6 Case 2	BWR/4 Case 3
1	0.183	0.23**	0.235
2	0.183	0.23*	0.288
3	0.317	0.398*	0.288
4	0.366	0.459*	0.333
5/ADS	0.482	0.607	0.333
FIST Test	6PMC1 6PMC2A	6SB1 6SB2C	4PMC1

*Not Activated in Tests 6SB2C and 6SB1

**Not Activiated in Test 6SB2C

Table 4.2-2
FIST S/RV OPERATION (BWR/6)

Pressure Setpoint, Open/Close (PSIG)

S/RV No.	Normal Relief	Low/Low set Relief
1	1103/1003	1003/926
2	1113/1003	1073/936
3	1113/1003	1113/946
4	1113/1003	-
5	1123/1003	-

Table 4.2-3
FIST S/RV OPERATION (BWR/4)

S/RV No.	Pressure Setpoint, Open/Close (PSIG) Normal Relief	Low/Low set Relief
1	1115/985	1085/985
2	1127/997	1097/997
3	1137/1007	1107/1007
4	1148/1018	1118/1018
5	1163/1033	1113/1033

*Normal to Low/Low Set at T = 10 Sec., Based on REDY Susquehanna Plant Inputs

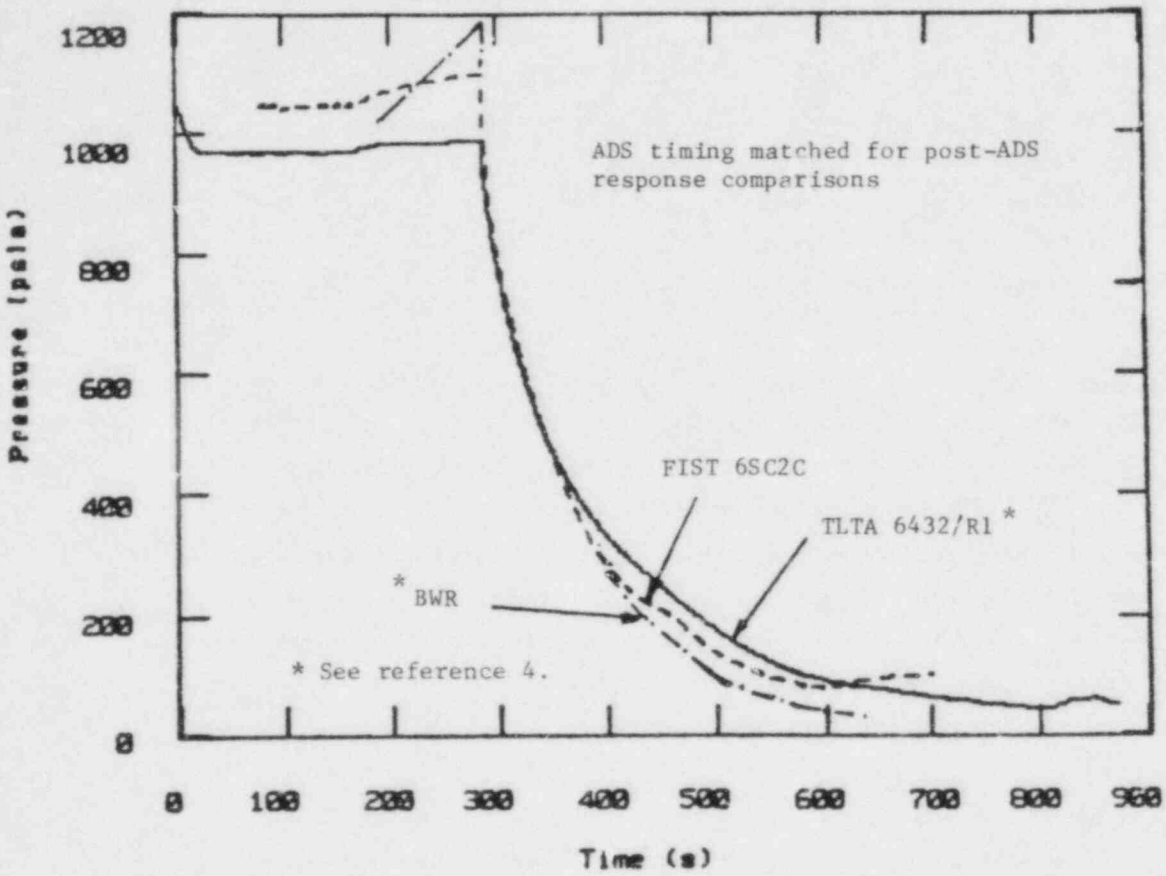

Figure 4.2-1. Comparisons of System Pressures After ADS

4.4 FEEDWATER SUPPLY

The FIST feedwater supply system includes a hot water line and a cold water line. This system has been designed mainly for achieving a steady state operation. The hot water supply is used for the water level control, while the cold water supply is to maintain water temperature in the downcomer.

The FIST is not capable of simulating the gradual closing and/or control in a BWR feedwater system. Similar to the MSIV operation, the FIST feedwater supply is activated to have a step closure at about the half time of the expected closing duration, so the total feedwater supply into the vessel is correctly simulated.

4.5 POWER TRANSIENT TEST SIMULATION

In a BWR power transient the bundle power and its distribution is strongly affected by local void fraction, due to the neutronic feedback. FIST uses a bundle with electric heater rods, which has a fixed power profile and peaking factor distribution among the rods. Therefore, the kinetic feedback and coupling between the bundle power and void fraction is not simulated in the FIST test. Because the primary objective and interest of the power transient tests are to investigate the system response, rather than local phenomena in the bundle, the test is based on simulating the core average power expected in the event.

GE transient code analyses of the BWR power transients reported in references 5 & 6 are used as bases for the FIST power transient test simulation study. The FIST heater rods bundle power is programmed to simulate the core average rod surface heat flux in a BWR as calculated by the transient code.

A TRAC deck modeled with heater rods was developed and used to determine the FIST power input. The power was obtained by matching the TRAC calculated rod surface heat flux with that of the transient code. (Figure 4.5-1).

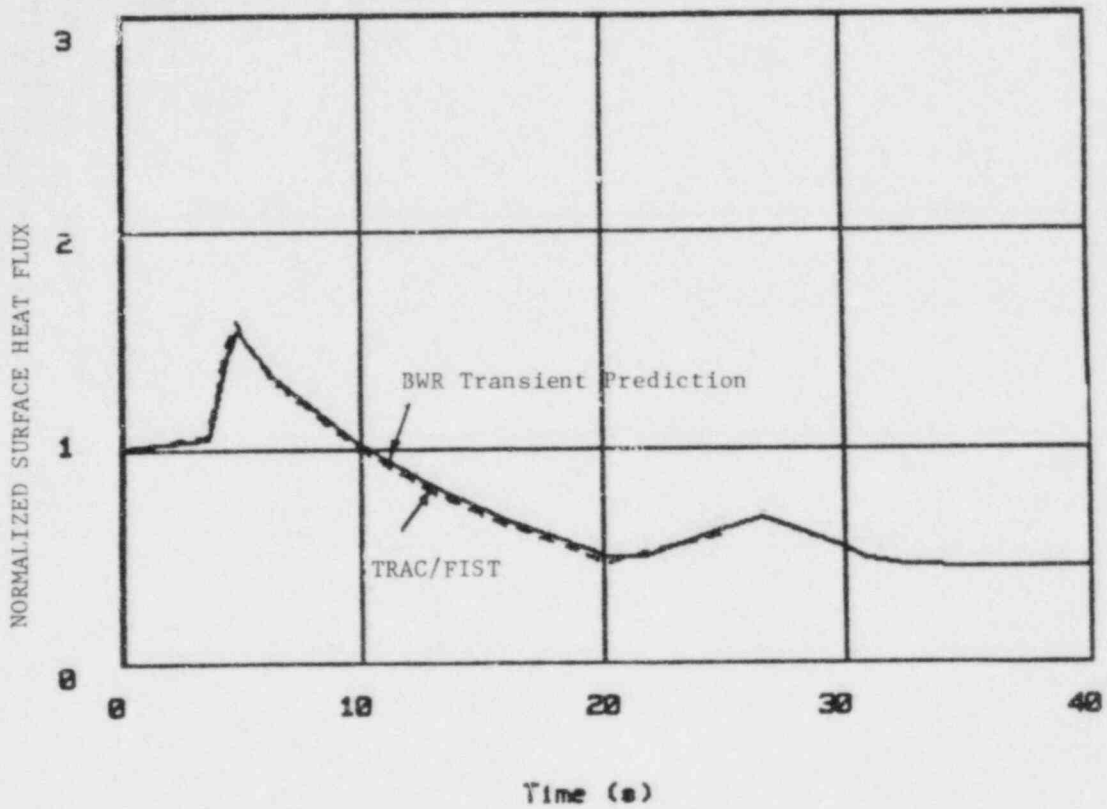

Figure 4.5-1. Normalized Surface Heat Flux

5. MEASUREMENT SYSTEM

The FIST measurement system has been developed to obtain sufficient measurements to characterize the system responses to various transients and to provide test data for assessing analytical codes. The measurements obtained include: system pressure, nodal differential pressure, flow differential pressure, fluid temperature, wall temperature, rod cladding temperature, conductivity probe signal, valve position, pump speed, power, volumetric flow etc. More than 400 measurement channels are used to collect data in each test.

The output signals from the measuring devices are recorded on a data tape with a Hewlett-Packard data acquisition system. Raw data is reduced for further processing with the same H-P computer. Details of measurements, data acquisition data processing and application are given in Reference 1.

6. TEST DATA

Two types of data are presented in this report. They include the direct measurements, as indicated in Section 5, and derived quantities. Derived quantities are generally a result of combining one or more measurements. While the direct measurements are self-evident to interpret, understanding of the system response and governing phenomena is required for interpreting the derived quantities. Derived quantities include nodal density, mass, void fraction, water level and flow rate.

During the test, a standard data plot package was developed to reduce the most important and useful measurements with the H-P computer. These results were used to quickly evaluate test results and judge the test acceptance immediately after the tests. Most of the plots used in this report are reduced with this standard package. Data of all Phase I matrix tests have been stored in the INEL data bank for further applications.

7. DISCUSSIONS AND RESULTS OF PHASE I MATRIX TESTS

FIST Phase I has a total of 8 matrix tests. Highlights, key system responses, and governing phenomena observed in all tests are discussed in this section. Two LOCA tests, 6DBA1B and 6SB2C, are TLTA tie-back tests. Comparisons of these two tests with their TLTA counterpart tests are discussed in Section 8. Pretest predictions performed with the TRAC code for these two LOCA tests are discussed in Section 9.

7.1 LARGE BREAK TEST 6DBA1B

7.1.1 General Description

Test 6DBA1B is a recirculation suction line break test with a "central average" bundle power of 5.05 MW and average ECC flow rate. This test is a tie-back test of the TLTA reference test 6425/R2. Sequence of significant events observed in the test is shown in Table 8.1-1, in comparing with the TLTA test results.

7.1.2 System Pressure

The system pressure transient is shown in Figure 7.1-1. The system begins to depressurize very rapidly after the recirculation line suction is uncovered at about 8 seconds. This depressurization leads to lower plenum flashing beginning at about 11.5 seconds. HPCS injection begins at 27 seconds and LPCS and LPCI at 64 and 75 seconds, respectively.

7.1.3 Rod Temperature

The rod temperatures measured at various elevations (Figure 7.1-2) indicate that the bundle begins to heatup at about 40 seconds as the bundle is uncovered. The rod temperature increase is limited by the rewet due to ECC cooling and a PCT of 710°F is observed. All rods are completely quenched before or during the bundle reflood at about 125 seconds.

7.1.4 System Mass and Regional Mass

Figures 7.1-3 through 11 show the total system mass and regional mass responses. The system inventory decreases rapidly during the blowdown phase and begins to recover after ECCS are initiated.

The jet pump is nearly empty at about 40 seconds (Figures 7.1-4 and 5), indicating that the lower plenum water level uncovers the jet pump exit. It begins to recover at about 90 seconds. Fluctuation is seen in the jet pump mass response particularly beyond 200 seconds during the refill/reflood phase.

Similar mass fluctuations are observed in other regions during the same period (Figures 7.1-4 to 12). The jet pump mass response is also given in these plots, in order to compare the timings of peaks and troughs of fluctuations among these regions. It can be seen that mass fluctuation responses in regions of the jet pump, lower plenum, bundle and upper plenum are generally in phase, while the bypass and guide tube respond in different phase from the above group. This regional mass fluctuation response is attributed mainly to stored heat in the bypass/guide tube region. The governing phenomena are discussed below.

7.1.5 Bypass Stored Heat Effect and Governing Phenomena

FIST has relatively heavy metal flanges, plates, and vessel wall which contain over-scaled amounts of stored heat, particularly in the lower bypass region (figure 7.1-13). The excess stored heat is transferred to the fluid to generate extra steam which affects the system performance in the transient as the system depressurizes.

Figures 7.1-14 to 16 provide aids to explain the governing phenomena of these mass fluctuations and interactions among various regions. As the system blows down, large steam generation results in CCFL at various locations, as shown in Figure 7.1-14. HPCS and LPCS water is held in the upper plenum by CCFL at the upper tieplate and top

of the bypass. LPCI water injected into the bypass either vaporizes when it contacts the bypass hot wall or is diverted into the upper plenum by the large steam upflow coming from the lower bypass. No significant increase of mass is seen in the bundle and bypass before 120 seconds (Figures 7.1-8 and 11), although LPCS and LPCI are initiated at 64 and 75 seconds, respectively.

Most ECC water is initially accumulated in the upper plenum. This eventually becomes subcooled and leads to a subcooled CCFL breakdown at both upper tieplate and top of the bypass at about 120 seconds. The bundle and bypass are quickly refilled with ECC flow and water from the upper plenum, while CCFL at the Side Entry Orifice (SEO) limits water draining into the lower plenum from the bundle. Flow in the bundle and bypass becomes stagnant once these two regions are completely refilled.

While flow in the bypass is stagnant, the vessel wall stored heat vaporizes the water, particularly in the lower bypass region (Figure 7.1-15). As vapor moves upward, LPCI water is again diverted into the upper plenum. Some water in the bypass is also driven into the lower plenum and bundle as the vapor volume rapidly expands. Accumulation of ECC water in the upper plenum results in an increase of water level (i.e. the upper plenum-to-lower plenum pressure head) which is balanced with a higher water level (or water head) in the jet pumps. Some water in the jet pump may spill over into the downcomer. During this period, regions of the jet pump, lower plenum, bundle and upper plenum show an increase in mass, but the bypass and guide tube have a decrease in mass.

Vapor generated in the bypass rises and then collapses as it meets subcooled LPCI water in the upper bypass region. ECC flow and water in the upper plenum rushes into and again fills the bypass and guide tube (Figure 7.1-16). This contributes to a decrease of water level in the upper plenum. The jet pump water level subsequently drops to maintain a pressure balance. Once the bypass refilling is completed the bypass flow becomes stagnant and a new cycle of the above response starts again. After several repeated cycles, a significant amount of stored heat is removed and the mass fluctuation and redistribution subsides.

Fluid temperatures measured in the bypass region (Figures 7.1-17 and 18) indicate the stored heat effects on movements of hot and cold water in the bypass during the refilling and vaporizing process. When the bypass is full of water, the lower region is affected by the stored heat and becomes hotter than the upper region. Saturated fluid is observed during the inventory depletion.

It should be noted that the above oscillation behavior, attributed to stored heat, is a FIST characteristic and is not expected in a BWR. Stored heat has negligible effect on the BWR bypass response during the refill/reflood phase. In addition, the three-dimensional nature of BWR bypass region allows LPCI flow and water in the upper plenum to drain easily and continuously into the bypass. A smooth and earlier refill and reflood of the core is therefore expected in a BWR.

7.1.6 Summary (Test 6DBA1B)

Key phenomena observed in the FIST test 6DBA1B are similar to the corresponding tests conducted in the TLTA and other facilities, except for the stored heat effect during the reflood period. Test results can be summarized as follows:

(1) The system blows down very rapidly after the break is uncovered. The system depressurization leads to a system bulk flashing and eventually ECCS injections.

(2) CCFL is observed at various locations such as SEO, UTP, top of the bypass and top of the guide tube.

(3) The jet pump exit is uncovered at about 40 seconds and later recovered due to the inventory makeup by ECC water.

(4) The bundle uncovery at about 40 seconds results in a general bundle heatup. ECC cooling effectiveness is clearly demonstrated in this test which limits the rod temperature increase. A PCT of 710°F was measured.

(5) The vessel wall stored heat affects and delays CCFL breakdown at top of the bypass and hence delays the core refill/reflood. Both the bundle and bypass are refilled mainly by subcooled CCFL breakdown at top of the core.

(6) Flow oscillation is observed during the reflood period. This is attributed to the stored heat effect in the bypass/guide tube regions. This reflood response is a FIST facility effect and is not expected in a BWR. The PCT is observed before the ocurrence of flow oscillation.

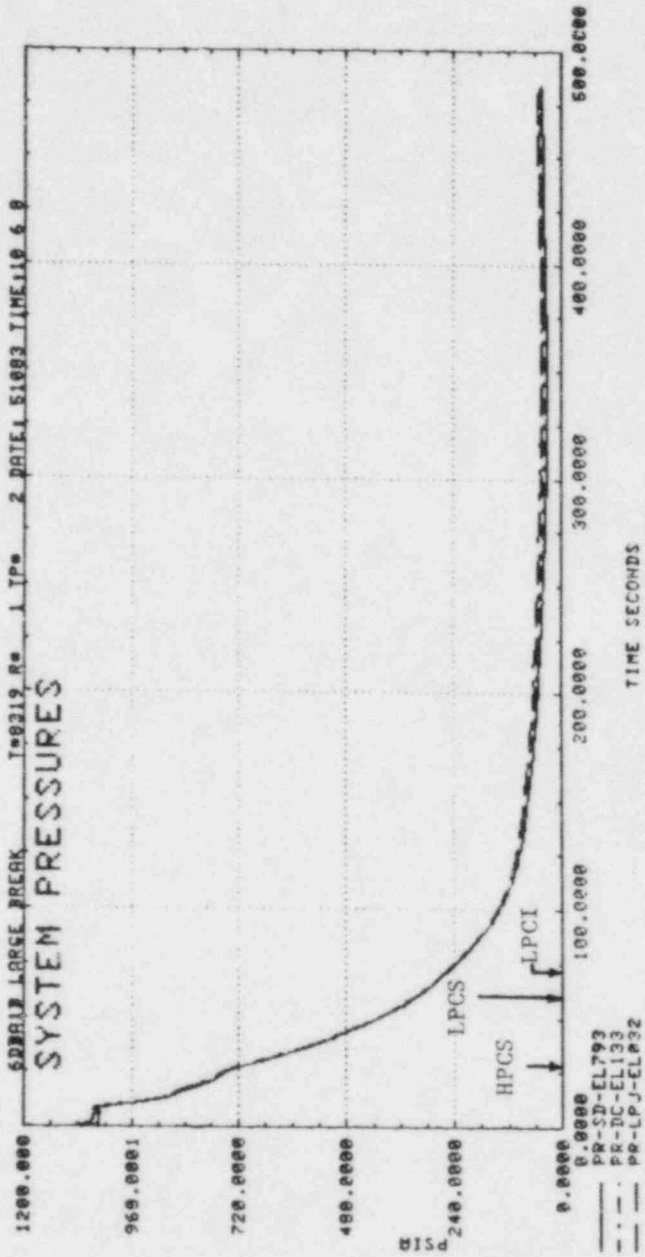

Figure 7.1-1. System Pressure

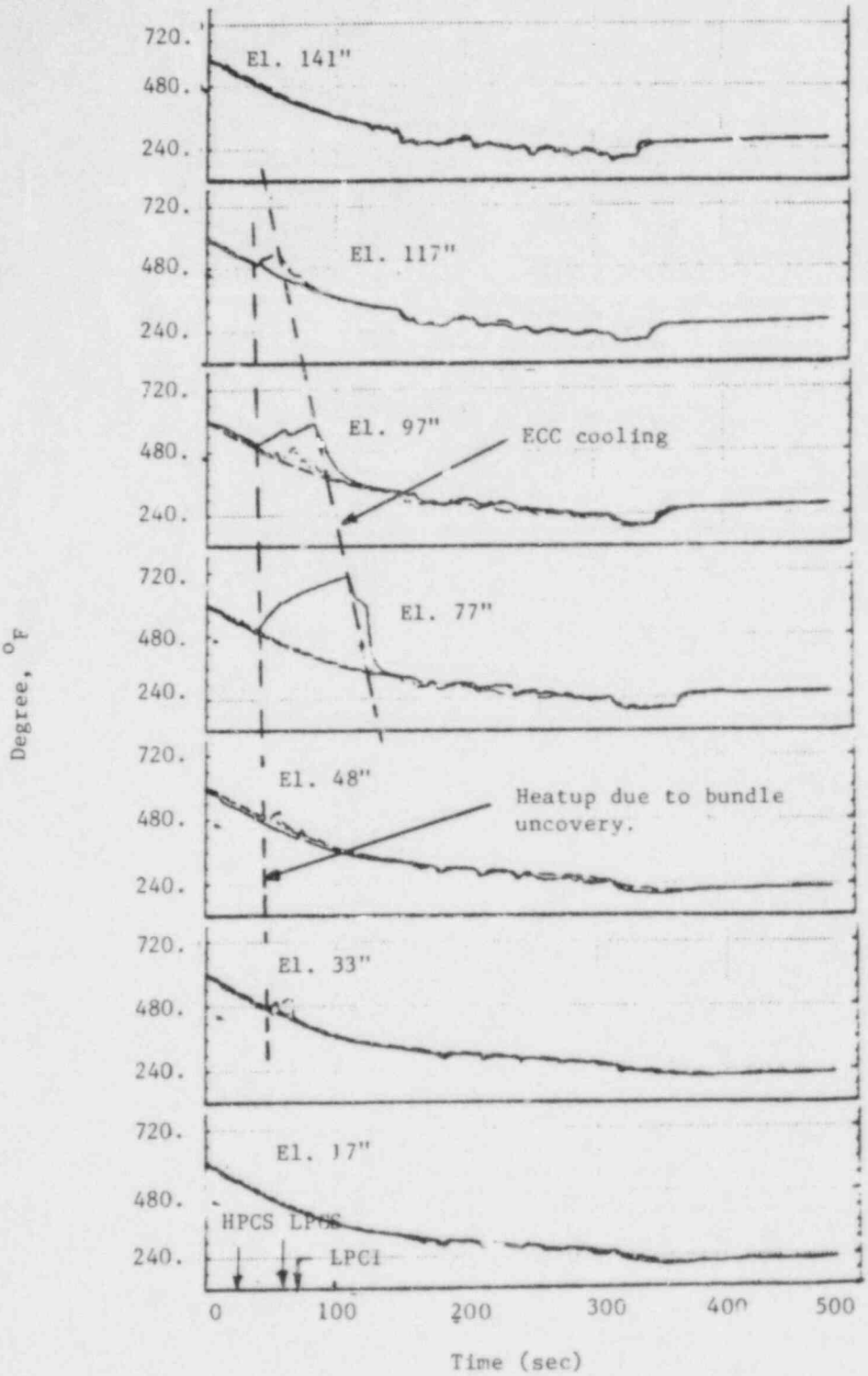

Figure 7.1-2. Rod Temperatures

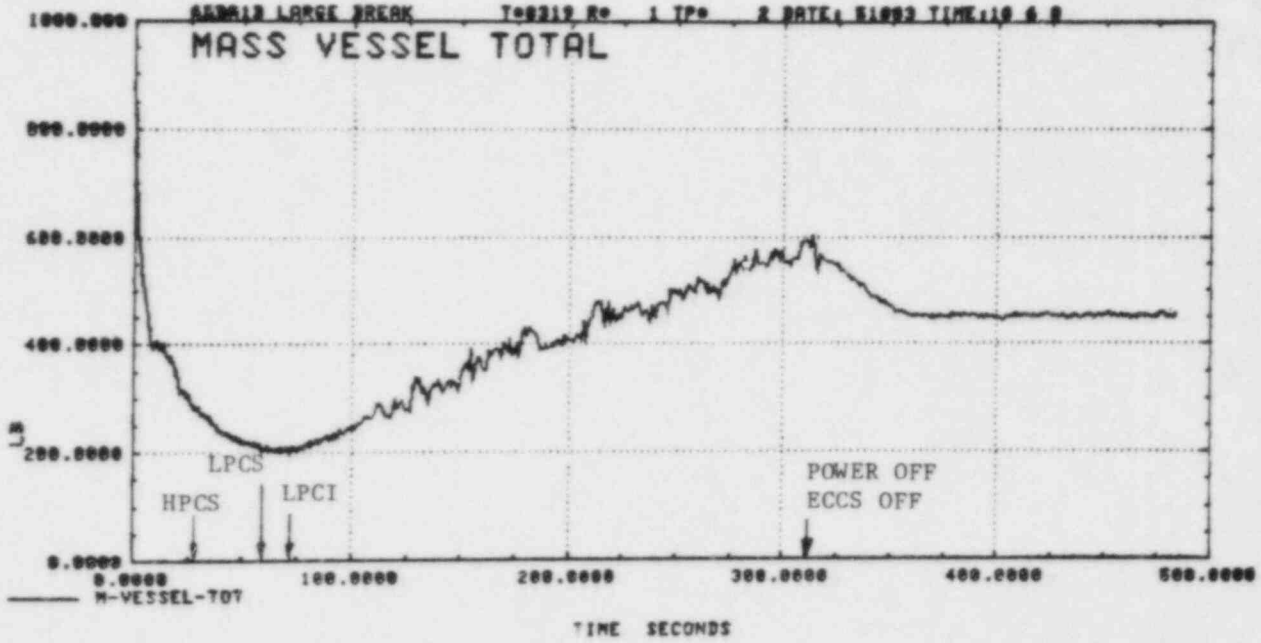

Figure 7.1-3. System Total Mass

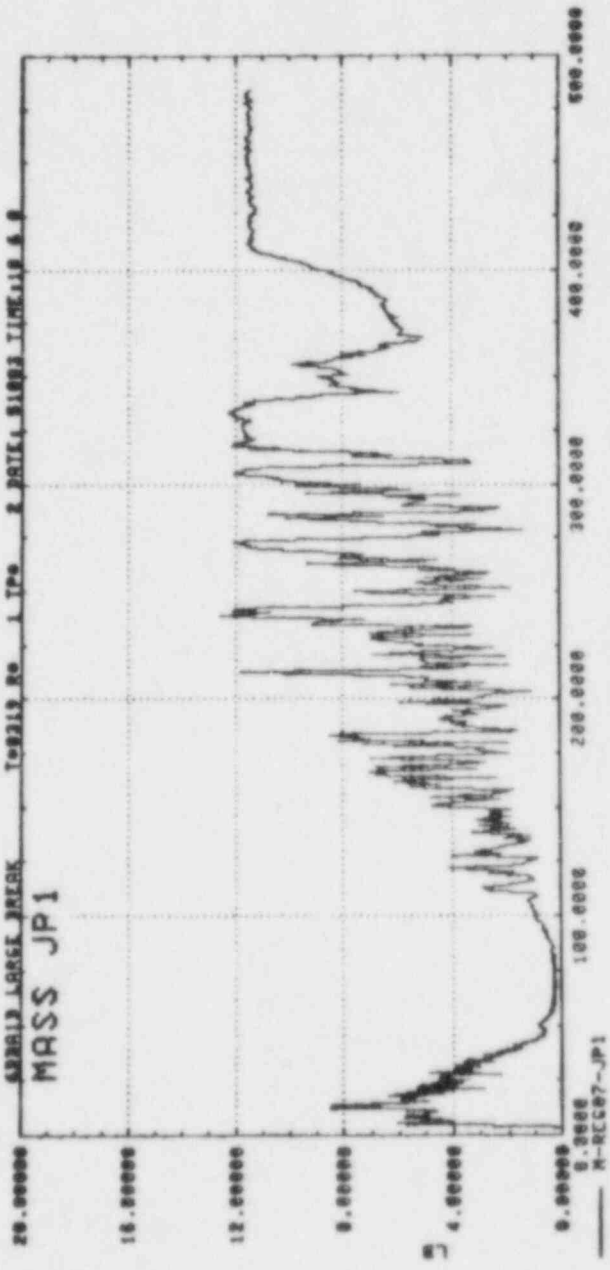

Figure 7.1-4. Intact Loop Jet Pump Mass

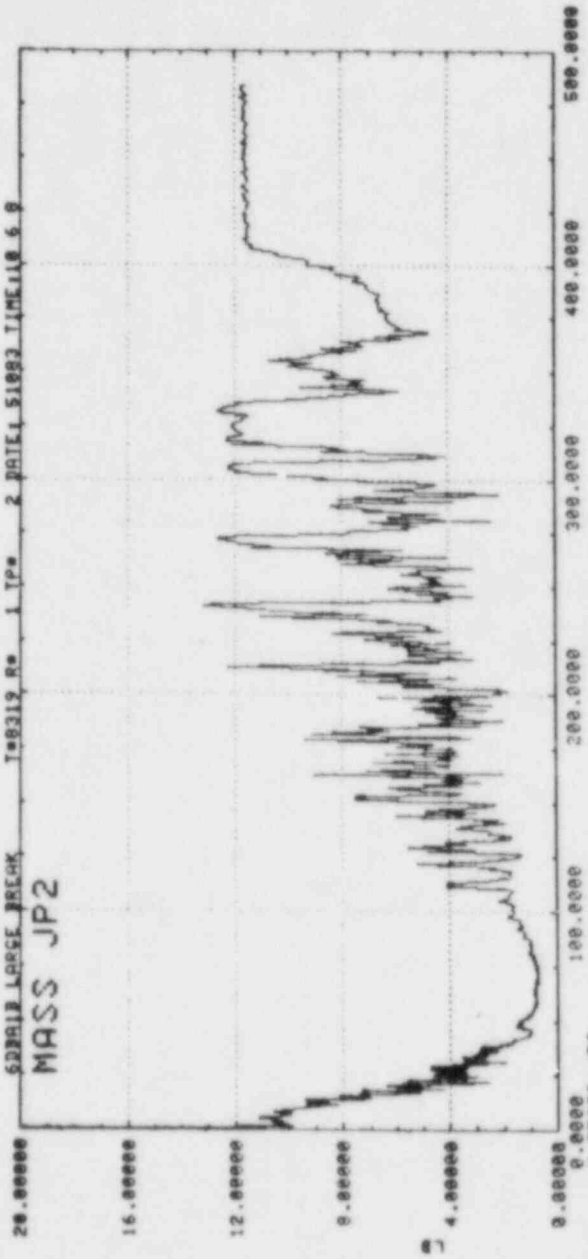

Figure 7.1-5. Broken Loop Jet Pump Mass

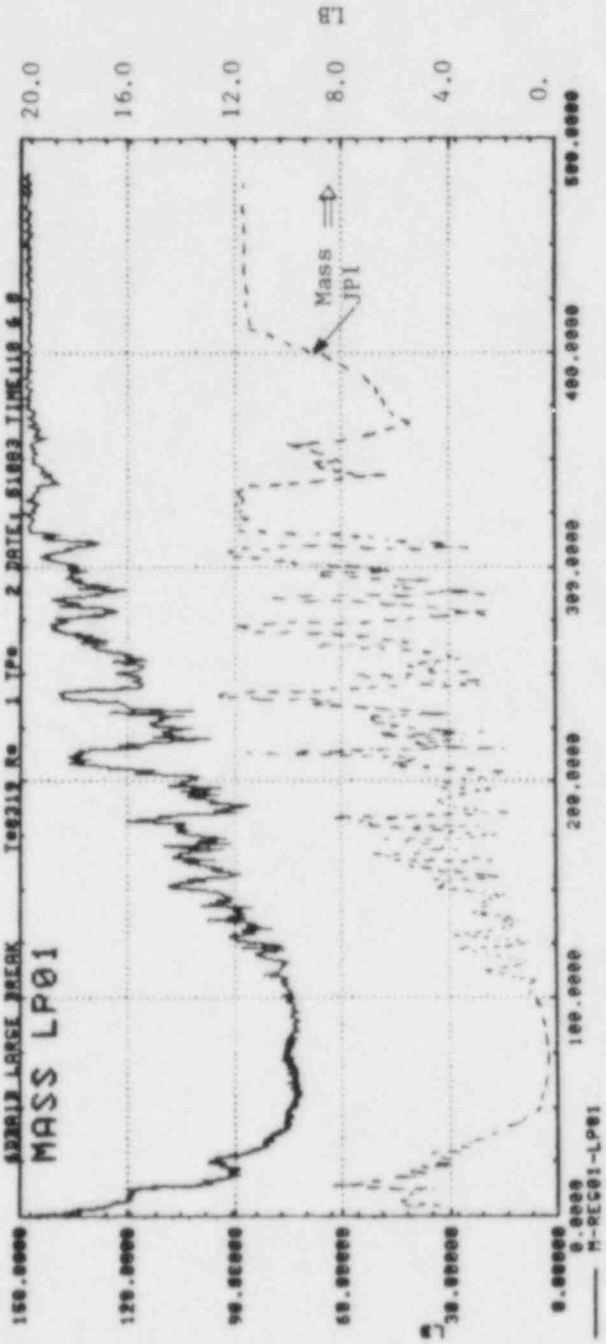

Figure 7.1-6. Mass of Lower Plenum Below Jet Pump Exit Plane

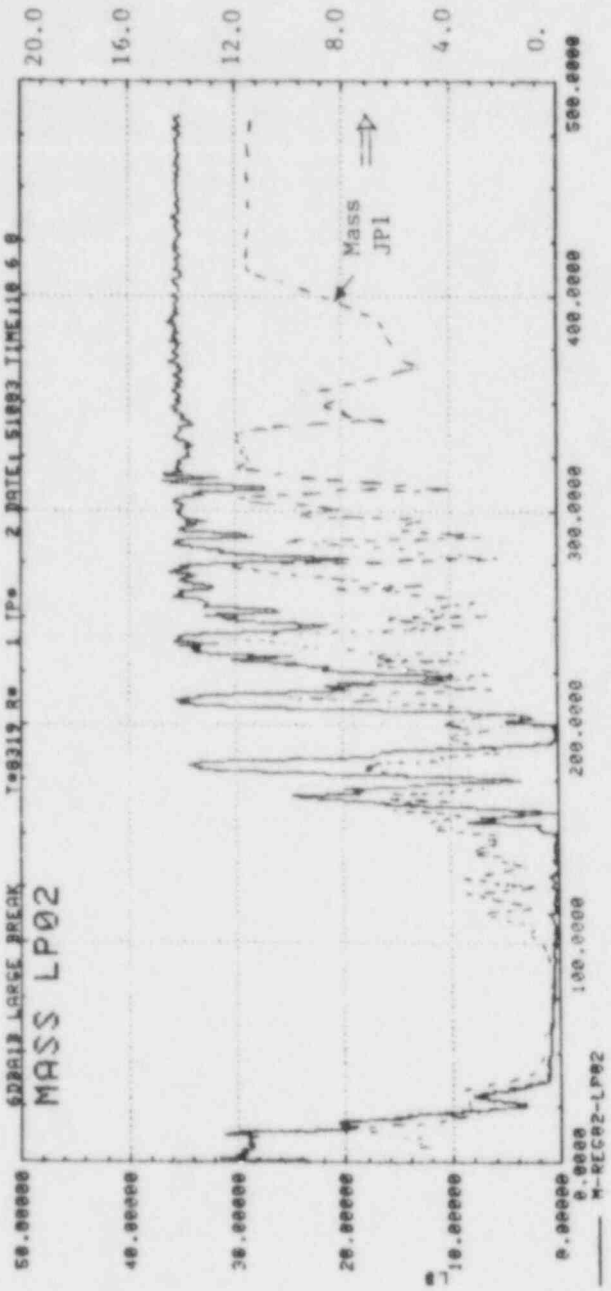

Figure 7.1-7. Mass of Lower Plenum Above Jet Pump Exit Plane

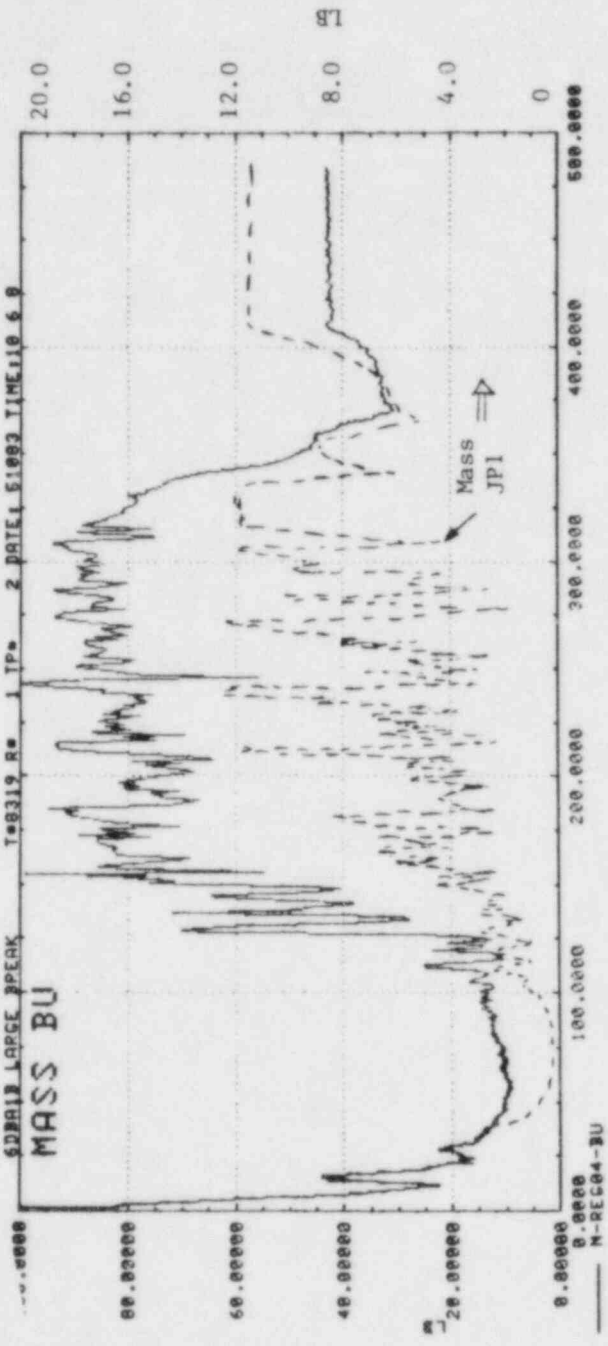

Figure 7.1-8. Bundle Mass

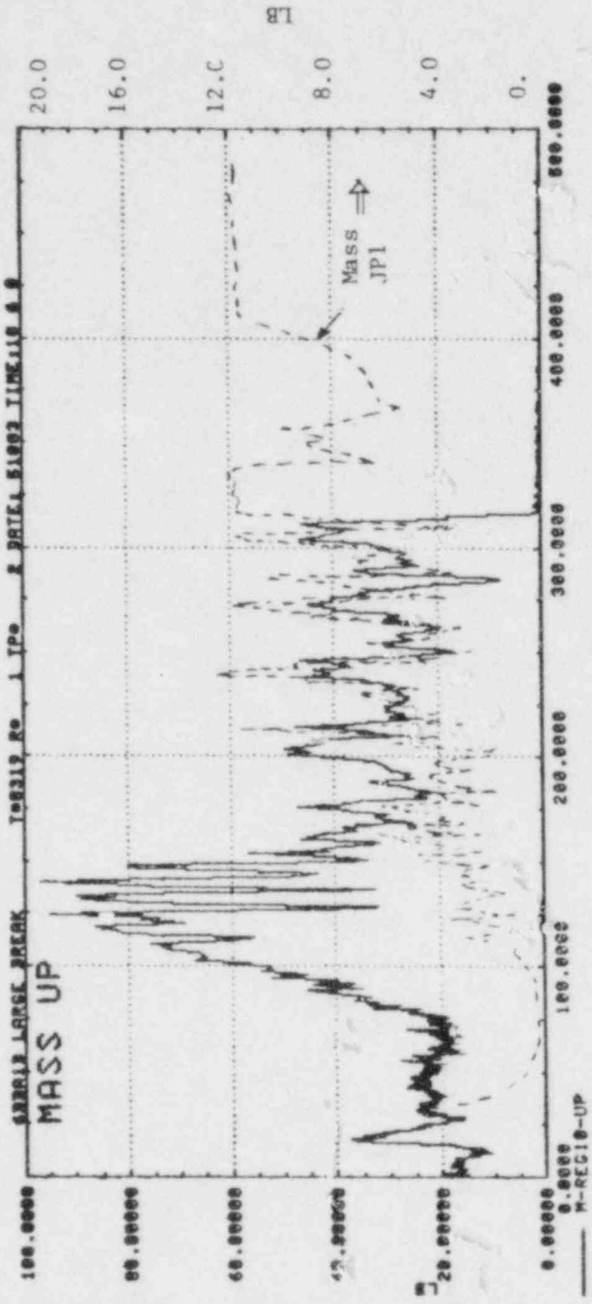

Figure 7.1-9. Upper Plenum Mass

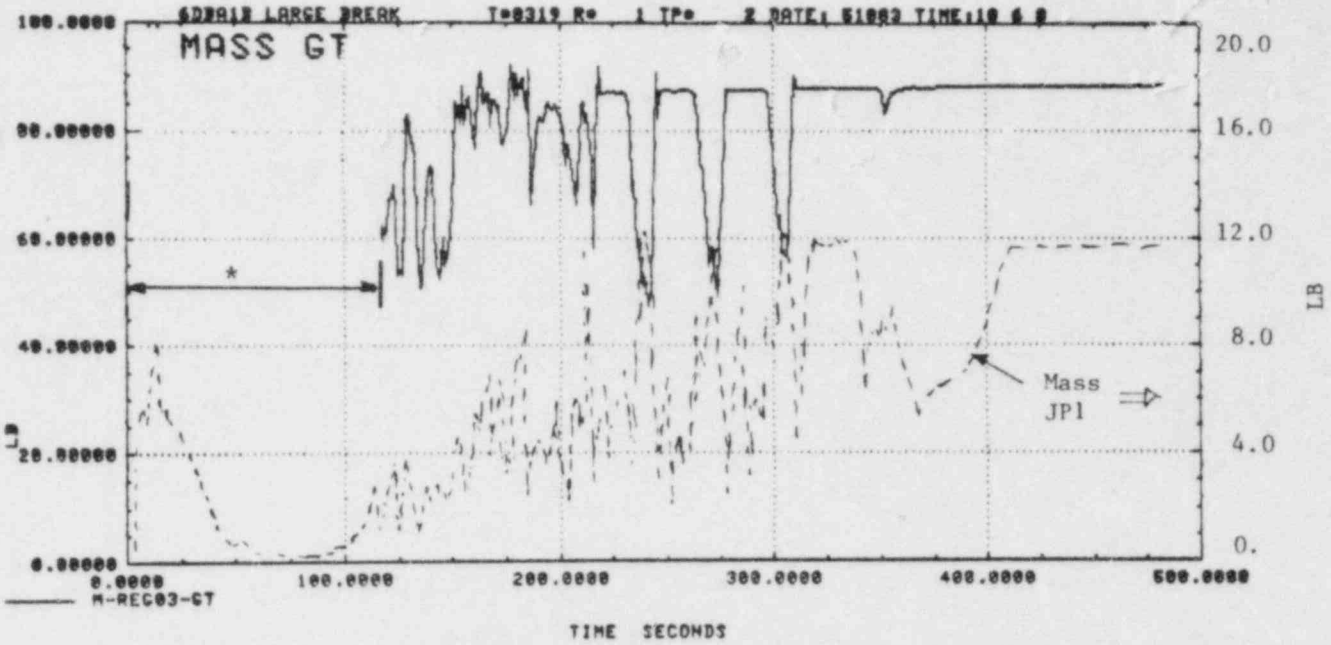

* Data not shown due to bad measurement in this period.

Figure 7.1-10. Guide Tube Mass

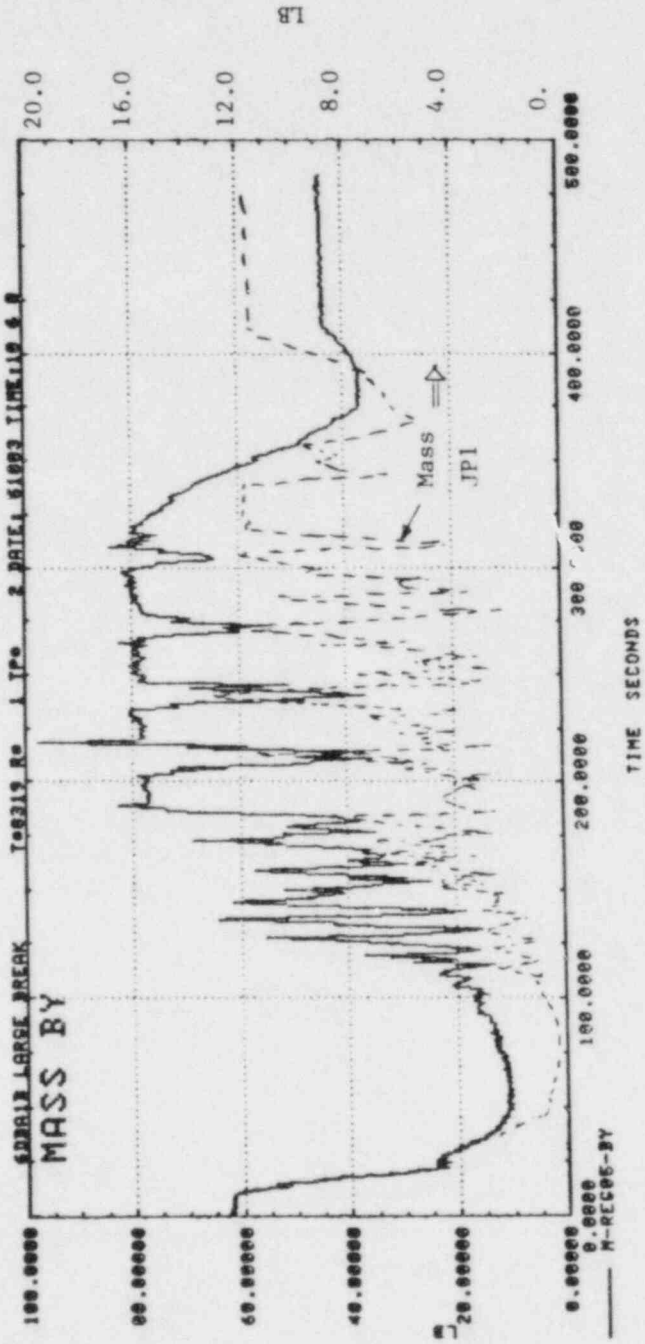

Figure 7.1-11. Bypass Mass

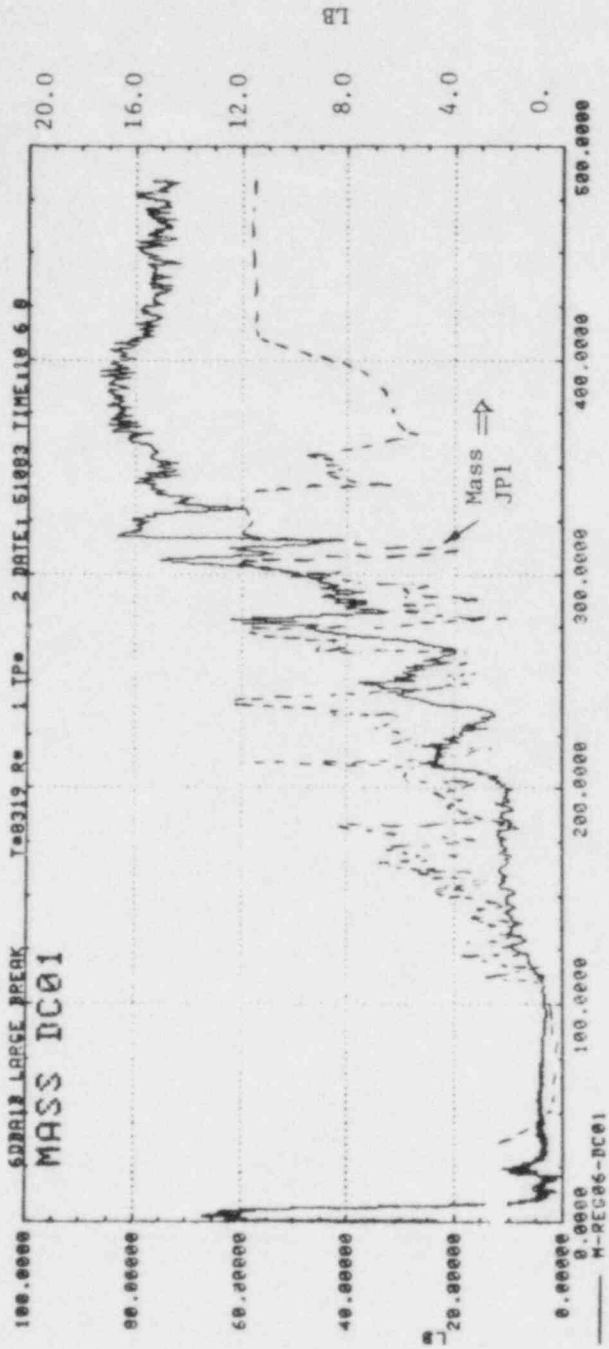

Figure 7.1-12. Mass of Downcomer Below Top of Jet Pump

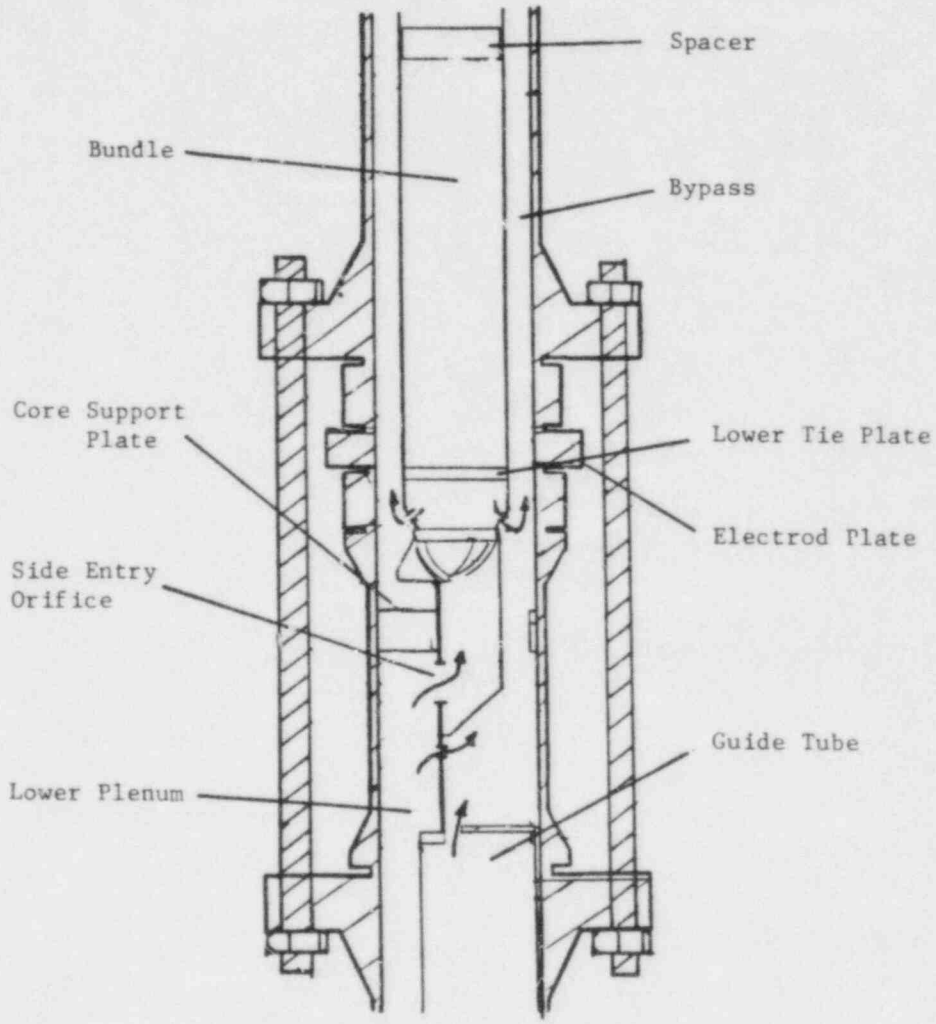

Figure 7.1-13. FIST Bypass, Guide Tube and Bundle Inlet Configuration

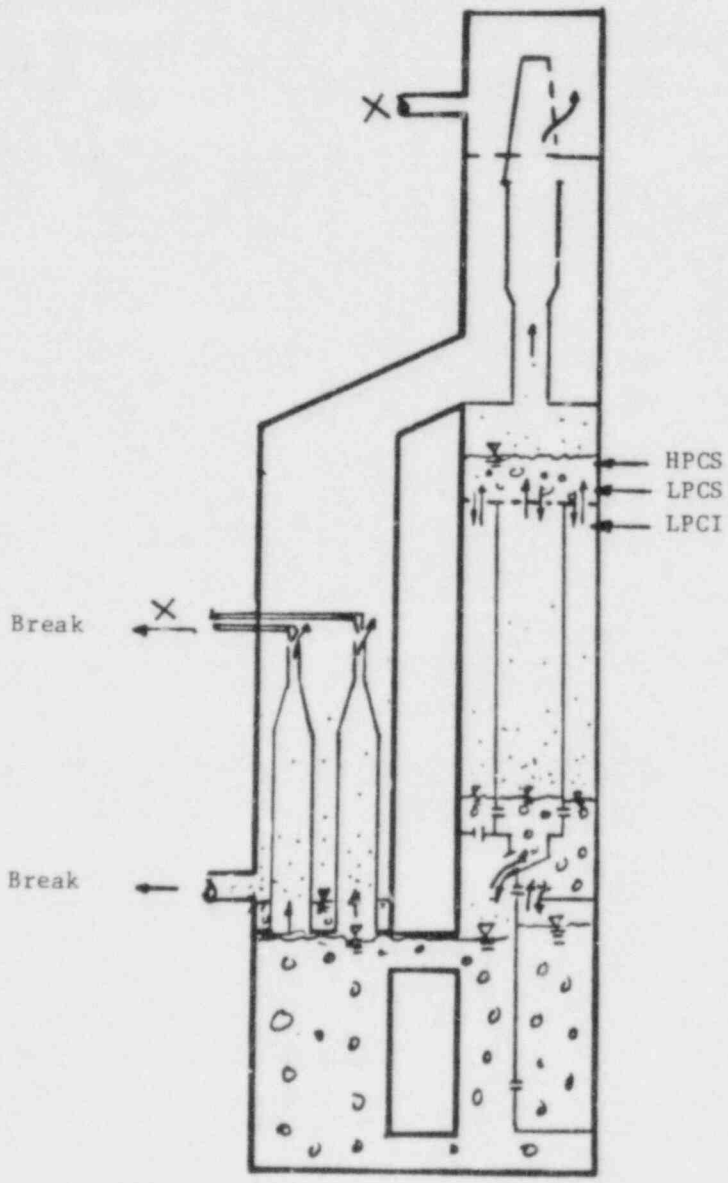

Figure 7.1-14. System Condition at About 60 seconds

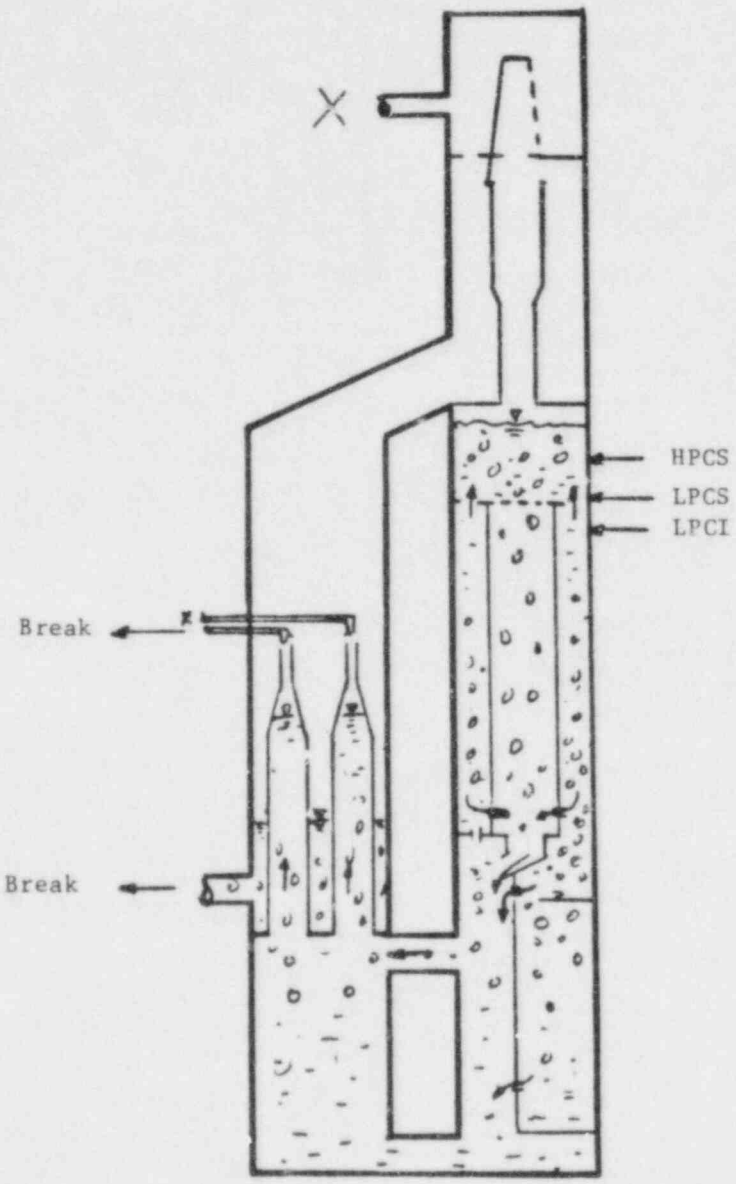

Figure 7.1-15. System Condition During The Bypass Vapor Generation

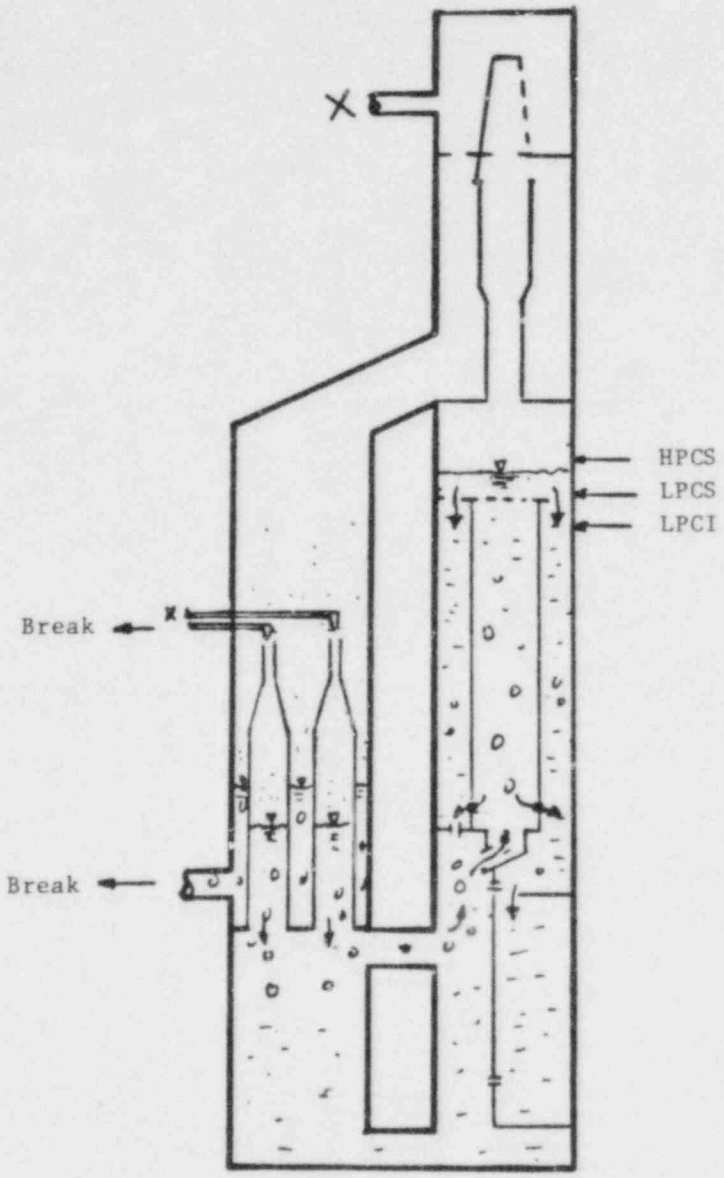

Figure 7.1-16. System Condition During the Bypass Refilling

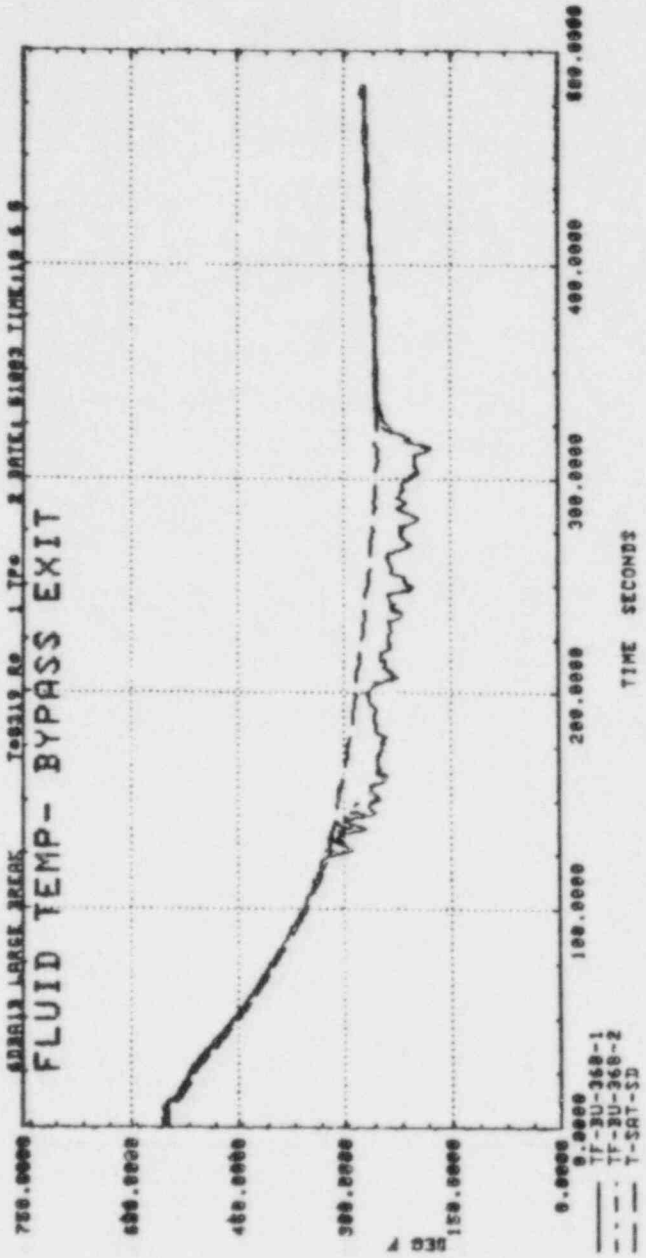

Figure 7.1-17. Fluid Temperature at Bypass Exit

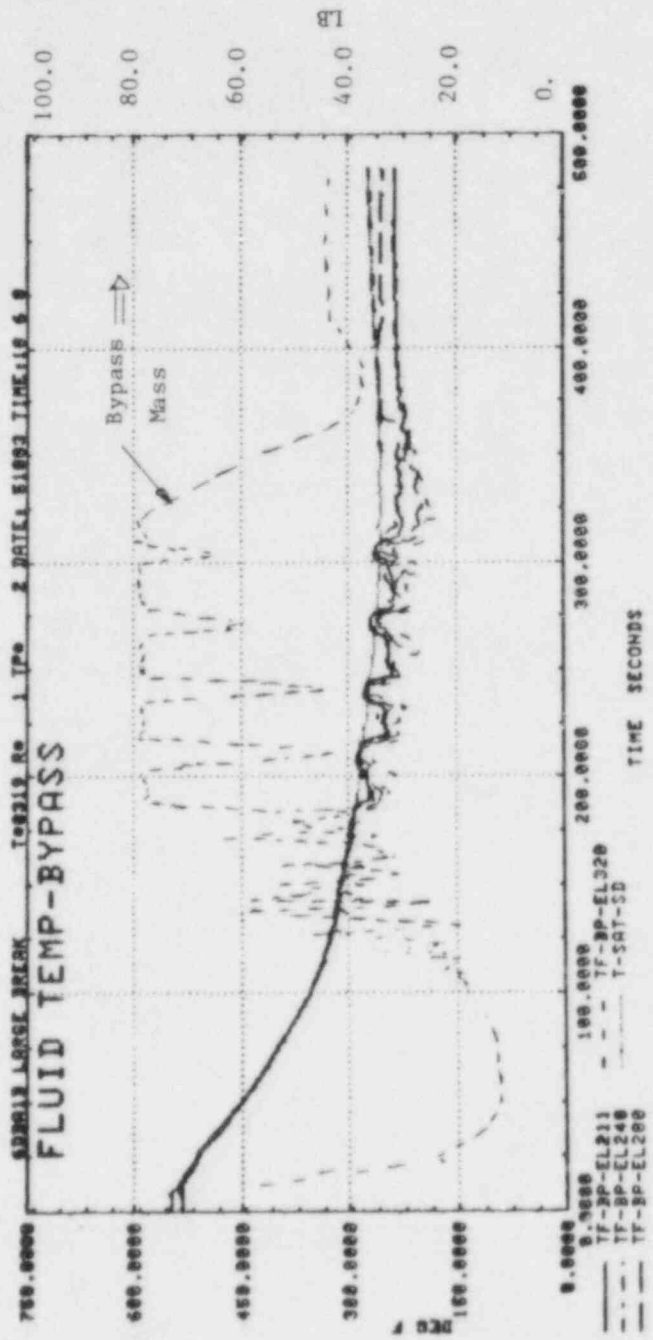

Figure 7.1-18. Bypass Fluid Temperature

7.2 SMALL BREAK TEST, 6SB2C

7.2.1 General Description

The small break test, 6SB2C, simulates a BWR/6 recirculation suction line break of 0.05 ft^2 with HPCS assumed to be unavailable. This test is also a TLTA tieback test. Test conditions of the TLTA test 6432/R1 including an initial bundle power of 5.05 MW, core flow of 42 lb/sec, ADS time delay of 120 second, and ECC water temperature of 90°F, are used in this test (Figure 7.2-1). In addition to the test results discussed below, comparisons between this test and the TLTA counterpart test, 6432/R1 are given in Section 8. A pretest prediction made using the TRAC code for this test is discussed in Section 9.

7.2.2 Key Events and System Pressure

Key events observed in the test are listed in Table 7.2-1. Upon break initiation and simultaneous start of bundle power decay, trip of recirculation pumps, and trip of feedwater supply, the steam generation in the core begins to decrease. The system pressure (Figure 7.2-2), however, is maintained nearly constant by the pressure regulator until the Main Steam Isolation Valve (MSIV) is tripped to close at 75 seconds when the water level reaches level 1. The Automatic Depressurization System (ADS) is also activated at level 1, with a time delay of 120 seconds. The MSIV closure results in an increase of the system pressure. The subsequent rapid depressurization by ADS leads to initiations of LPCS and LPCI at 310 and 335 seconds, respectively.

7.2.3 Water Level and Scenario

Water level determined from differential pressure (DP) and conductivity probe (CP) measurements in various regions is illustrated in Figures 7.2-3 and 4. "Snap shot" views of system conditions during the transient (Figures 7.2-5 to 13) provide aids for discussing the scenario observed in this test.

Water level drop in the downcomer during the early transient is due mainly to loss of inventory through the break and the steamline. Water level in the downcomer reaches level 1 (Figures 7.2-3 and 7.2-6) and trips MSIV and ADS at 75 seconds. Following the downcomer water level drop, the water level inside the core shroud also begins to drop after the core flow coastdown is completed and reaches the top of the core at about 130 seconds (Figure 7.2-4). Water level continues to drop in the bypass thereafter, while the bundle remains covered with two phase mixture for about another 30 seconds. During this period natural circulation drives water into the bundle from the bypass, through the bypass leakage path. The lower density of the boiling mixture maintains a higher two phase mixture level in the bundle.

The rapid depressurization by ADS at 195 seconds (Figure 7.2-2) leads to system flashing and level swell (Figures 7.2-4 and 8). The swollen mixture level begins to fall back as the depressurization rate decreases and flashing subsides.

Shortly after ADS, a mixture level is observed in the lower plenum and later the jet pump exit plane is uncovered at about 290 seconds (Figures 7.2-4 and 9). Steam generation in the lower plenum leads to counter current flow limiting (CCFL) at the SEO, which holds some water in the core. The jet pumps have high steam flow at this time and CCFL is observed at the top of the jet pumps. This results in a mixture level in the downcomer that is higher than the bundle mixture level (Figure 7.2-9).

As the mixture level falls back after the flashing surge, the core becomes completely uncovered (Figure 7.2-4), leading to rod heatup (Figure 7.2-14). Shortly after ECCS initiation, the core starts to refill. The bypass refill is completed at 380 seconds, followed by the bundle reflood at about 420 seconds (Figure 7.2-4). This refilling process is similar to that observed in most TLTA LOCA tests but

different than the FIST large break test 6DBA1B as discussed in Section 7.1. In the test 6DBA1B, both the bundle and bypass were refilled at about the same time by the subcooled CCFL breakdown at the top of the core. Differences in steam generation and ECC flow affect the refilling process in these two tests, as discussed below.

At the time of the LPCI injection, the steam generation in the bypass region of the small break test is smaller than the large break test 6DBA1B, due to less water being left in the bypass/guide tube region (Figure 7.2-4) and a slower depressurization rate (Figure 7.2-2). Test 6DBA1B was performed with one LPCI simulated, while this small break test simulated 3 LPCI systems. The relatively large LPCI flow is able to condense a significant amount of the steam upflow and change the CCFL condition at the top of the bypass, allowing LPCS water in the upper plenum to drain into the bypass. This leads to a quick refilling of the bypass, while CCFL at the upper tieplate limits water draining into the bundle from the upper plenum. Later in the transient, the bundle is reflooded by both top-down and bottom-up refilling (Figure 7.2-11) which is also evident in the rod temperature response (Figure 7.2-14).

After the core is reflooded the subcooled ECC water arrives at the core inlet and results in a CCFL breakdown at the SFO. This leads to lower plenum refill at 465 seconds (Figure 7.2-4 and 13).

7.2.4 Rod Temperature and Mass Responses

Figure 7.2-14 shows that all rods heatup during the bundle uncovery and are completely quenched before or during the bundle reflood (420 seconds). A PCT of 920°F is measured. The regional mass responses of various regions are shown in Figures 7.2-15 to 24. The flashing surge at ADS results in a mass redistribution throughout the entire system. These mass responses reflect the scenario and system performance discussed in the previous sections.

7.2.5 Summary (Test 6SB2C)

In summary, the following responses are observed in the FIST small break test, 6SB2C:

(1) The system pressure does not reach the S/RV opening setpoint after MSIV and there is no S/RV activation

(2) The bundle and bypass are partially uncovered before ADS and recovered at ADS by the flashing surge. These two regions are completely uncovered after ADS and later refilled by ECC water.

(3) CCFL is observed at SEO, UTP, top of the bypass and top of the jet pump during the post-ADS depressurization.

(4) The downcomer water level remains relatively high after ADS.

(5) The jet pump exit is uncovered and later recovered,

(6) A relatively smooth refill/reflood in the bypass/guide tube is observed.

(7) The bundle is reflooded with top-down and bottom-up refilling.

(8) A PCT of 925^{o}F was measured.

Table 7.2-1

KEY EVENTS, 6SB2C

		Time (sec)
1.	Break Initiation	0
2.	Bundle Power Trip	0
3.	Jet Pump Trip	0
4.	Feedwater Trip	0
5.	Recirculation Loop Isolation	20
6.	Water Level Reached L1	75
7.	MSIV Closure	77
8.	ADS Activation	195
9.	Bundle Uncovery (Top)	
	(A) Before ADS	155
	(B) After ADS	237
10.	Bypass Uncovery (Top)	133/235
11.	Jet Pump Suction Uncovery	165
12.	Bundle Heatup Begins	250
13.	Final Rod Rewet	420
14.	LPCS Activation	35
	LPCS Injection	310
15.	LPCI Activation	35
	LPCI Injection	335
16.	Bypass Refill Begins	362
	Bypass Refill Completed	380
17.	Bundle Refill Begins	370
	Bundle Refill Completed	420
18.	Jet Pump Exit Uncovery	290
19.	Jet Pump Exit Recovery	420
20.	SEO CCFL Breakdown	465
21.	Lower Plenum Refilled	465
22.	PCT (925°F)	400
23.	End of Test	510

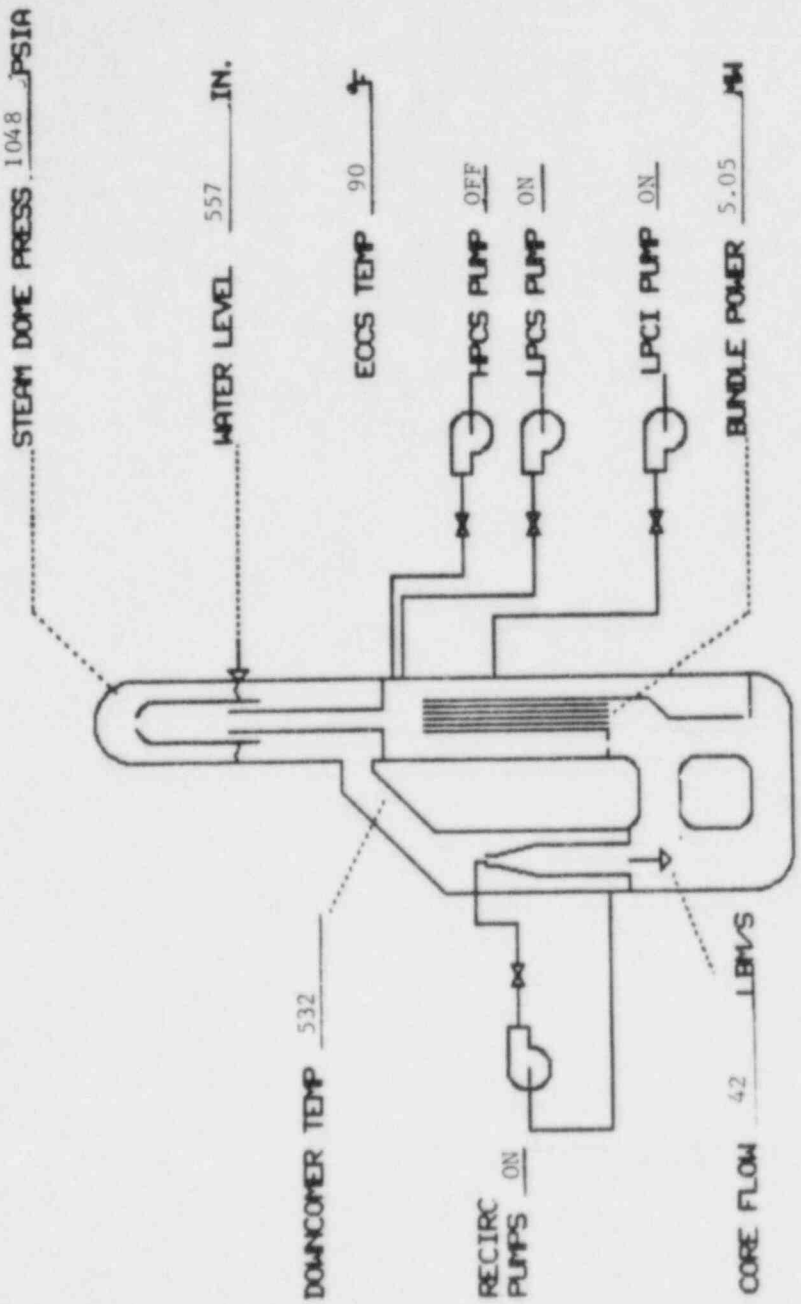

Figure 7.2-1. Initial Conditions - Test 6SB2C

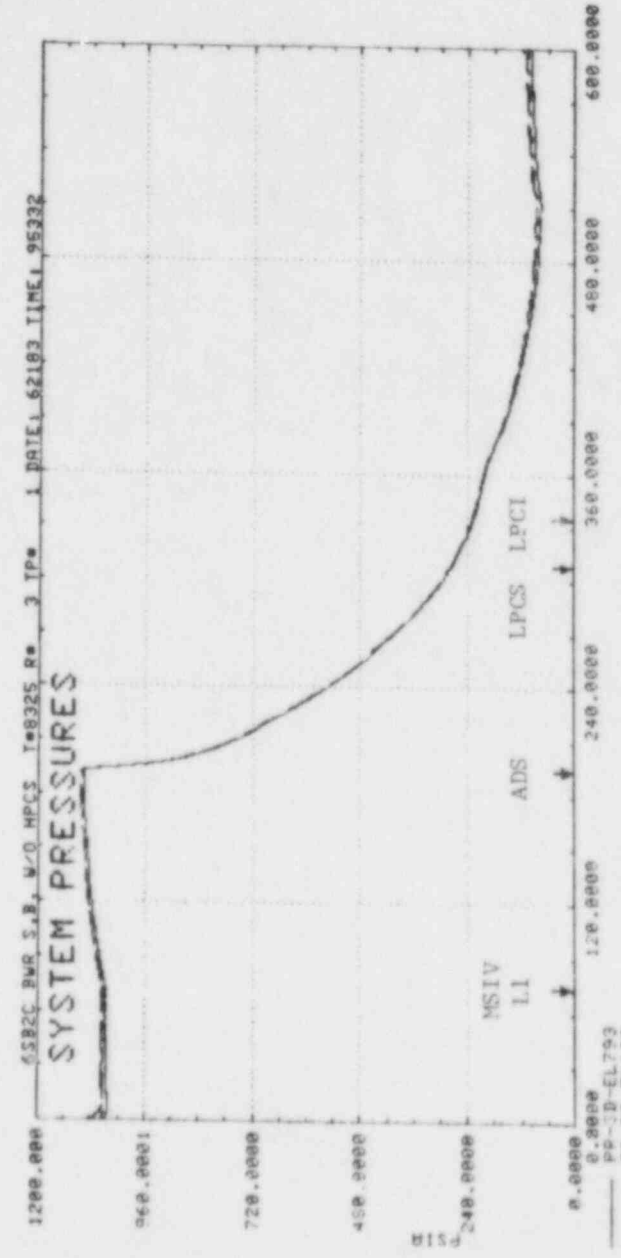

Figure 7.2-2. System Pressure

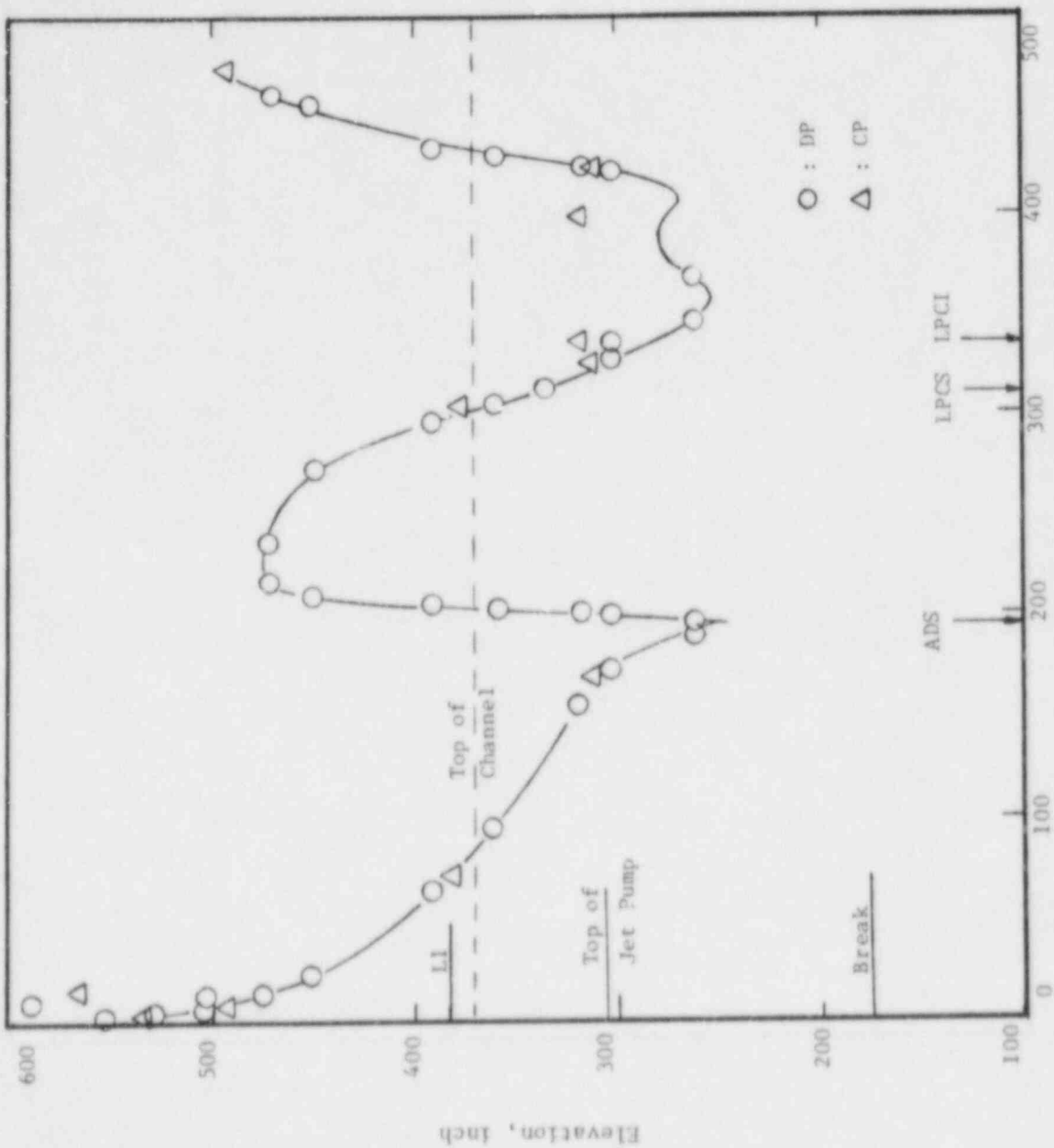

Figure 7.2-3. Downcomer Water Level, Test 6SB2C

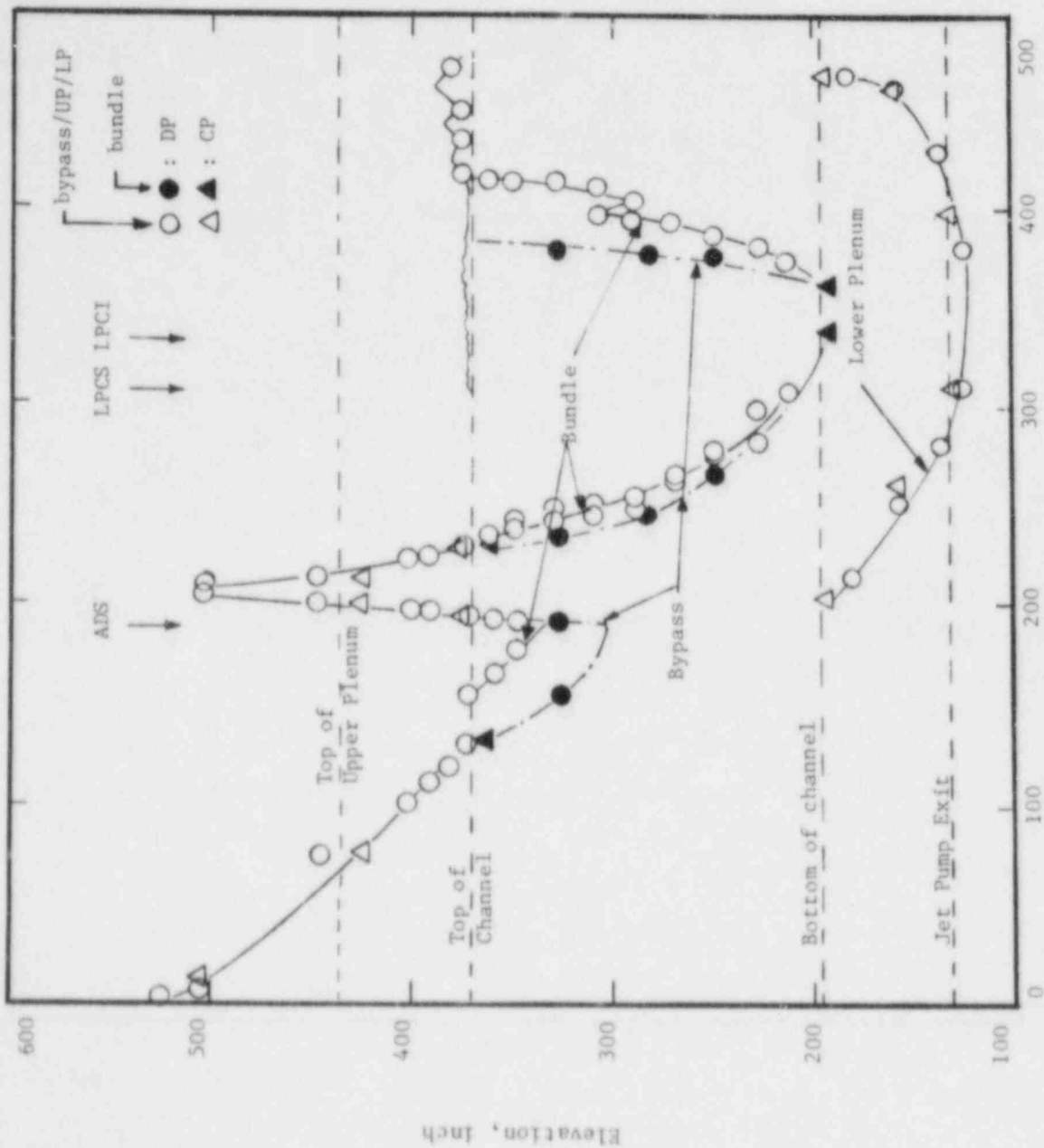

Figure 7.2-4. Inside Water Level, Test 6SB2C

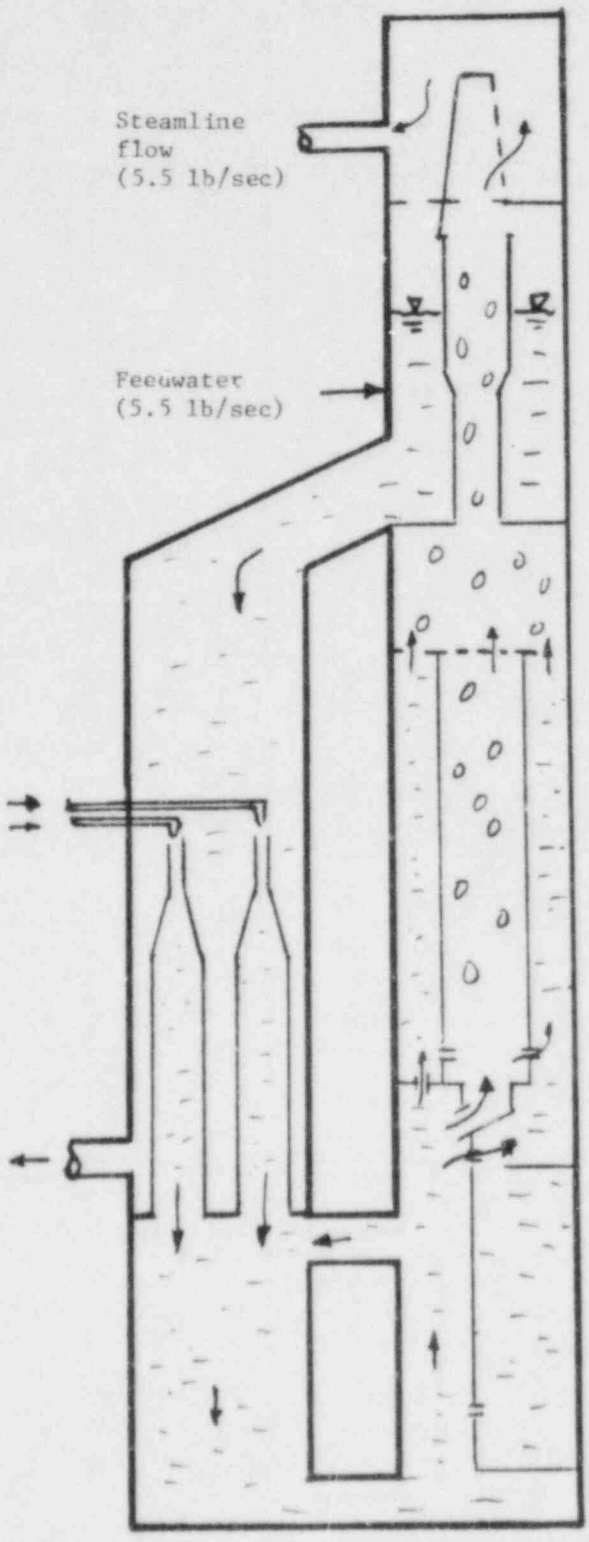

Figure 7.2-5. System Condition at T=0 Sec

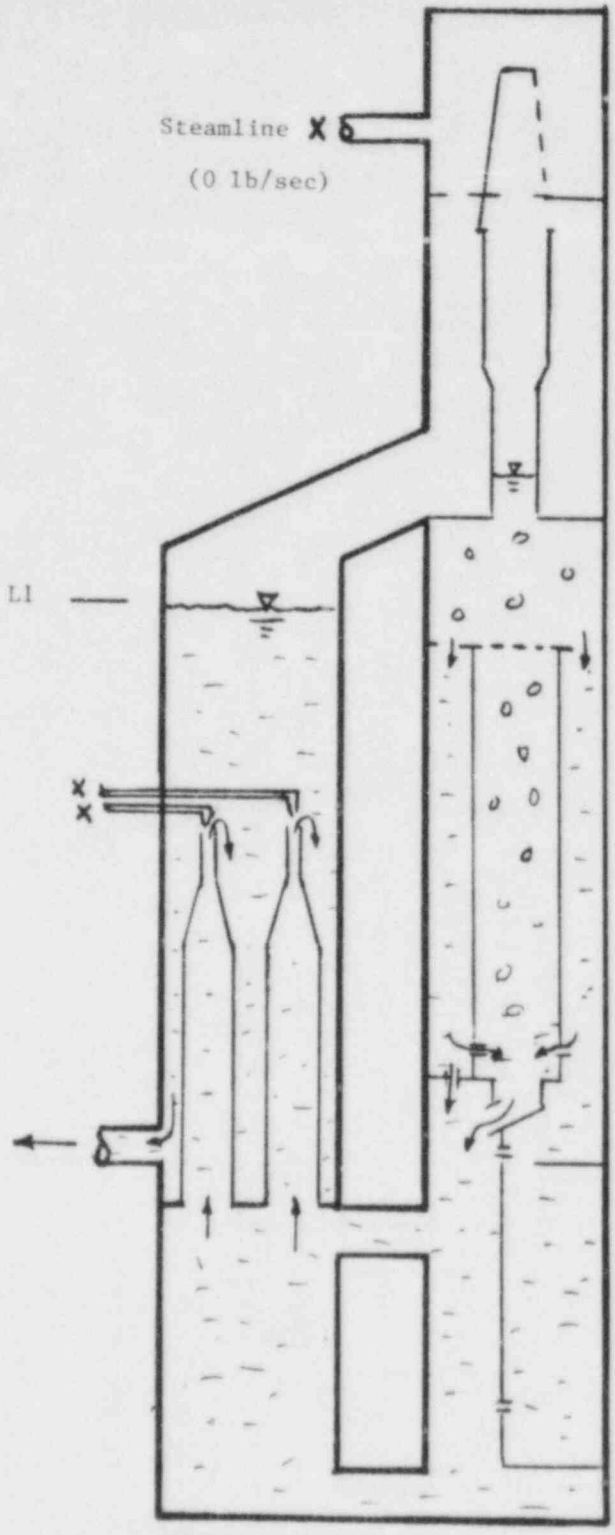

Figure 7.2-6. System Condition at T=75 sec

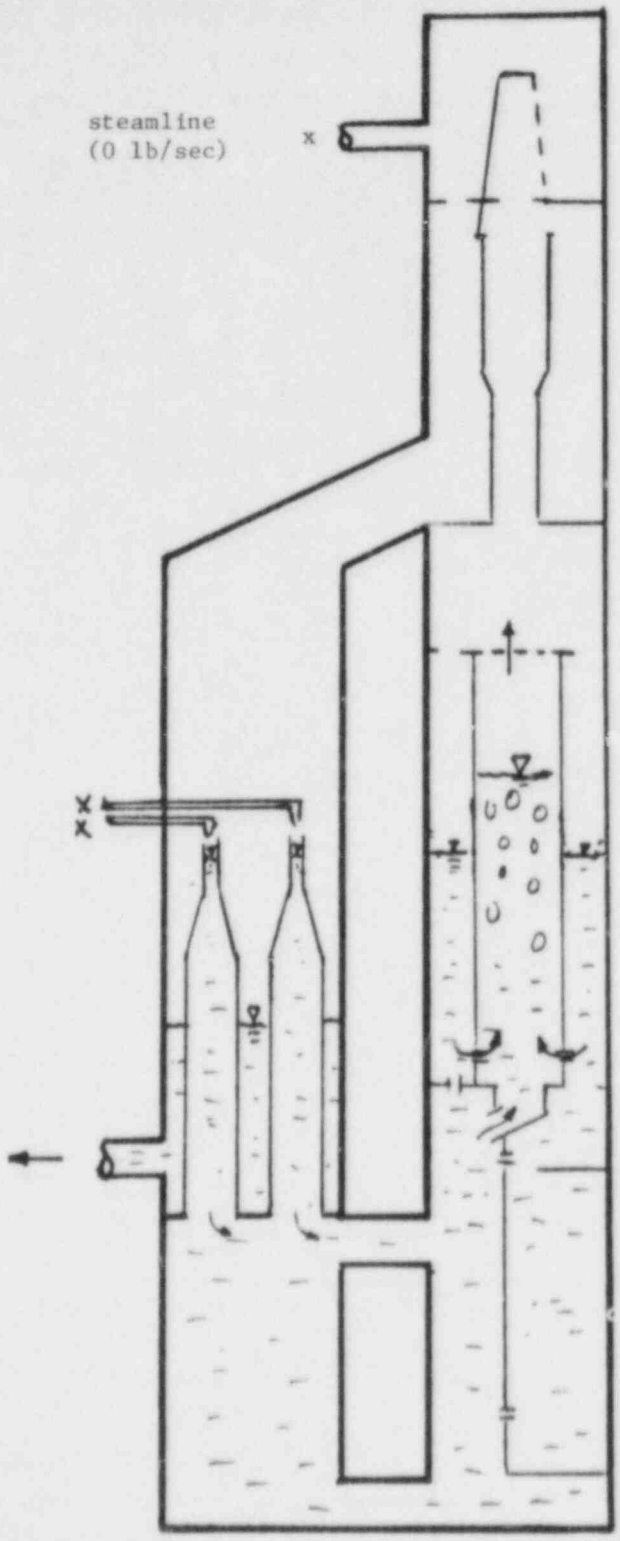

Figure 7.2-7. System Condition at T=190 sec

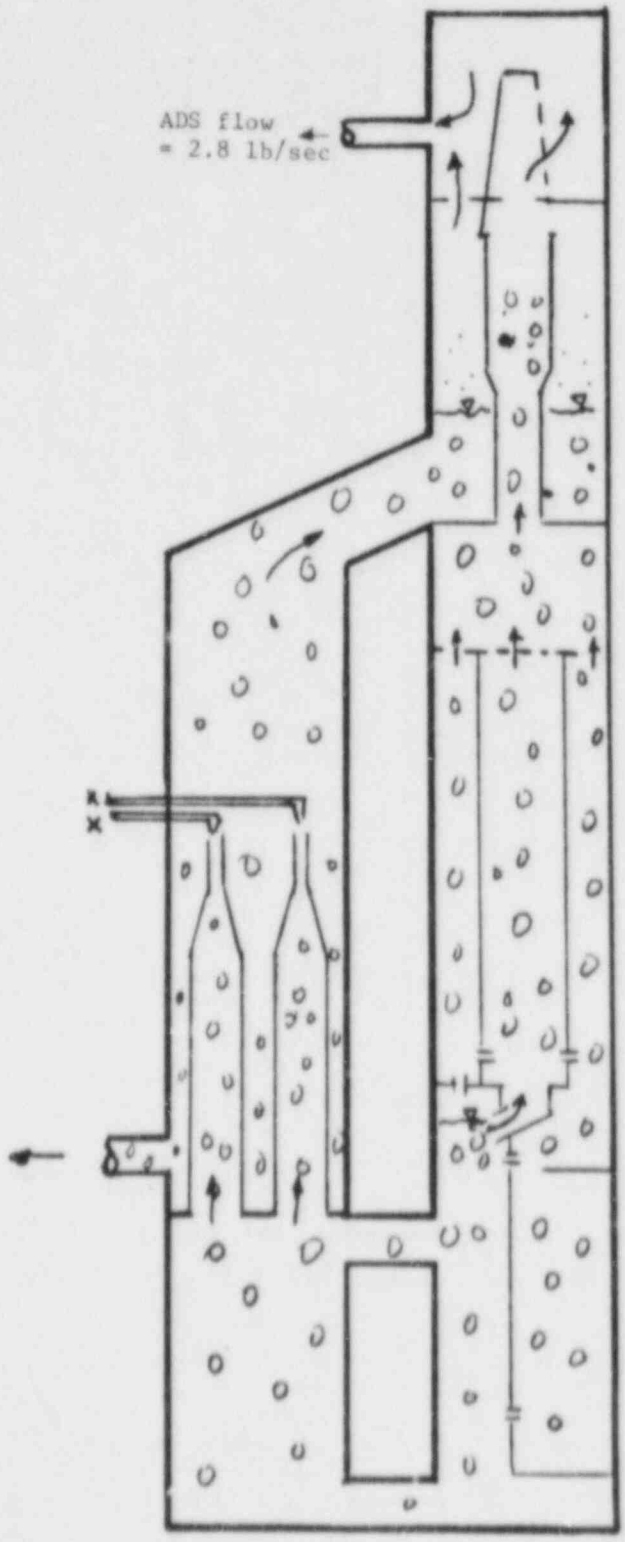

Figure 7.2-8. System Condition at T=210 sec

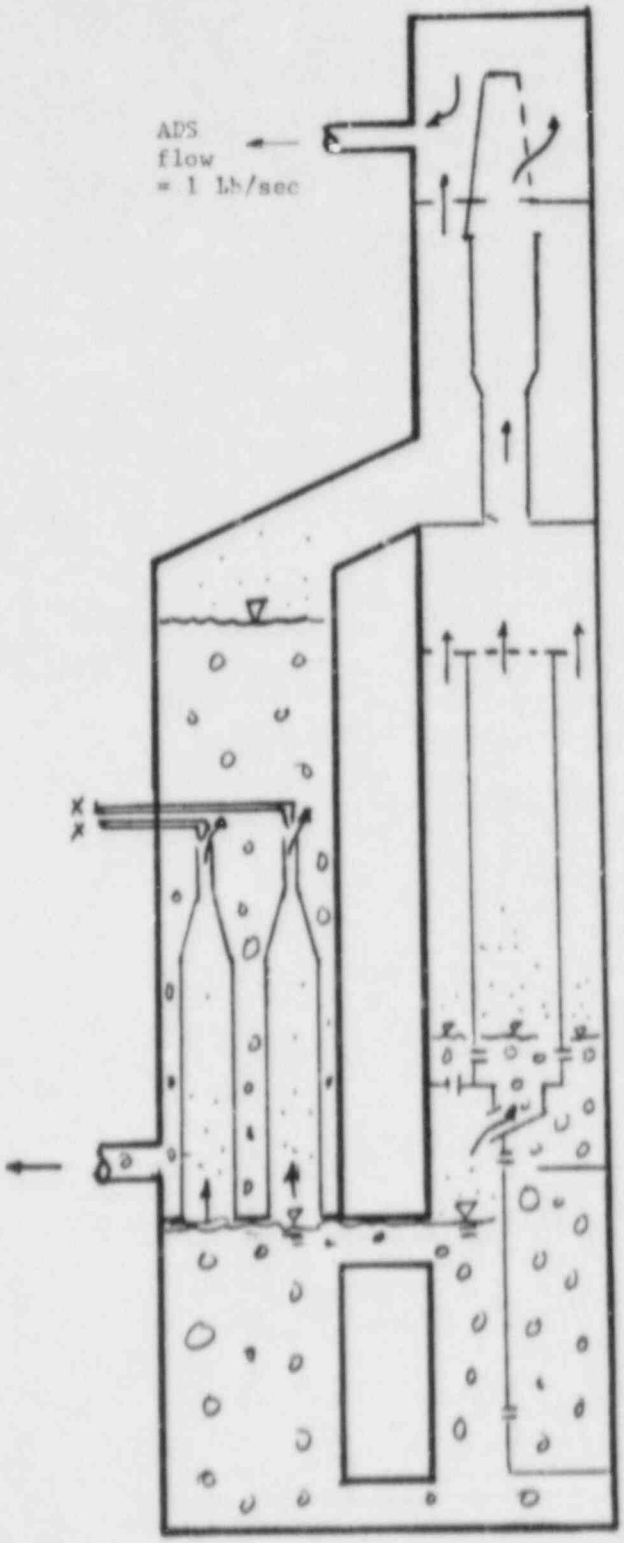

Figure 7.2-9. System Condition at T=300 sec

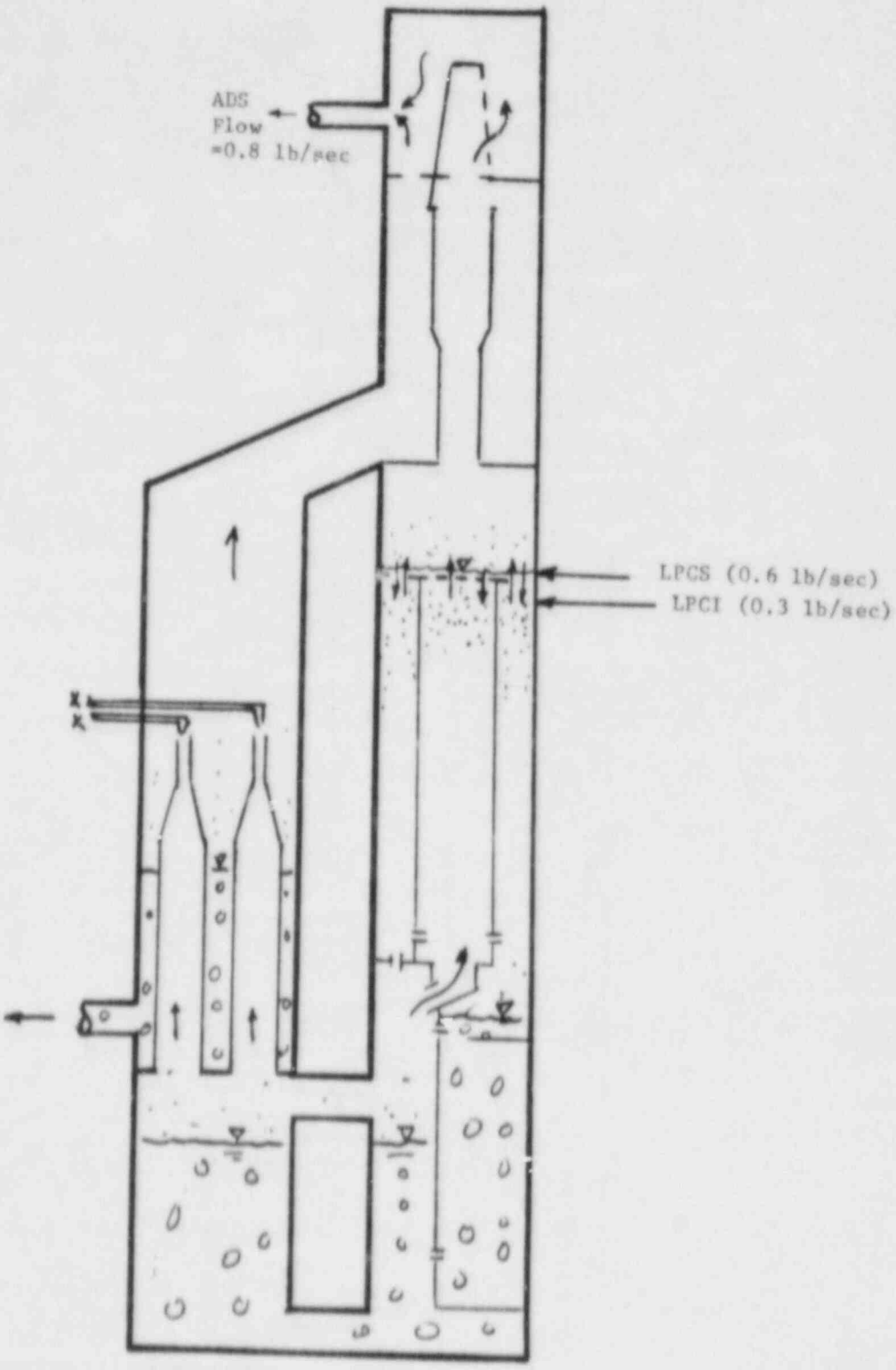

Figure 7.2-10. System Condition at T=350 sec

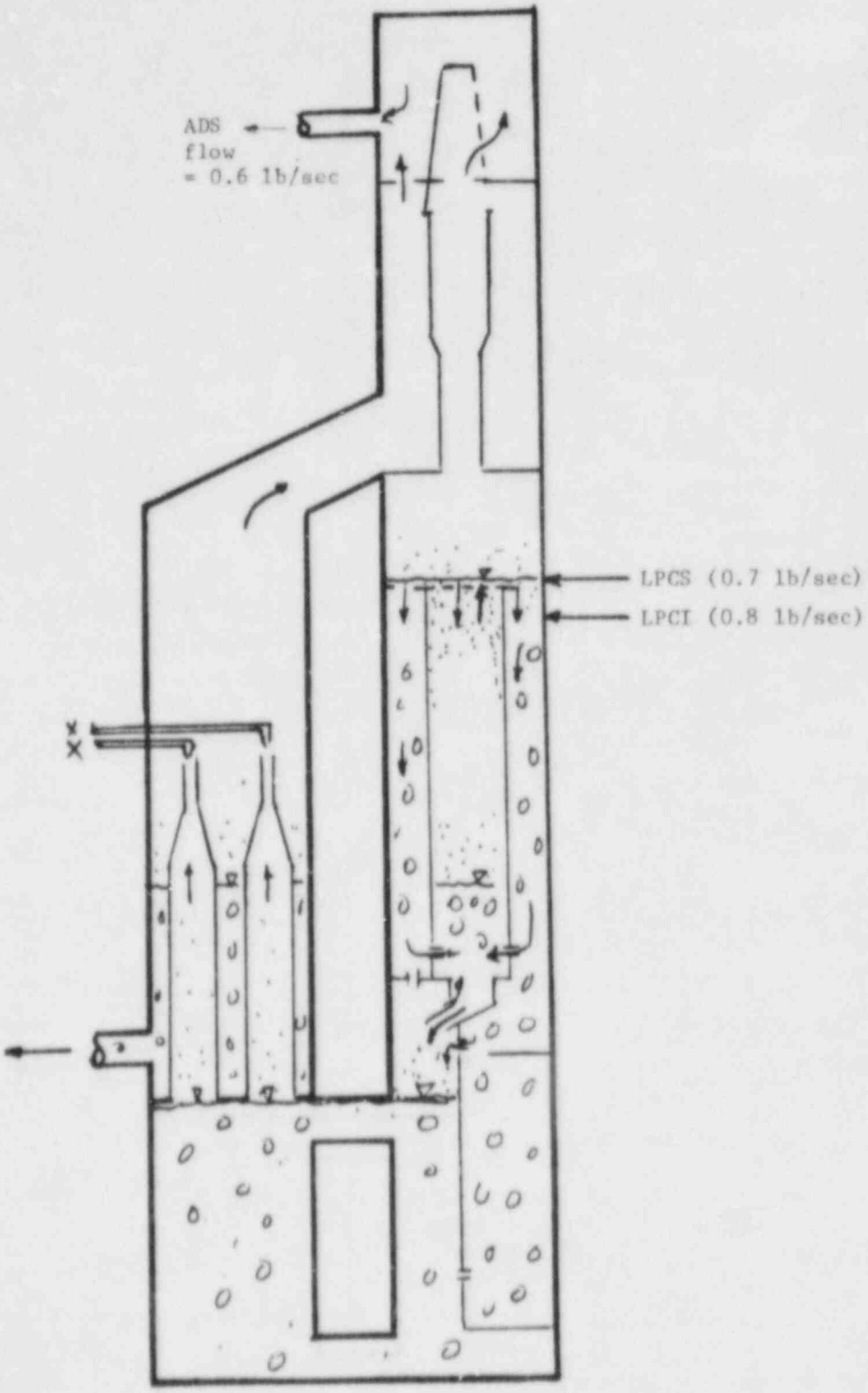

Figure 7.2-11. System Condition at T=380 sec

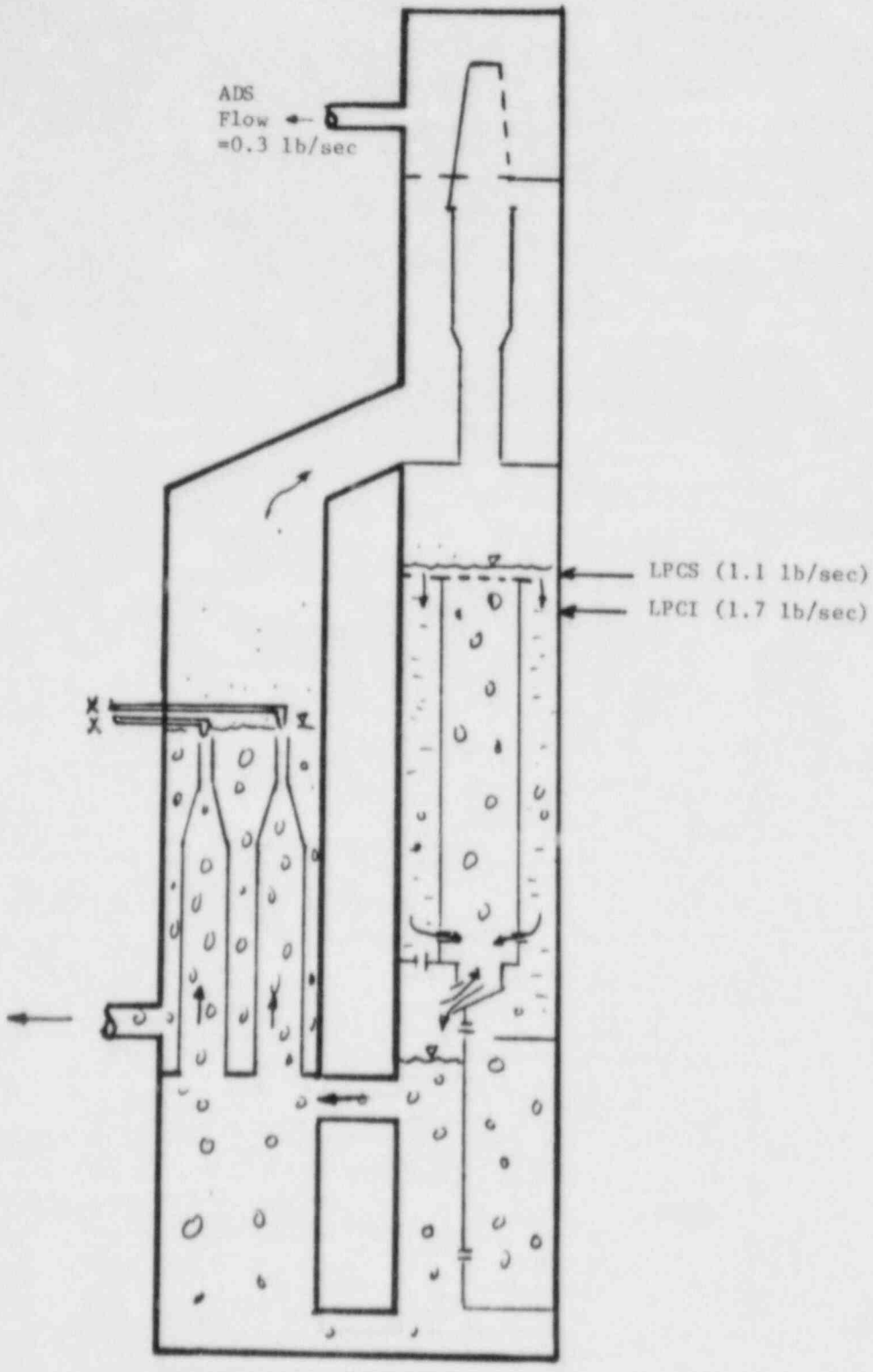

Figure 7.2-12. System Condition at T=420 sec

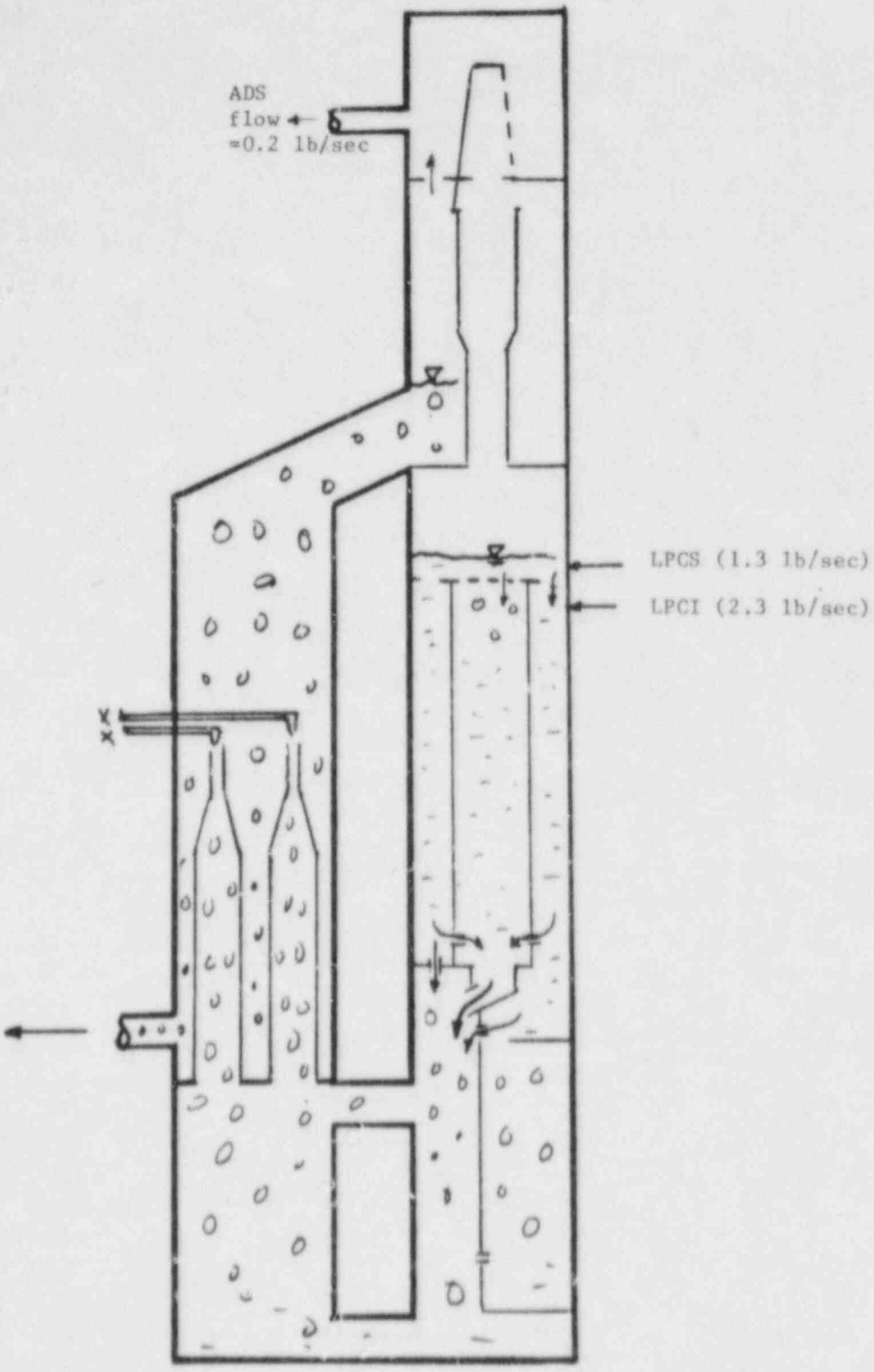

Figure 7.2-13. System Condition at T=460 sec

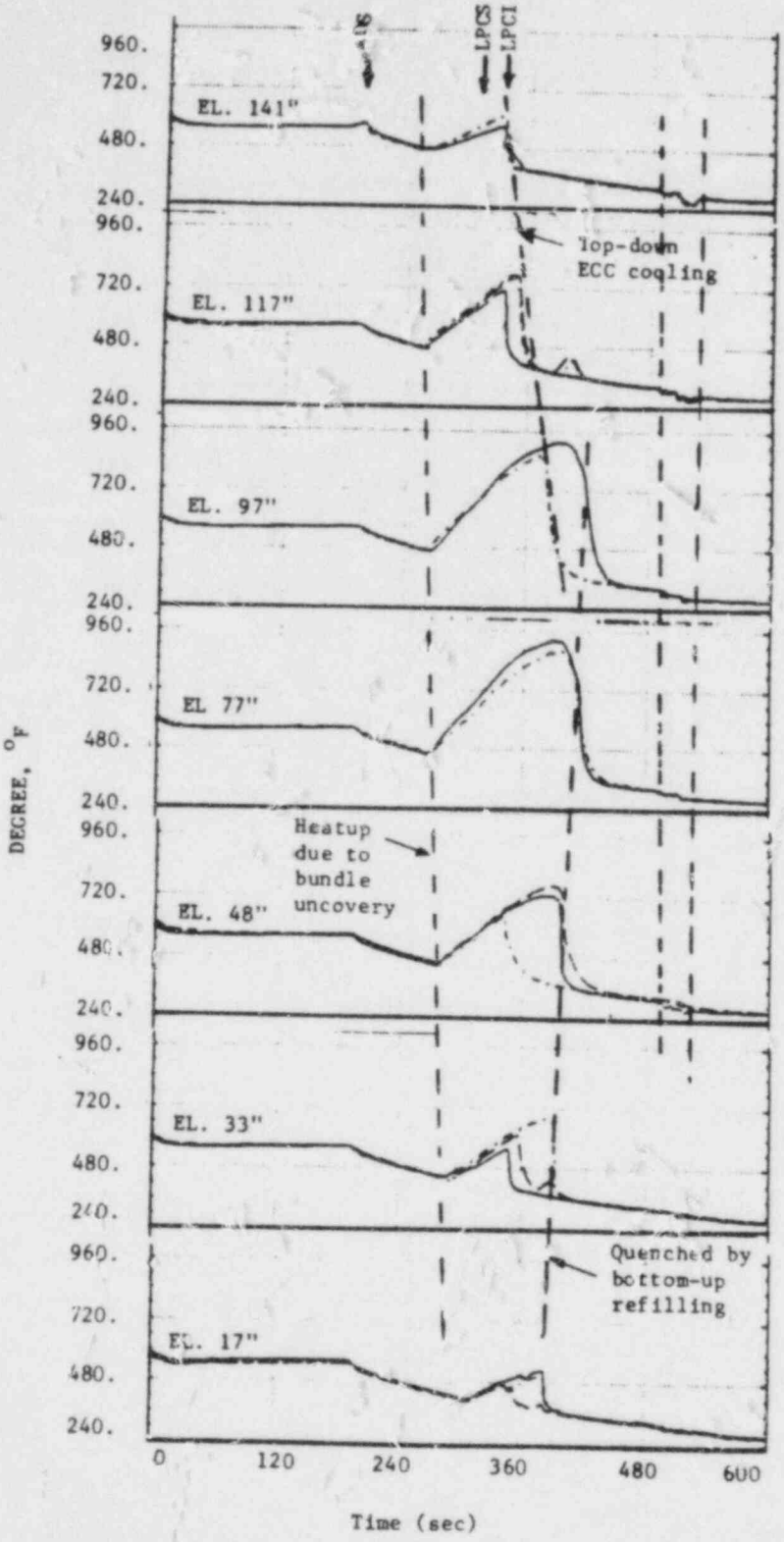

Figure 7.2-14. Rod Temperature, Test 6SB2C

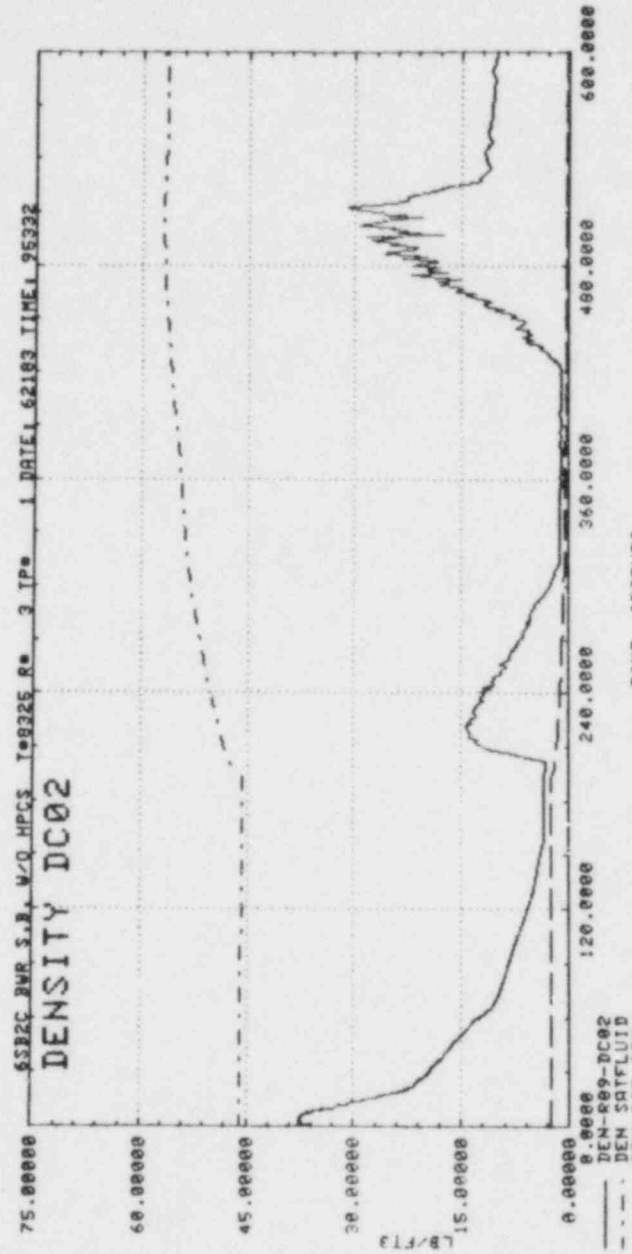

Figure 7.2-15. Regional Density of Downcomer Above Top of Jet Pump

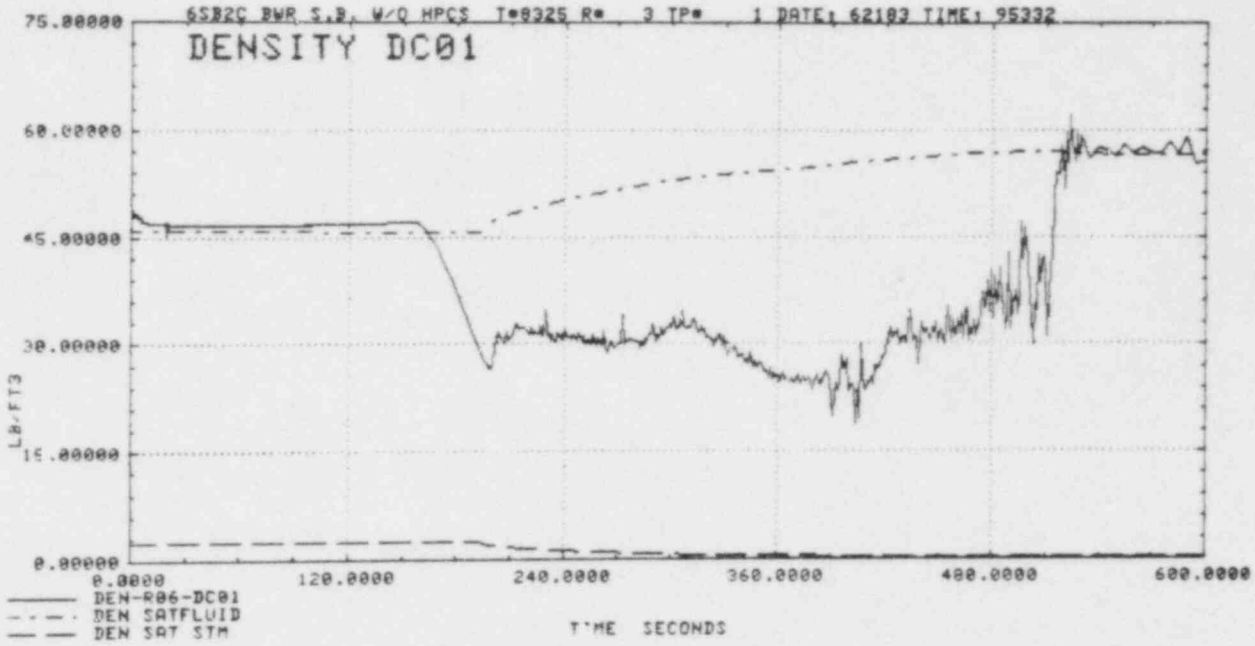

Figure 7.2-16. Regional Density of Downcomer Below Top of Jet Pump

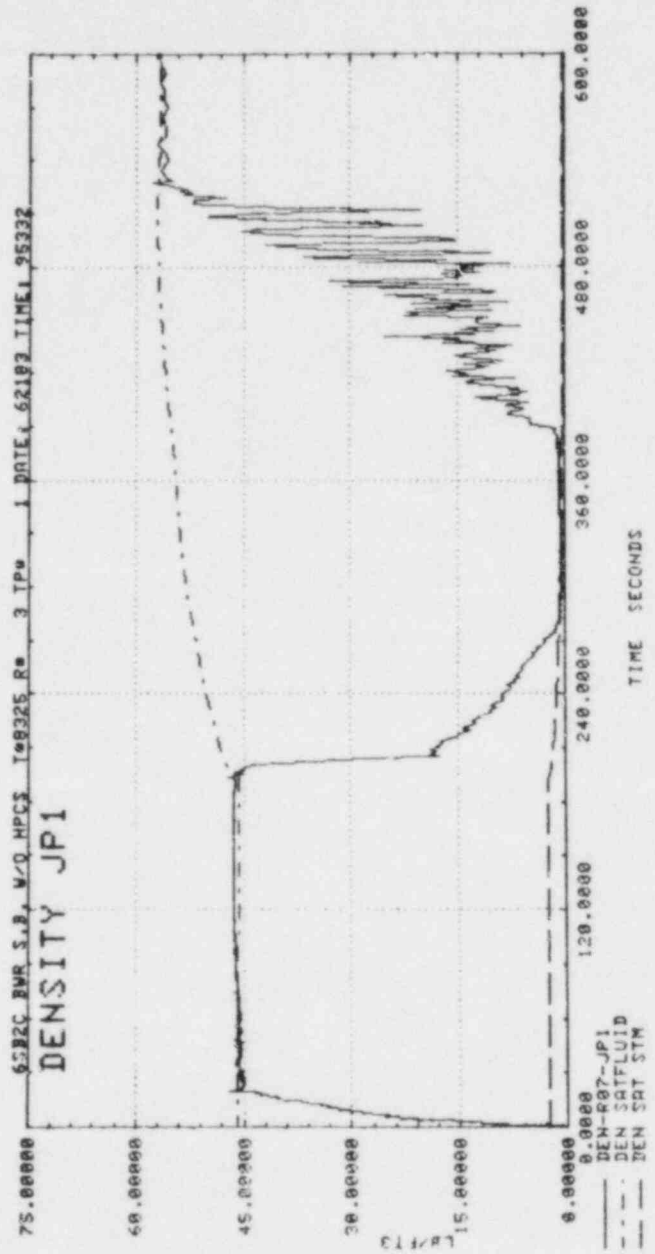

Figure 7.2-17. Regional Density of Intact Loop Jet Pump

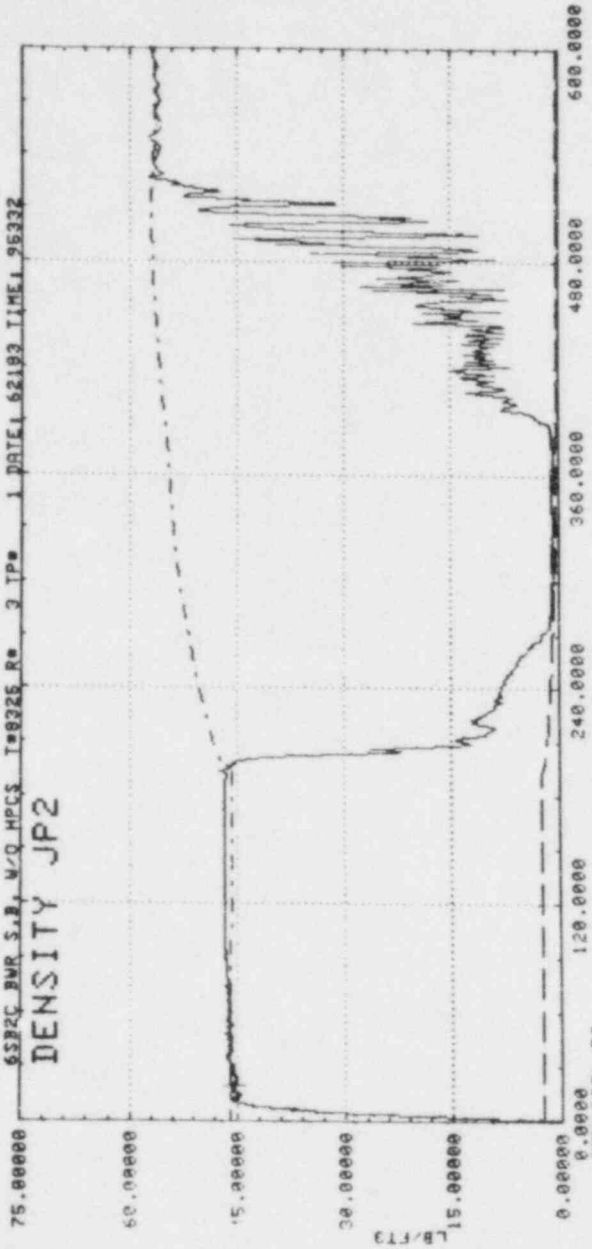

Figure 7.2-18. Regional Density of Broken Loop Jet Pump

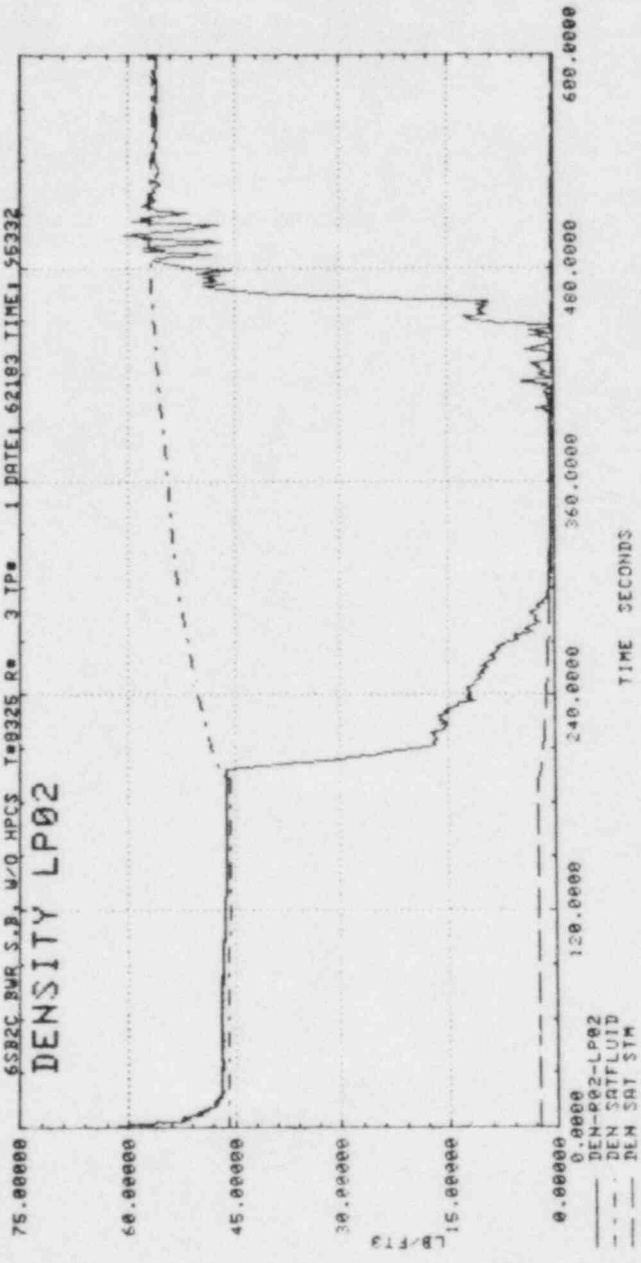

Figure 7.2-19. Regional Density of Lower Plenum Above Jet Pump Exit Plane

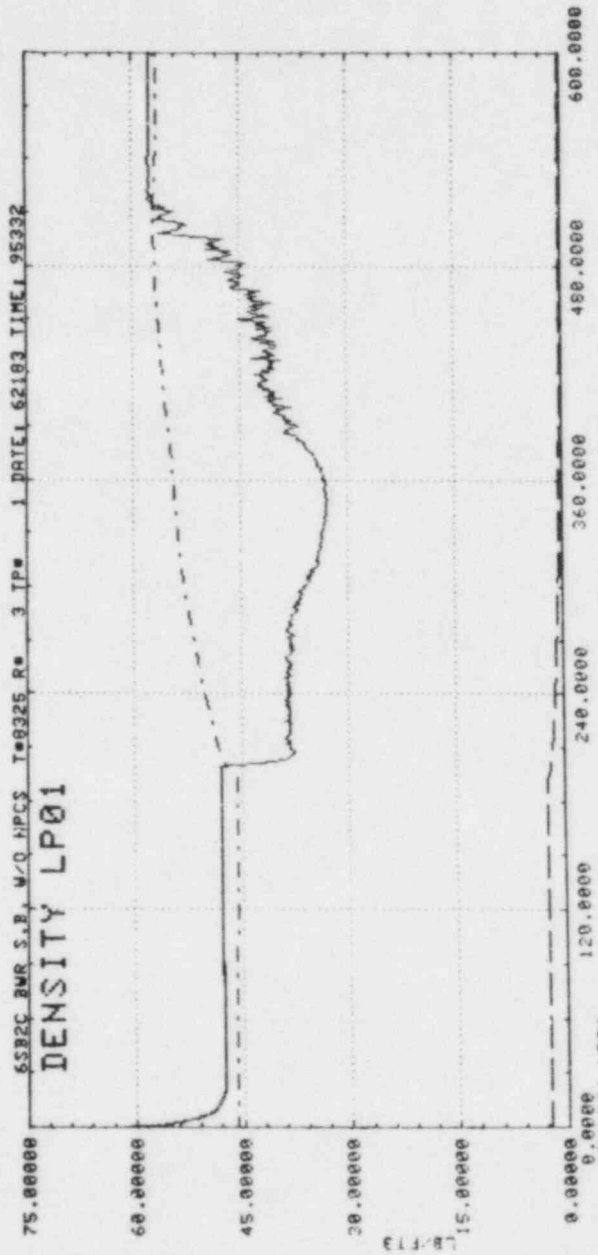

Figure 7.2-20. Regional Density of Lower Plenum Below Jet Pump Exit Plane

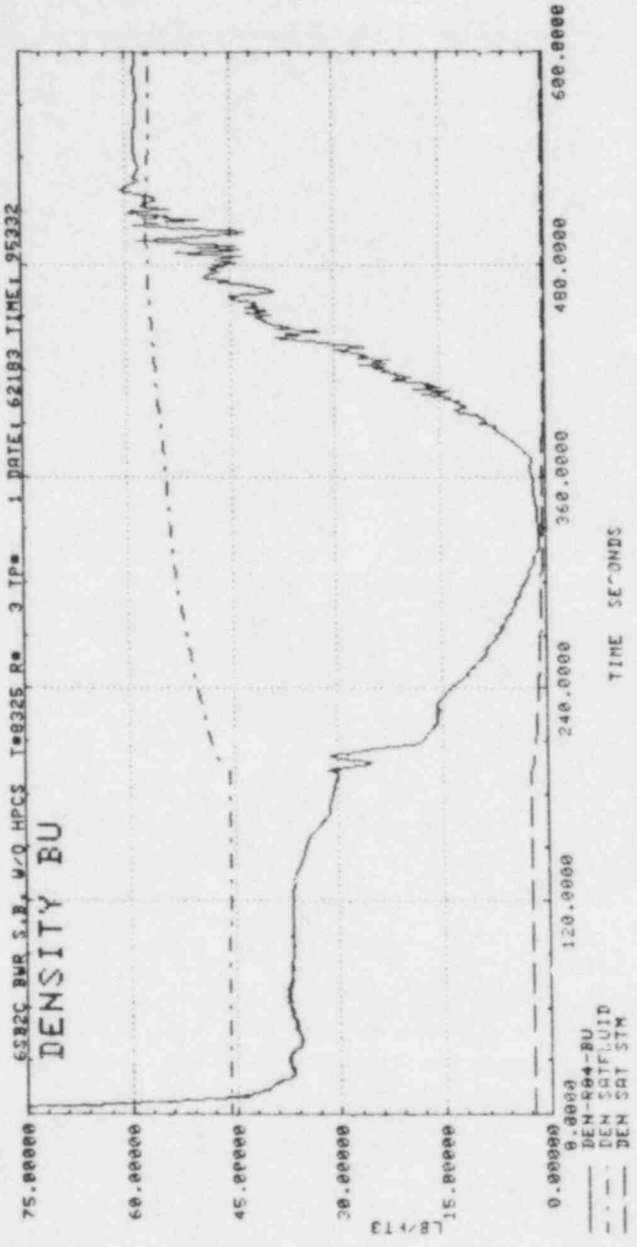

Figure 7.2-21. Regional Density of Bundle

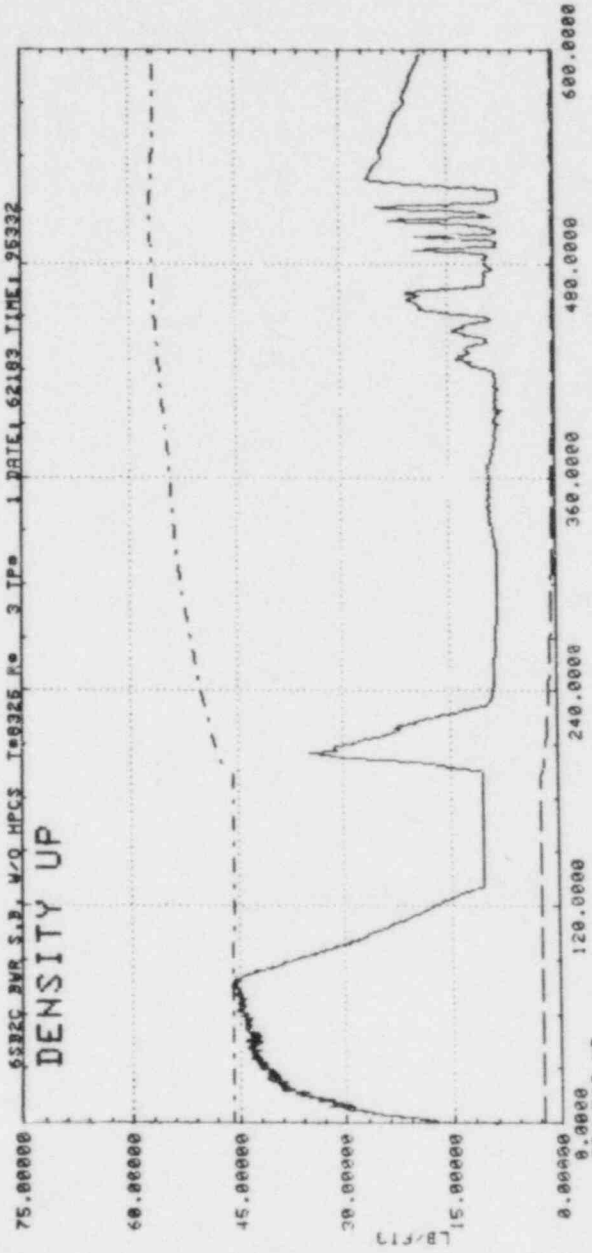

Figure 7.2-22. Regional Density of Upper Plenum

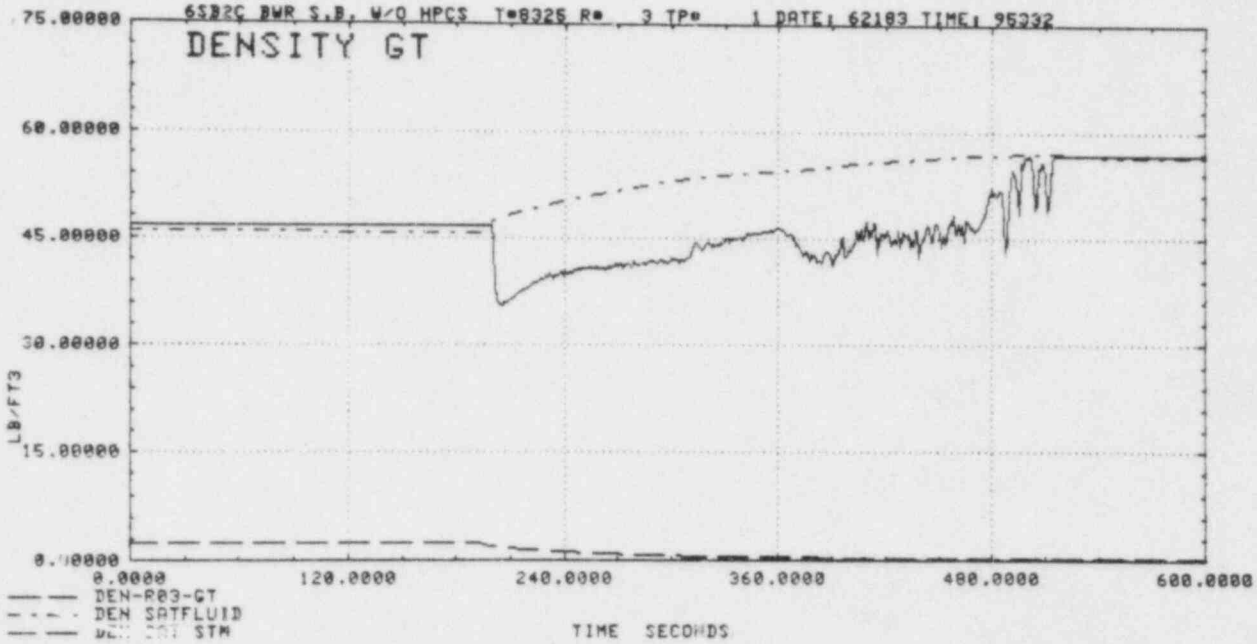

Figure 7.2-23. Regional Density of Guide Tube

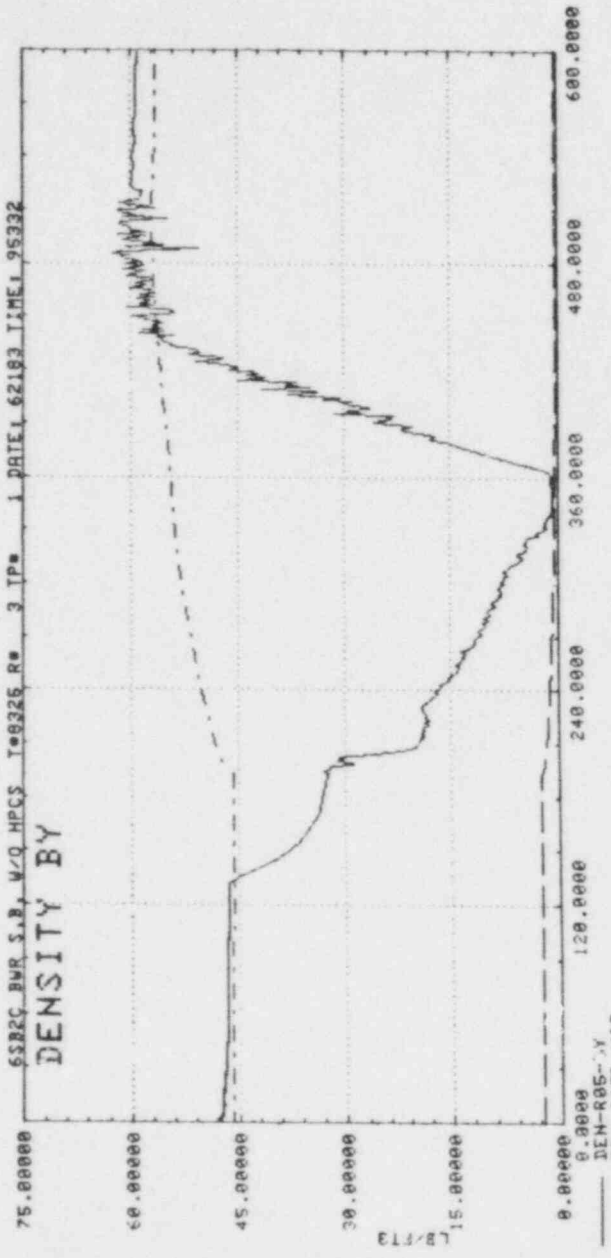

Figure 7.2-24. Regional Density of Bypass

7.3 SMALL BREAK WITH STUCK SAFETY RELIEF VALVE TEST, 6SB1

7.3.1 General Description

Test 6SB1 simulates a BWR/6 recirculation line break of 0.05 ft^2 with a stuck open safety relief valve. In addition, similar to test 6SB2C, HPCS is assumed to be unavailable.

Test 6SB1 is performed with a BWR/6 core average power of 4.64 MW. This power is slightly lower than the TLTA tieback test, 6SB2C, which simulates a central average power of 5.05 MW. Consequently, the initial core flow, steamline flow, and feedwater supply of this test are also slightly different from test 6SB2C (Figures 7.3-1 vs 7.2-1). A nominal ADS time delay of 105 seconds, rather than 120 seconds, is used in this test. ECC water temperature is 120°F, 30°F higher than test 6SB2C.

It should be noted that, based on realistic operator guideline calculations for a BWR/6 with 0.05 ft^2 break, the system pressure does not reach the SRV opening setpoint during the period between MSIV closure and ADS activation. Thus, the combination of a stuck open safety relief valve with a 0.05 ft^2 break is not expected in a BWR. However, the current licensing calculation, based on bounding assumptions, indicates that SRV #1 is activated to open at 45 seconds after the MSIV closure. The test 6SB1 is conducted with the SRV#1 activated at 45 seconds after the L1 signal (or the MSIV closure).

7.3.2 Key Events and System Behavior

Key events observed in this test are summarized in Table 7.3-1. Generally, the system performance and governing phenomena of this test are similar to the test 6SB2C which is discussed in detail in section 7.2. Those discussions are not repeated here for this test. Comparisons between these two tests are shown in data plots to demonstrate the similarity of the system behavior.

7.3.3 System Pressure

The system pressure is shown in Figure 7.3-2. The system pressure in the early transient is identical to test 6SB2C. Upon activation of SRV#1, system pressure begins to decrease. The major depressurization occurs at ADS, leading to the ECCS initiations (Figures 7.3-3 and 4). The post ADS pressure response is similar to test 6SB2C. The slightly lower pressure in this test is attributed to an earlier ADS activation (190 vs 195 seconds) and a lower pressure at ADS.

7.3.4 Rod Temperature

Figure 7.3-5 shows the rod temperatures measured at various elevations. Similar to test 6SB2C, the entire bundle experiences rod heatup during the bundle uncovery. The heatup in this test is relatively mild due to the lower power and a PCT of 720^{o}F is measured.

7.3.5 System Mass and Regional Mass

The total system mass and regional mass are shown in Figures 7.3-6 to 16. These plots clearly demonstrate the similarity of the system responses between the two small break tests. The earlier refill and reflood in test 6SB1 for various regions are due to the earlier ECC initiations (Figures 7.2-3 and 4).

7.3.6 Summary (Test 6SB1)

System responses of the small break test with a stuck relief value, 6SB1, are found to be very similar to the test 6SB2C. The activation of S/RV #1 has small effect on the system performance. Key phenomena such as CCFL at various locations and uncovery/recovery of the bundle observed in the test 6SB2C are also seen in this test. A PCT of 720^{o}F was measured.

Table 7.3-1

KEY EVENTS, TEST 6SB1

		Time (Sec)
o	Break Initiation	0
o	Bundle Power Trip	0
o	Feedwater Trip	0
o	Recirculation Pump Trip	0
o	Recirculation Loop Isolation	20
o	Level 1 Reached	85
o	MSIV Closure	87
o	SRV #1 Opens	130
o	ADS Opens	190
o	LPCS Begins	290
o	LPCI Begins	320
o	Jet Pump Exit Uncovered/Recovered	230/360
o	Lower Plenum Refill Completed	450
o	Bypass Refill Begins/Completed	350/380
o	Bundle Reflood Begins/Completed	355/420
o	End of Test (Power Off)	485

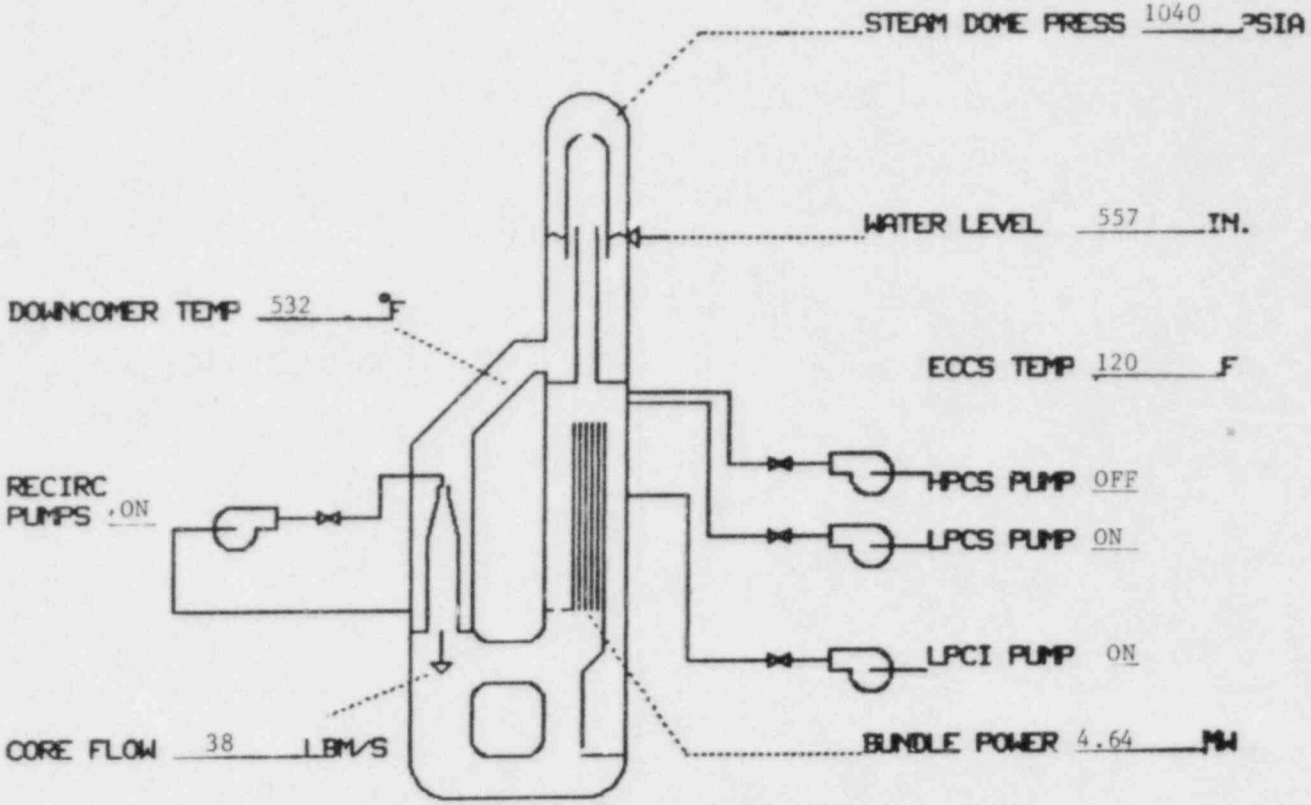

Figure 7.3-1. Initial Conditions - Test 6SB1

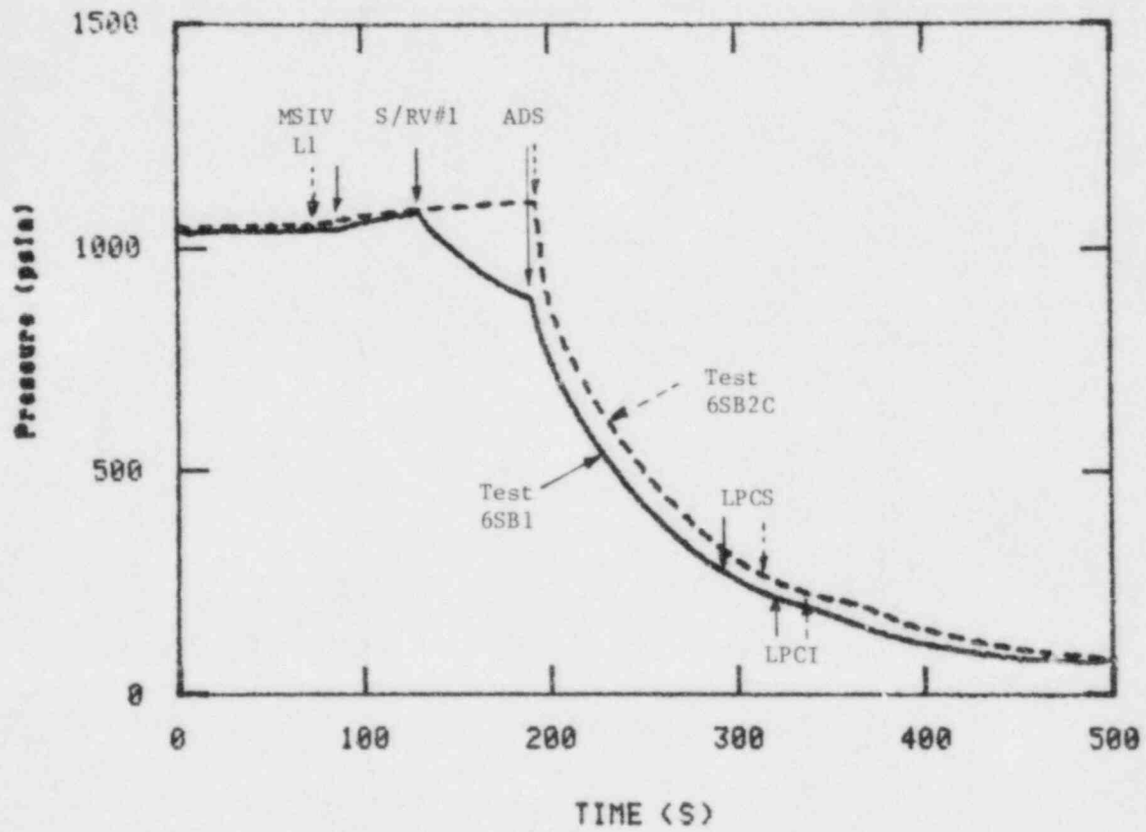

Figure 7.3-2. System Pressure

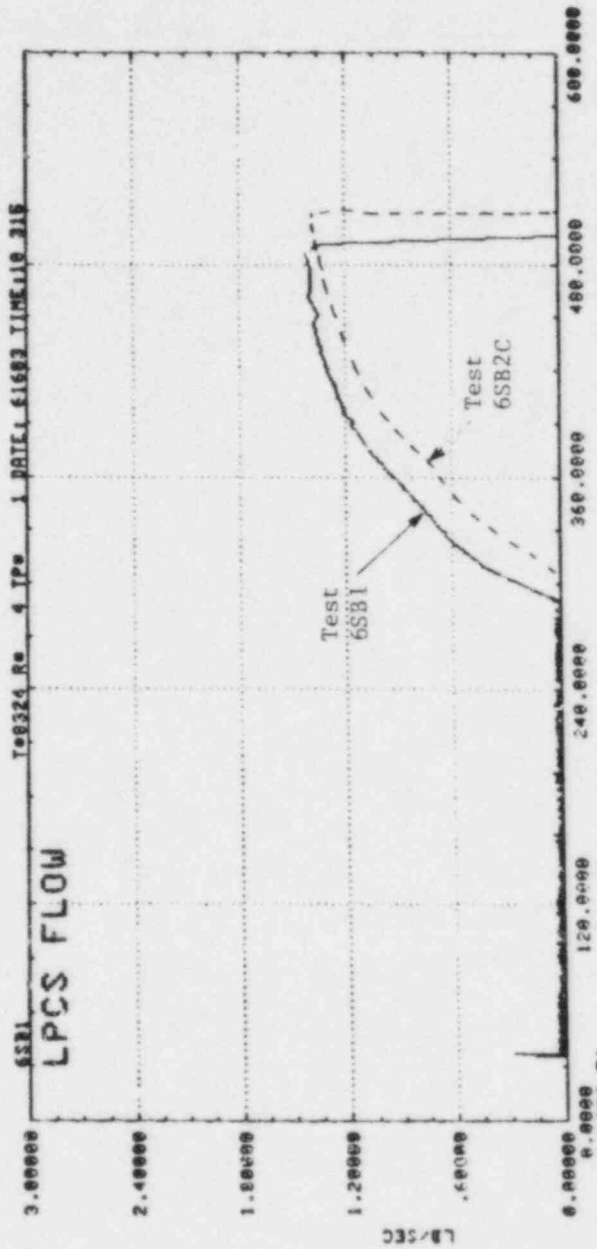

Figure 7.3-3. LPCS Flow

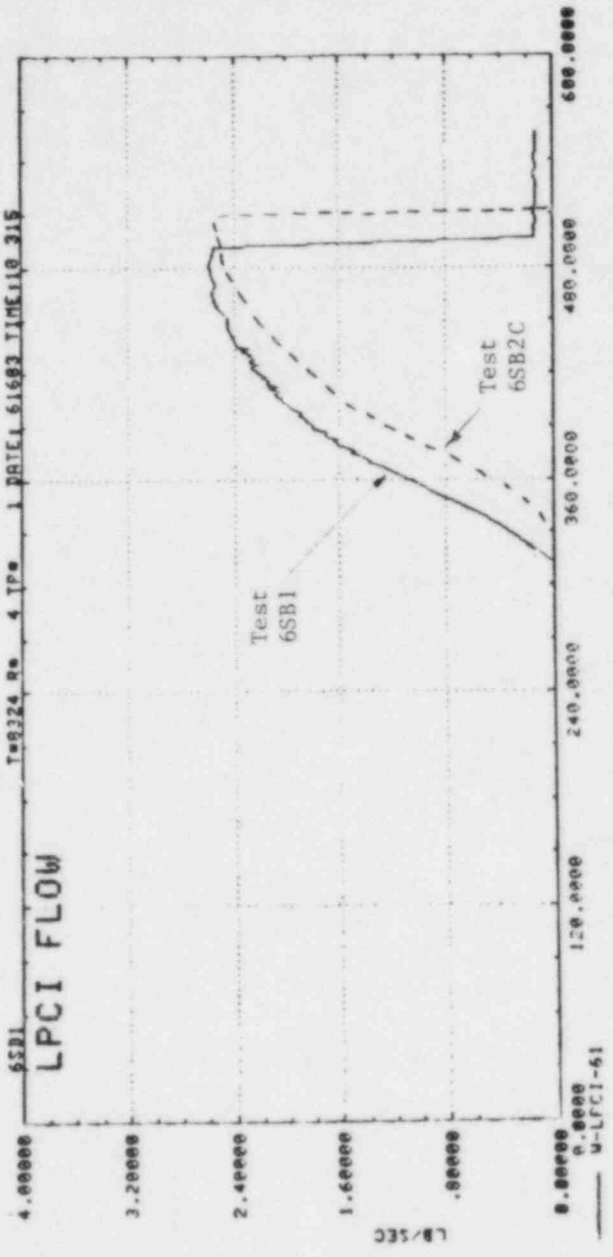

Figure 7.3-4. LPCI Flow

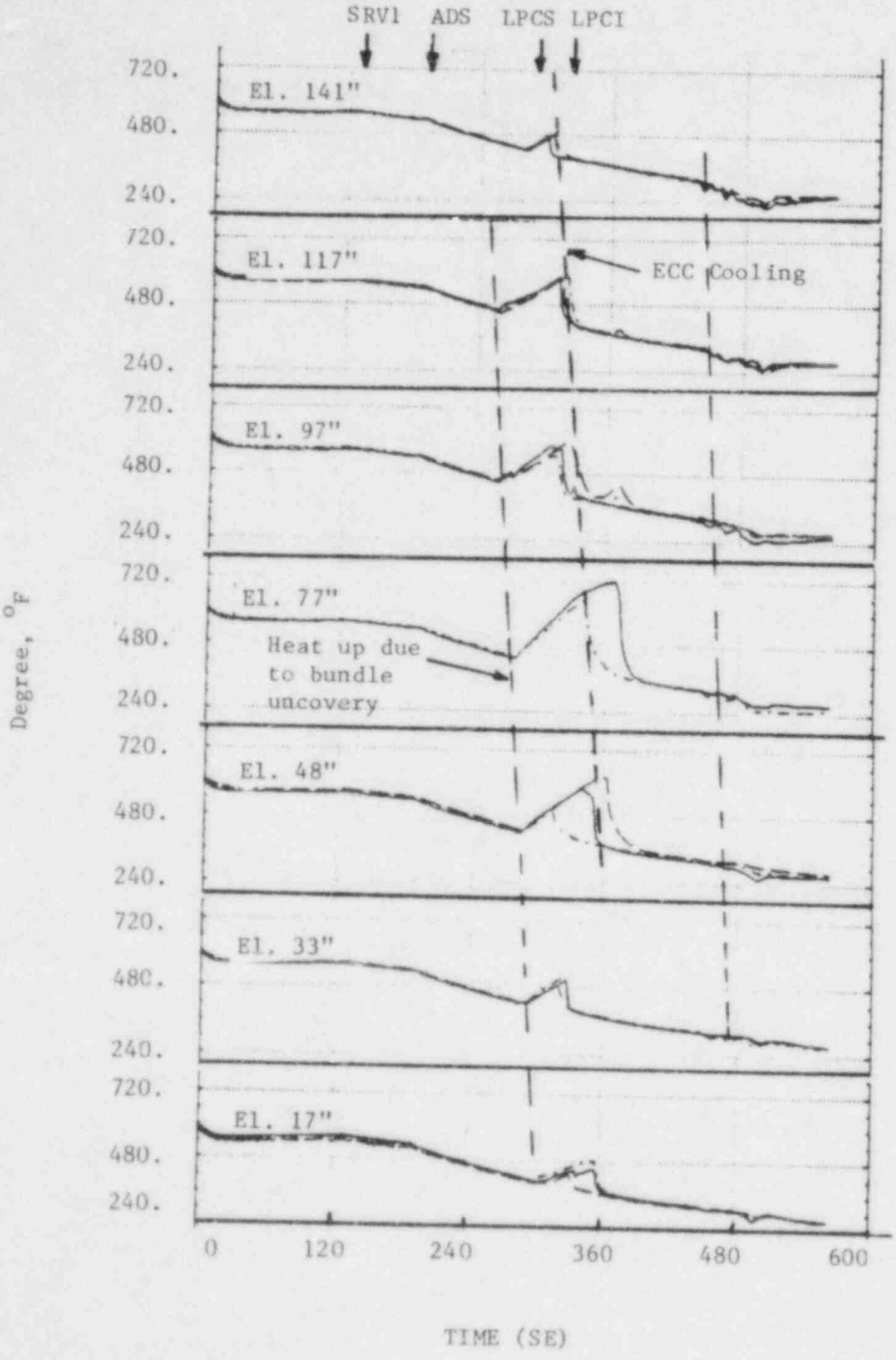

Figure 7.3-5. Rod Temperature, Test 6SB1

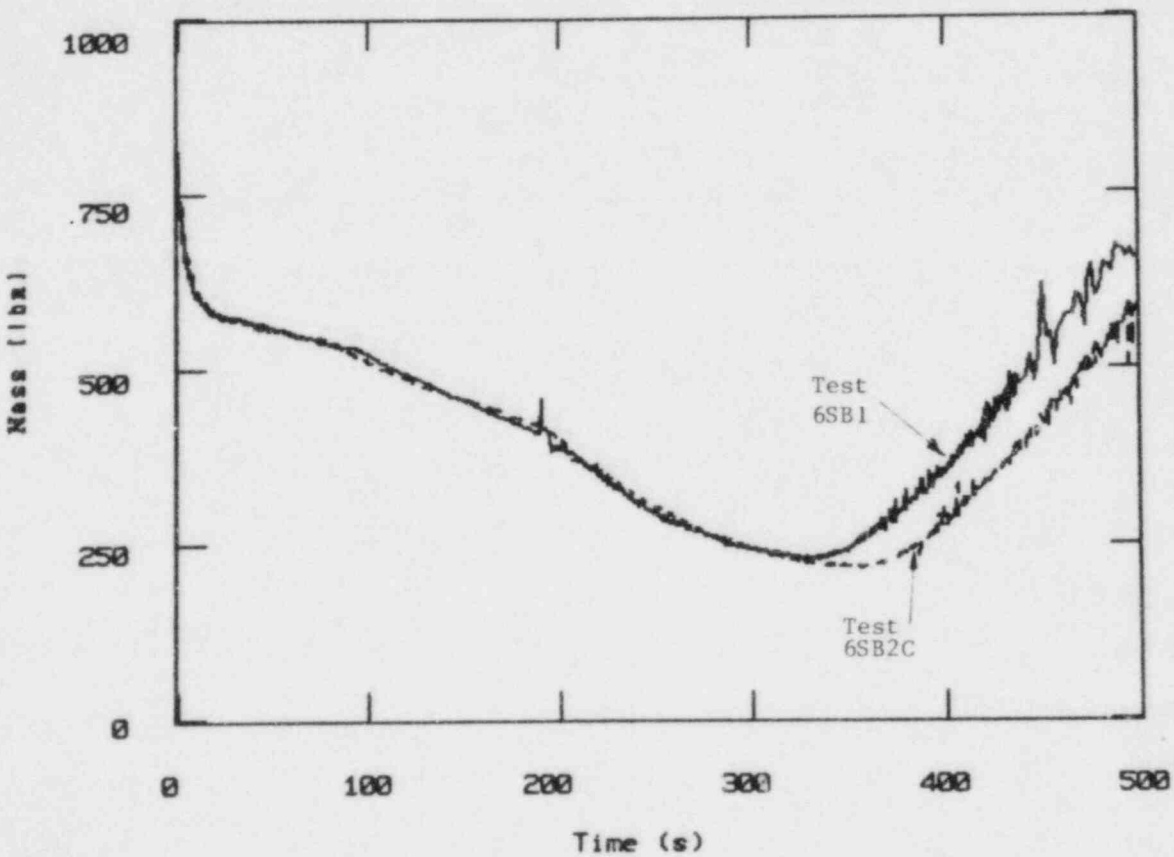

Figure 7.3-6. System Total Mass

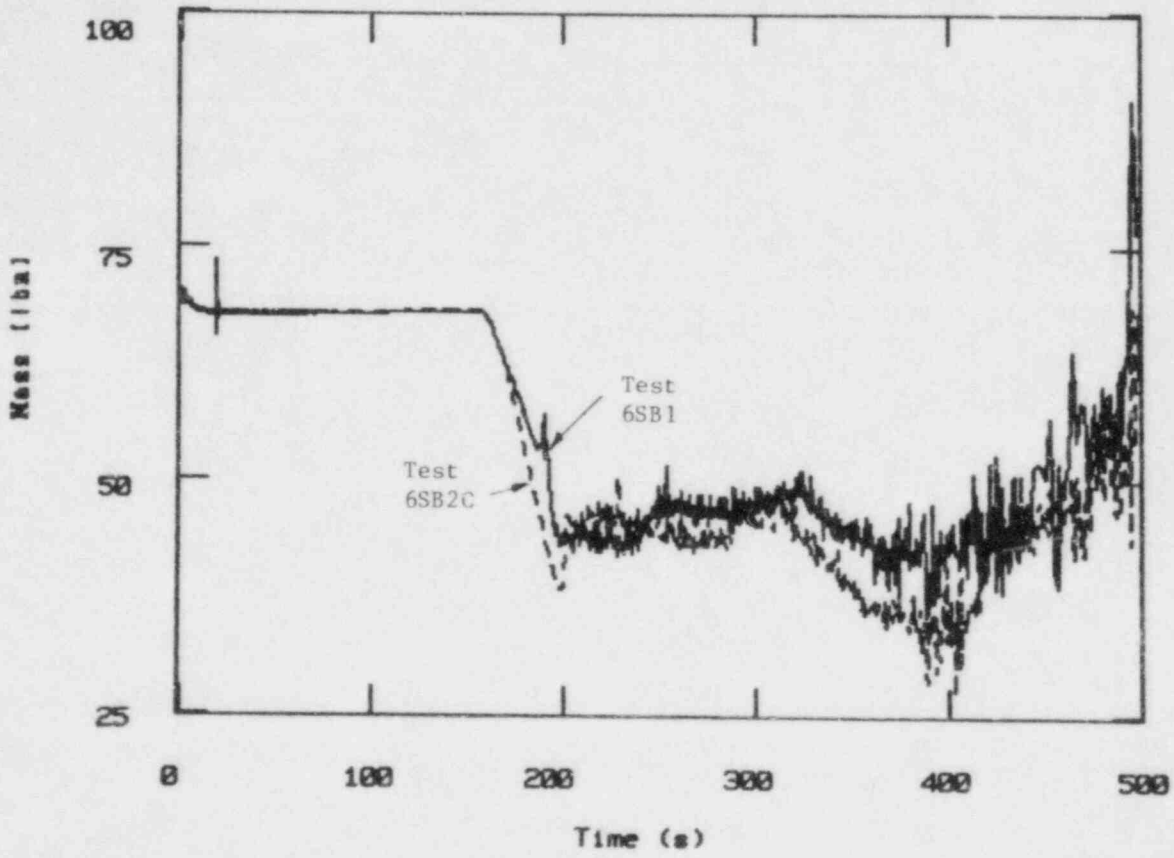

Figure 7.3-7. Mass of Downcomer Below Top of Jet Pump

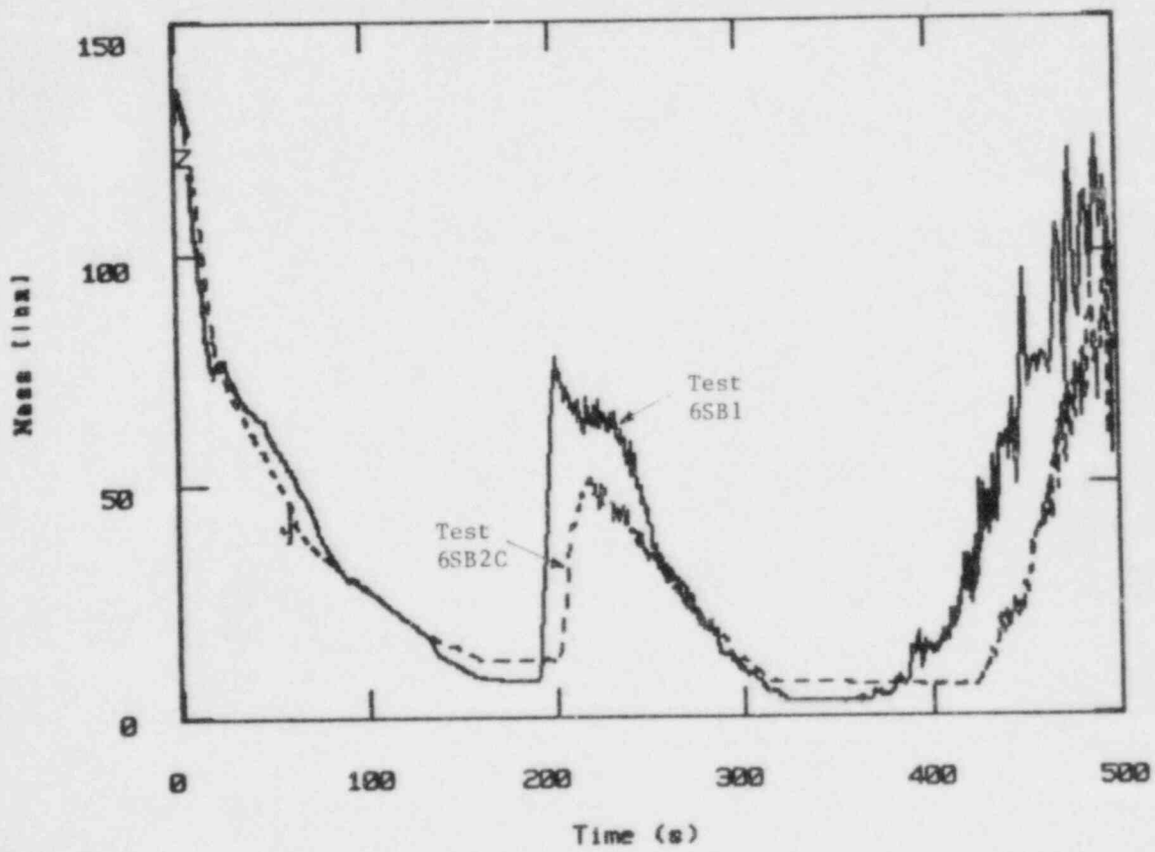

Figure 7.3-8. Mass of Downcomer Above Top of Jet Pump

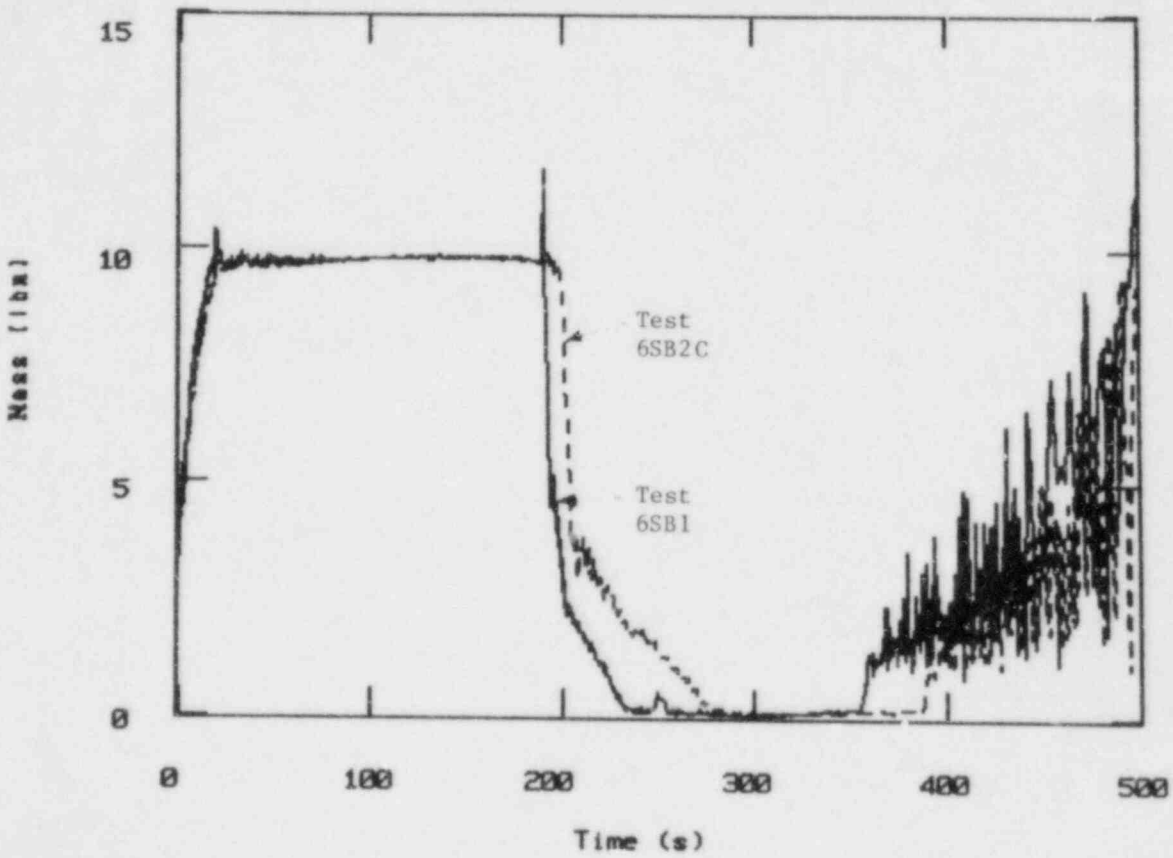

Figure 7.3-9. Intact Loop Jet Pump Mass

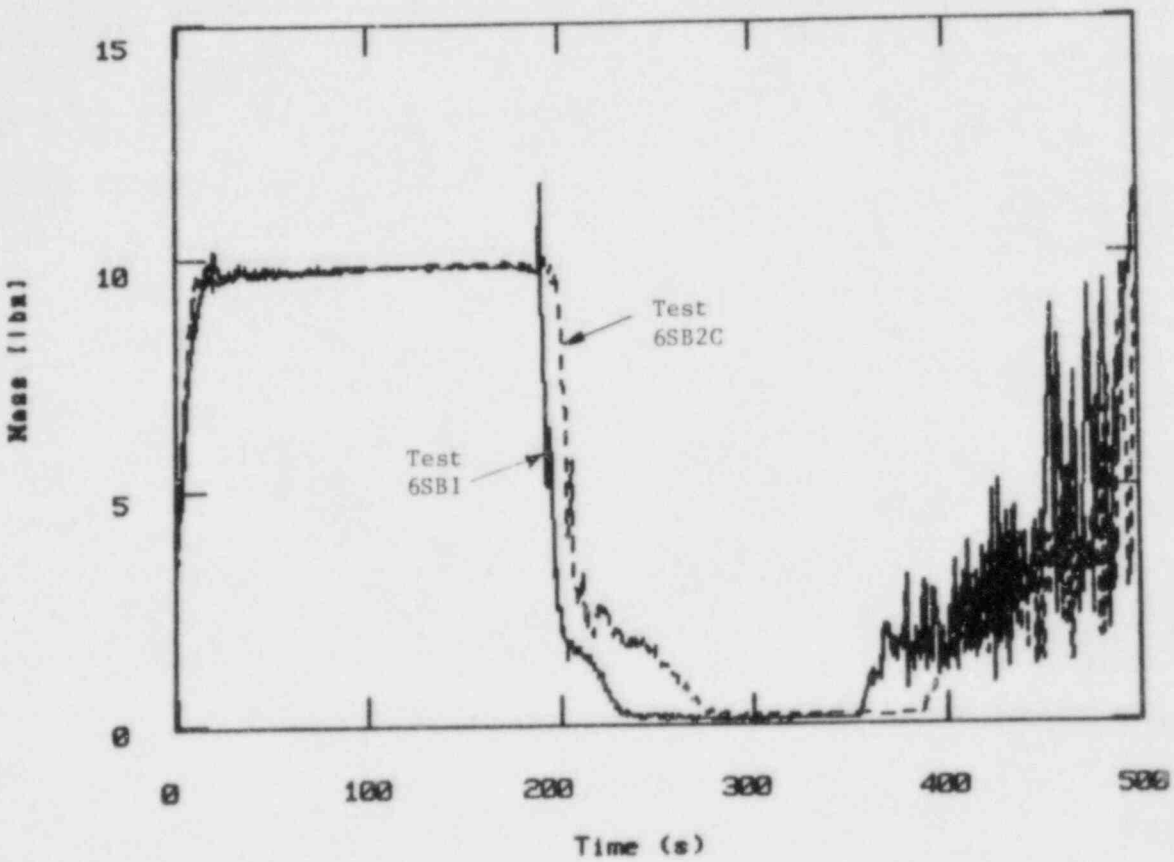

Figure 7.3-10. Broken Loop Jet Pump Mass

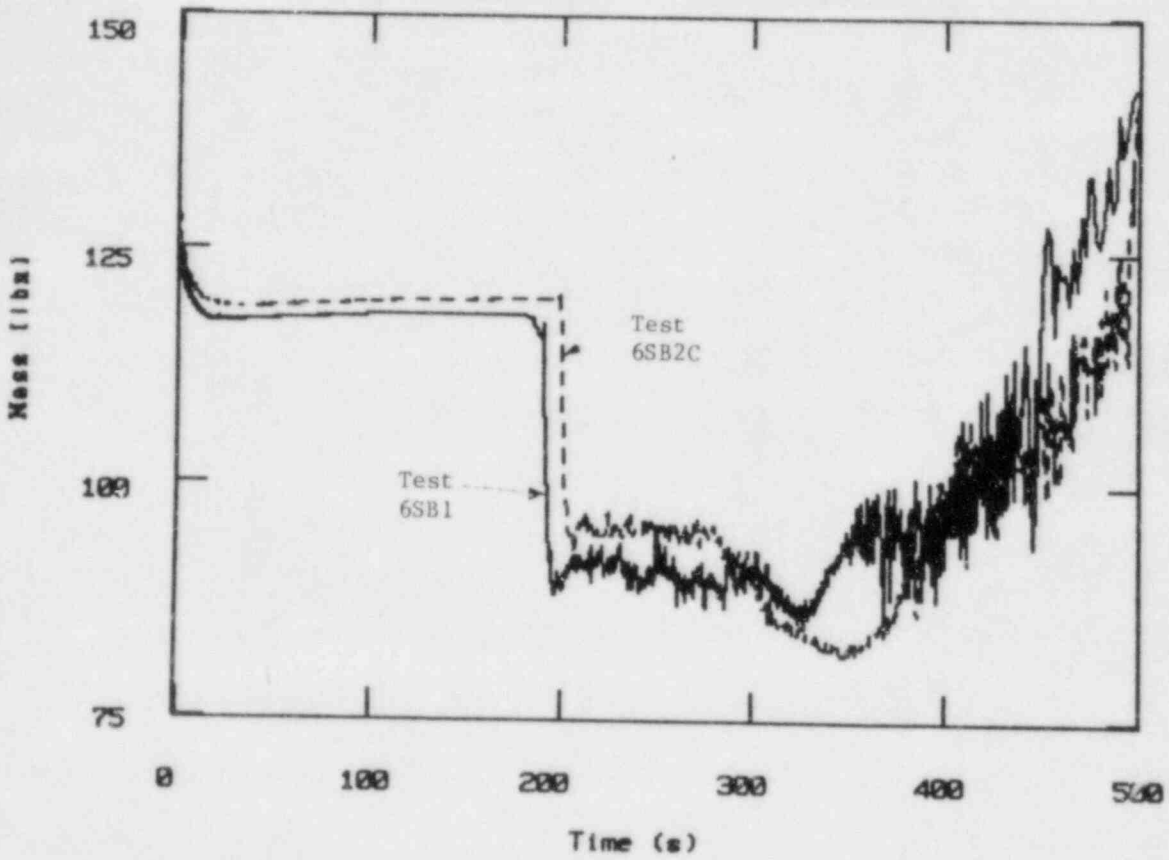

Figure 7.3-11. Mass of Lower Plenum Below Jet Pump Exit Plane

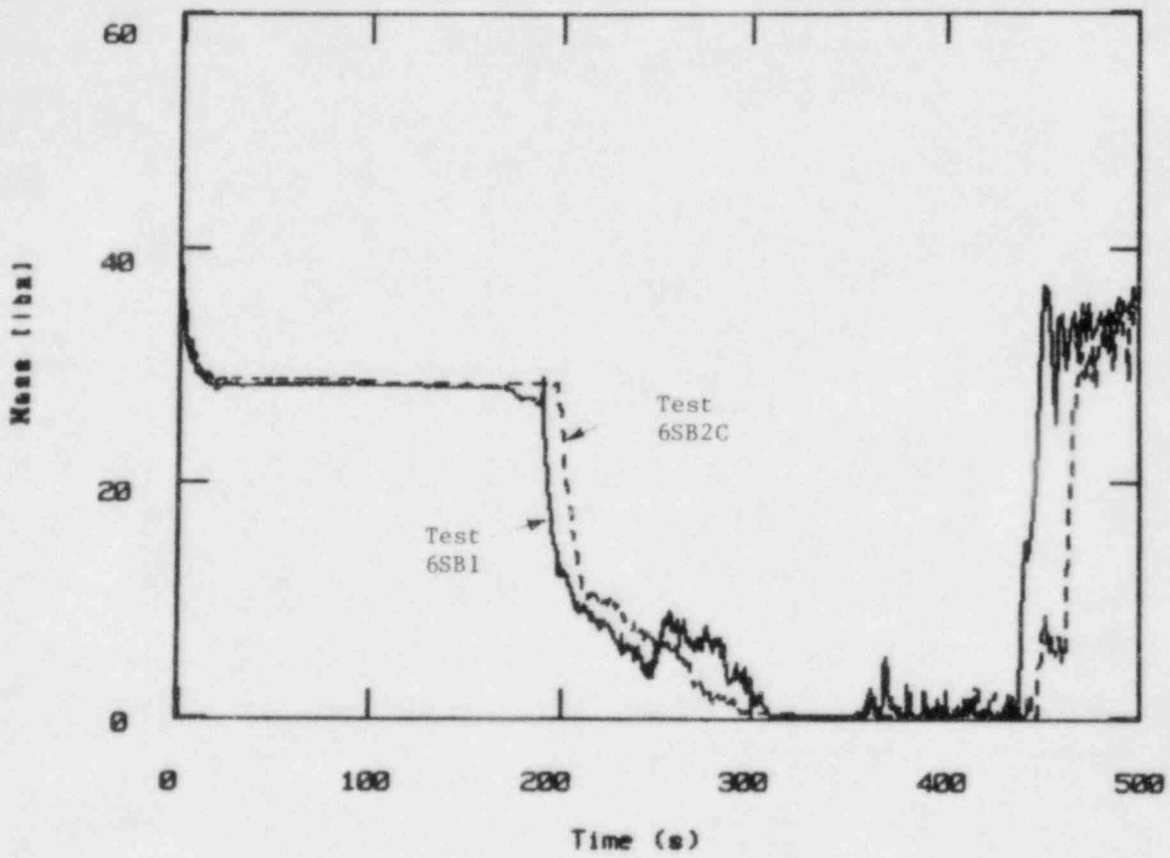

Figure 7.3-12. Mass of Lower Plenum Above Jet Pump Exit Plane

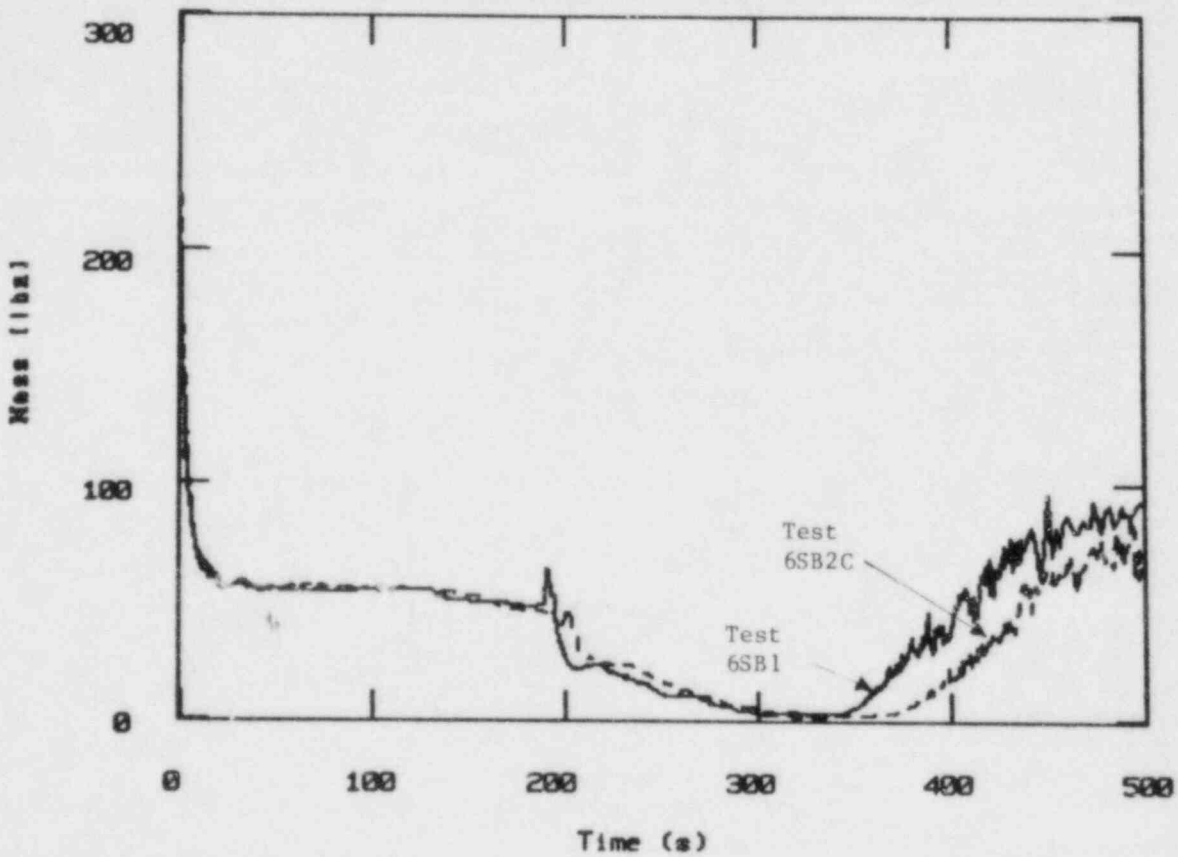

Figure 7.3-13. Bundle Mass

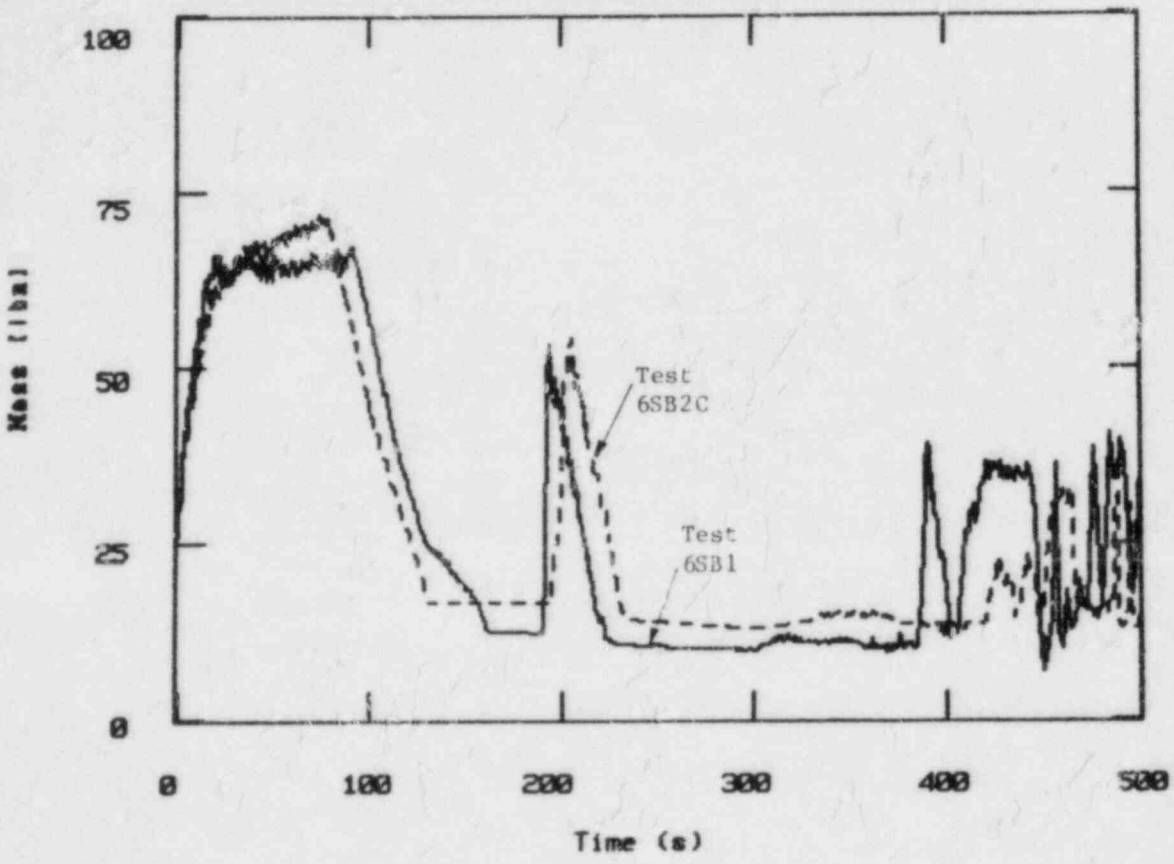

Figure 7.3-14. Upper Plenum Mass

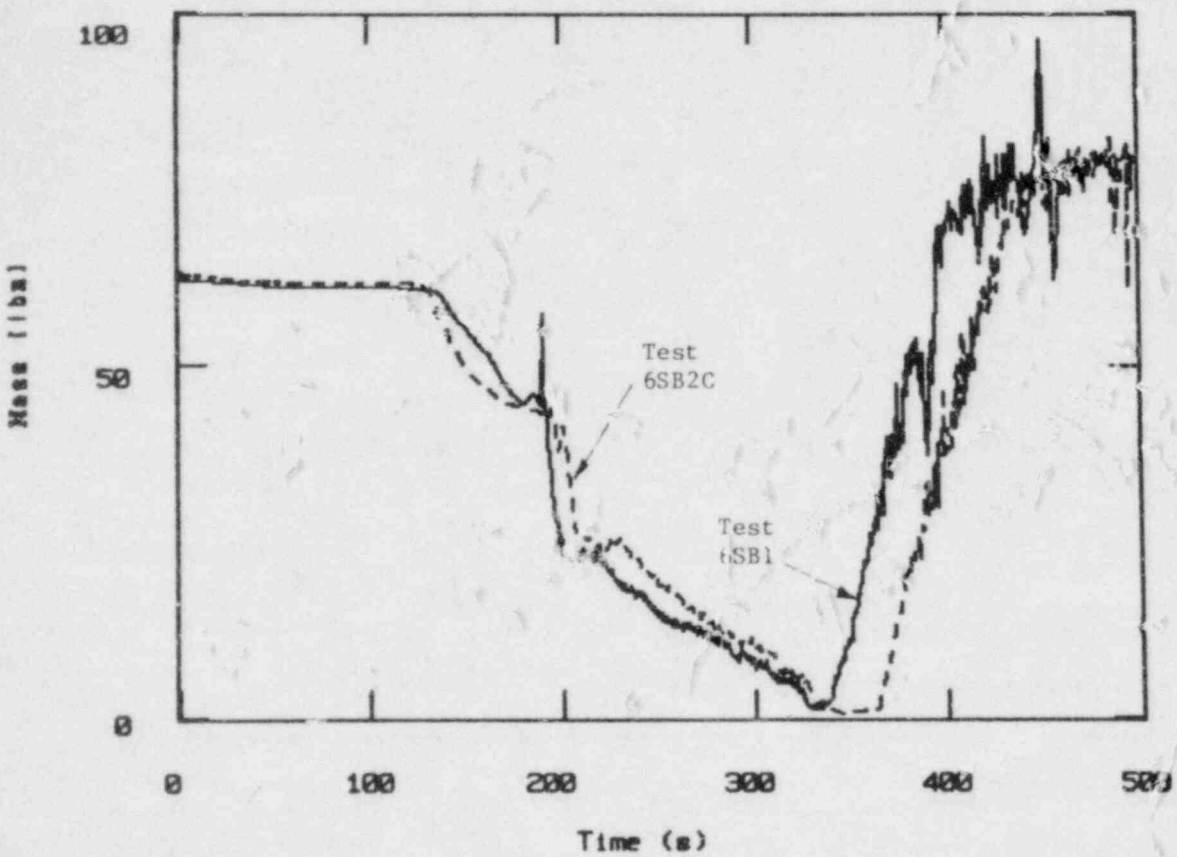

Figure 7.3-15. Bypass Mass

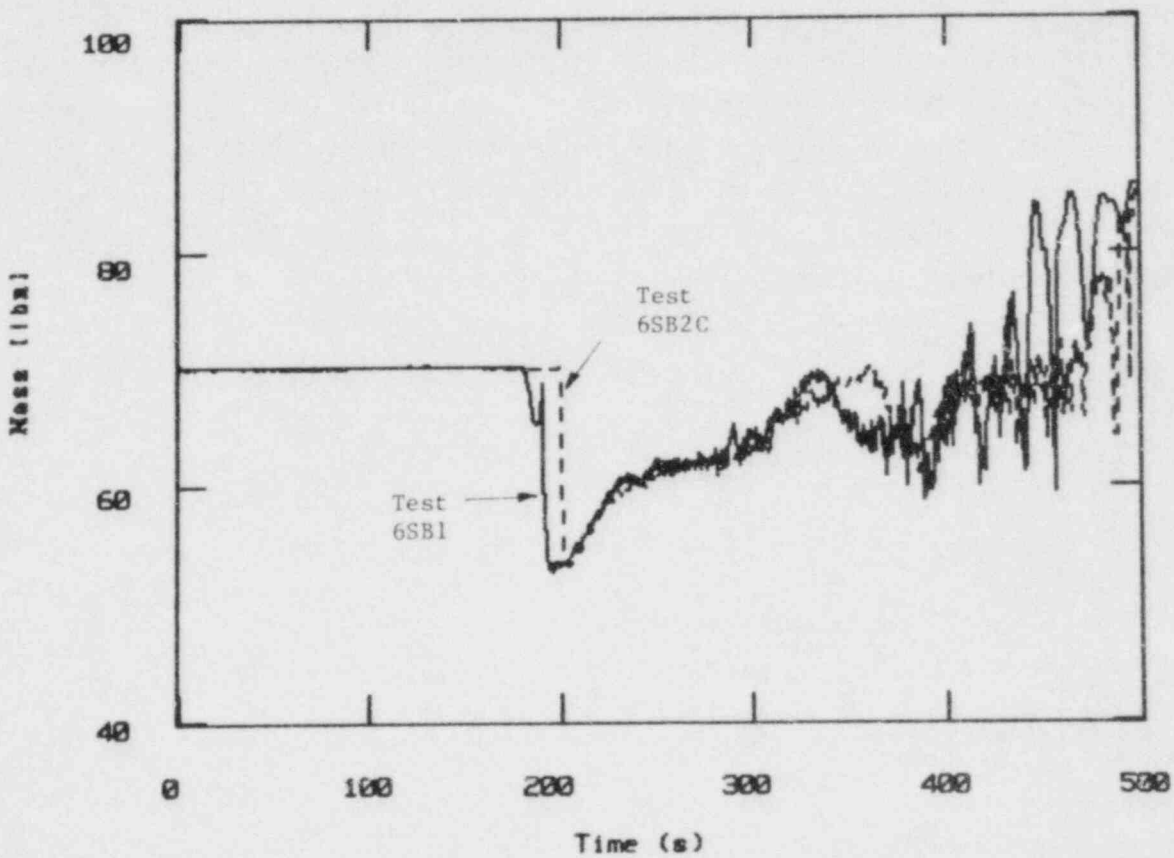

Figure 7.3-16. Guide Tube Mass

7.4 MAIN STEAMLINE BREAK TEST 6MSB1

7.4.1 General Description

The main steamline break test 6MSB1 simulates a BWR/6 response with a double ended break upstream of the flow limiter in one of the four main steamlines.

7.4.2 Break Simulation

Figure 7.4-1 illustrates the steamline control response in a BWR under the break condition. The turbine is isolated almost immediately (0.1 sec) upon the break initiation. The effective break area consists of one main steamline flow area and one steam line flow limiter, due to back flow via the bypass header. The turbine bypass opens at about 1 second and the effective break flow area at this time also includes the bypass line area. By about 5.5 seconds, the main steam isolation valve is closed and the break is limited to one main steamline. For simplifying the test operation, and having a bounding simulation, the test was performed with full turbine bypass flow area from 0 to 5.5 seconds and one steamline flow area beyond 5.5 seconds.

7.4.2 Key Events and System Pressure

Table 7.4-1 lists timings of key events observed in this test. The system pressure (Figure 7.4-2) drops very rapidly upon break initiation, due to a large steam discharge through the break (Figure 7.4-3). The depressurization rate is reduced as the break changes to a smaller size at 5.5 seconds. HPCS injection begins at 27 seconds and LPCS and LPCI at 88 and 95 seconds, respectively.

7.4.4 Water Level and Governing Phenomena

Mixture levels observed in various regions are shown in Figures 7.4-4 and 5. Void distribution derived from nodal ΔP's in the bundle

and upper plenum is also shown in Figure 7.4-5. These plots plus "snap shot" views of the system conditions (Figures 7.4-6 to 10) are used to discuss the system performance.

A major result of fast depressurization upon the break initiation is that water in various regions begins to flash into steam and the water level swells up very rapidly. Two phase mixture level in the downcomer reaches and covers the steamline inlet at about six seconds (Figures 7.4-4 and 6).

As the initial flashing surge begins to subside, two phase mixture levels are formed in the upper and lower downcomer regions (Figures 7.4-4 and 7). This is attributed to the large steam generation rate and the FIST configuration in these regions. The strong steam upflow leads to CCFL at locations with small flow areas such as the top of the jet pumps and top of the dryer skirt. In addition, the elbow shape connection of the FIST side-arm downcomer vessel to the main vessel and strong steam upflow retards fluid in the upper downcomer from draining into the lower region (Figures 7.4-7 to 9). The steamline inlet is uncovered at about 80 seconds. Following LPCS and LPCI injection the system begins to accumulate inventory and the water level in the downcomer begins to recover.

After the early flashing surge, a mixture level begins to form in the lower plenum (Figure 7.4-5). The mixture level drops below the jet pump exit at about 70 seconds and begins to recover after ECCS injection.

CCFL at the SEO limits the core drainage into the lower plenum; hence, and the core remains covered throughout the entire transient. The void fraction distribution, shown in Figure 7.4-5, provides insight into the thermal hydraulic performance in these regions during the transient. A relatively uniform distribution of void fraction throughout the bundle, due to the flashing surge, is seen in the early period of the transient. As the flashing surge subsides, a stratified void distribution is observed in the bundle.

Although HPCS begins to inject water into the upper plenum at 27 seconds, the void fraction in the upper plenum remains relatively high for a long period of the transient. This indicates that HPCS flow does not condense all steam upflow coming from the core and cold HPCS water does not penetrate into the lower regions. During this period, the void fraction in the bundle continues to increase due to boil off.

Two phase mixture in the upper plenum becomes single phase saturated water immediately following the LPCS and LPCI injections at about 90 seconds. In this period of the transient the middle of the bundle has a high void fraction. However, the rods are well cooled and no heatup is seen in the bundle (Figures 7.4-11 and 12).

Continuous injection of subcooled ECC water eventually leads to the upper plenum water becoming subcooled. The subcooled water reaches the upper tieplate and results in a CCFL breakdown at that location at 150 seconds. Water drains into the bundle filling it with single phase saturated water, with CCFL at the SEO holding the water in the bundle.

The water level rise in the lower plenum after 160 seconds is due to the drainage at the SEO which, in turn, allows subcooled water in the upper region to flow into the bundle. Most of the bundle is subcooled beyond 180 seconds. A subcooled CCFL breakdown at the SEO occurs at about 200 seconds which leads to a complete refill of the lower plenum. A water level is seen in the upper plenum during the later transient of the refill/reflood phase.

7.4.5 System Mass and Regional Mass

Figures 7.4-13 to 25 are plots of the system total mass and regional mass. Similar to the large break test 6DBA1B, fluctuations are seen in the regional mass responses during the reflood period after about 160 seconds. This is again attributed to stored heat in the bypass/guide tube region. The governing phenomena are as discussed in detail in Section 7.1.

7.4.6 Summary (Test 6MSB1)

A summary of key phenomena observed in the steamline break test, 6MSB1, is given below:

(1) Upon the break initiation, water level swells and reaches the steamline elevation. The steamline inlet is uncovered at 80 seconds.

(2) CCFL is observed at various locations such as SEO, top of the dryer skirt and top of the jet pumps.

(3) The bundle is always covered with two phase misture and there is no rod heatup.

(4) The jet pump exit is uncovered and recovered later.

Table 7.4-1
KEY EVENTS, TEST 6MSB1

		Time (Sec)
o	Break Initiation	0
	Break Size Change ($0.00539 \rightarrow 0.00406$ FT^2)	5.5
o	Power Trip	0
o	Feedwater Trip	0
o	Recirculation Pump Trip	0
o	ECCS	
	HPCS	27
	LPCS Activation/Injection	35./88.
	LPCI Activation/Injection	35./95.
o	Steamline Inlet Covered	6
	Steamline Inlet Uncovered	80
o	Jet Pump Exit Uncovered	65
	Jet Pump Exit Recovered	120
o	Lower Plenum Completely Refilled	205
o	End of Test (Power Off)	335

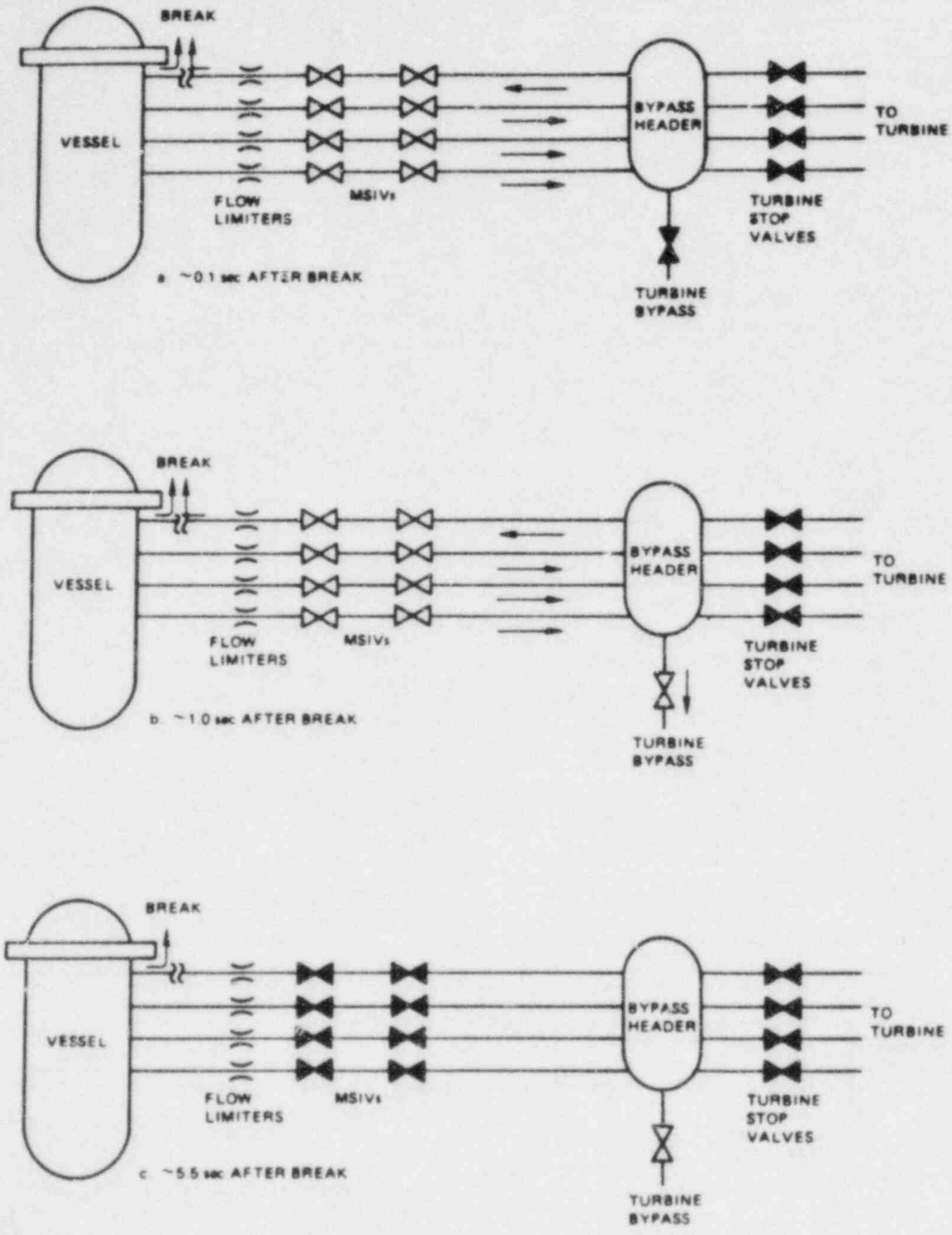

Figure 7.4-1. BWR/6 Main Steam Line Break

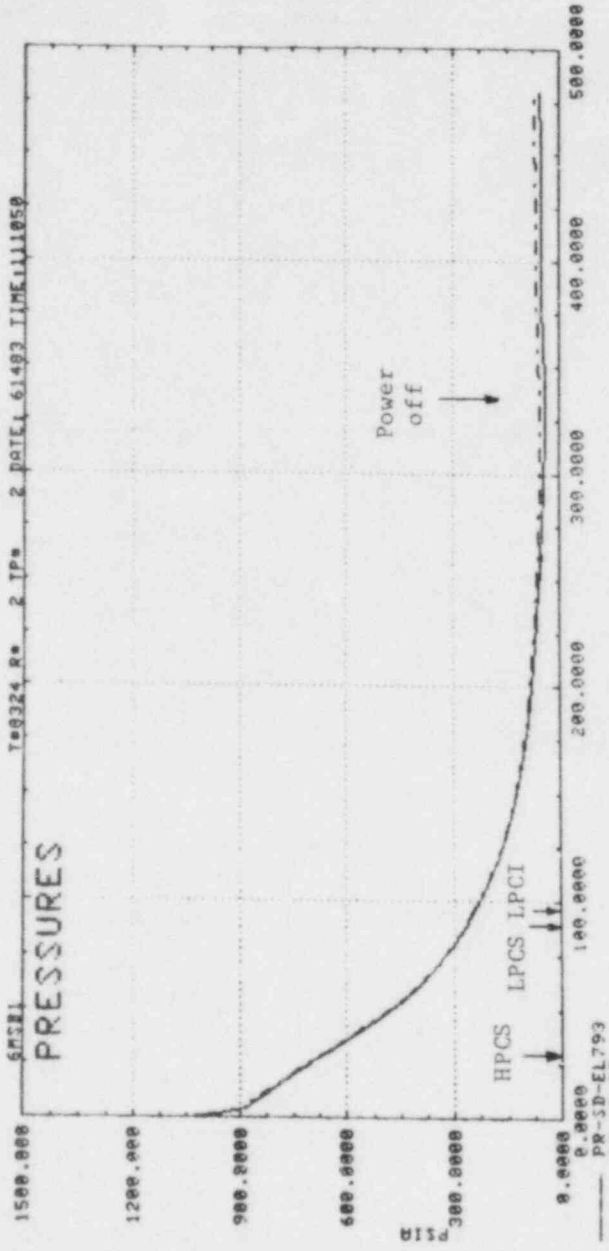

Figure 7.4-2. System Pressure

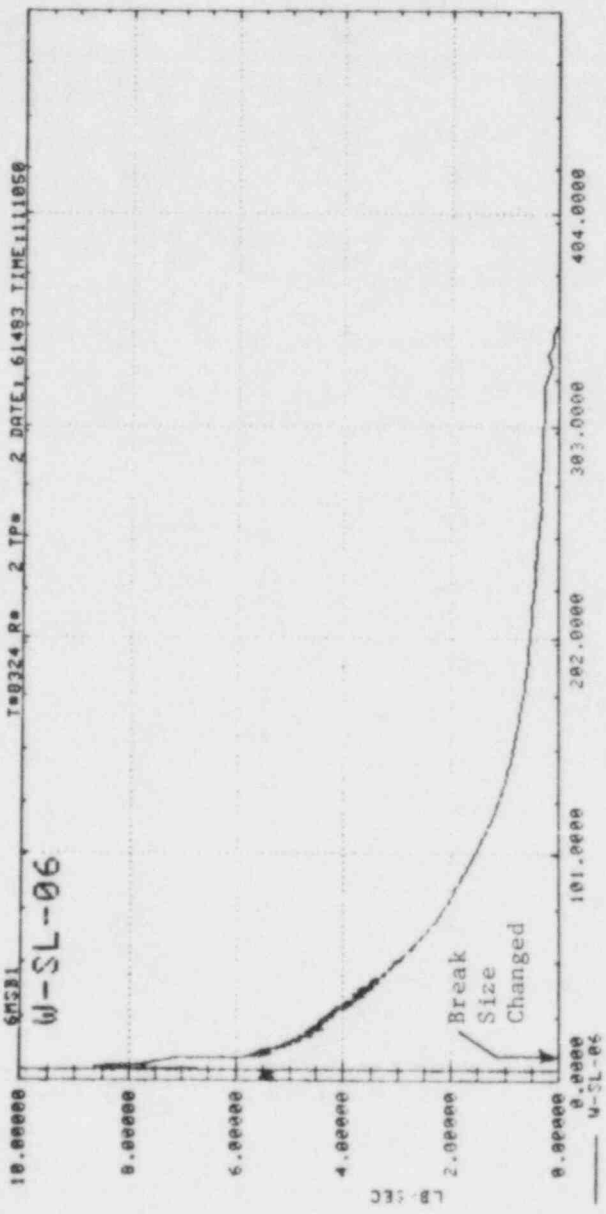

Figure 7.4-3. Steamline Flow

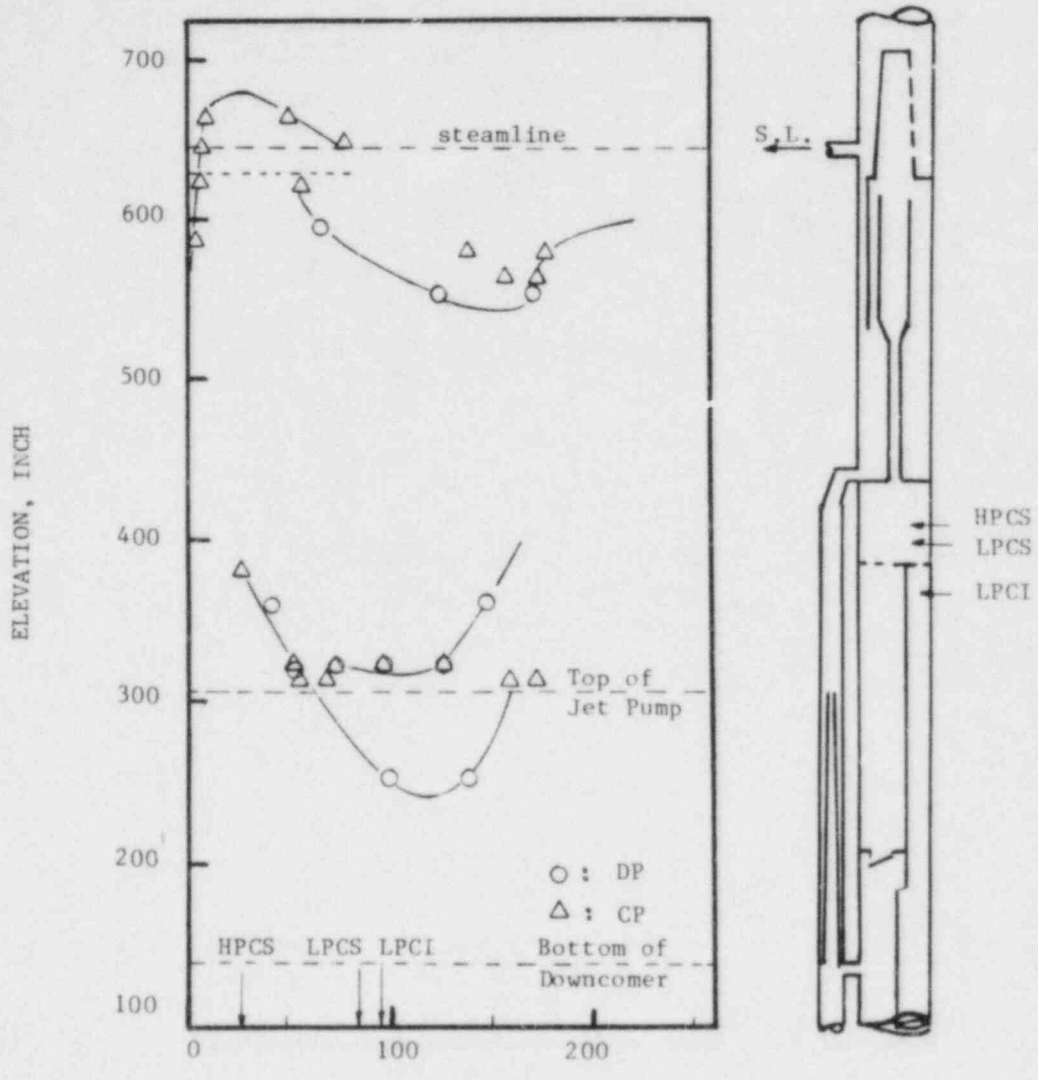

Figure 7.4-4. Downcomer Water Level, Test 6MSB1

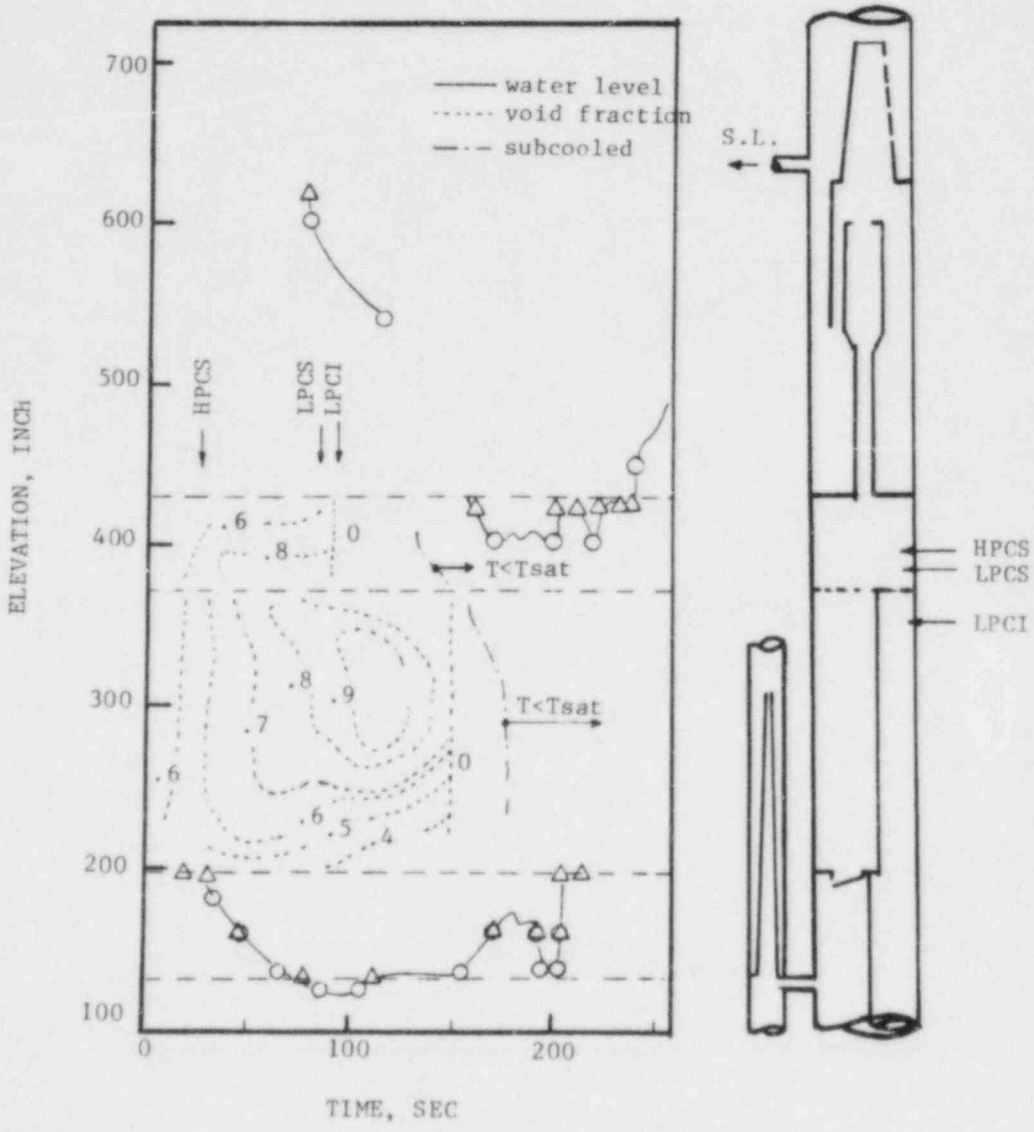

Figure 7.4-5. Inside Water Level and Void Fraction Distribution, Test 6MSB1

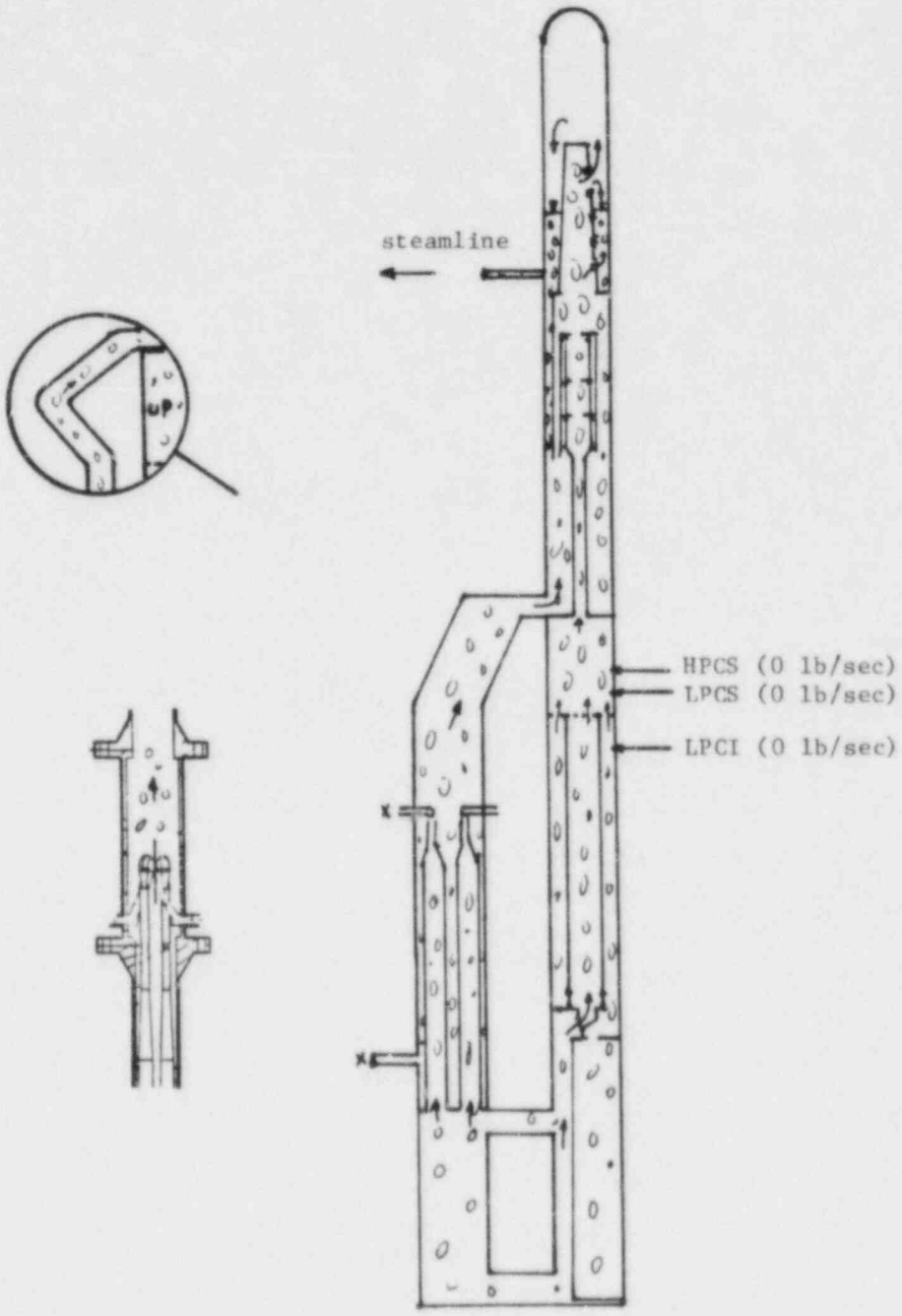

Figure 7.4-6. System Condition at T=20 sec

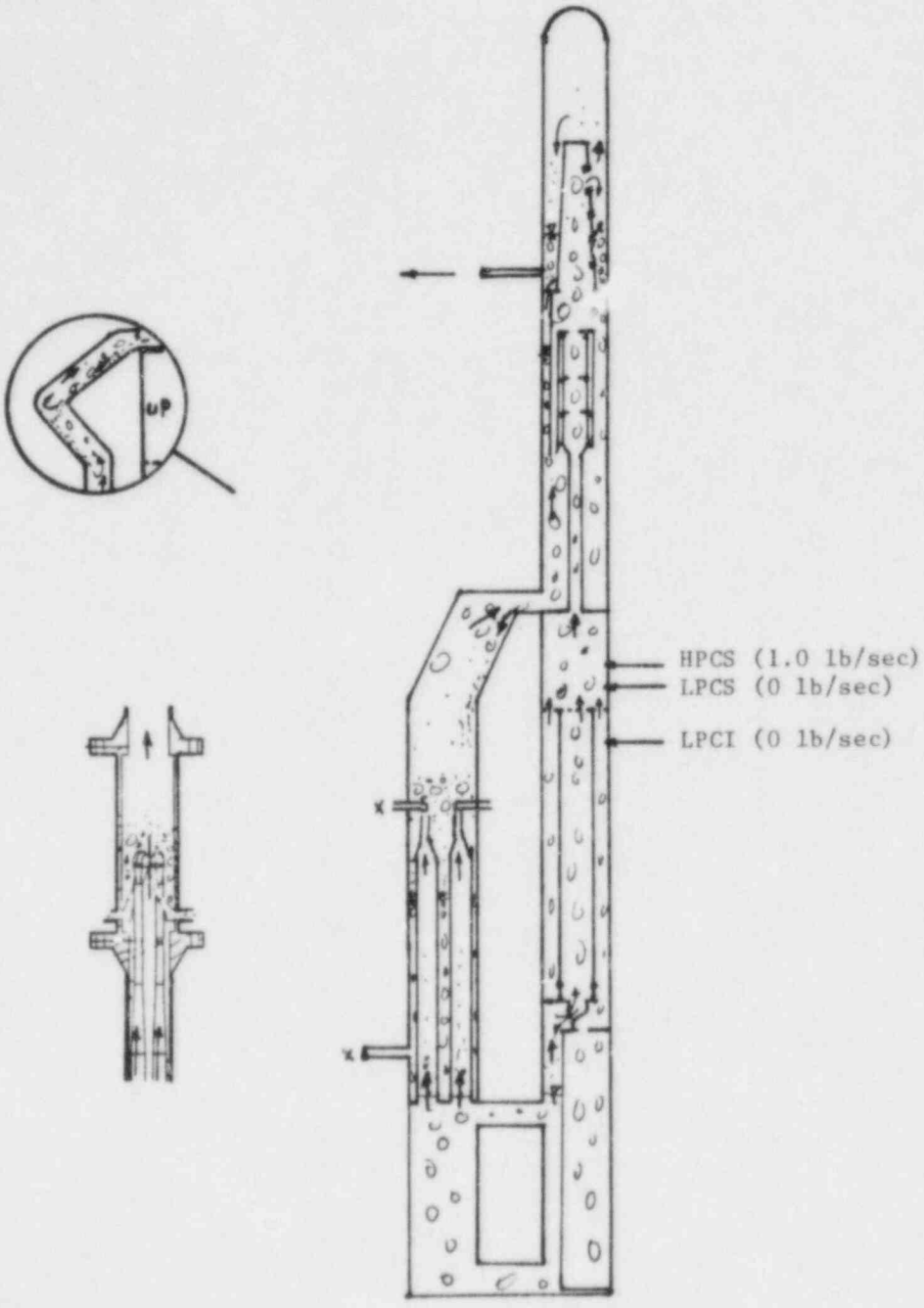

Figure 7.4-7. System Condition at T=60 sec

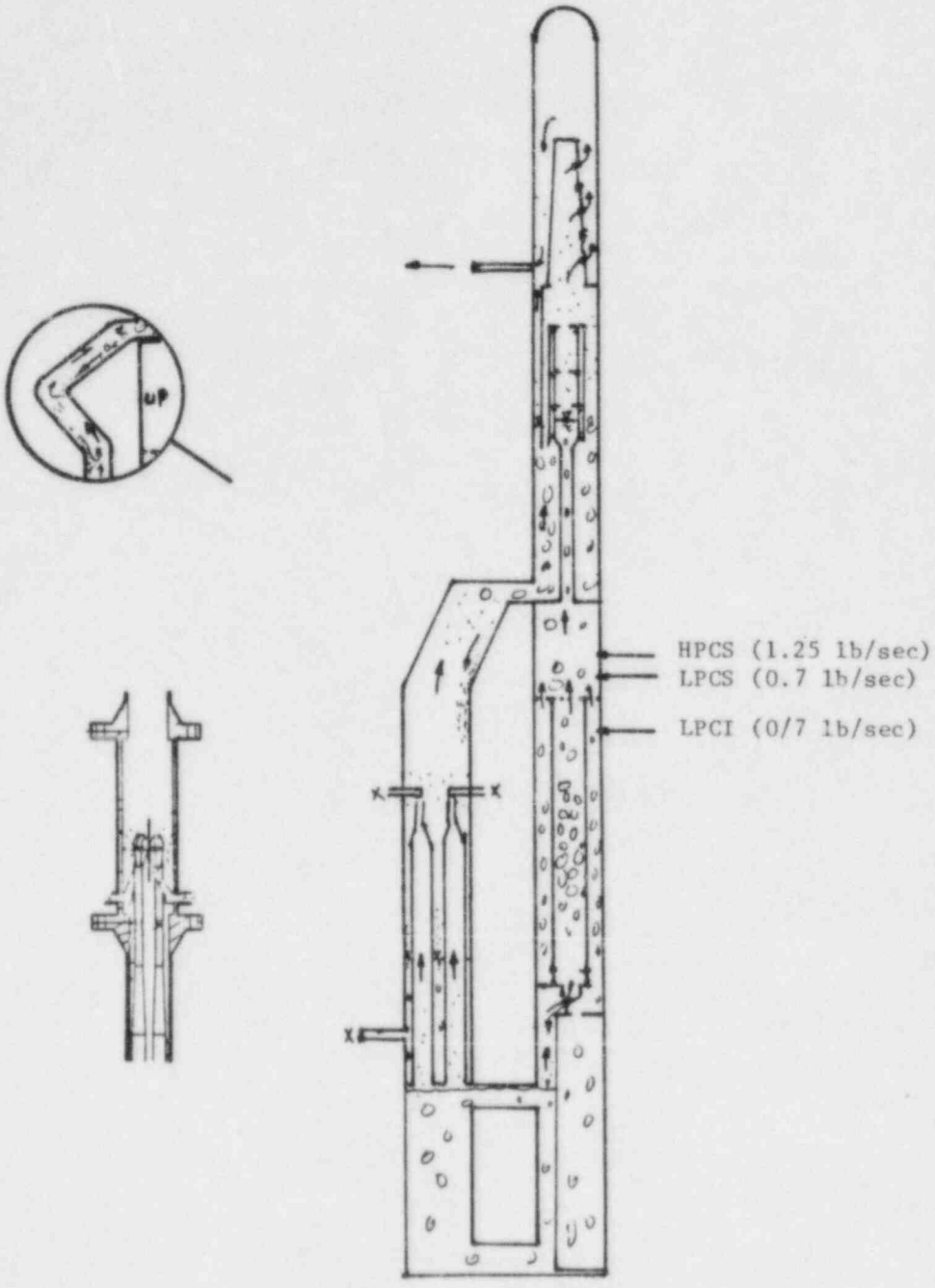

Figure 7.4-8. System Condition at T=120 sec

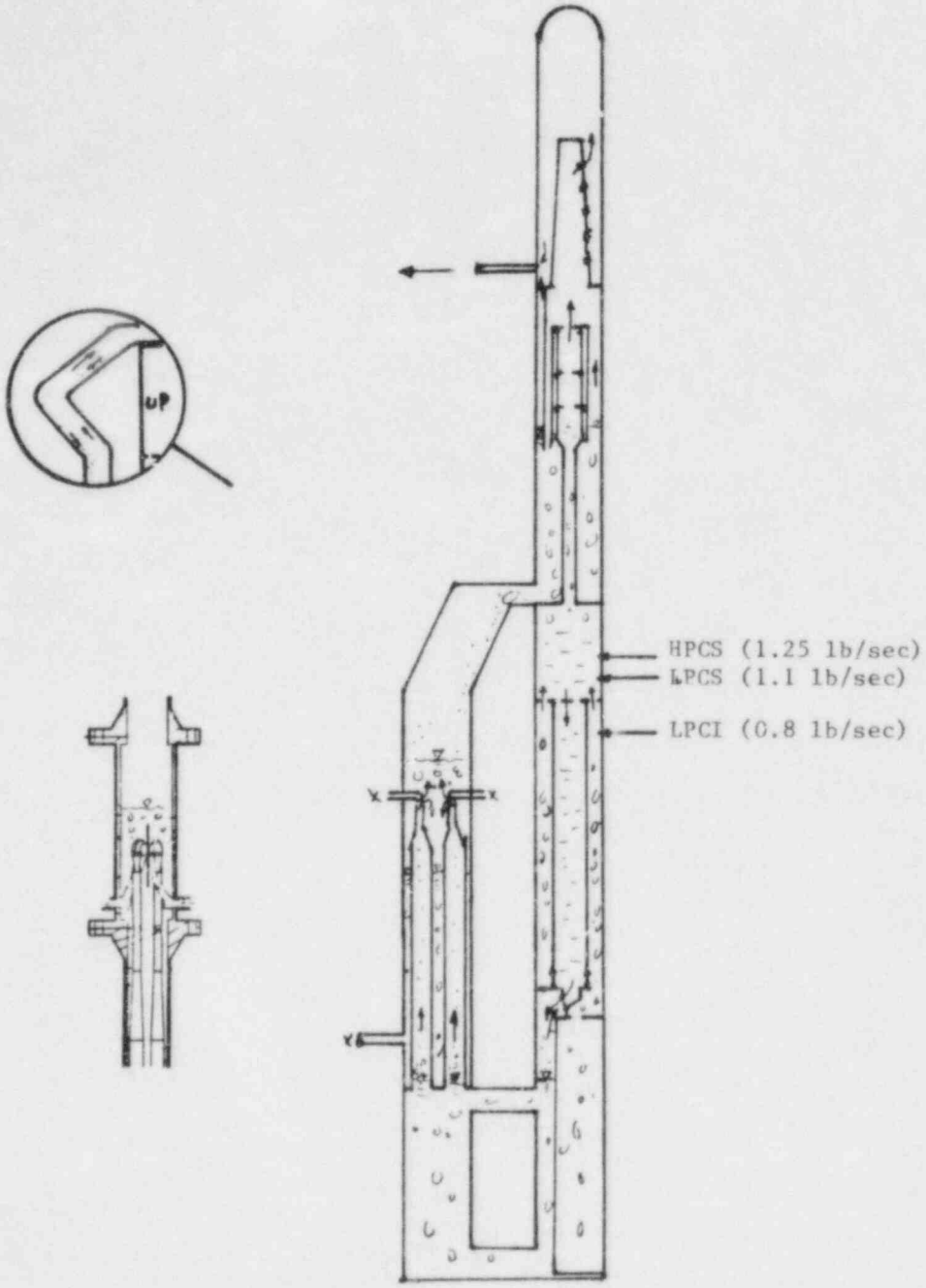

Figure 7.4-9. System Condition at T=150 sec

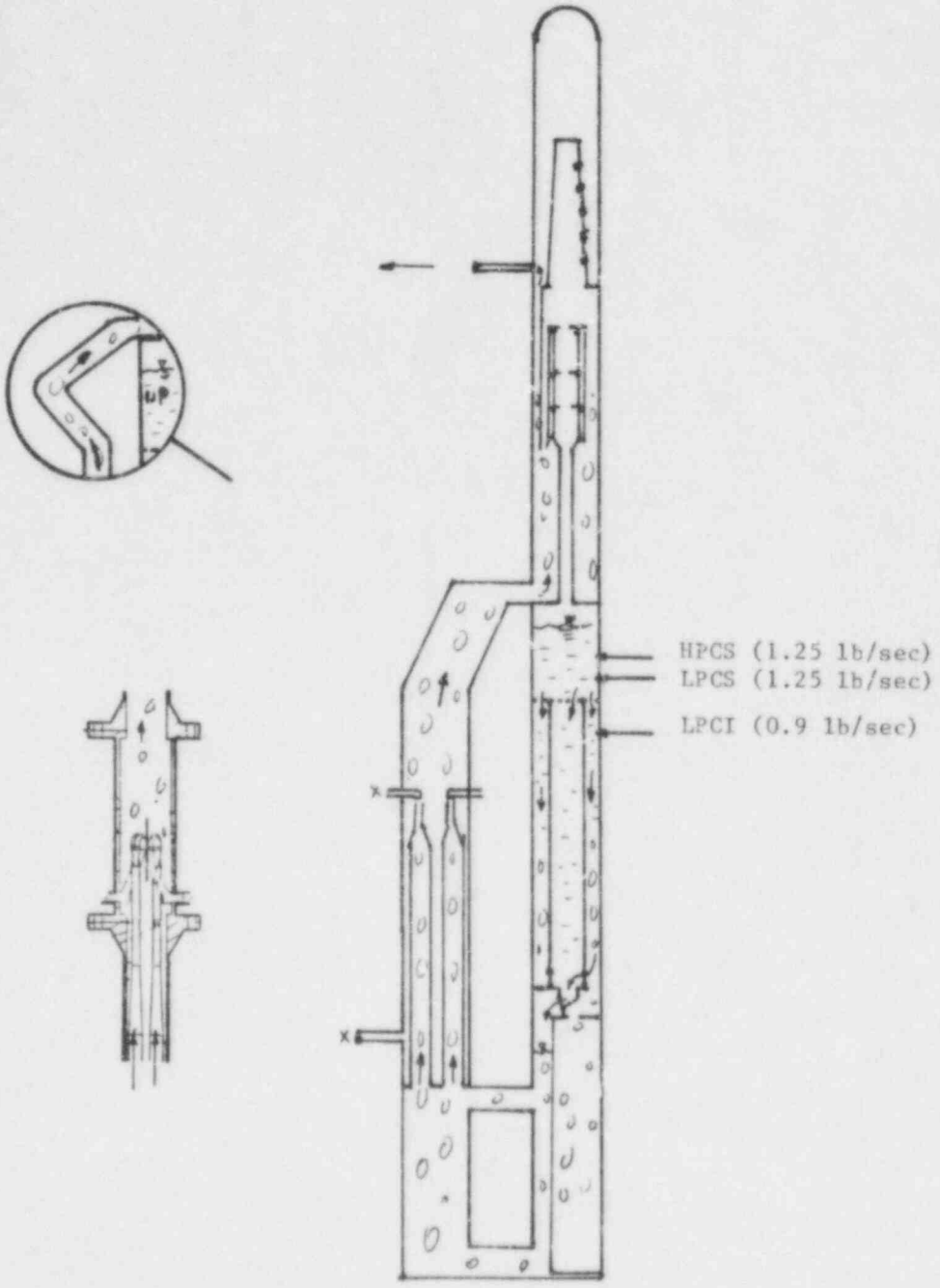

Figure 7.4-10. System Condition at T=180 sec

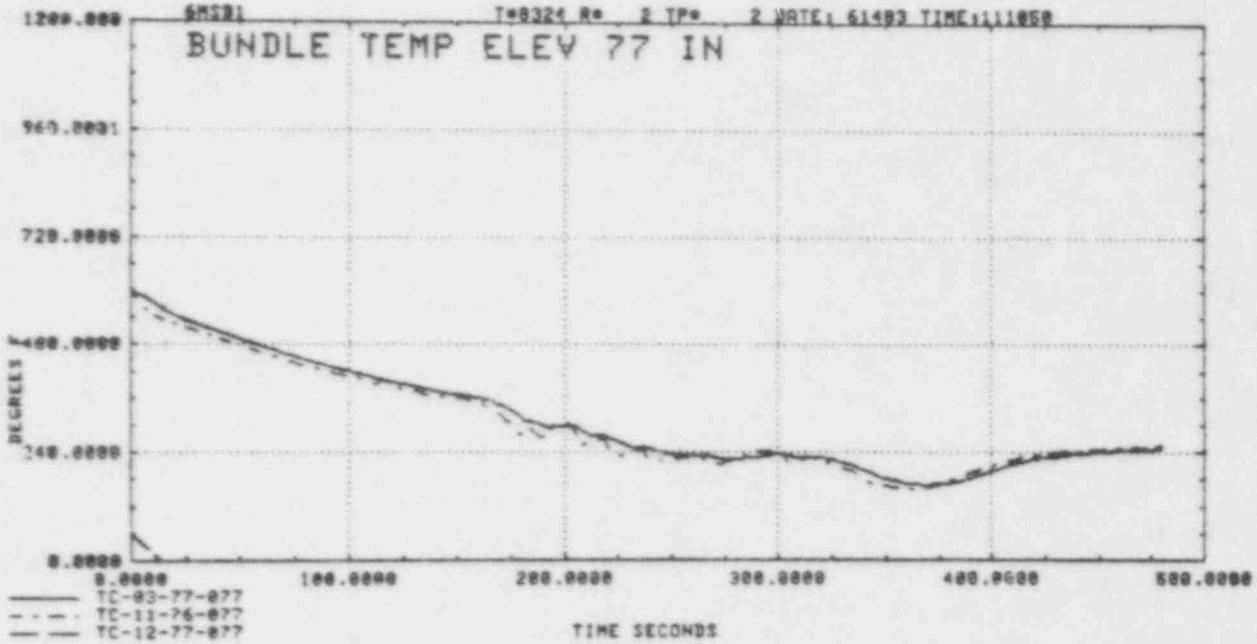

Figure 7.4-11. Rod Temperature, Elev 77"

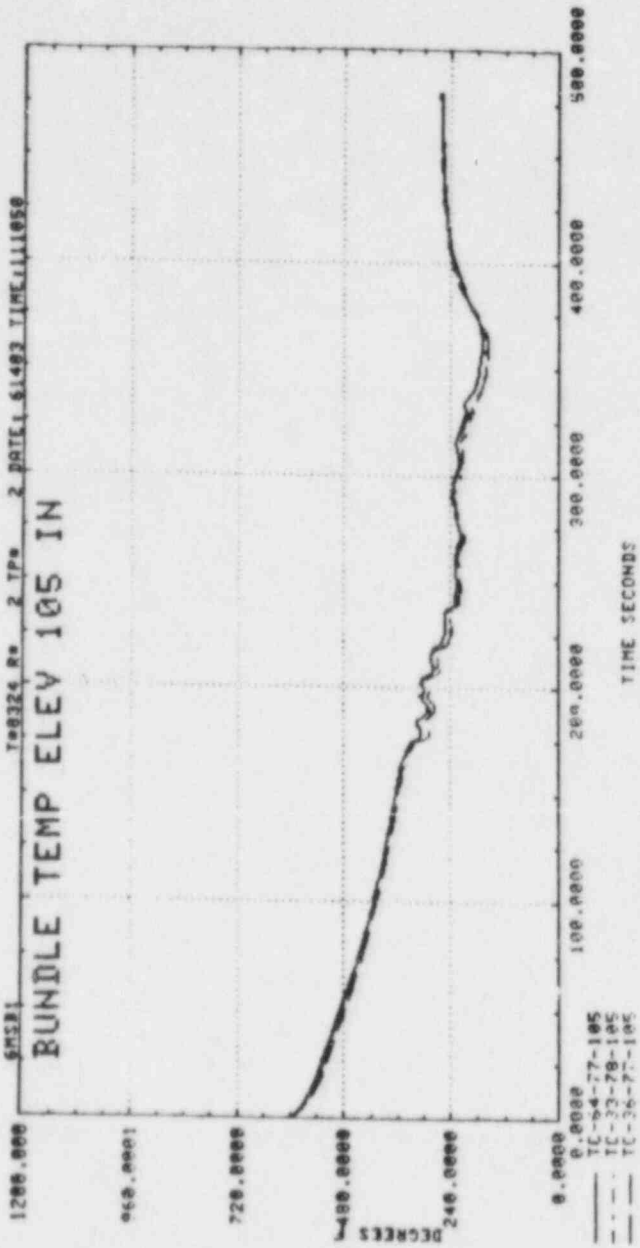

Figure 7.4-12. Rod Temperature, Elev 105"

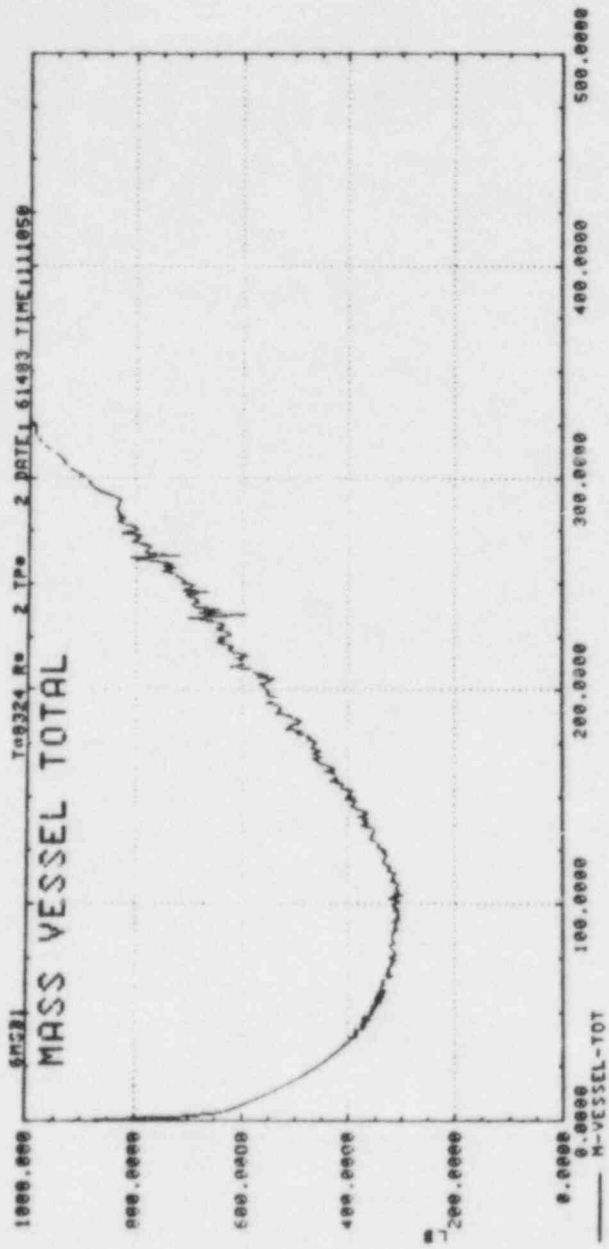

Figure 7.4-13. System Total Mass

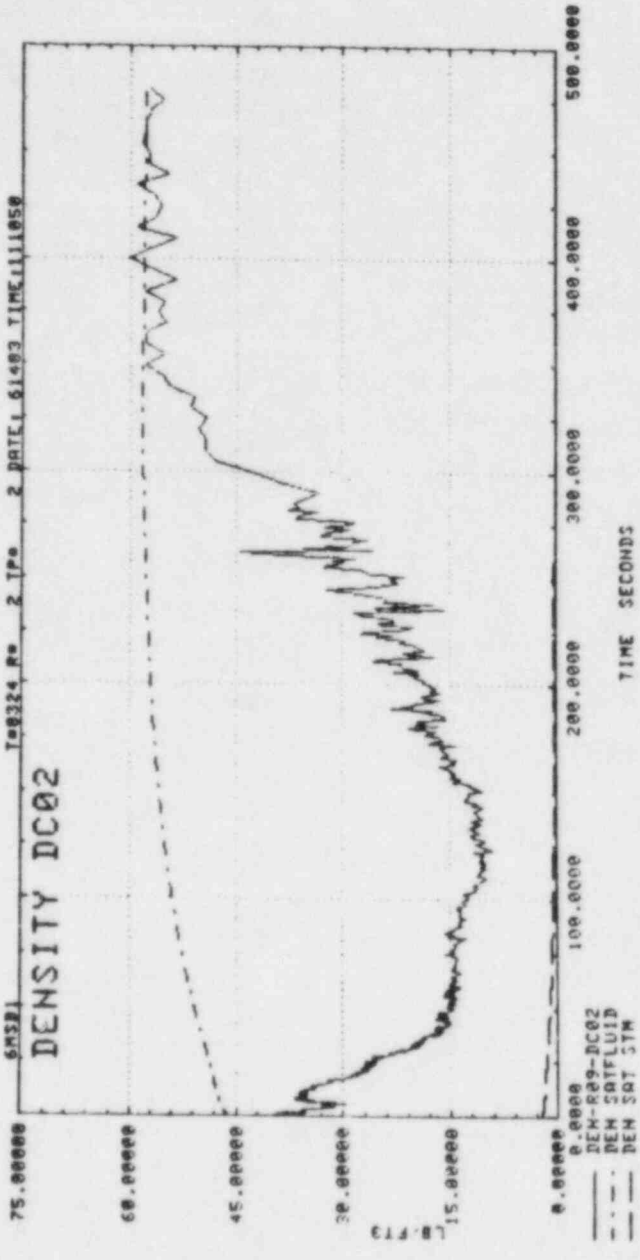

Figure 7.4-14. Regional Density of Downcomer Above Top of Jet Pump

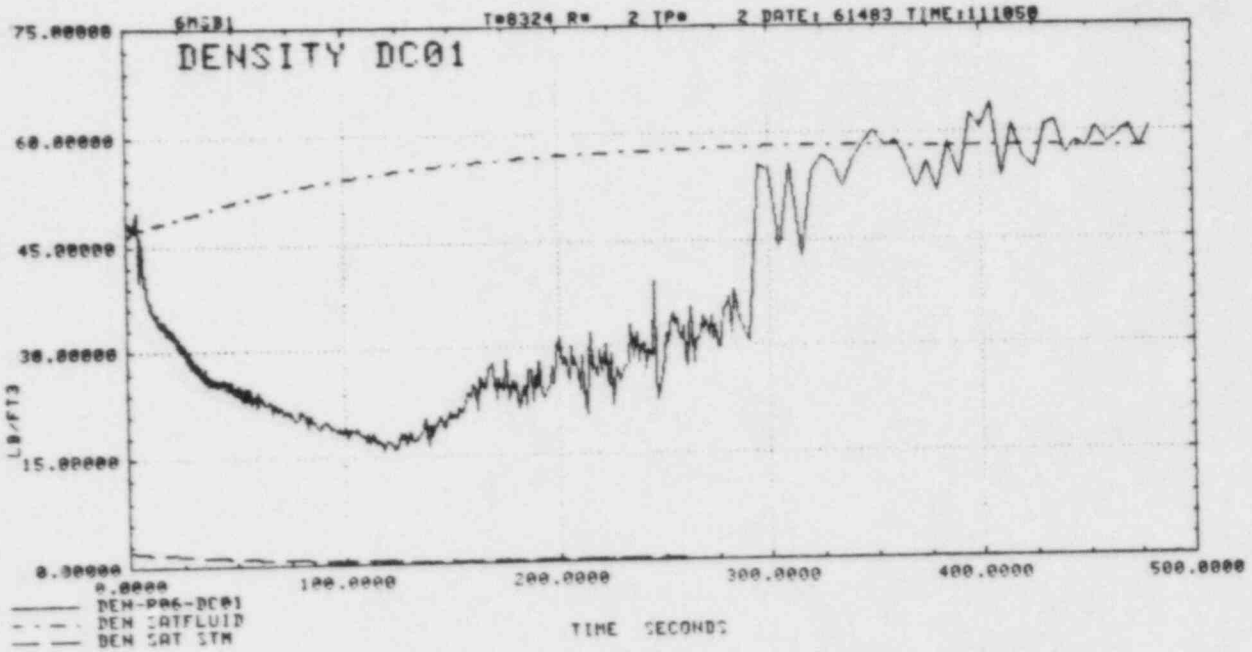

Figure 7.4-15. Regional Density of Downcomer Below Top of Jet Pump

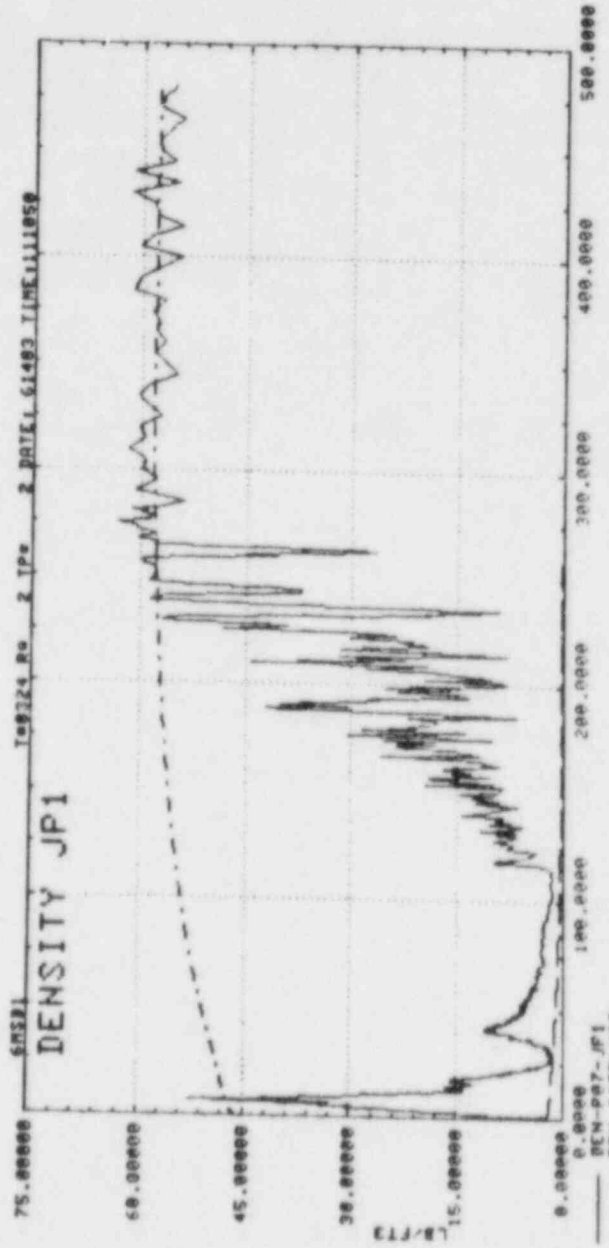

Figure 7.4-16. Intact Loop Jet Pump Density

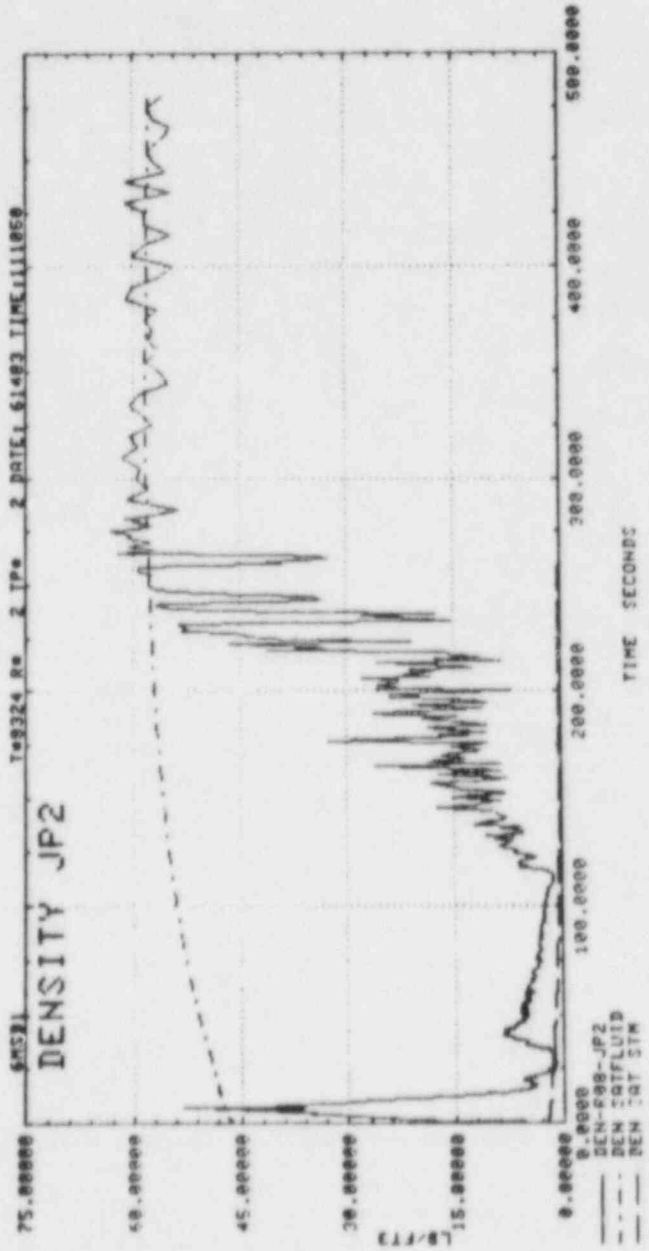

Figure 7.4-17. Broken Loop Jet Pump Density

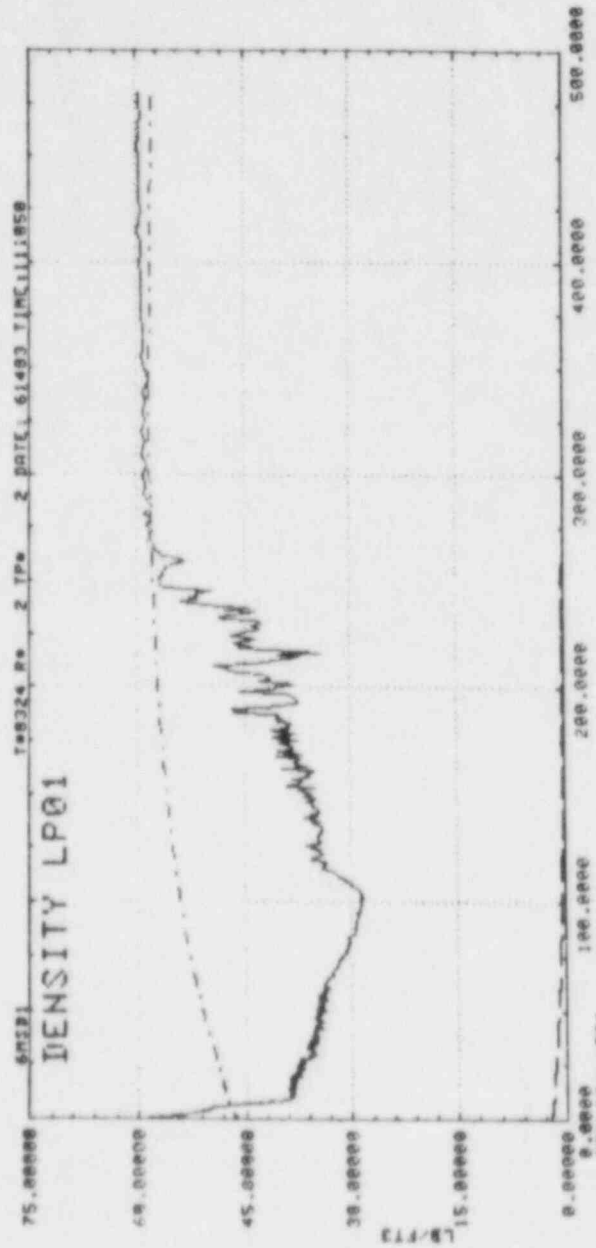

Figure 7.4-18. Regional Density of Lower Plenum Below Jet Pump Exit Plane

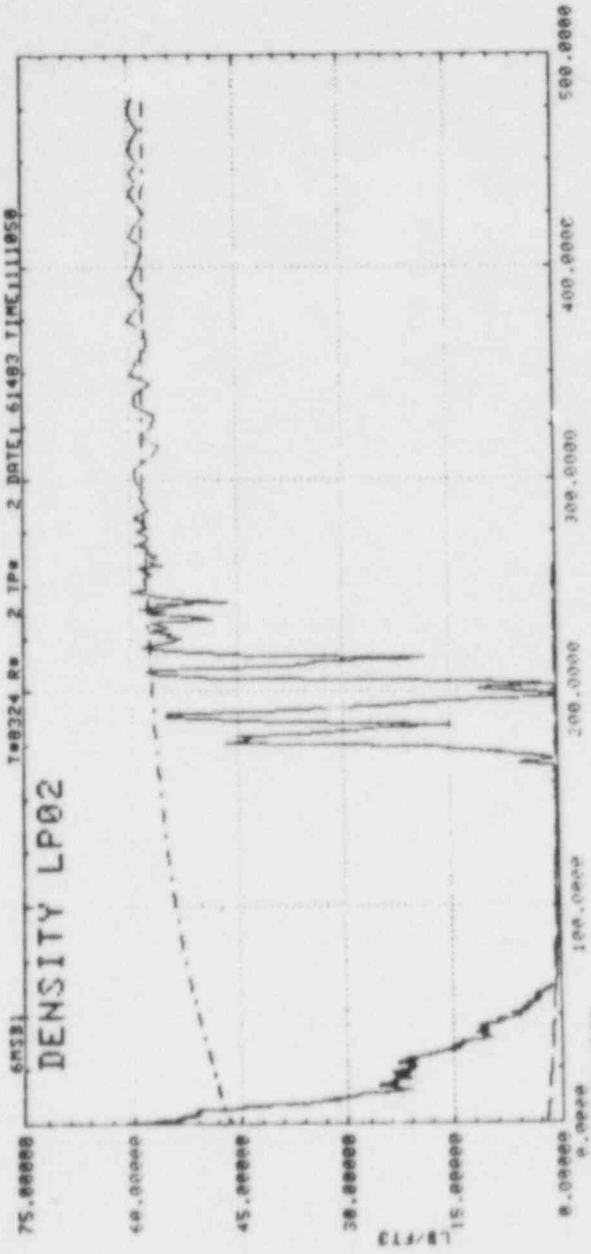

Figure 7.4-19. Regional Density of Lower Plenum Above Jet Pump Exit Plane

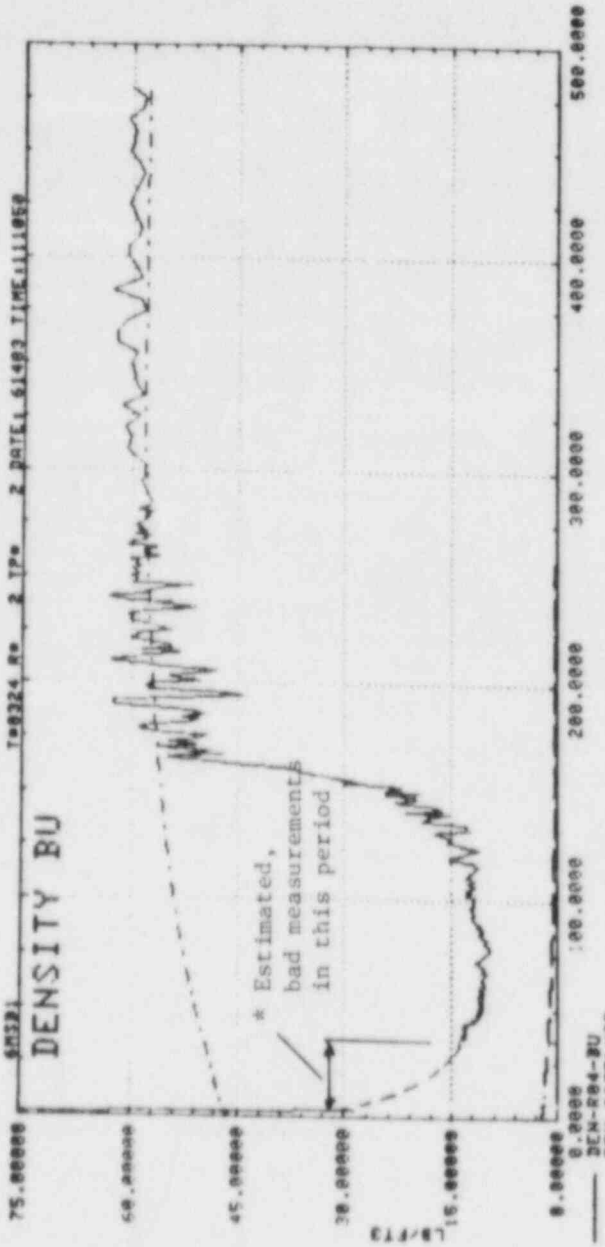

Figure 7.4-20. Bundle Density

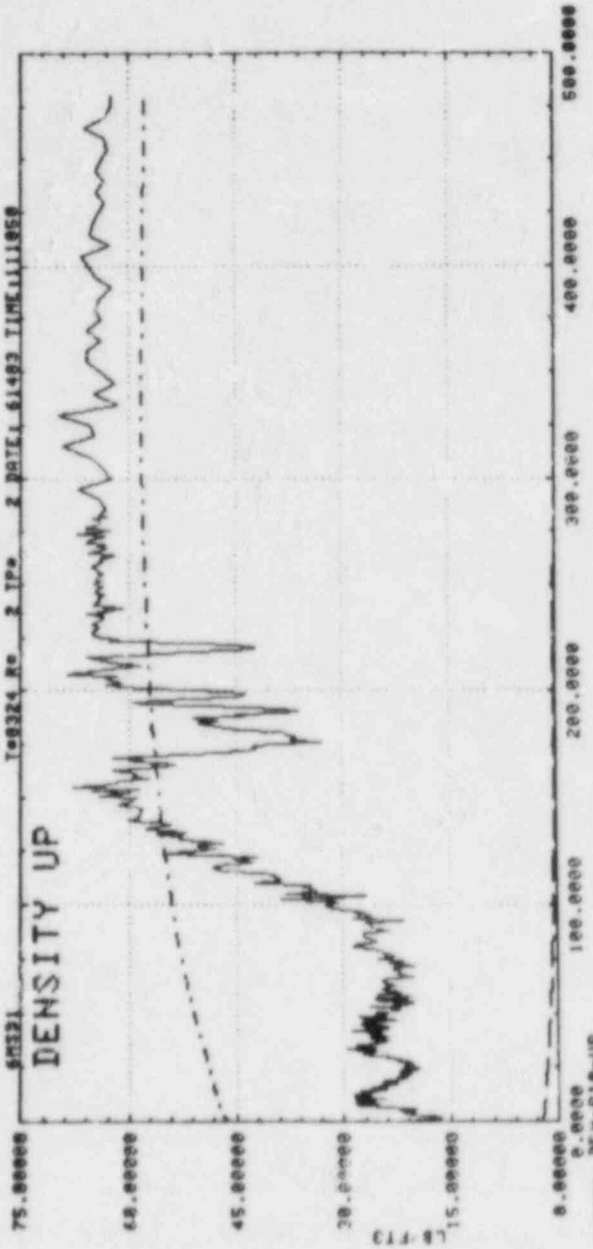

Figure 7.4-21. Upper Plenum Density

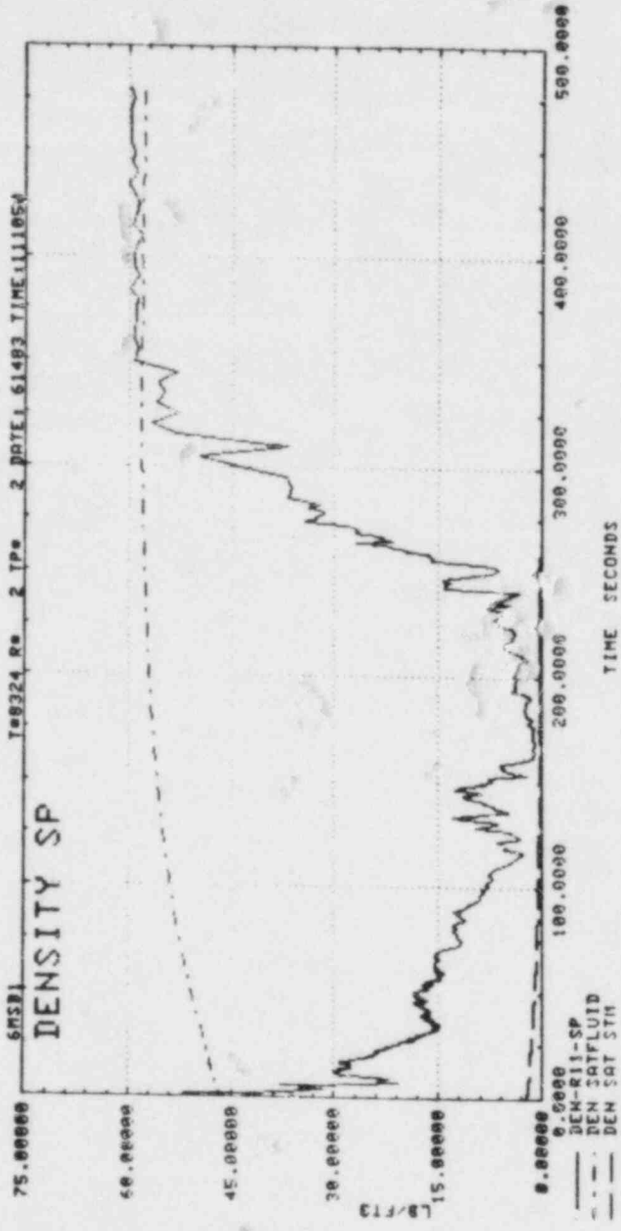

Figure 7.4-22. Stand Pipe Density

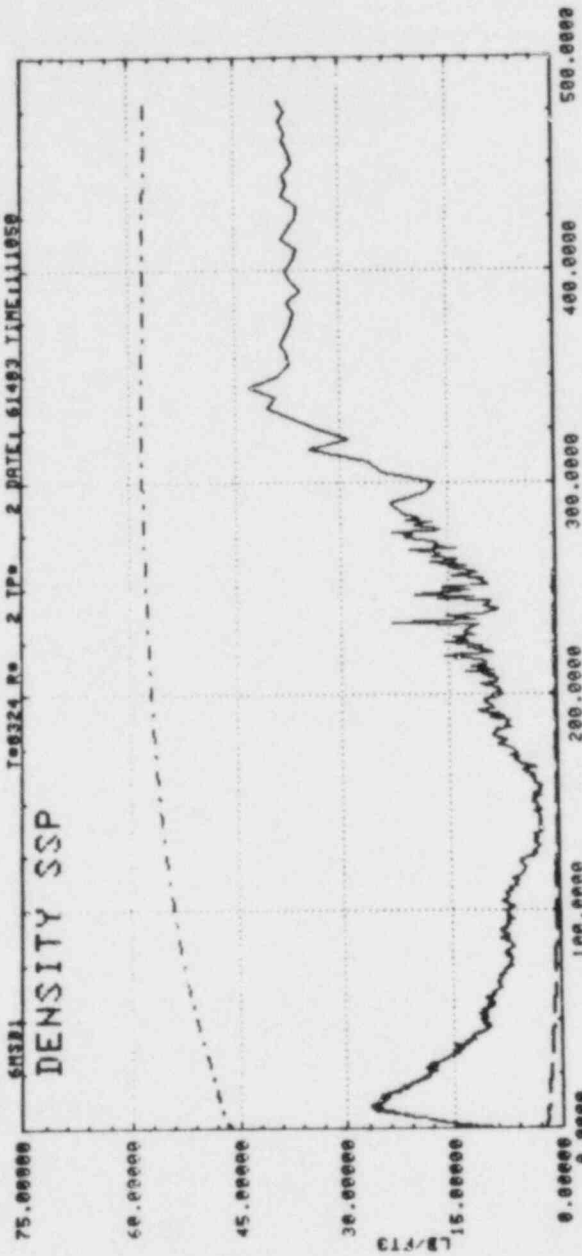

Figure 7.4-23. Steam Separator Density

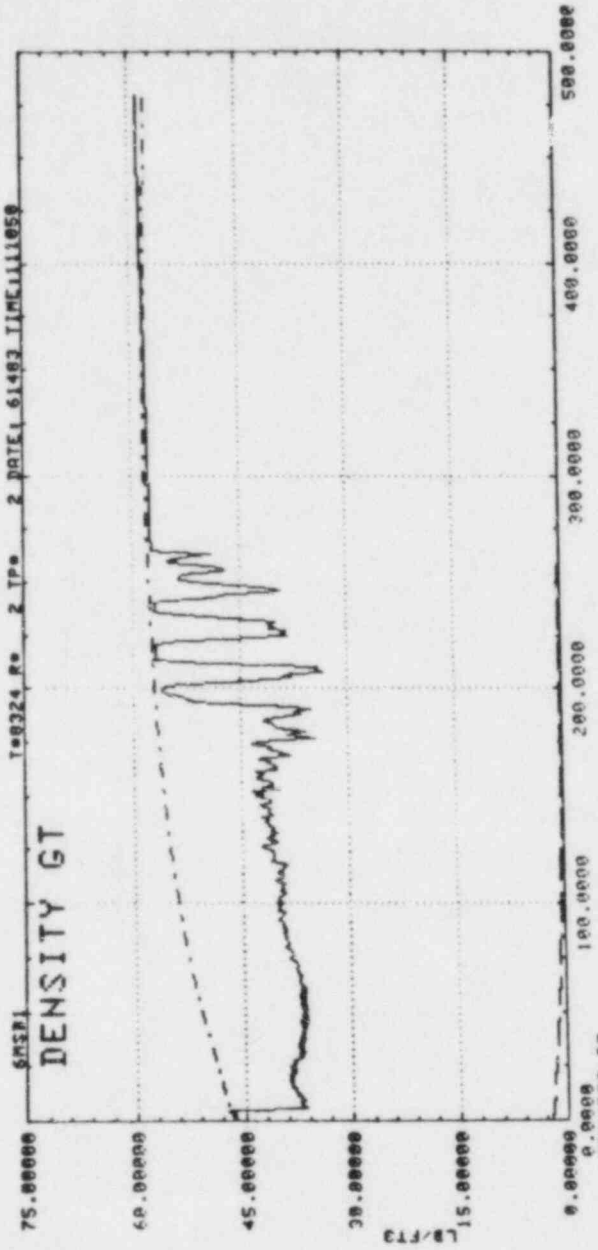

Figure 7.4-24. Guide Tube Density

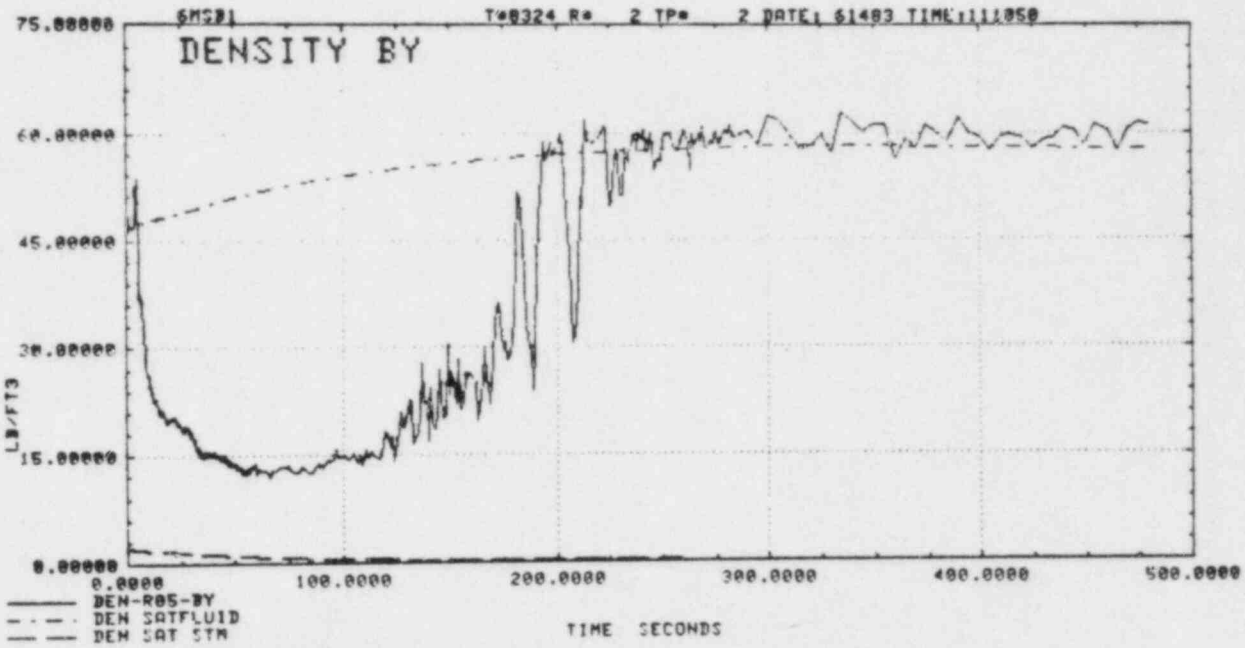

Figure 7.4-25. Bypass Density

7.5 NATURAL CIRCULATION TEST 6PNC1

7.5.1 General Description

A unique and important feature of the BWR is the natural circulation performance. The FIST test 6PNC1 is to investigate and demonstrate the natural circulation characteristics.

7.5.2 Test Conditions

A series of seven tests with bundle powers of 0.5 to 3.0 MW were performed to investigate the system performance. Of these, the 2.0 MW test (6PNC1-4) is the reference case and most of the data presented below are obtained from that test. All tests were conducted with saturated water in the downcomer except test 6PNC1-7A in which subcooled feedwater was injected into the vessel.

Data were collected while the system was maintained at a quasi steady state condition. System pressure was kept constant at 1040 PSIA (Figure 7.5-1), and bundle power at the desired level (Figure 7.5-2), while water level in the downcomer decreased very slowly at a rate of less than 0.5 in/sec (Figure 7.5-3). The tests began at normal water level and ended when water level neared the top of the core.

7.5.3 Natural Circulation Flow

Figure 7.5-4 shows that the total natural circulation core flow decreased as water level dropped (Figure 7.5-3). Similar data were obtained for all tests. These data are combined and replotted to show the relationship between the natural circulation flow and bundle power, with water level at various elevations (Figure 7.5-5). It can be seen that the natural circulation flow is affected by bundle power as well as water level.

At normal water level (37" BWR level), a natural circulation flow of about 10 lbm/sec is measured for bundle power higher than 1.5 MW. This flow is more than 25% of the core flow at normal operating conditions.

7.5.4 Internal Circulation

In addition to the natural circulation from the downcomer to the core, there are several internal circulation flows. Figures 7.5-6 to 8 illustrate these internal flows with water level at three different elevations, as observed in the 2.0 MW test. As water level drops, the natural circulation flow from the downcomer decreases, but the bypass-to-bundle flow increases. Increasing internal flow is due to an increase in the driving head between the bypass and the bundle resulting from a higher void fraction (Figures 7.5-9 and 11) in the bundle.

7.5.5 Water Level Measurements

In a BWR, water level in the downcomer is monitored with a wide range water level measurement. Results given in Figures 7.5-4 and 5 show the same wide range water level measurement in FIST. Water level can also be determined based on the uncovery of differential pressure (DP) taps and conductivity probes (CP). Figure 7.5-12 shows that these different measurements agree well with the wide range water level measurement.

7.5.6 Summary (Test 6PNC1)

A series of natural circulation tests which cover a wide range of bundle powers has been conducted in FIST. These tests provide an excellent set of natural circulation data which can be used for various applications such as code qualification.

Test results have demonstrated that natural circulation provides adequate cooling in the core of a BWR. There was no rod heatup observed in any of the tests. Natural circulation flow rate is affected by bundle power and water level. Also secondary circulations are observed in various regions.

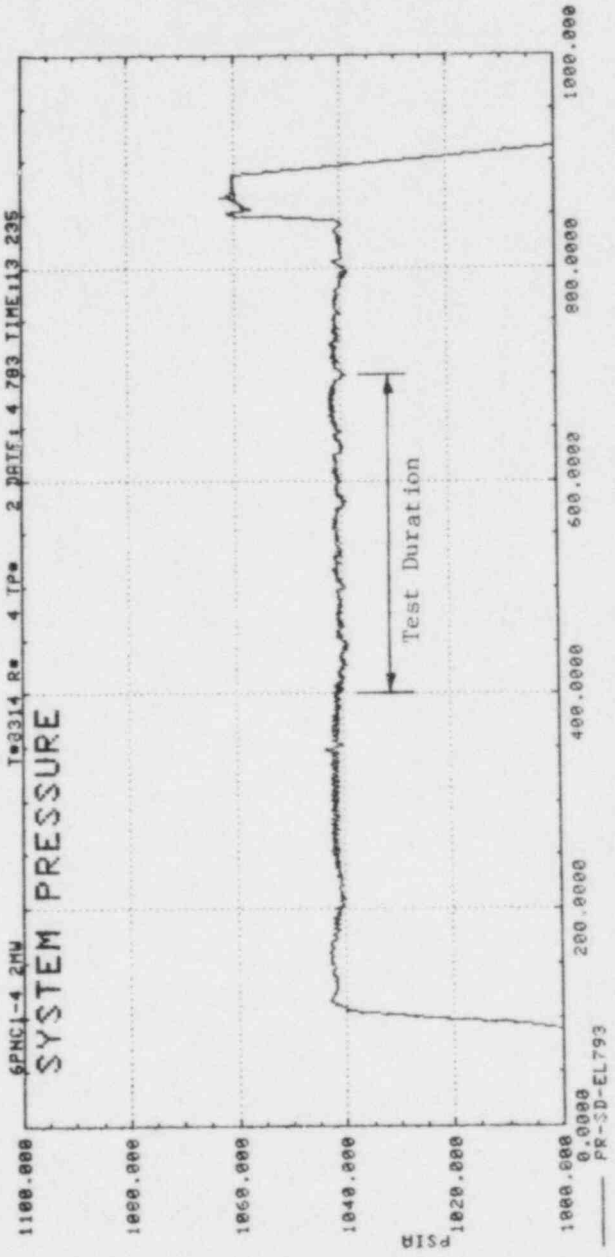

Figure 7.5-1. System Pressure, Test 6PNC104

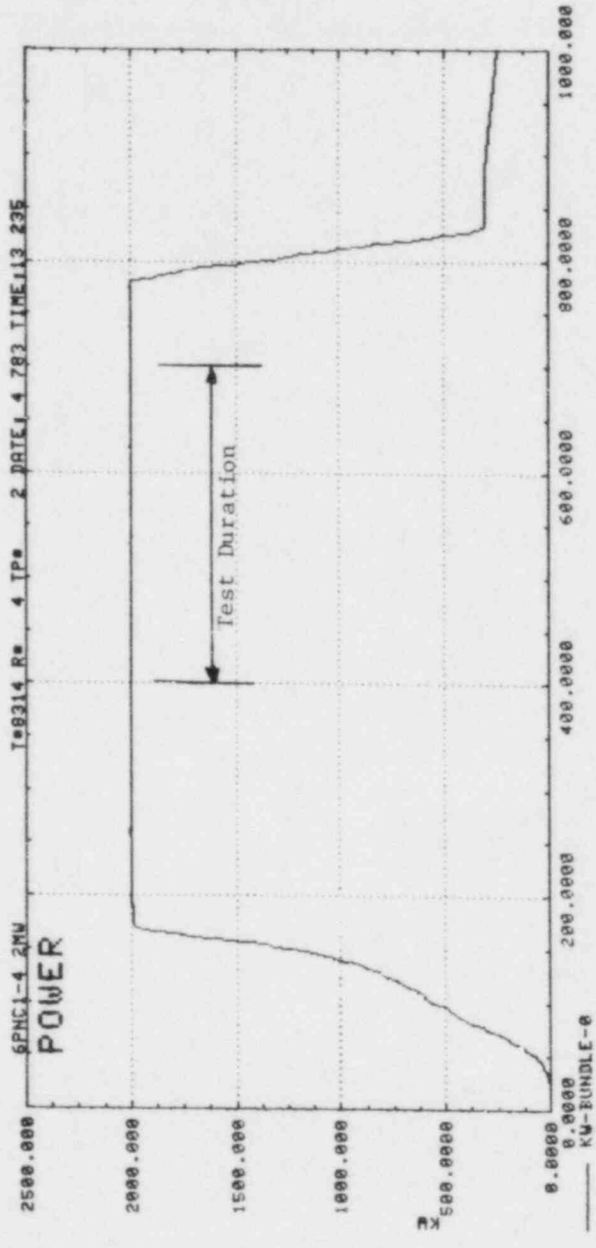

Figure 7.5-2. Bundle Power, Test 6PNC1-4

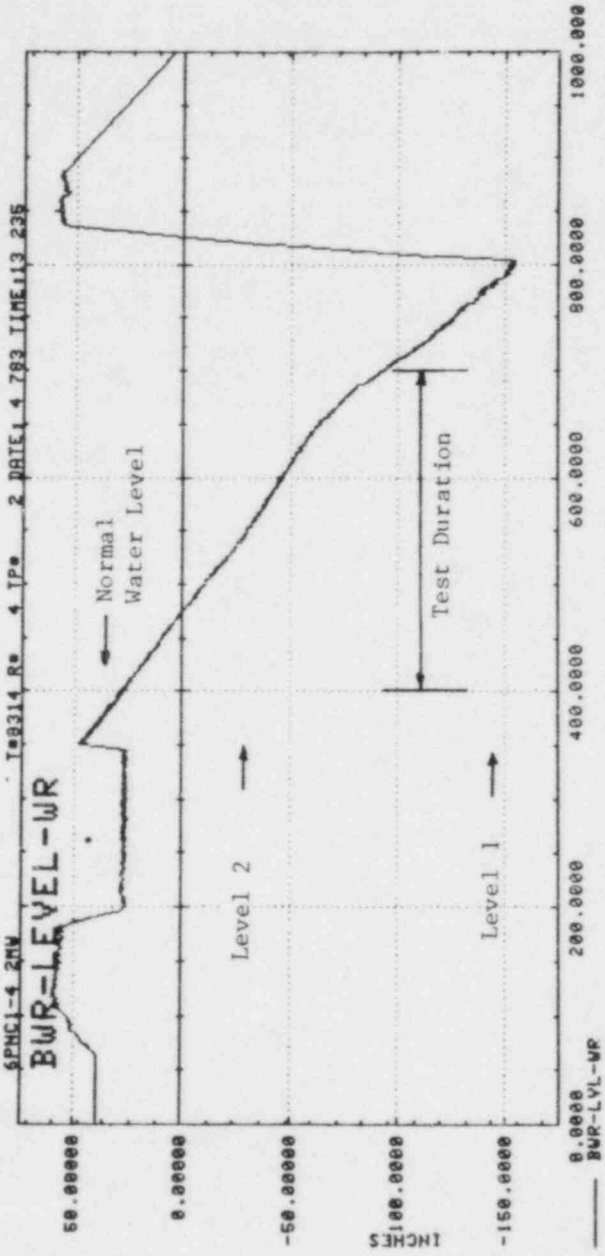

Figure 7.5-3. Downcomer Water Level, Test 6PNC1-4

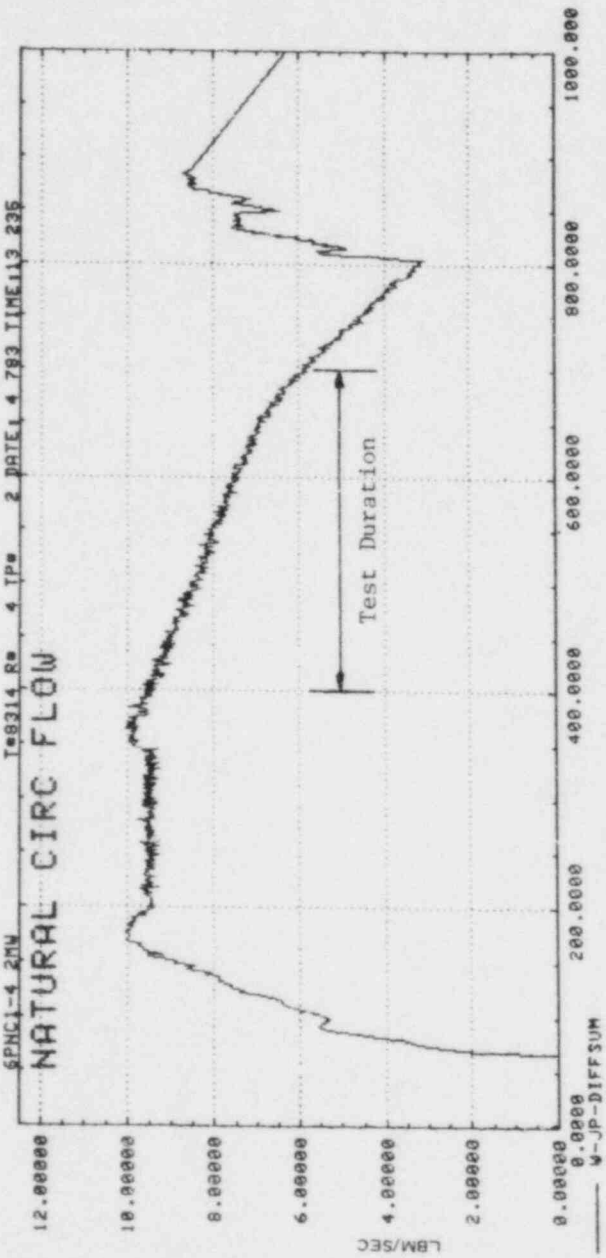

Figure 7.5-4. Core Flow, Test 6PNC1-4

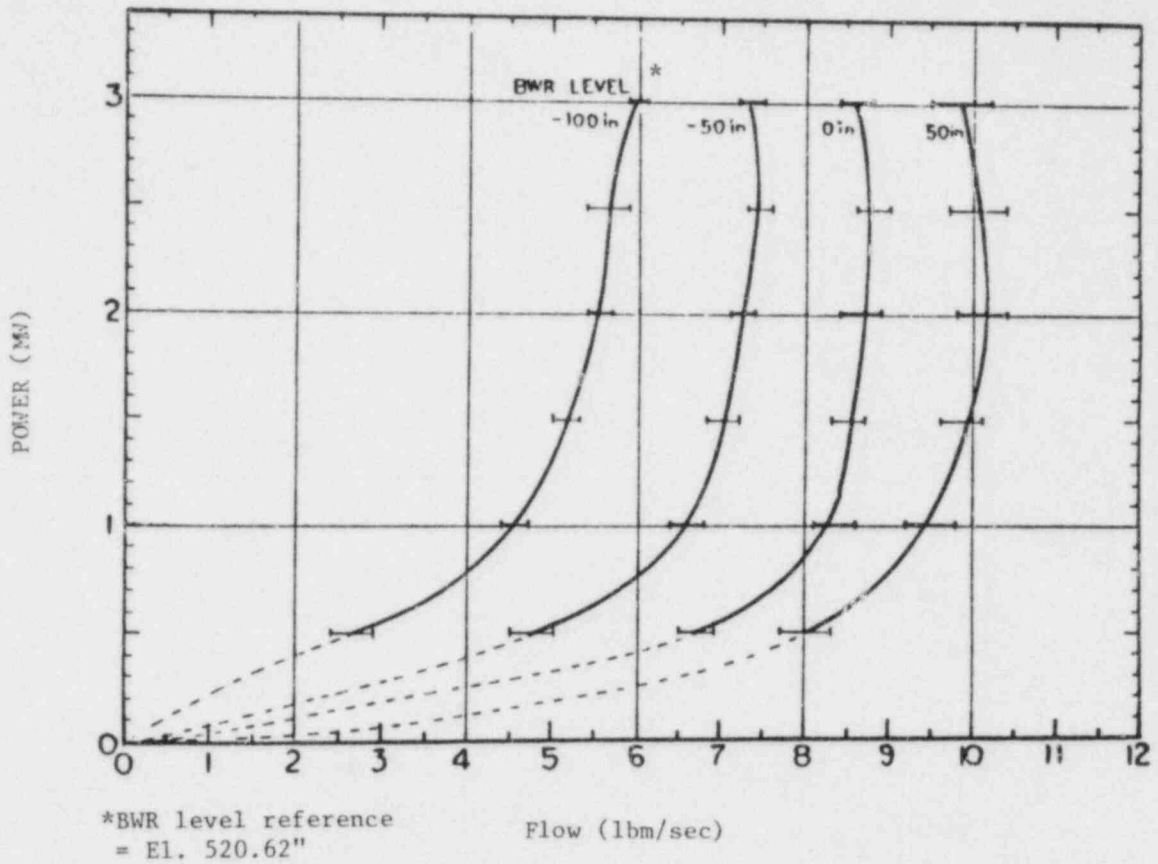

*BWR level reference
= El. 520.62"

Figure 7.5-5. Natural Circulation Flow

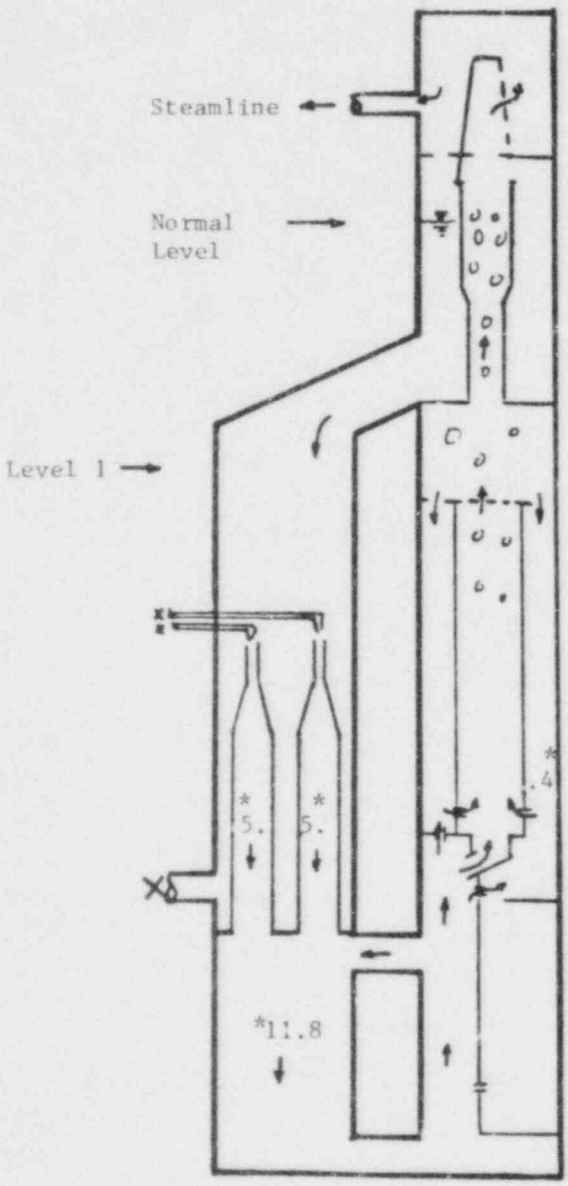

Figure 7.5-6. Flow Circulation versus Water Level at El. 560", Test 6PNC1-4

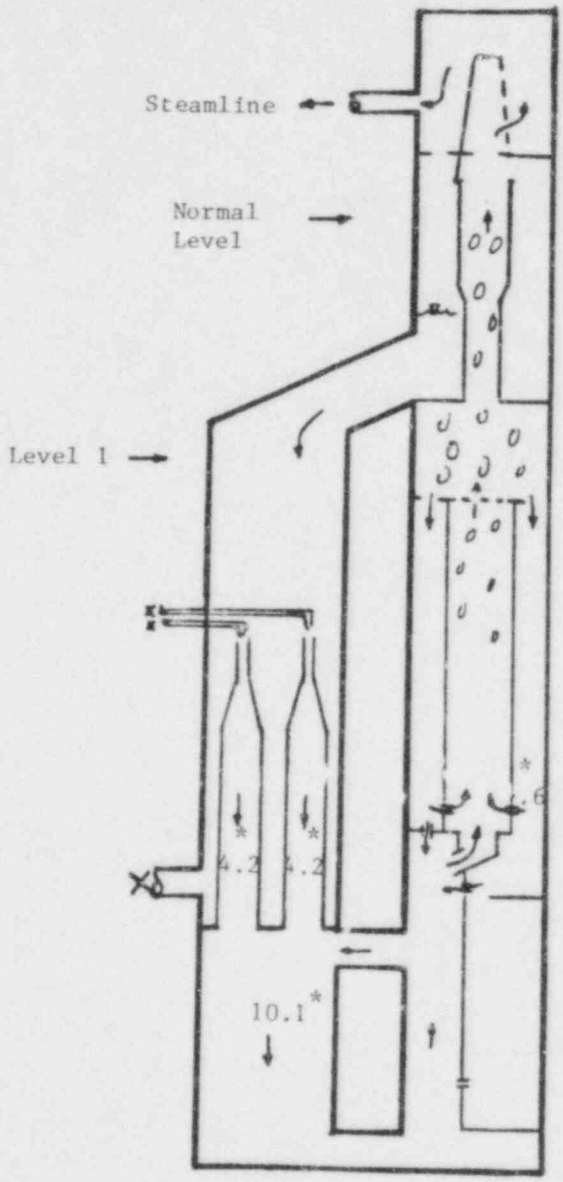

Figure 7.5-7. Flow Circulation versus Water Level at El. 490", Test 6PNC1-4

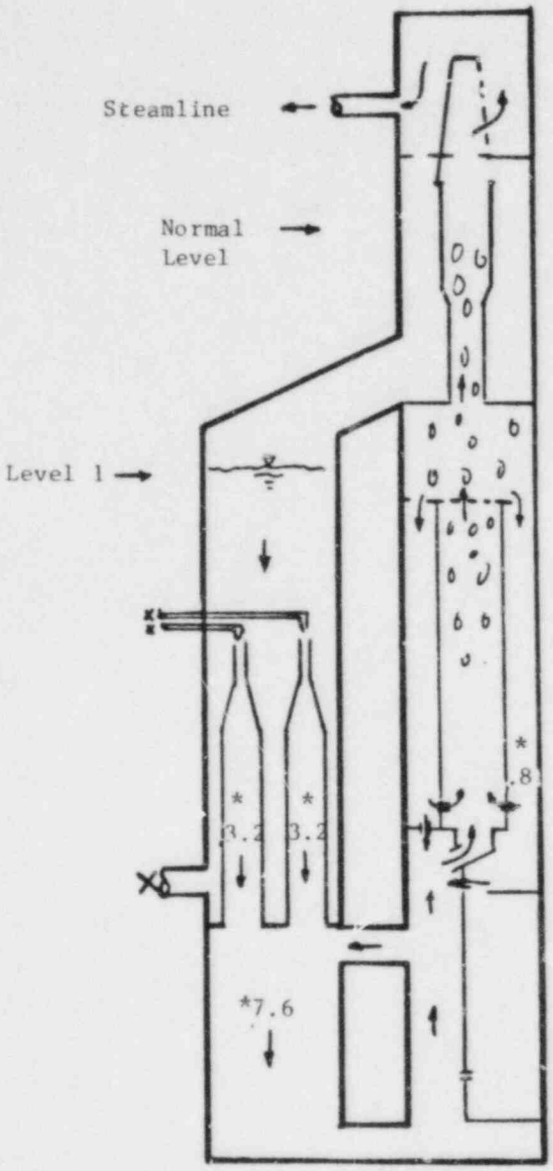

Figure 7.5-8. Flow Circulation versus Water Level at El. 430", Test 6PNC1-4

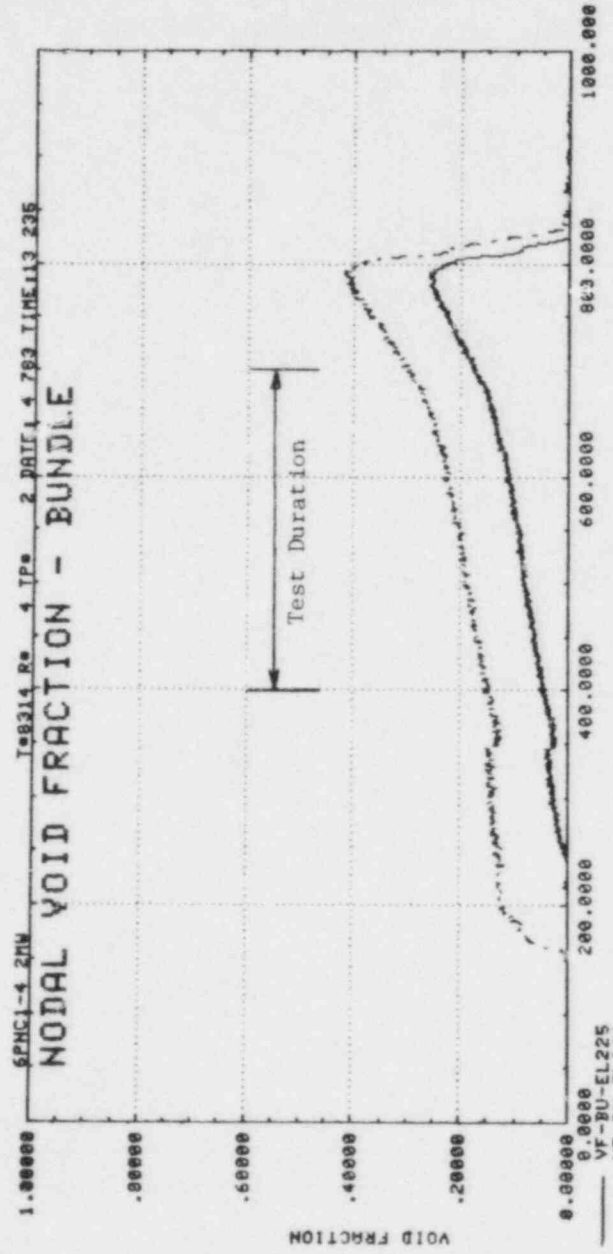

Figure 7.5-9. Bundle Nodal Void Fraction, El. 225" to 266", Test 6PNC1-4

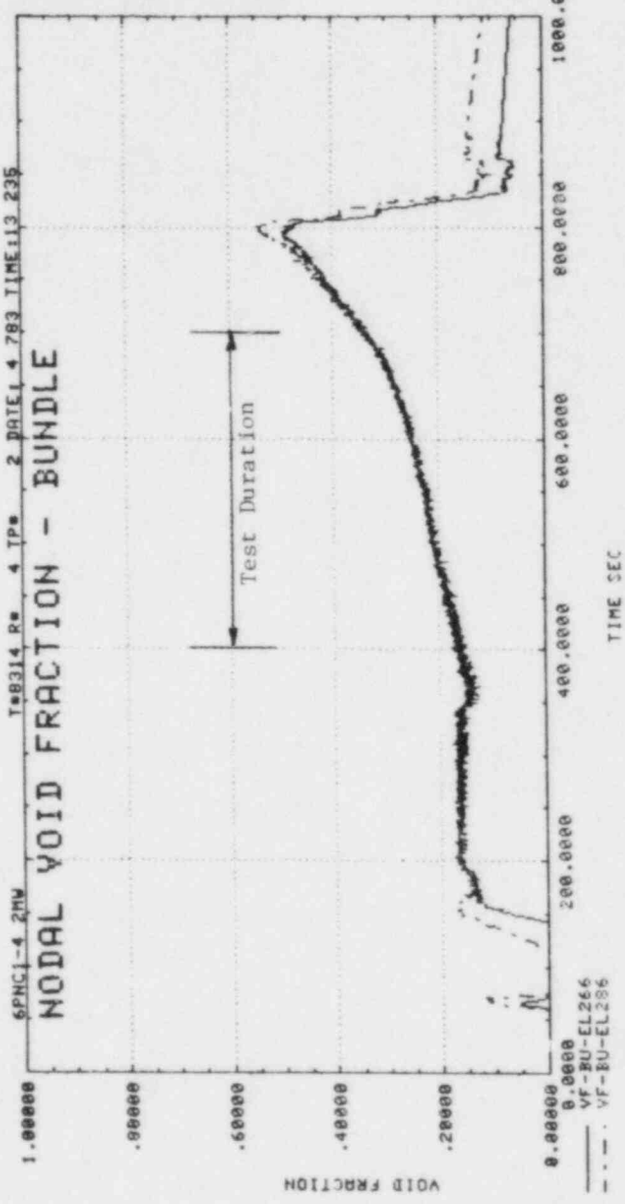

Figure 7.5-10. Bundle Nodal Void Fraction, El. 266" to 306", Test 6PNC1-4

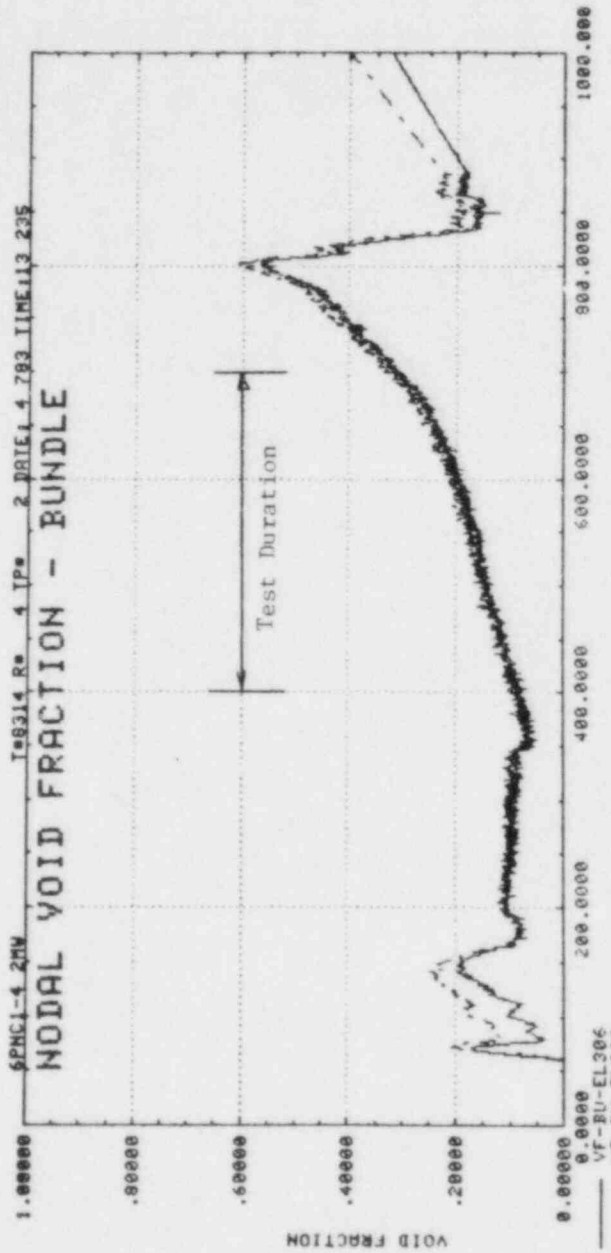

Figure 7.5-11. Bundle Nodal Void Fraction, El. 306" to 346", Test 6PNC1-4

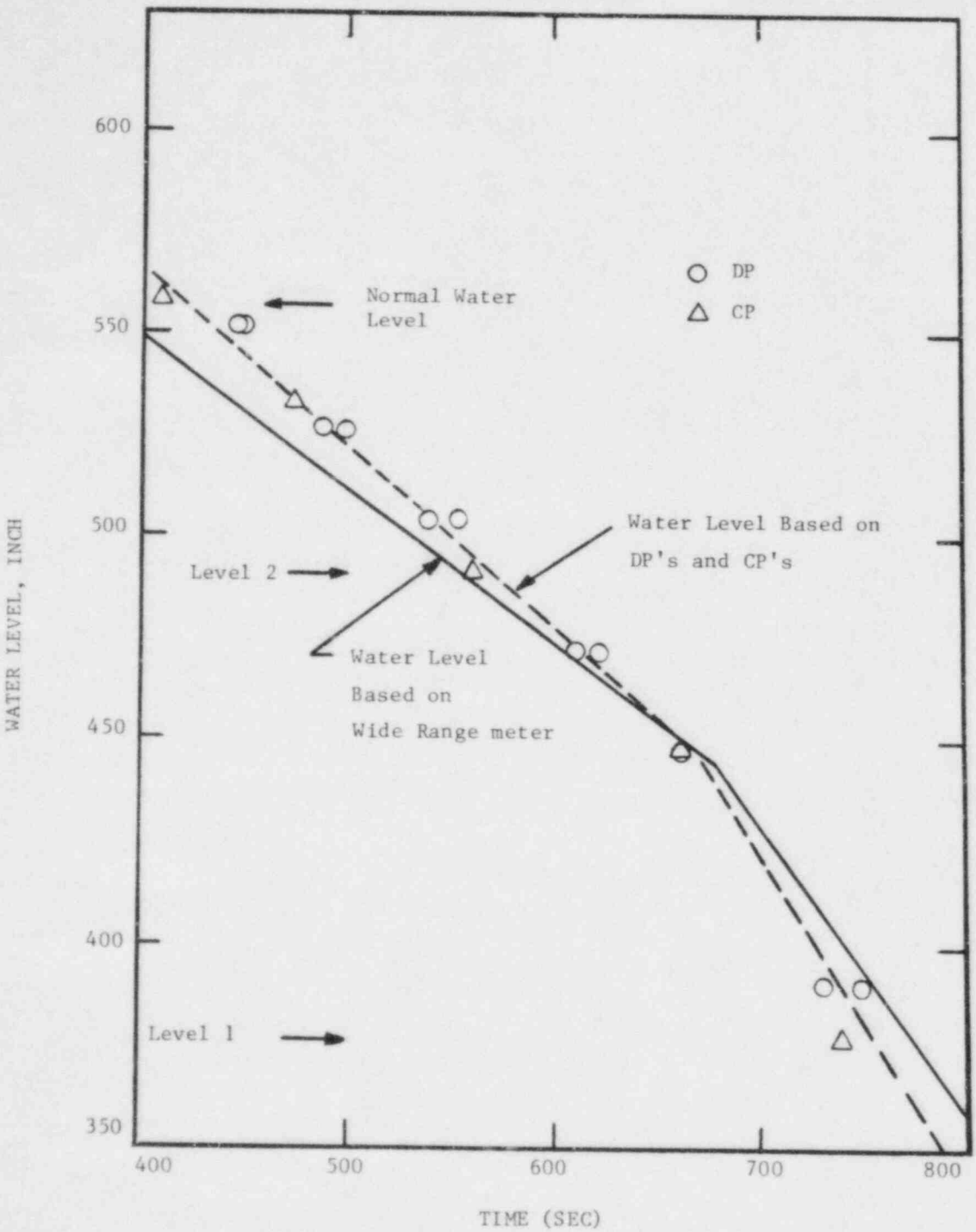

Figure 7.5-12. Downcomer Water Level Based on Different Measurements

7.6 BWR/6 POWER TRANSIENT WITH MSIV CLOSURE TEST 6PMC1

7.6.1 General Description

Test 6PMC1 simulates a BWR/6 Main Steamline Isolation Valve (MSIV) closure without power scram. HPCS and RCIC are assumed to be functional. This event is the severest case based on the BWR power transient analysis reported in reference 5. As discussed in Section 4.5, the power transient test simulation is based on a transient code calculation for a BWR. Results of this BWR study are shown in Table 7.6-1. Table 7.6-2 lists the test conditions and trips employed in the test.

7.6.2 Key Events and Bundle Power

Timings of major events of the test are given in Table 7.6-3. Figure 7.6-1 shows the bundle power applied in the test throughout the transient and Figure 7.6-2 is a short term plot for the same power which indicates a power surge to 7.3 MW at about 4 seconds.

7.6.3 Pressure Response and S/RV Operation

The system pressure is presented in Figure 7.6-3. Following the MSIV closure, the system isolation and increasing steam generation rate in the bundle causes the system pressure to increase rapidly, reaching the opening setpoints (Table 4.2-2) of the normal relief of all five S/RV's. Steam discharge through these five valves (Figure 7.6-4), plus the reduction in the bundle power (Figure 7.6-2), decreases the system pressure. As in a BWR, once the normal relief of S/RV #2, 3, 4, or 5 is activated, the operation of all S/RV's is switched to the low/low set relief for the remainder of the transient. Thus, the system pressure is maintained within the pressure range of the low/low set relief of S/RV's by opening and closing S/RV valves. (Figure 7.6-4).

7.6.4 Water Level

Water level in the downcomer (Figure 7.6-5) drops rapidly in the early transient due to inventory loss through S/RV's. Level 2 is reached at 22 seconds activating HPCS and RCIC systems with a time delay of 20 seconds. However, a minor difficulty in the time delay control was experienced in this test. Data have indicated that both HPCS and RCIC flows were initiated at 50 seconds (Figures 7.6-6 and 7). These minor differences in time delays from the test specifications have negligible effect on the system response. Also, feedwater was terminated at an earlier time than specified due to the back pressure (vessel pressure) being higher than the feedwater pump pressure.

The system begins to rebuild the inventory in the later transient due to continuous HPCS and RCIC injections and less inventory loss through S/RV's (Figure 7.6-4). Water level in the downcomer is completely recovered (Figure 7.6-5) and reaches level 8 at 1355 seconds (Figure 7.6-5). At level 8 both HPCS and RCIC are turned off.

7.6.5 Nodal Density

Nodal densities measured in the downcomer (Figures 7.6-8 and 9) show the sequence and timings of the uncoveries of these measuring taps as water level drops. The top of the jet pumps (elev. 311") is uncovered at about 100 seconds. Similar measurements in the bypass are given in Figure 7.6-10. It can be seen that bypass densities begin to decrease significantly (ie. losing inventory) shortly after the jet pump is uncovered. The boil-off by bundle power prior to the jet pump uncovery is made up by water from the downcomer and is then supplied from the bypass. The bundle is full of two phase mixture throughout the transient (Figure 7.6-11) and no heatup is observed (Figure 7.6-12).

7.6.6 Summary (Test 6PMC1)

Results of the FIST power transient test, 6PMC1, are summarized below:

(1) Water level in the downcomer drops and uncovers the top of the jet pump.

(2) The bypass is partially uncovered. The bundle, however, is always covered and there is no rod heatup.

(3) Water level is completely recovered by HPCS and RCIC injections.

Table 7.6-1

BWR/6 RESPONSES OF TRANSIENT CODE CALCULATION

		Time (Sec)
o	MISV Closure	0 - 4
o	Pressure and Power Rise Begins	0
o	Power Transient High Pressure (1113 PSIG) Reached	4
o	Relief Valve Lift	4
o	Vessel Pressure Peaks	6
o	Feedwater Limit Initiated	29
o	Feedwater Stop	44
o	L2 Reached	55
o	HPCS/RCIC Initiation	75
o	Maximum Neutron Flux (%)	638
o	Maximum Vessel Bottom Pressure (PSIG)	1204
o	Maximum Average Heat Flux (%)	154
o	Fuel Remains Covered at all Times	

Table 7.6-2

POWER TRANSIENT TEST, 6PMC1

- o BWR/6 MSIV Closure Without Scram
- o No ADS
- o HPCS and RCIC Function
- o Programmed Bundle Power
  - To Simulate the Calculated Rod Surface Heat Flux
- o Trips
  - HPCS On/Off: L2 + 20 Sec/L8
  - RCIC On/Off: L2 + 20 Sec/L8
  - SRV Open/Close: Pressure Setpoints
  - Pump Off: L2 or 1150 PSIG

- -

  - Feedwater Off: 22.5 Sec (44 Sec)
  - Loop Isolation: Pump Trip + 20 Sec

Table 7.6-3

MAJOR EVENT TIMING 6PMC1

Event	Time (s)
Programmed Power Started	0.0
Steam Valve Closure	0.0
Pump Trip	1
First Opening of SRV	1.5
Feed Water Termination	
hot	3
cold	8
Level 2	22
Loops Isolated	40
HPCS, RCIC Initiated	50
Minimum Level	600
Level 8, (HPCS, RCIC Off)	1,355
Bundle Power Terminated	1,580

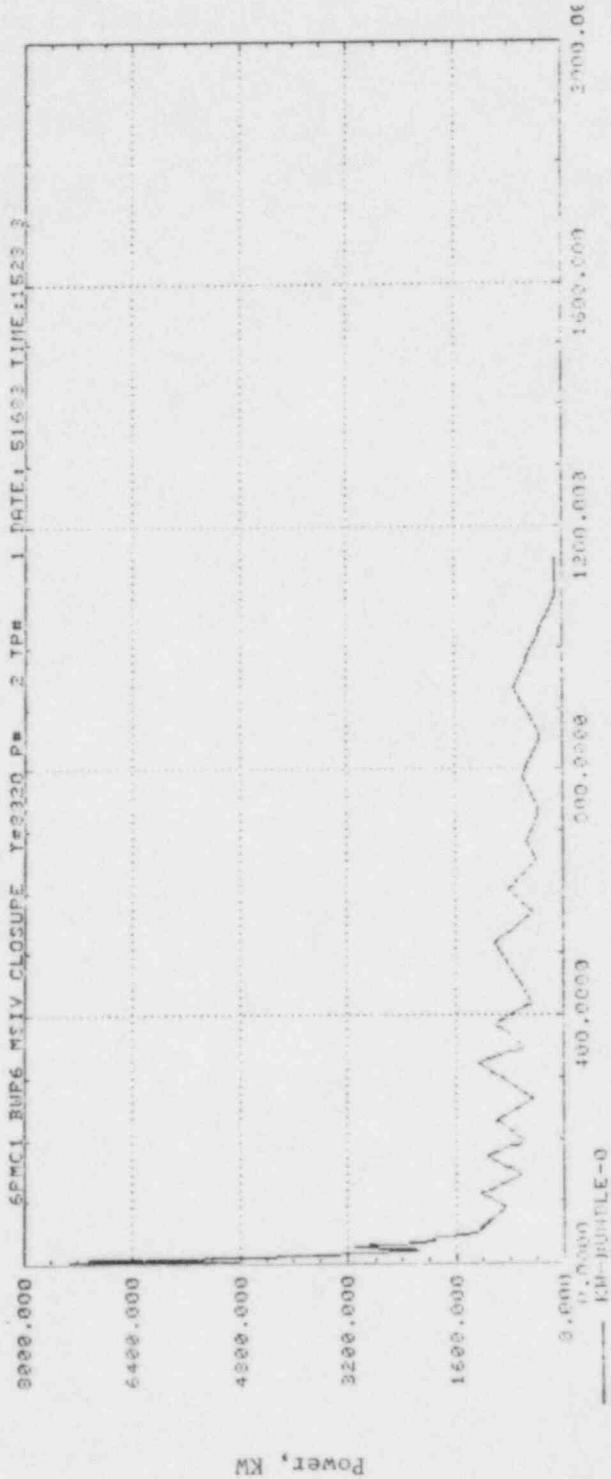

Figure 7.6-1. Bundle Power

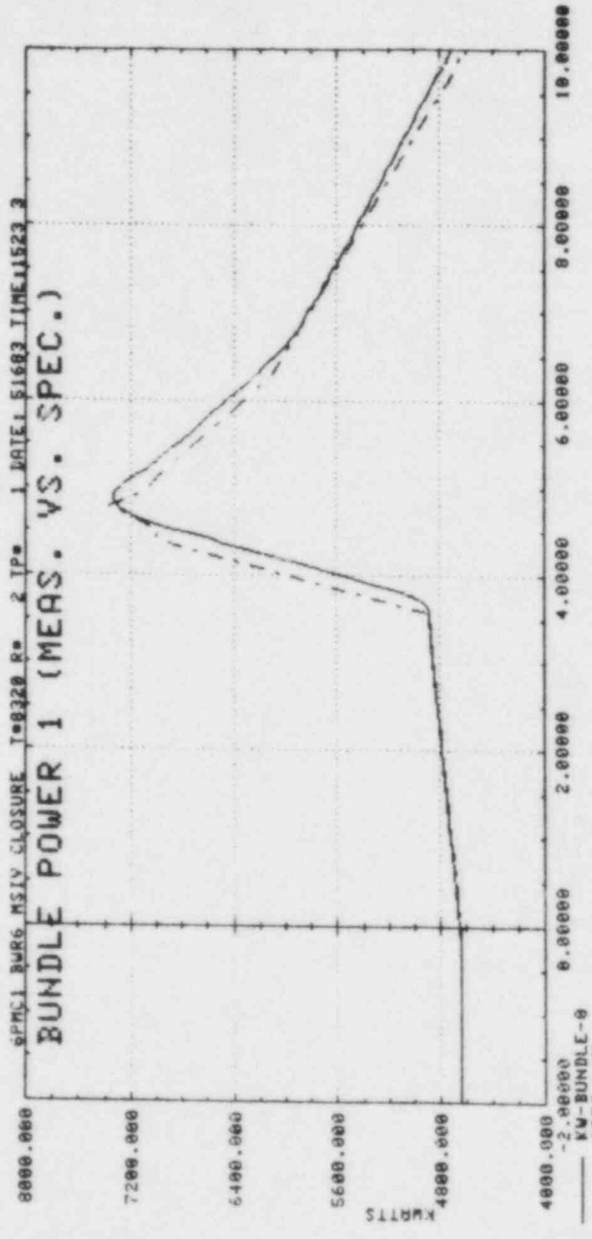

Figure 7.6-2. Bundle Power (Short Term)

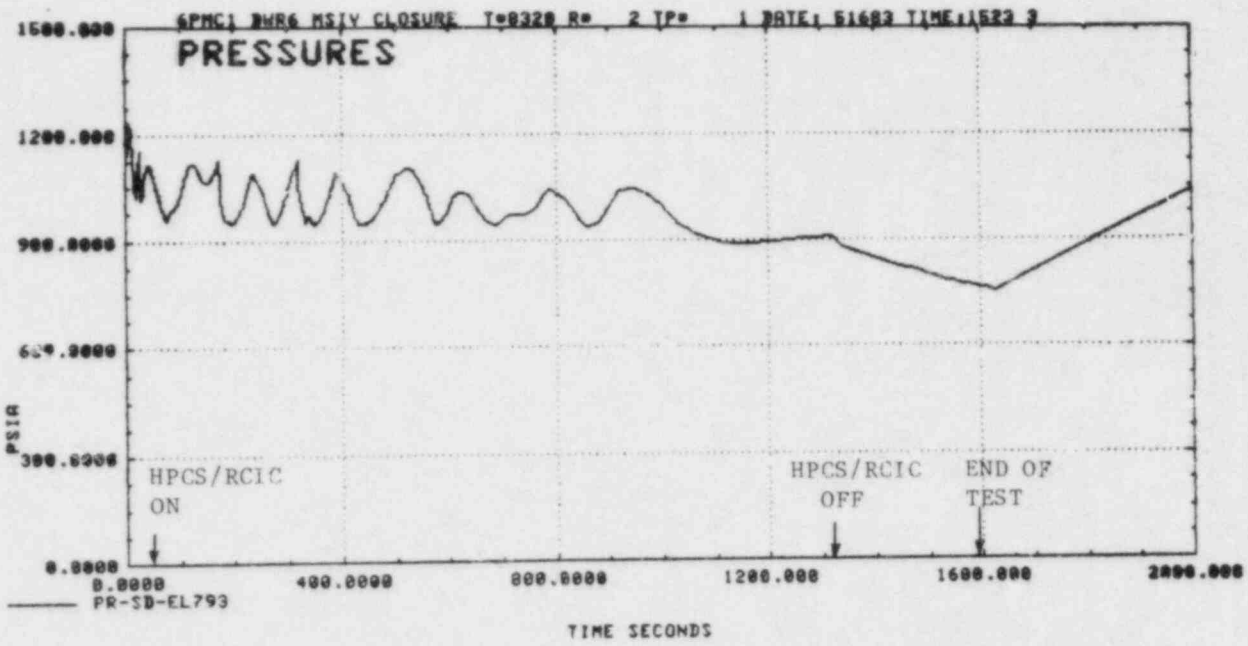

Figure 7.6-3. System Pressure

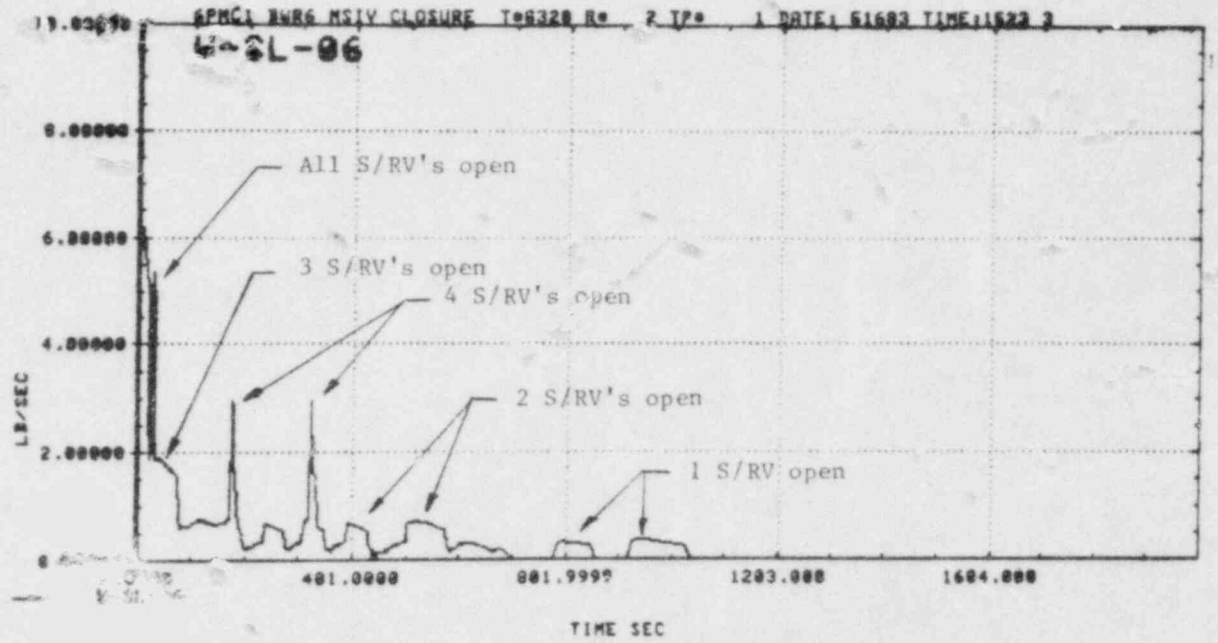

Figure 7.6-4. Steamline Flow

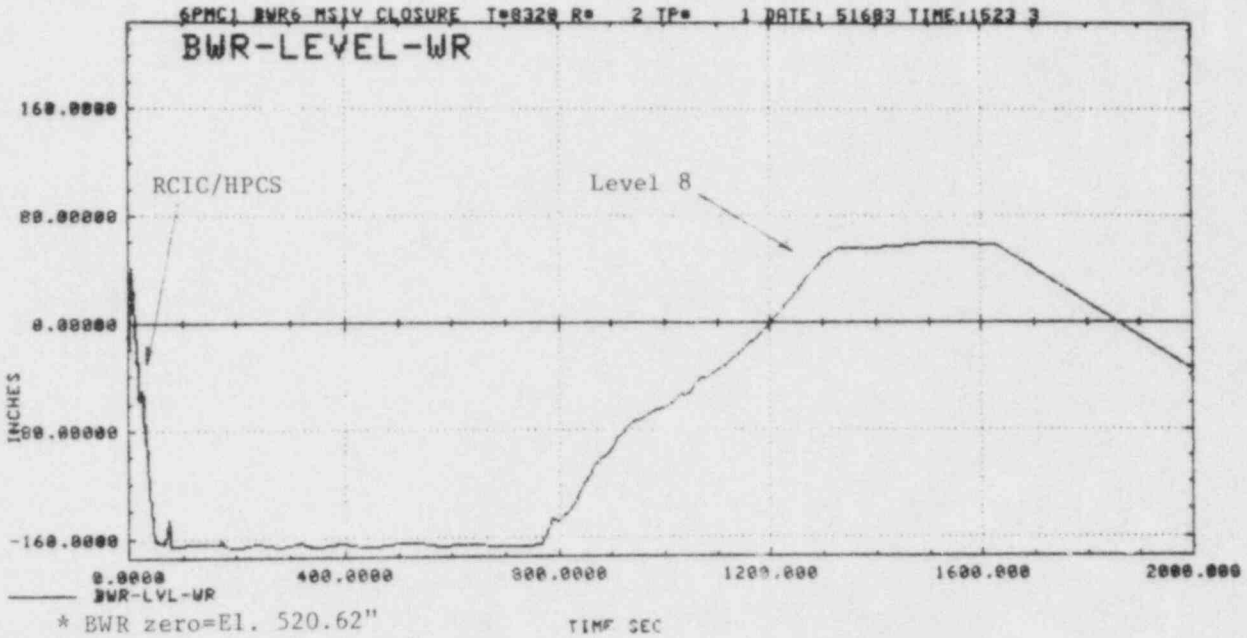

Figure 7.6-5. Downcomer Water Level

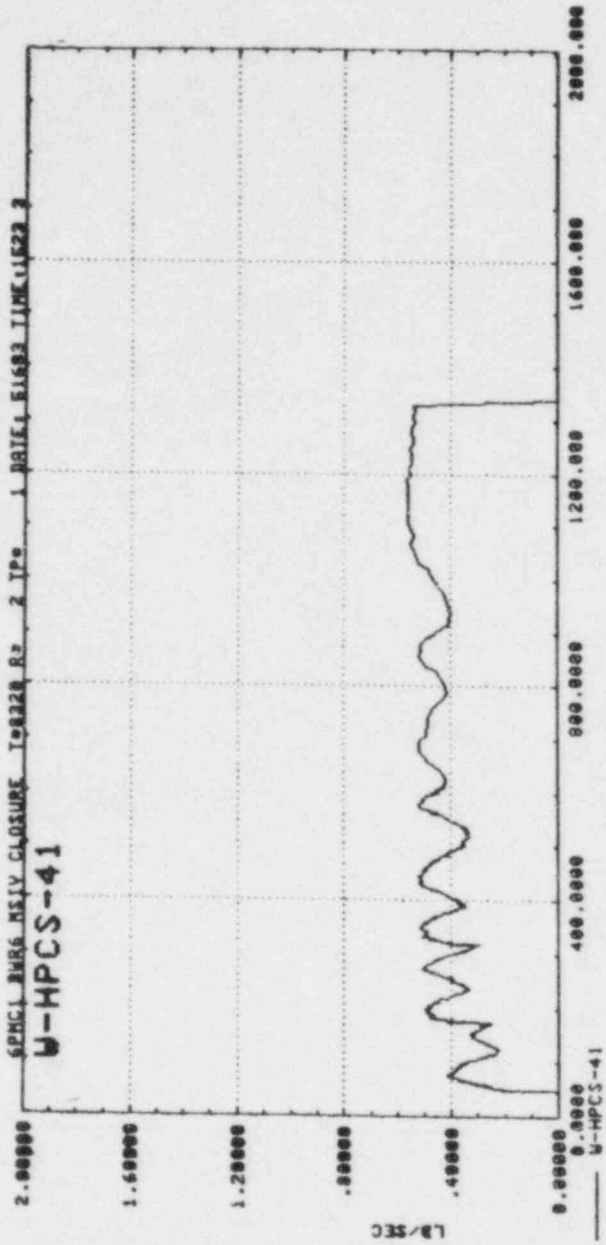

Figure 7.6-6. HPCS Flow

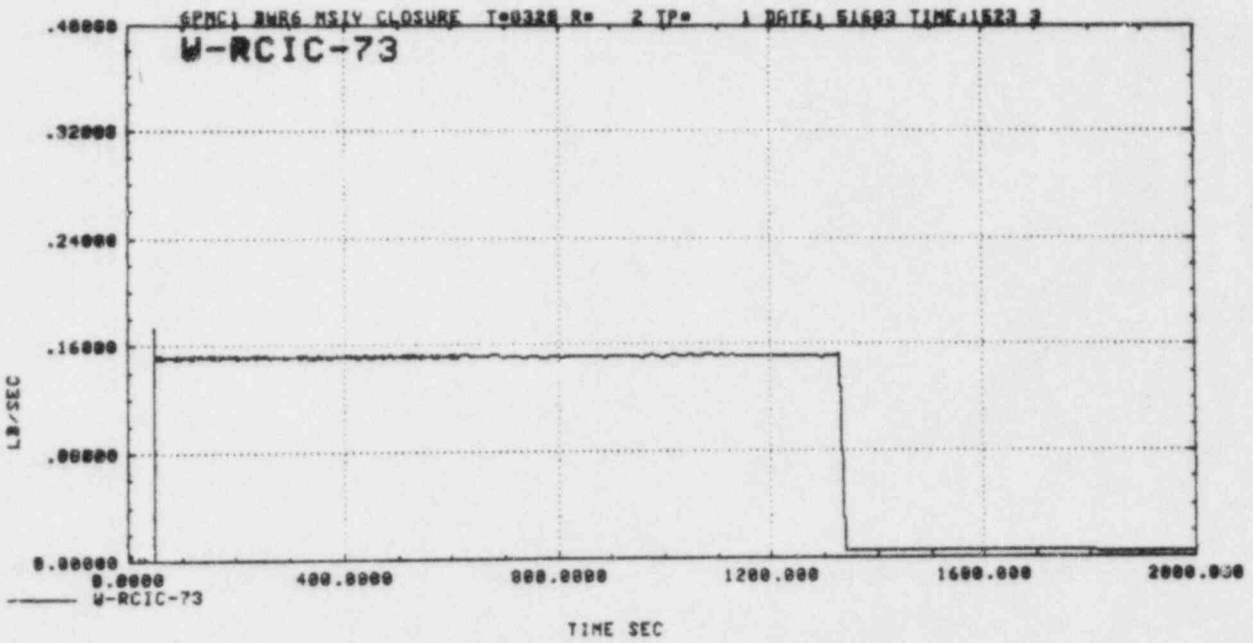

Figure 7.6-7. RCIC Flow

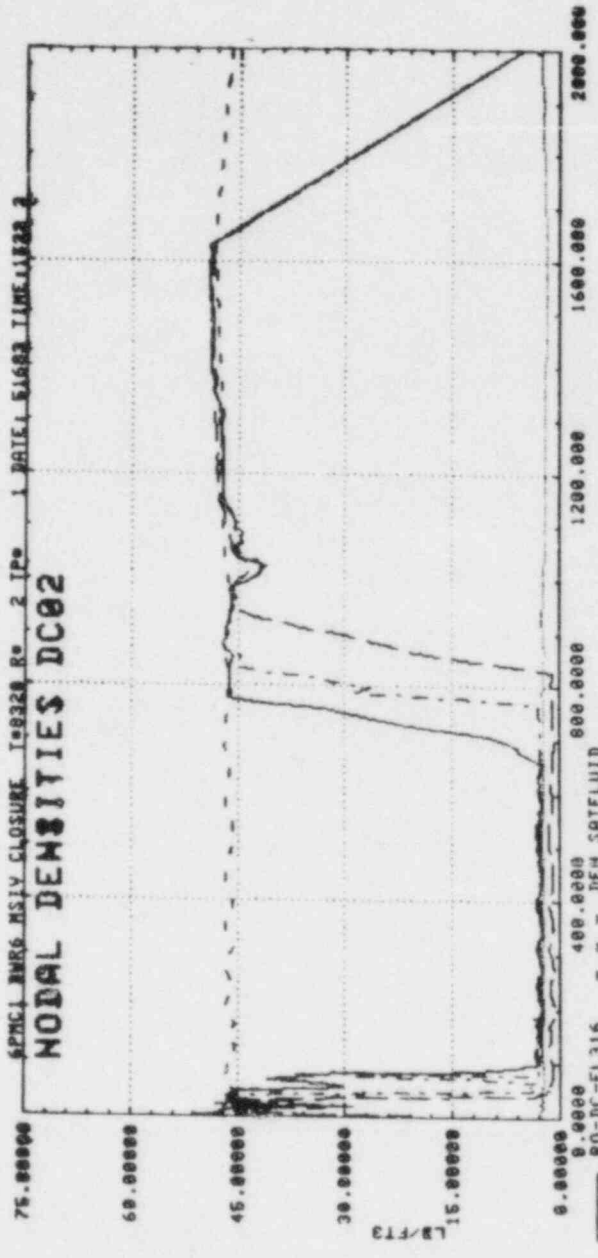

Figure 7.6-8. Nodal Densities in Downcomer Above Top of Jet Pump

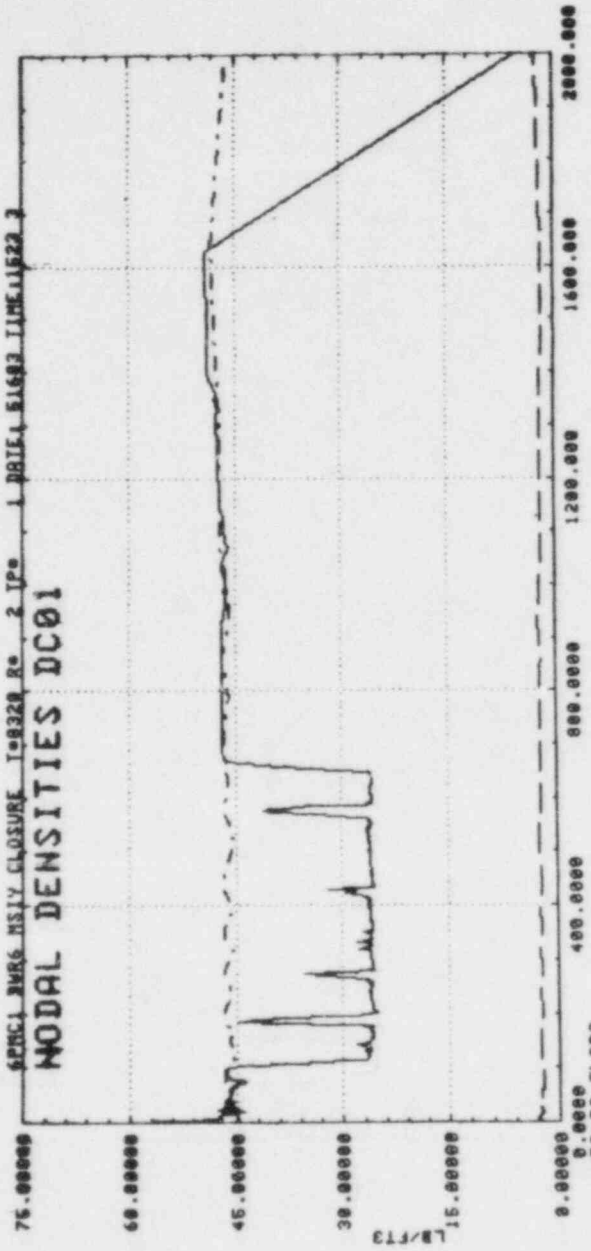

Figure 7.6-9. Nodal Density in Downcomer Near Top of Jet Pump

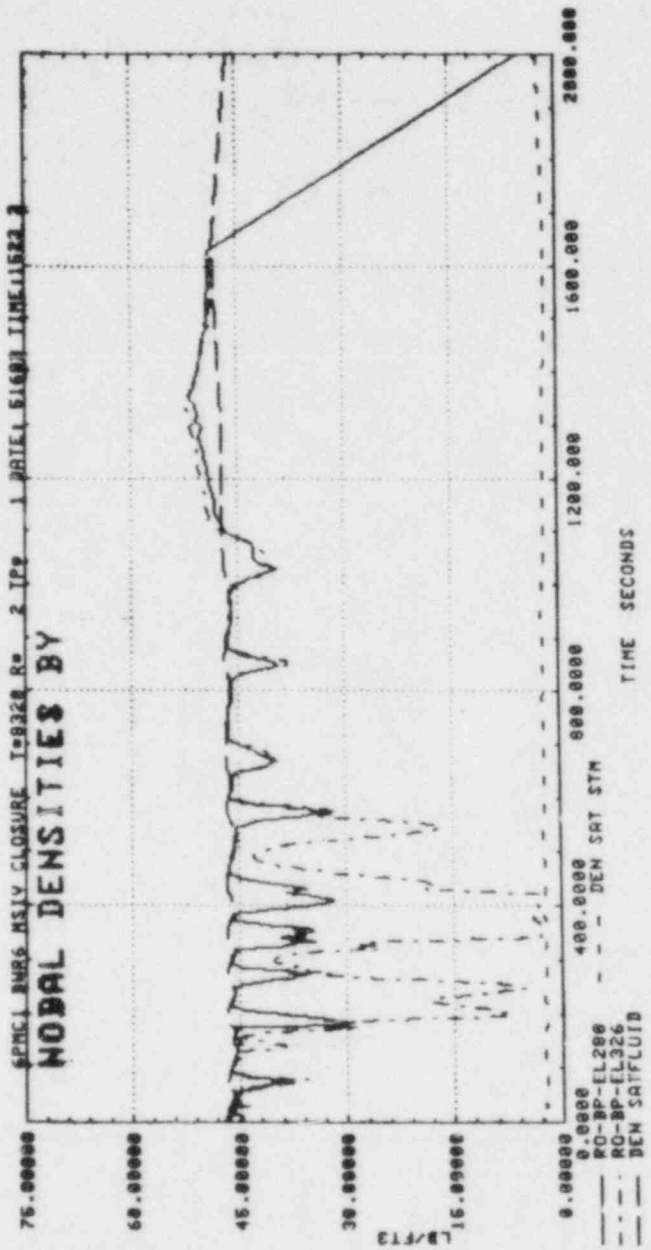

Figure 7.6-10. Nodal Densities in Bypass

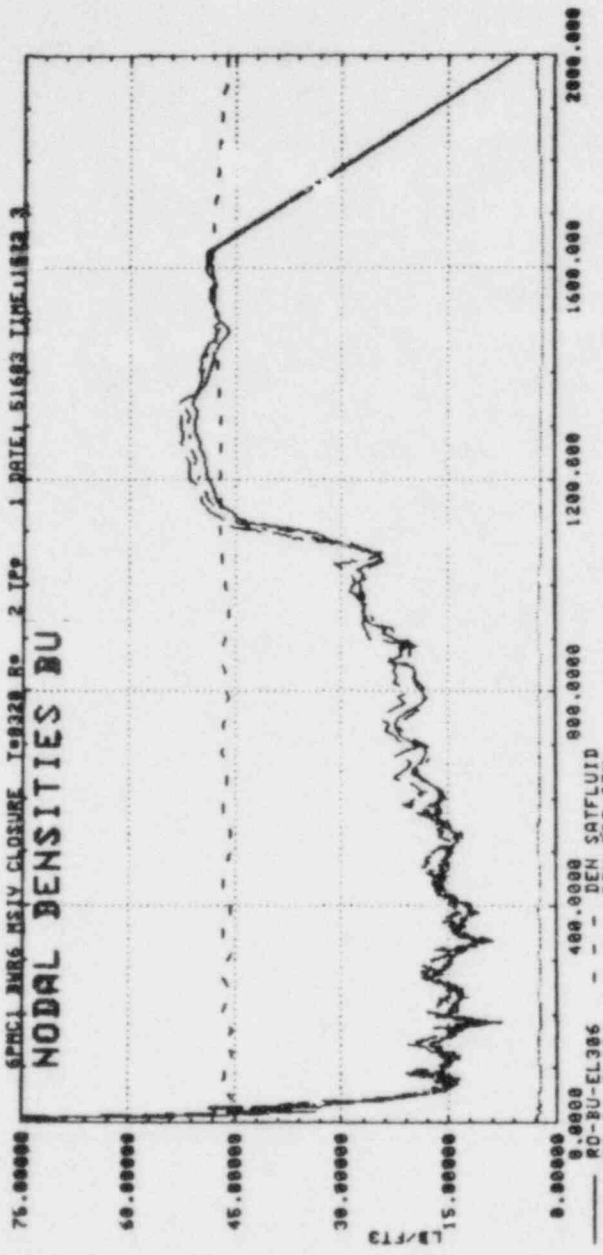

Figure 7.6-11. Nodal Densities in Upper Bundle

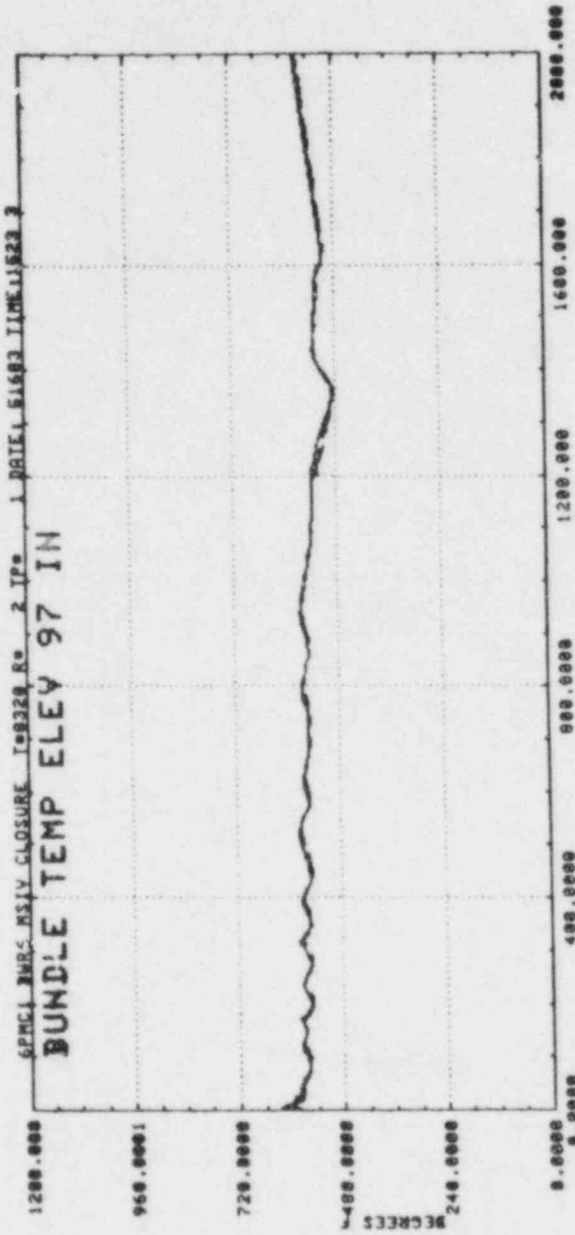

Figure 7.6-12. Rod Temperature

7.7 BWR/6 POWER TRANSIENT WITH MSIV CLOSURE AND NO HPCS TEST, 6PMC2A

7.7.1 General Description

Test conditions of the test 6PMC2A are identical to the test 6PMC1 except that HPCS is assumed to be unavailable. Only the RCIC system is available to supply the make-up water into the downcomer during the test. Without HPCS water entering the core in a BWR, the void fraction in the bundle remains high and thus the bundle power remains at a lower level for the transient.

7.7.2 Bundle Power

Similar to power transient test 6PMC1, the bundle power employed in this test (Figure 7.7-1) is based on a BWR transient code calculation. The bundle power for this test is lower than test 6PMC1 beyond 75 seconds, the calculated HPCS initiation time.

7.7.3 System Pressure and S/RV Operation

Smaller steam generation is expected in this test due to the lower bundle power. A smooth system pressure response (Figure 7.7-2) and no S/RV operation (Figure 7.7-3) are seen beyond about 130 seconds.

7.7.4 Water Level

Water level in the downcomer (Figure 7.7-4) decreases very rapidly in the early transient due to the inventory loss through S/RV activation. Shortly after RCIC initiation (Figure 7.7-5), water level begins to recover and increases continuously until the end of the test.

7.7.5 Nodal Density

Several nodal densities measured in the downcomer, bypass, and bundle are shown in figures 7.7-6 to 9. It can be seen that the node of Downcomer EL 316", (Figure 7.7-6) is always covered and water level

remains above the jet pump (El.311") The bundle and bypass are also covered throughout the transient. As in test 6PMC1, there is no heatup in this test.

7.7.6 Summary (Test 6PMC2A)

The power transient test, 6PMC2A, demonstrates that the power transient without HPCS is much milder than the case with HPCS. Without HPCS water entering the bundle, the bundle void fraction remains high and thus, the bundle power is kept low throughout the transient. This results in less steam generation. S/RV operations and inventory loss are significantly reduced. Water level remains above the jet pump. The core is never uncovered and there is no rod heatup. Water level is completely recovered by RCIC flow.

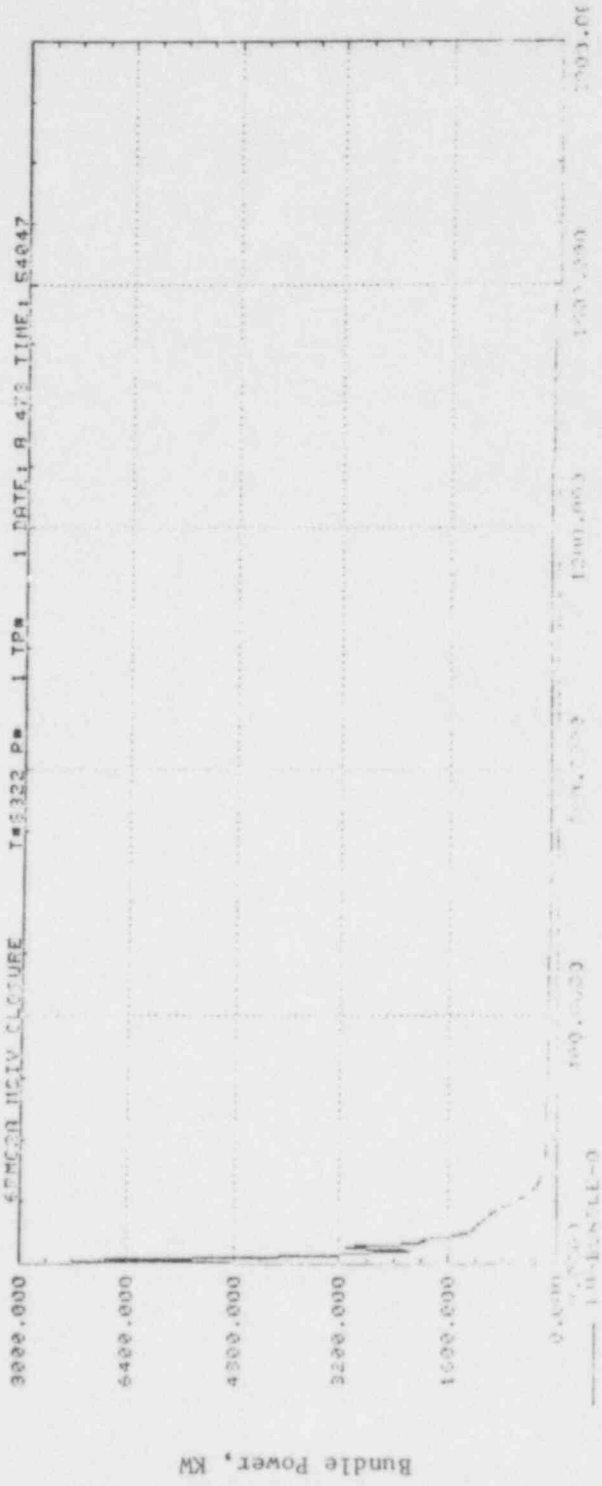

Figure 7.7-1. Bundle Power

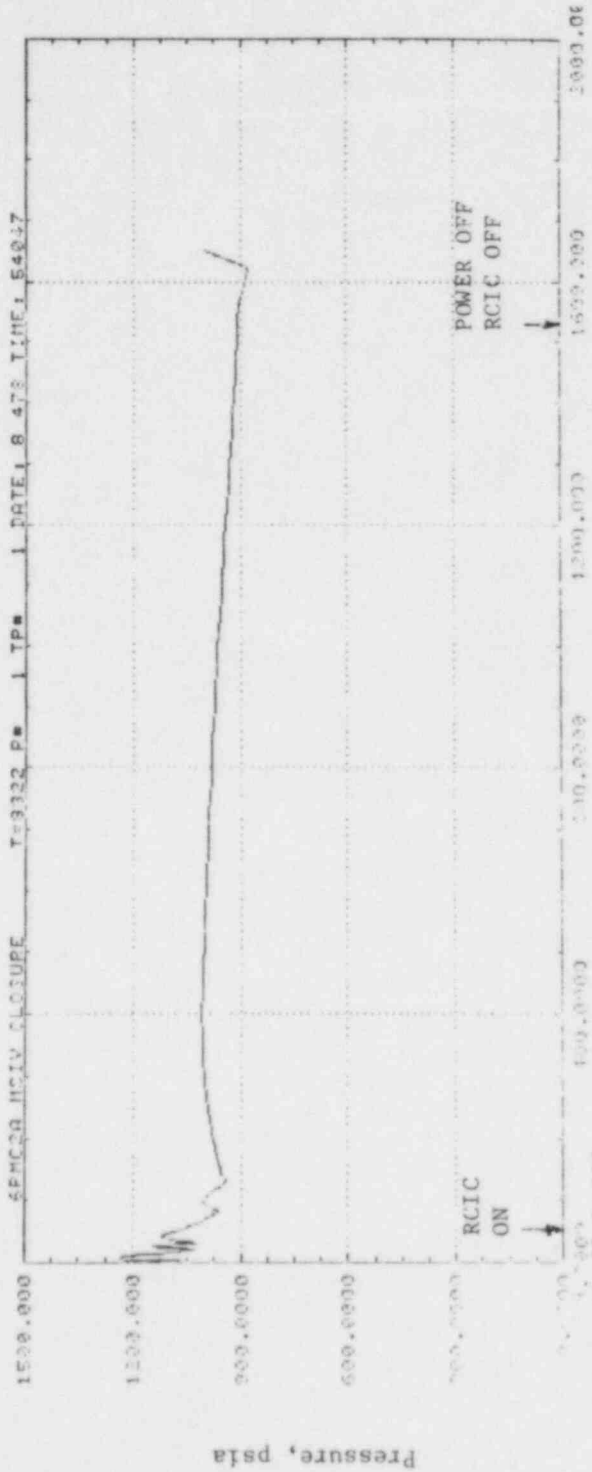

Figure 7.7-2. System Pressure

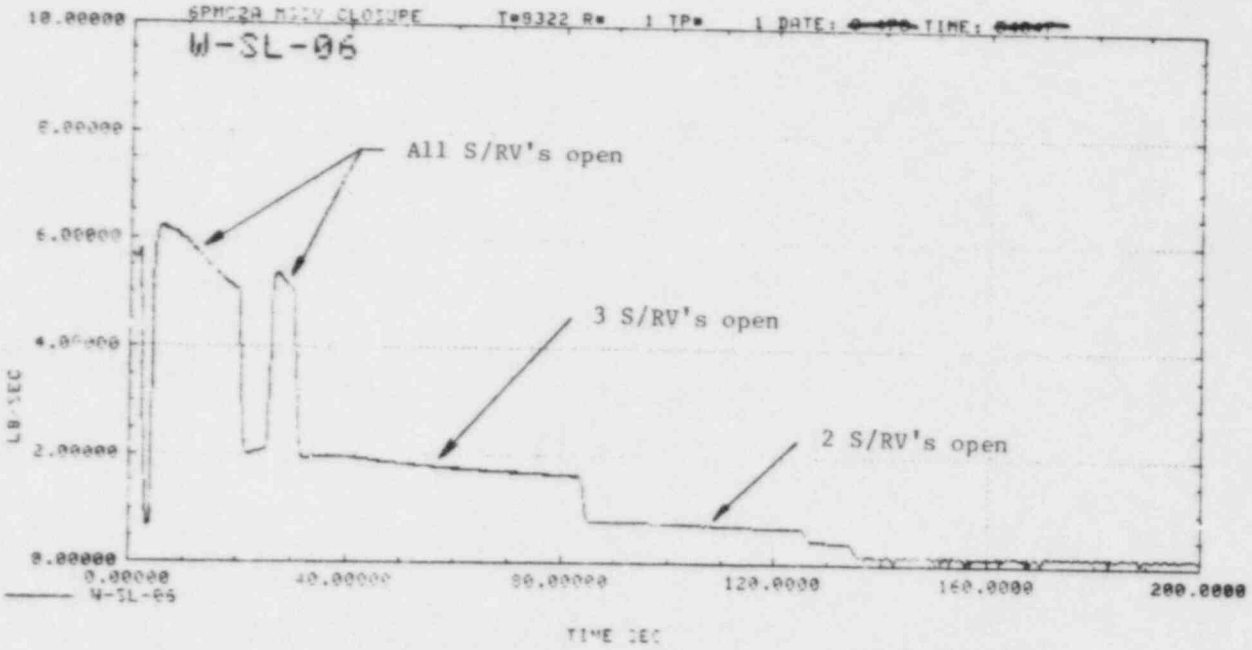

Figure 7.7-3. Steamline Flow

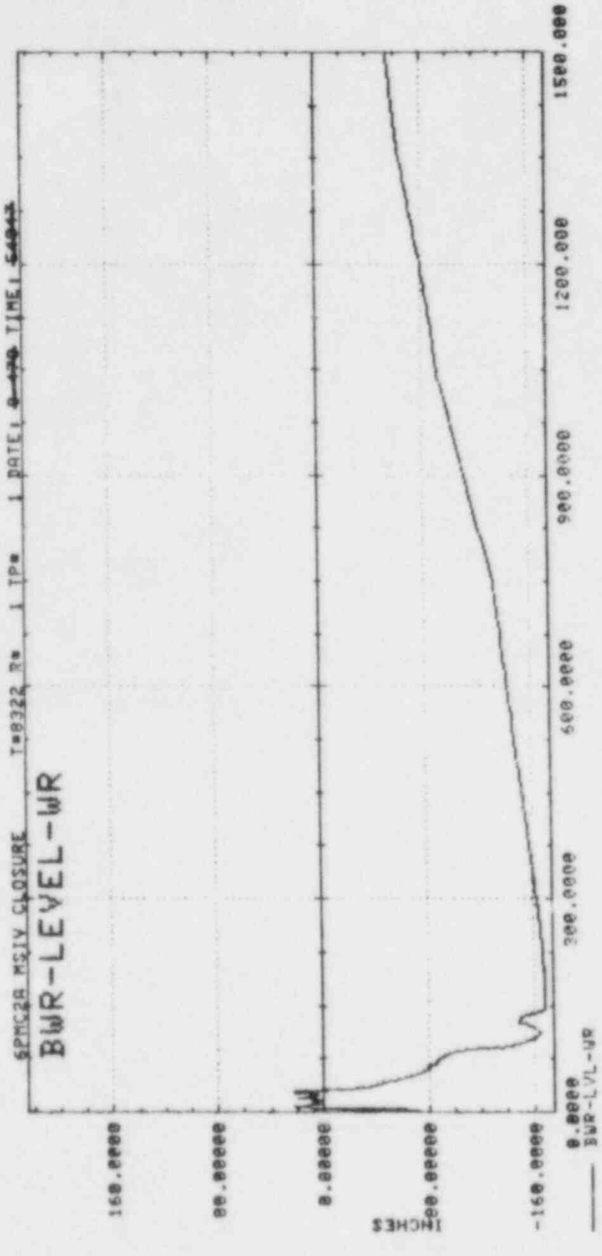

Figure 7.7-4. BWR Wide Range Water Level

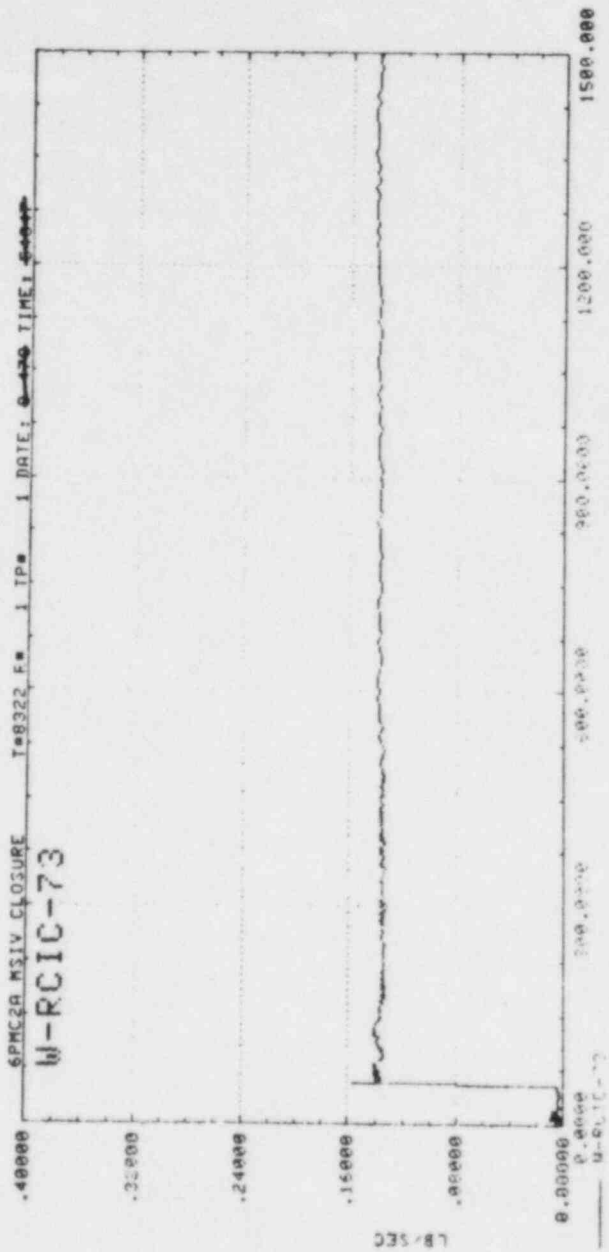

Figure 7.7-5. RCIC Flow

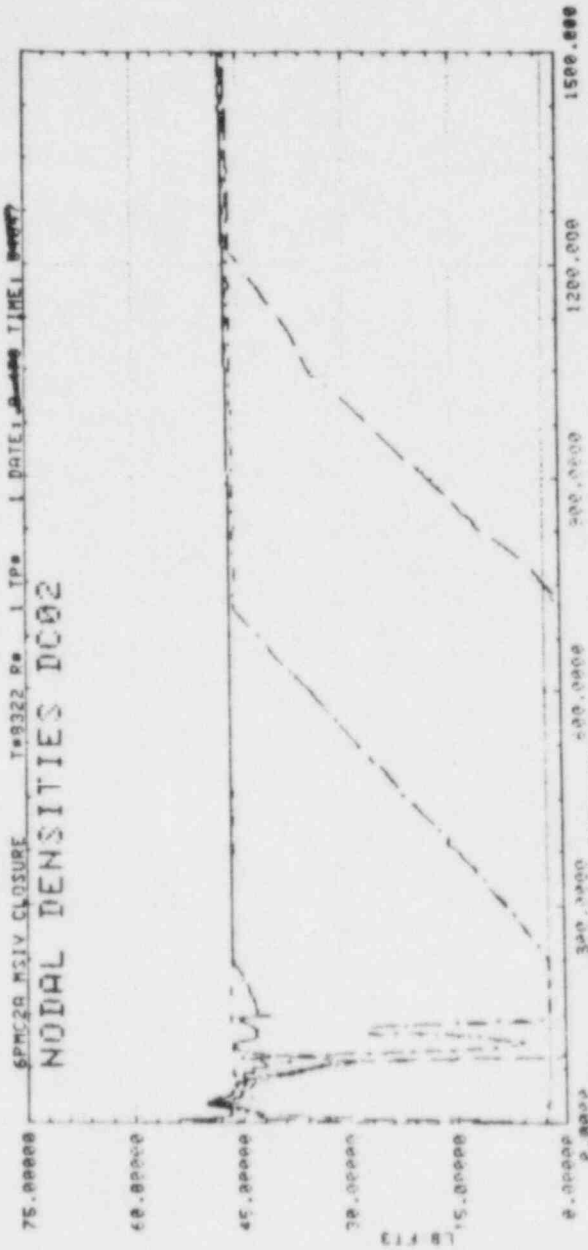

Figure 7.7-6. Nodal Densities in Downcomer Above Top of Jet Pump

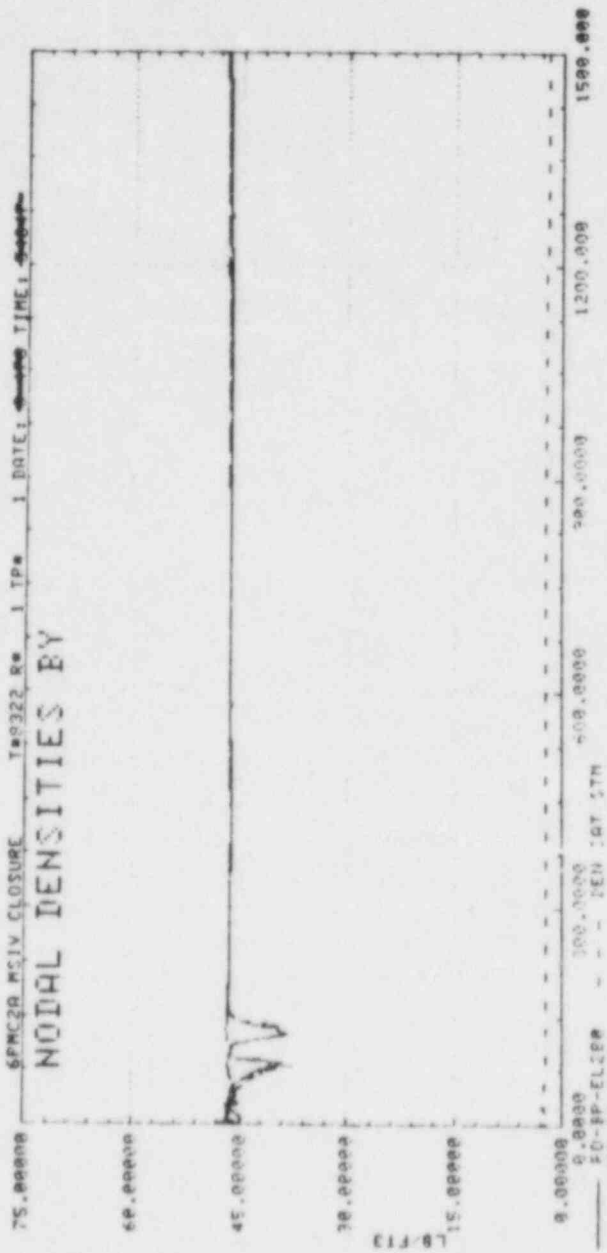

Figure 7.7-7. Bypass Nodal Densities

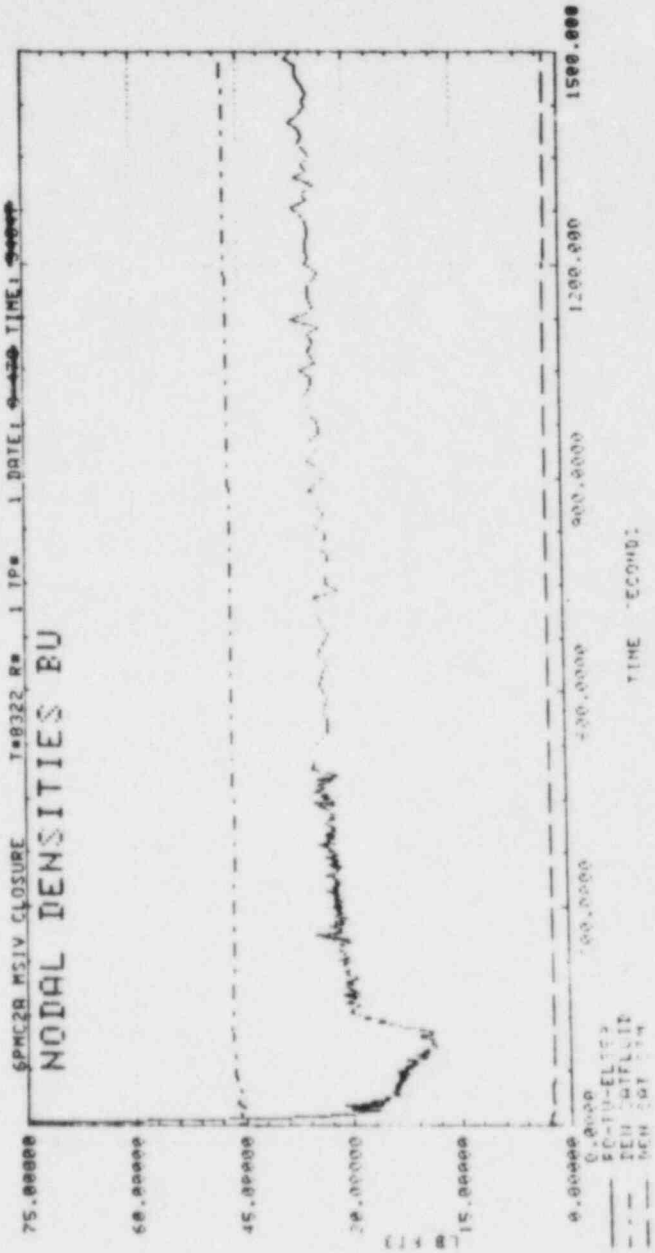

Figure 7.7-8. Nodal Density Near Top of Bundle

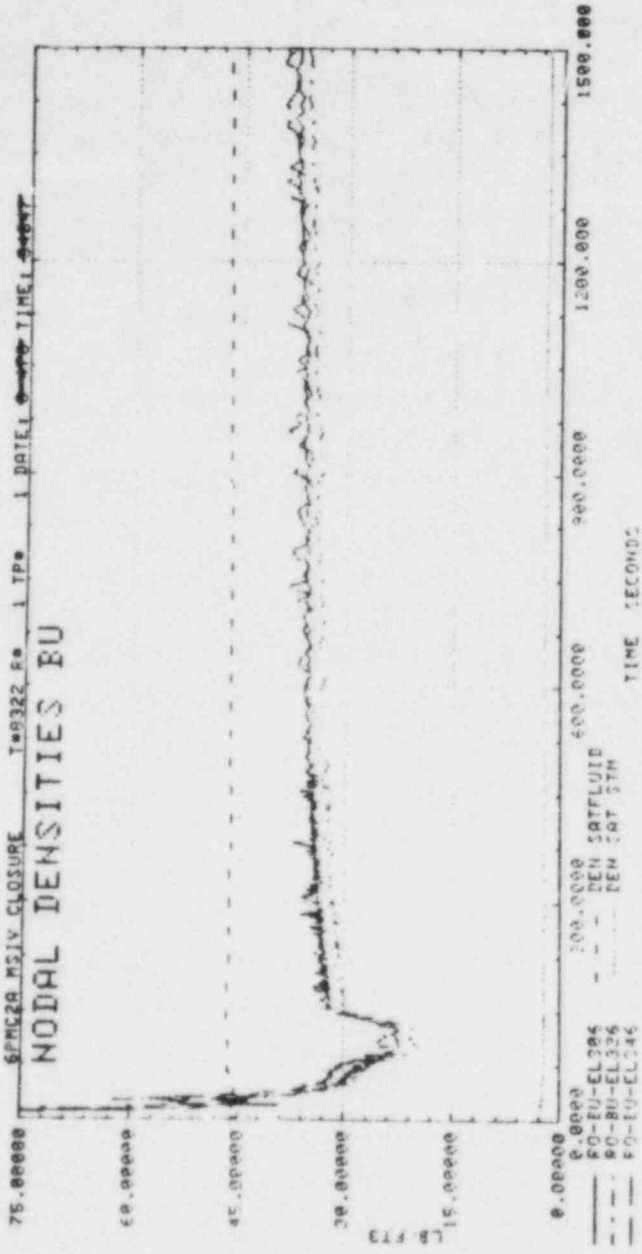

Figure 7.7-9. Nodal Densities in Upper Bundle

7.8 BWR/4 POWER TRANSIENT WITH MSIV CLOSURE TEST, 4PMC1

7.8.1 General Description and Test Simulation

Test 4PMC1 is a power transient simulation test for a BWR/4 with MSIV closure and without power scram. This test is similar to the BWR/6 counterpart test, 6PMC1, which is discussed in Section 7.6. Test conditions and trips of key events are given in Table 7.8-1.

Several components in FIST were modified for simulating a BWR/4. Both HPCI and RCIC flows in this test were injected through the feedwater line into the downcomer, whereas in the BWR/6 test HPCS was directly injected into the upper plenum. The orifice size and pressure setpoints of S/RV's (Tables 4.2-1 and 3) were changed to reflect the S/RV operation in a BWR/4.

Similar to two previous power transient tests, the bundle power used in this test was based on a transient code analysis for a BWR/4 power transient reported in reference 6. Figure 7.8-1 shows the bundle power employed in the test which simulates the calculated core average rod surface heat flux of a BWR/4 response.

7.8.2 Key Events and Pressure

Timings of major events observed in the test are shown in Table 7.8-2. Following the MSIV closure, the system pressure (Figure 7.8-2) increases very rapidly due to system isolation and steam generation from the bundle power surge. All five S/RV's open (Figure 7.8-3), resulting in a decreasing system pressure. The S/RV operation switches to the low/low set control at 10 seconds. The system pressure is then kept within the pressure range of the low/low set control by operating the S/RV valves.

7.8.3 Water Level

Water level response in the downcomer (Figure 7.8-4) indicates that level 2 is reached at 29 seconds, which activates the HPCI/RCIC injection with a time delay of 20 seconds (Figure 7.8-5). The injection of makeup water leads to the level increasing beyond 50 seconds and water level eventually reaches level 8 at 965 seconds. As in a BWR/4, HPCI/RCIC flow is terminated at level 8.

7.8.4 Bundle Response

As observed in the BWR/6 power transient test, the bundle is always covered and no rod heatup is observed in this test. Nodal void fraction responses in the bundle are shown in Figures 7.8-6 to 10. Void fraction of the nodes in the middle of the bundle shows only small variations in response to the system pressure and power swings (Figures 7.8-1 and 2).

7.8.5 Summary (Test 4PMC1)

Similar to the previous two tests, results of the present test show that the core of a BWR/4 is always covered and there is no rod heatup during a power transient. The system inventory is completely recovered with HPCI and RCIC injections.

Table 7.8-1

BWR/4 POWER TRANSIENT TEST, 4PMC1

- MSIV Closure Without Power Scram
- No ADS Activation
- HPCI/RCIC Functional
- Programmed Bundle Power
- Trips
  - Power: 0 Sec
  - Pump: L2 or P = 1150 PSIG
  - HPCI/RCIC: L2 + 20 Sec
  - Feedwater: 8 Sec
  - BWR/4 S/RV Setpoints

Table 7.8-2
MAJOR EVENT TIMING 4PMC1

Event	Time (Sec)
Start of Programmed Power	0
Steamline Valve Closure	2
First Opening of SRV	3
Pump Trip	3
Maximum Pressure in Vessel	4
Feedwater Termination	
Hot	5
Cold	8
Level 2	29
RCIC and HPCI Initiation	49
Minimum Level	49
Level 8	965
RCIC and HPCI Off	965
Bundle Power Off	1587
Test Termination	1640

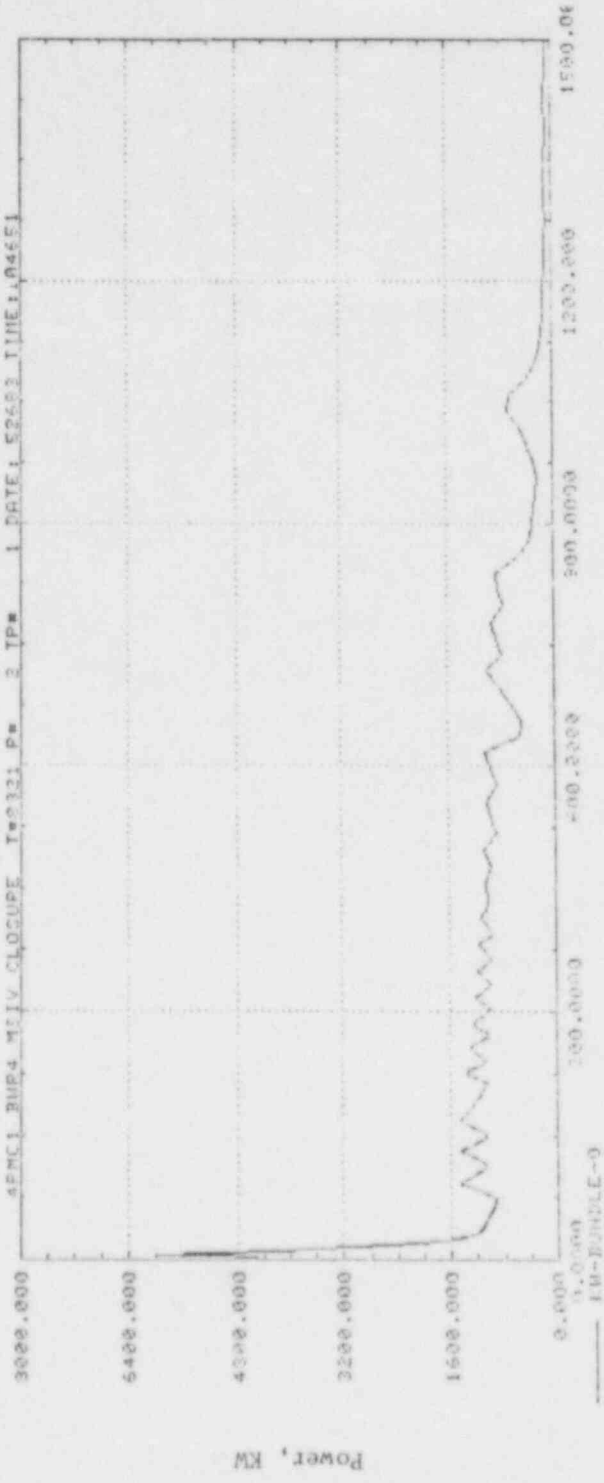

Figure 7.8-1. Bundle Power

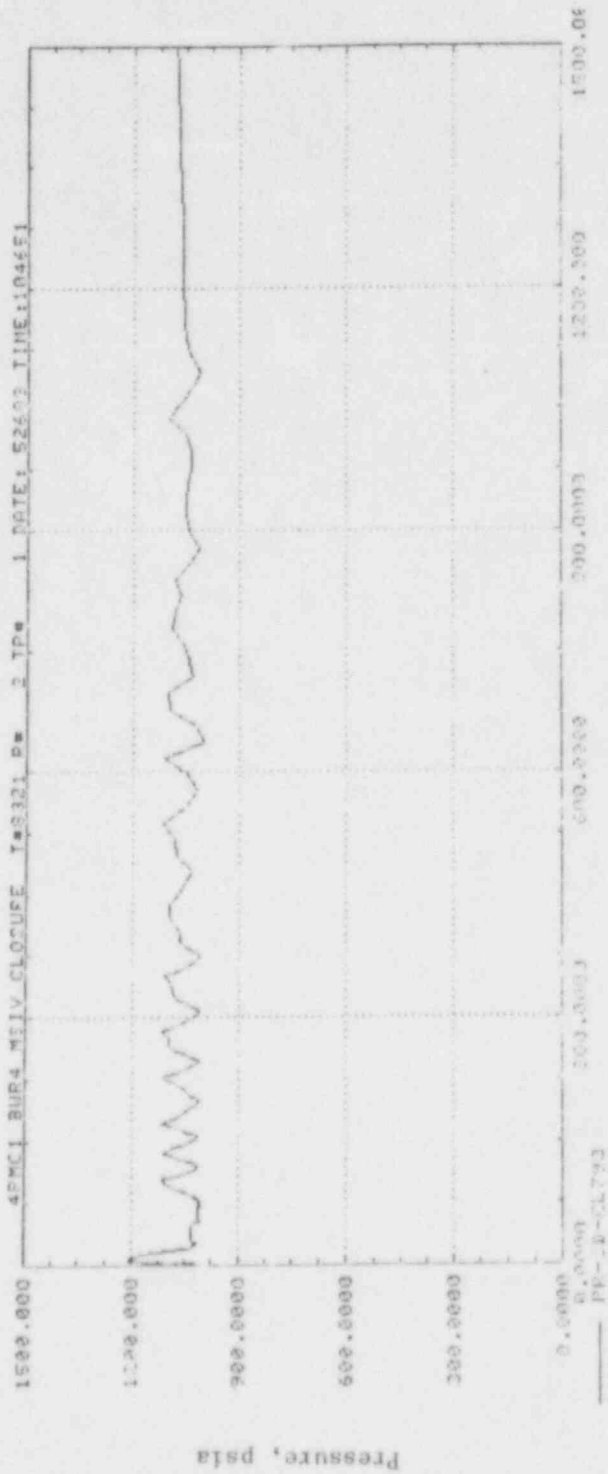

Figure 7.8-2. System Pressure

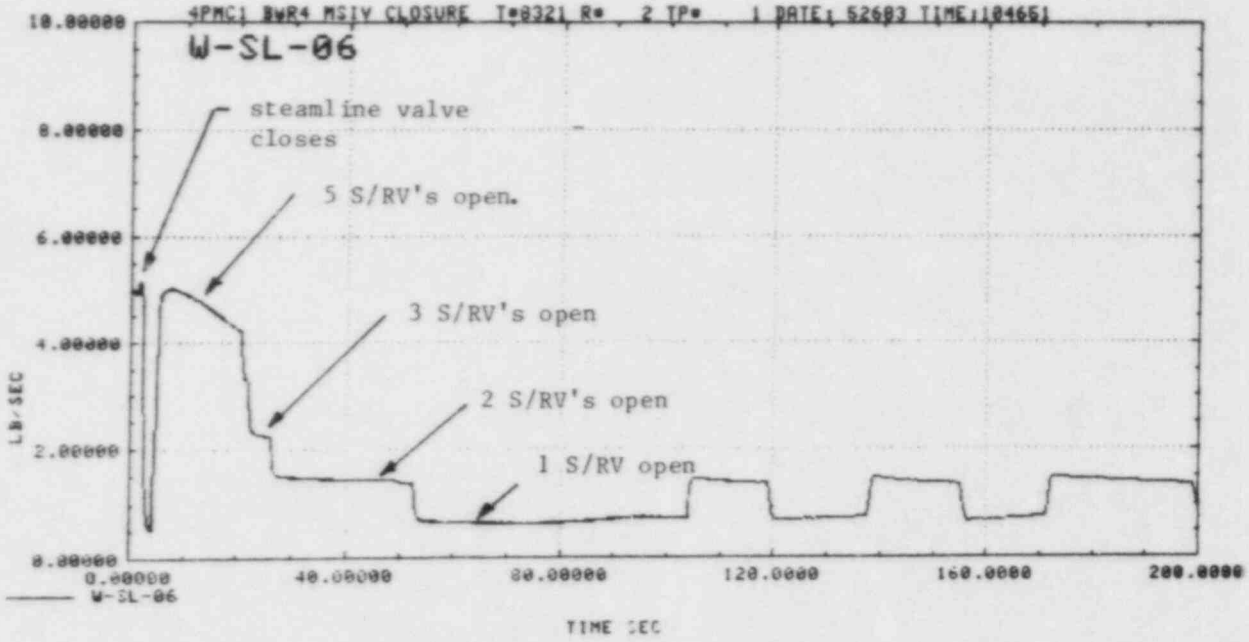

Figure 7.8-3. Steamline Flow

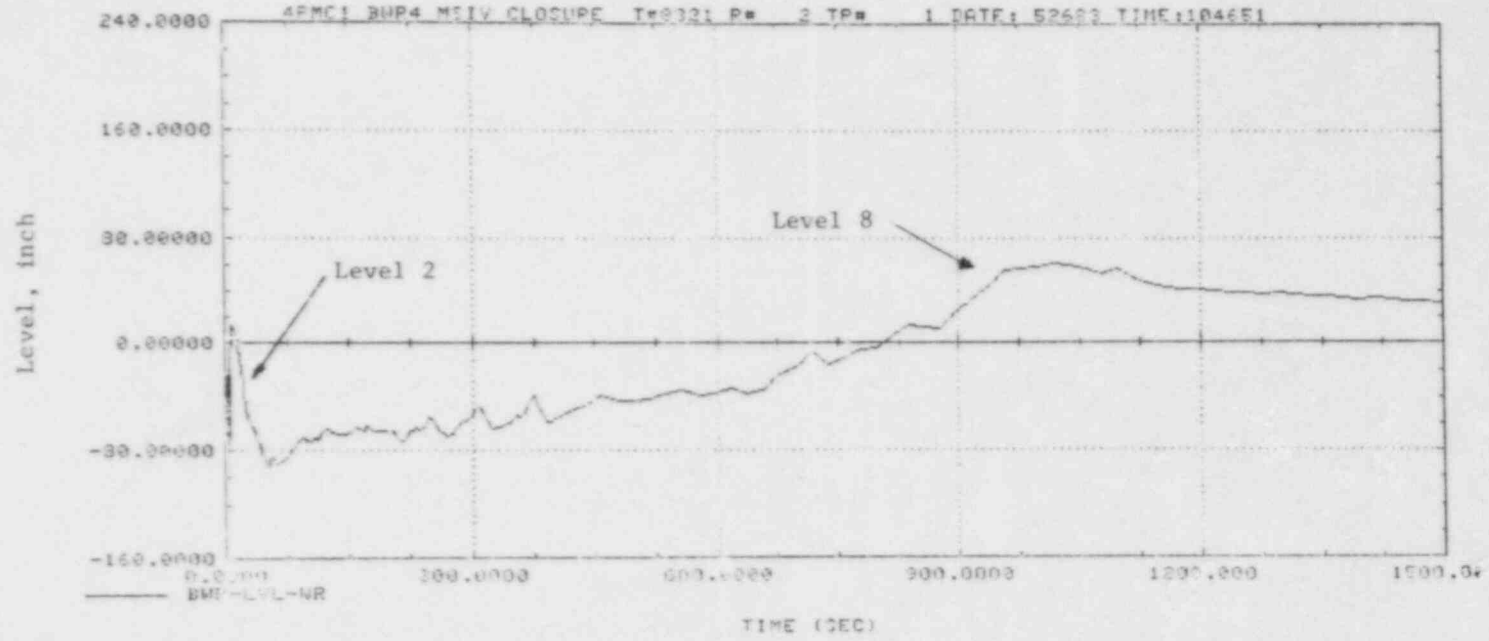

Figure 7.8-4. Downcomer Water Level

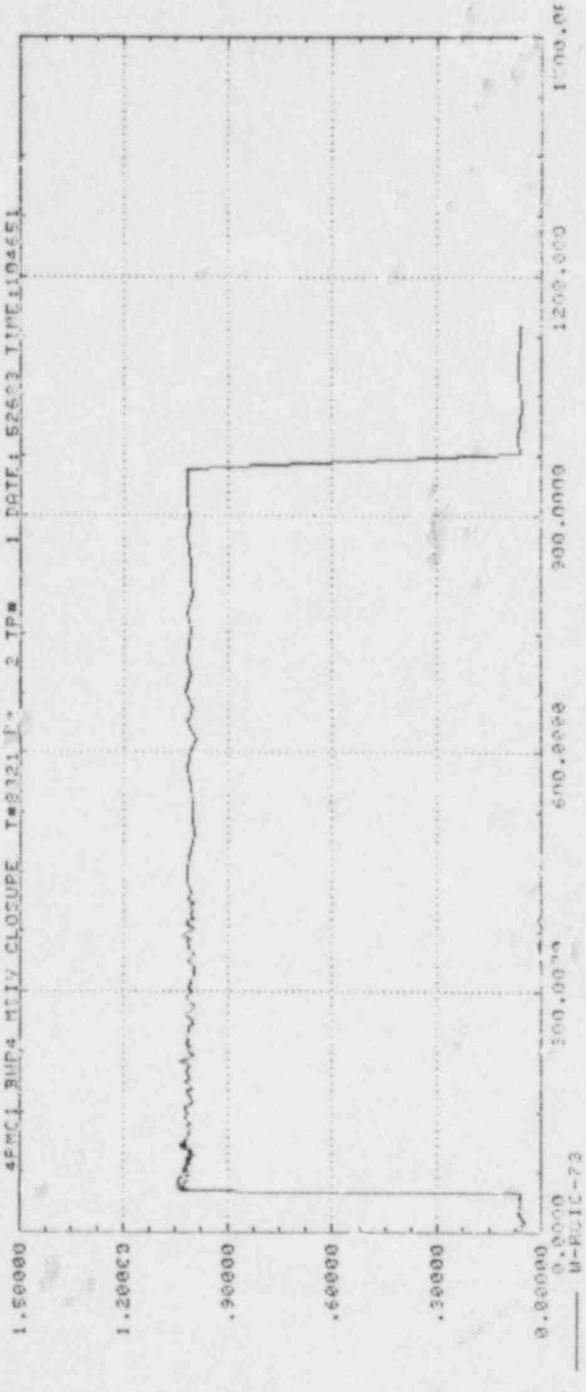

Figure 7.8-5. HPCI/RCIC Flow

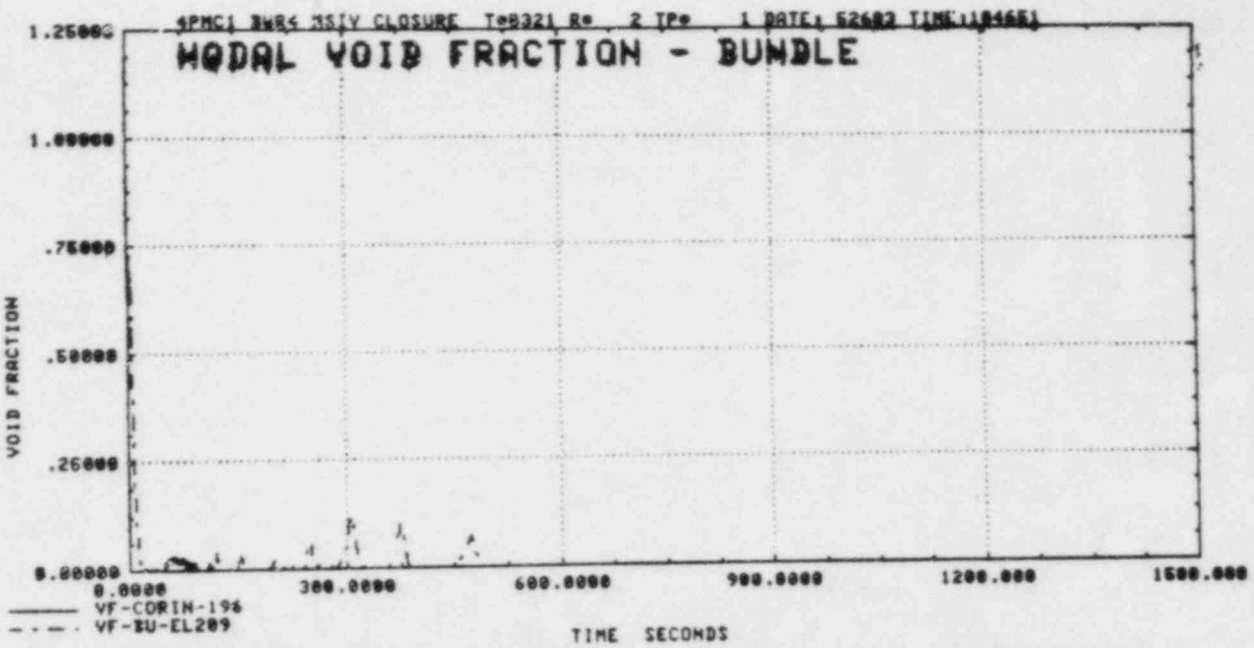

Figure 7.8-6. Bundle Nodal Void Fraction, El. 196" to 225"

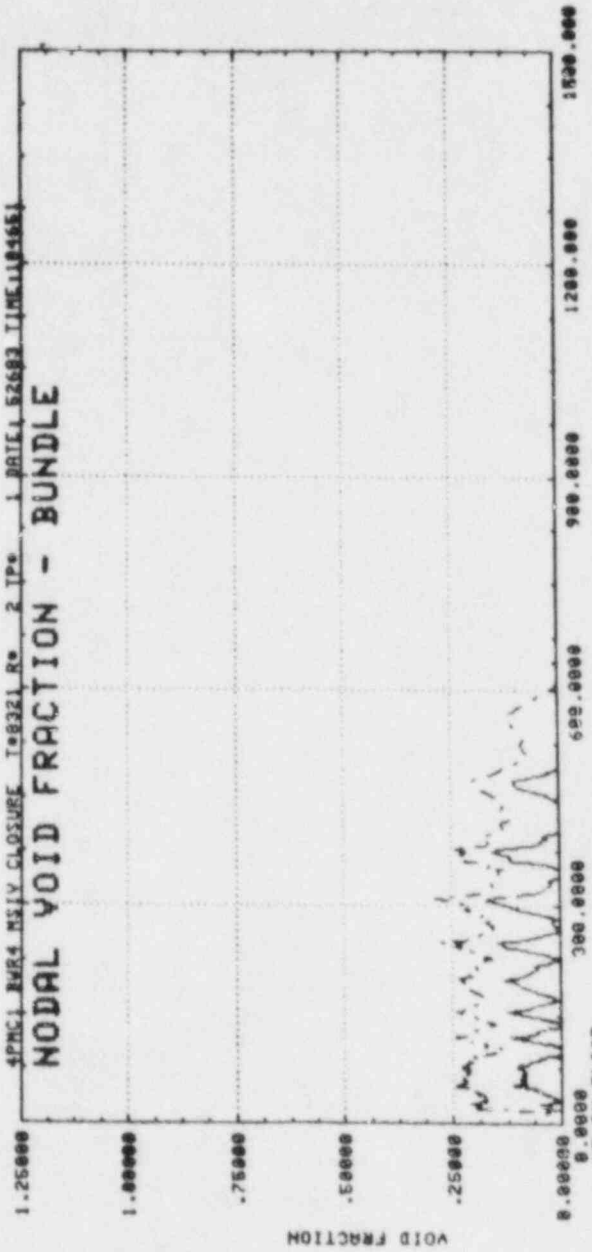

Figure 7.8-7. Bundle Nodal Void Fraction, El. 225" to 266"

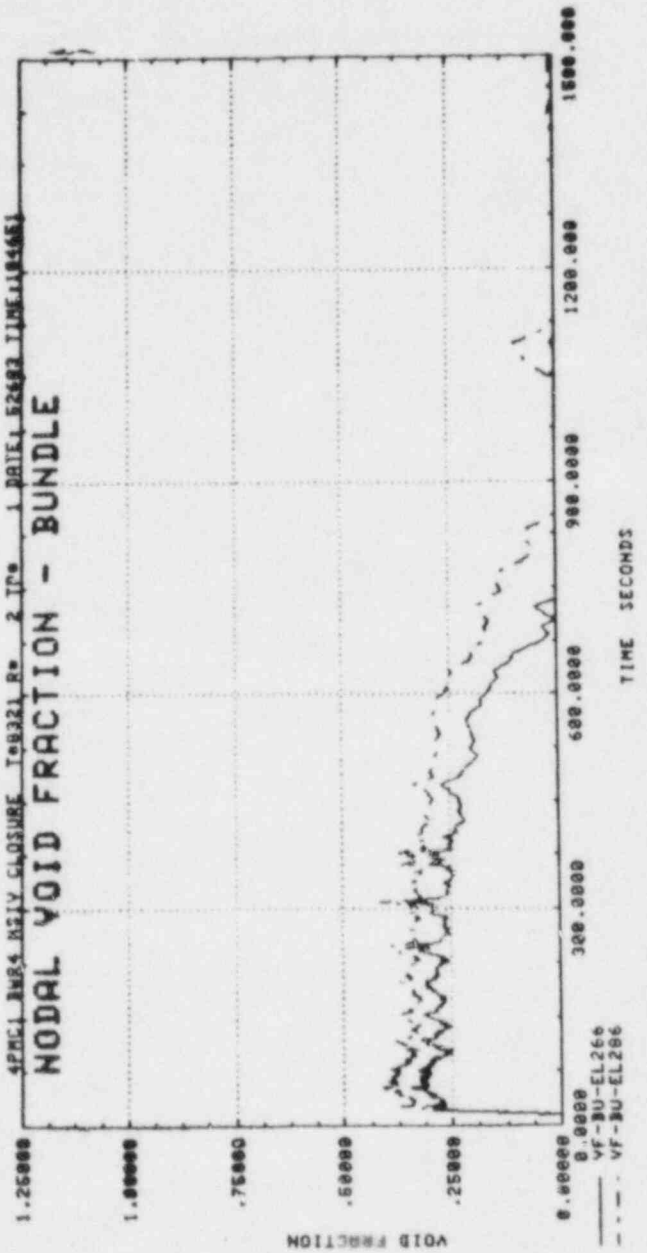

Figure 7.8-8. Bundle Nodal Void Fraction, El. 266" to 306"

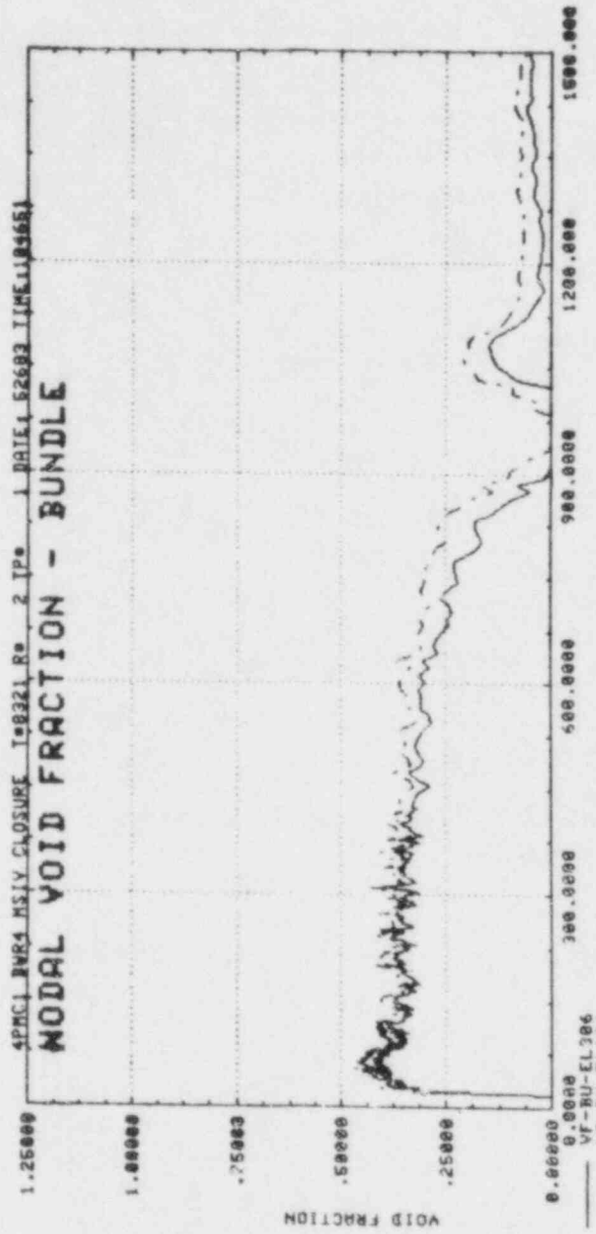

Figure 7.8-9. Bundle Nodal Void Fraction, El. 306" to 346"

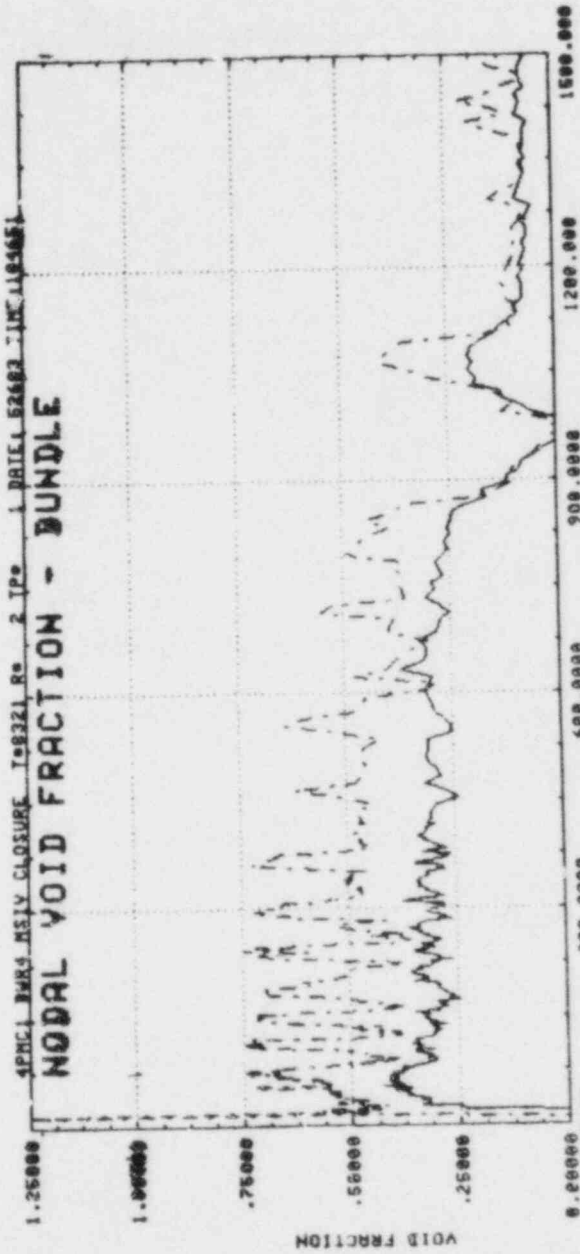

Figure 7.8-10. Bundle Nodal Void Fraction, El. 346" to 368"

8. COMPARISONS OF TLTA TIEBACK TESTS

The FIST phase I includes two TLTA tieback tests: a large break, 6DBA1B, and a small break, 6SB2C. These tests were performed to identify similarities and/or differences in the system responses between the corresponding tests.

Details of the system performance and governing phenomena of each test are given in References 3 and 4 for the TLTA tests and Sections 7.1 and 7.2 of this report for the FIST tests. Highlights and comparisons of these tests are discussed in this section.

8.1 LARGE BREAK TESTS, FIST 6DBA1B VS. TLTA 6425/R2

8.1.1 General Description

Large break test, 6DBA1B, is a counterpart test of the TLTA reference test, 6425/R2. Both tests were conducted with similar test conditions, except for initial water level elevation due to facility differences.

8.1.2 Pressure

Good agreement in the system pressure is seen in Figure 8.1-1, which leads to the same ECCS initiations and performance (Figures 8.1-2 to 4) in both tests.

8.1.3 Mass Distribution

Comparison of total system mass (Figure 8.1-5) indicates that more water remains in FIST, particularly during the refill/reflood phase of the transient. This is mainly attributed to the larger jet pump height. FIST has full height jet pumps, whereas the TLTA jet pumps are relatively short. Thus, the FIST jet pumps hold more water inside the shroud, resulting in less inventory loss through the break.

This jet pump effect on mass transfer across the shroud can be seen clearly in the regional mass comparisons (Figures 8.1-6 to 11). While FIST has less mass in the downcomer, more mass is seen in the lower plenum, bundle, and upper plenum as compared with the TLTA test. Fluctuations in the regional mass responses observed in FIST during the reflood period are discussed in Section 7.1 These fluctuations are caused by stored heat, particularly in the bypass region. A smooth refill/reflood is seen in the TLTA core region. Since the TLTA bypass consisted of four tubes which were separated from the vessel wall and bundle channel, there was no stored heat effect on the TLTA bypass hydraulic response.

Another significant effect of the bypass configuration and stored heat is on the bundle refill/reflood process. Both the bundle and bypass of FIST are refilled at about the same time by subcooled CCFL breakdown at the top of the core. The bypass in TLTA is refilled first, immediately following LPCI injection, and the bundle is then reflooded with water entering from the bypass leakage and the upper tie plate. Governing phenomena for these refilling and reflooding processes are discussed in Reference 3 and Section 7.1 of this report.

8.1.4 Rod Temperature

Rod temperature responses are compared in Figures 8.1-12 to 8.1-16. Both tests show rod heatups and similar responses. The measured PCT is less than 800°F in both tests.

8.1.5 Key Events

Table 8.1-1 is a comparison of timings of key events observed in the two experiments. The blowdown responses and ECCS initiations between the two tests are nearly identical. Differences in the refilling/reflood processes affect the hydraulic responses in the core during that period. The FIST test has a slight delay in beginning the core refill. However, both tests complete the core reflood at about the same time.

8.1.6 Summary

These comparisons, plus a review of the test responses and governing phemomena discussed in Reference 2 and Section 7.1 of this report, identify the similarity and difference between the FIST and TLTA large break tests. These observations are summarized in Table 8.1-2.

Table 8.1-1
SEQUENCE OF EVENTS FOR TLTA 6425 RUN 2 AND FIST 6DBA1B

Events	TLTA 6425/R2 Time (sec)	FIST 6DBA1B Time (sec)
Blowdown Valves Open	0.0	0.0
Bundle Power Decay Initiated	0.5	0.1
Bypass Flow Reverses	1.7	1.0
Jet Pump Suction Uncovers	6.7	5.0
Recirc. Suction Line Begins To Uncover	9.4	8.0
Lower Plenum Bulk Flashing	11.0	11.5
Guide Tube Flashing	11.2	12.0
Loop 1 Isolated	20.0	13.0
HPCS Injection Begins	27.0	27.0
LPCS, LPC1 Activated	37.0	35.0
LPCS Flow Begins	64.0	64.0
LPC1 Flow Begins	75.0	75.0
Bypass/Guide Tube Region Begins to Refill	85.0	115.0
CCFL Break Down at Bypass Outlet	95.0	115.0
Bundle Begins to Refill	114.0	125.0
Bypass Region Refilled	125.0	125.0
Bundle Reflood with Two-Phase Mixture	130.0	125.0
CCFL Breaks Down at Upper Tie Plate	125.0	125.0
Bundle Quenched	150.0	125.0
End of Test	480.0	320.0

TABLE 8.1-2

SUMMARY (FIST 6DBA1B VS. TLTA 6425/R2)

- o Similar Blowdown Responses
  - CCFL at SEO, UTP, Top of Guide Tube and Top of Bypass
  - Rod Heatup
- o CCFL Breakdown
  - TLTA: First at Top of Bypass After LPCI, Then at UTP After Bypass Refilled
  - FIST: Both Top of Bypass and UTP by Upper Plenum Subcooled Water
- o Bundle Refill/Reflood
  - TLTA: Refill by Bypass Leakage Plus Drainage at UTP, Later by CCFL Breakdown at UTP
  - FIST: Major Refill by CCFL Breakdown at UTP
- o Wall Stored Heat Affects Hydraulic Responses During Reflood in FIST
- o More Mass Remains in FIST during Refill/Reflood

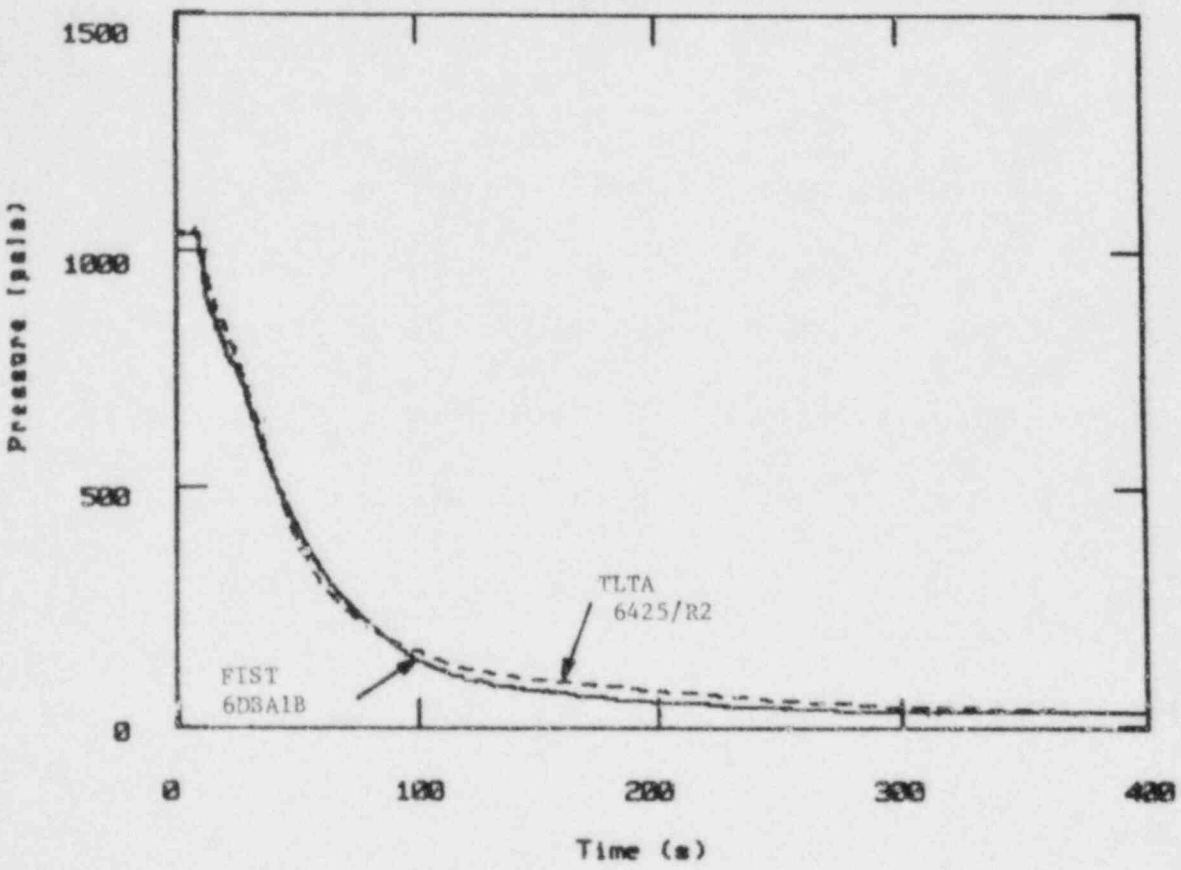

Figure 8.1-1. System Pressure

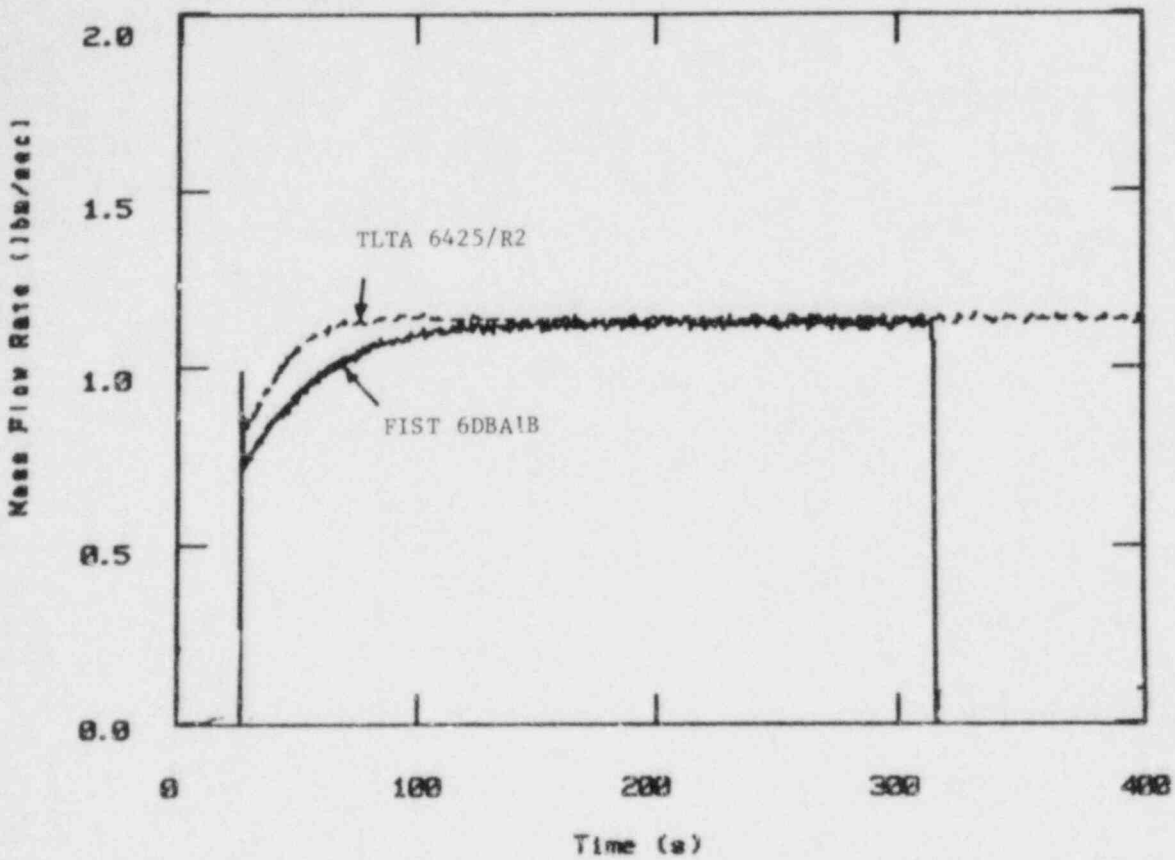

Figure 8.1-2. HPCS Flow

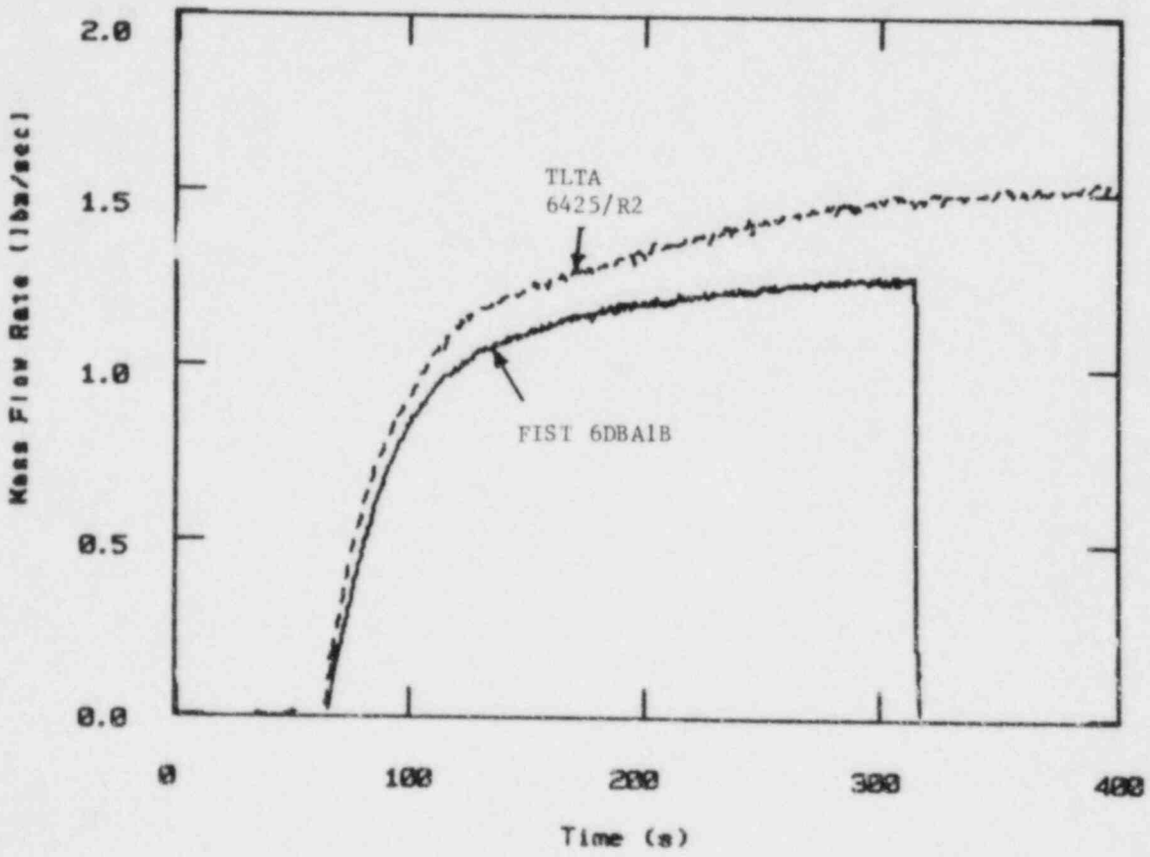

Figure 8.1-3. LPCS Flow

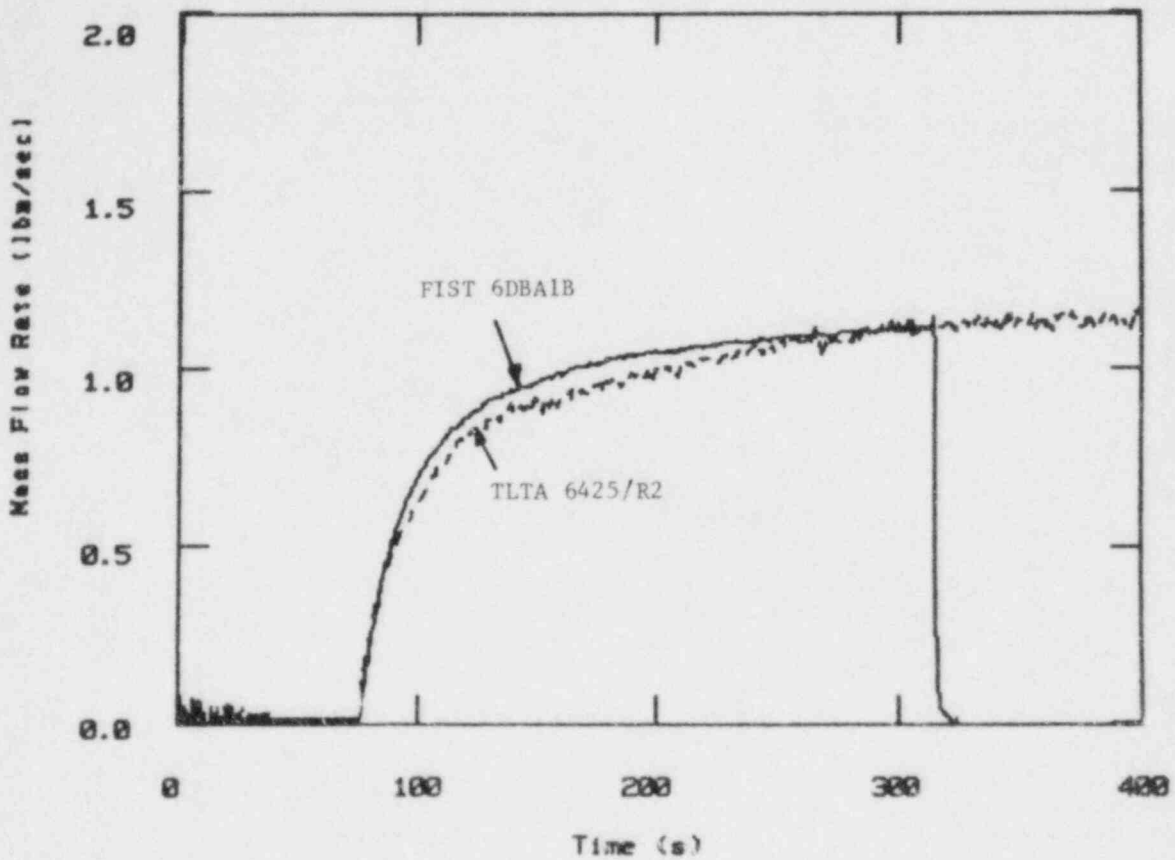

Figure 8.1-4. LPCI Flow

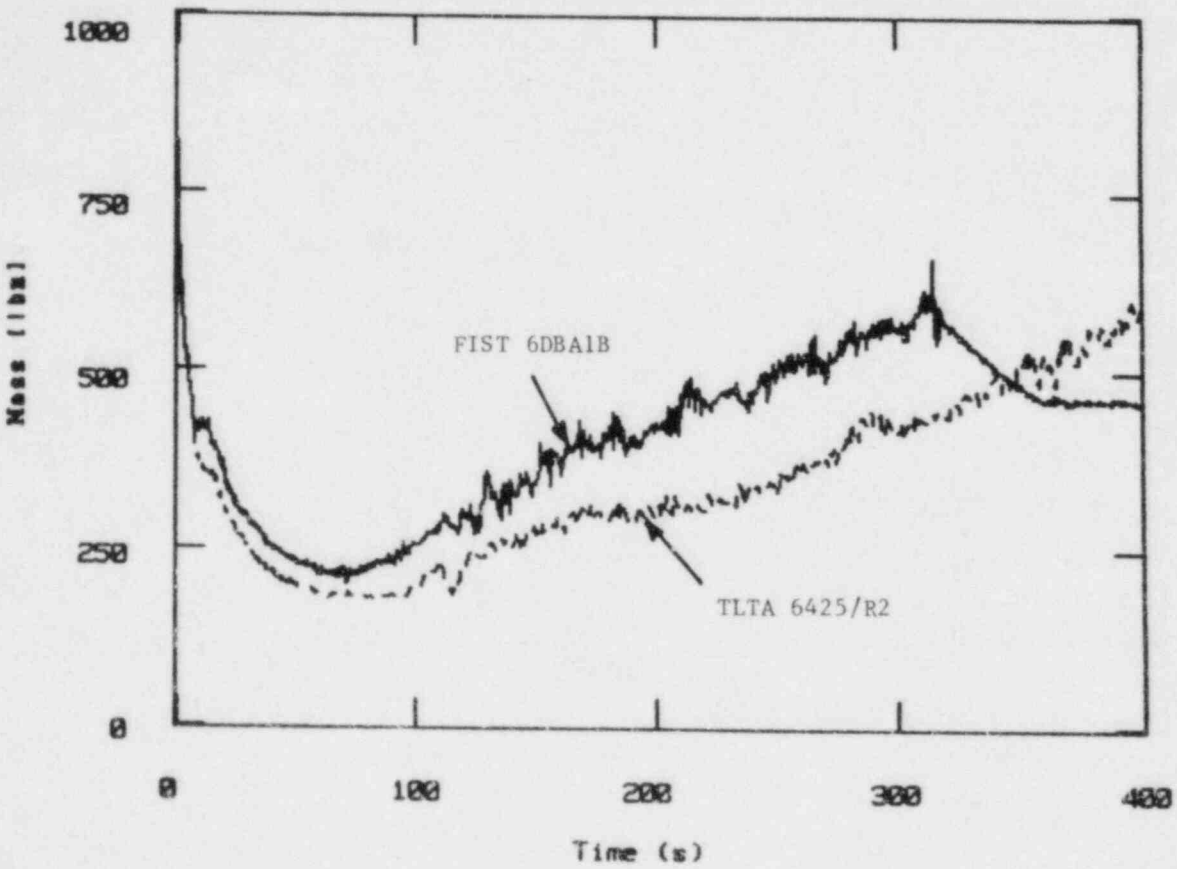

Figure 8.1-5. Total Mass

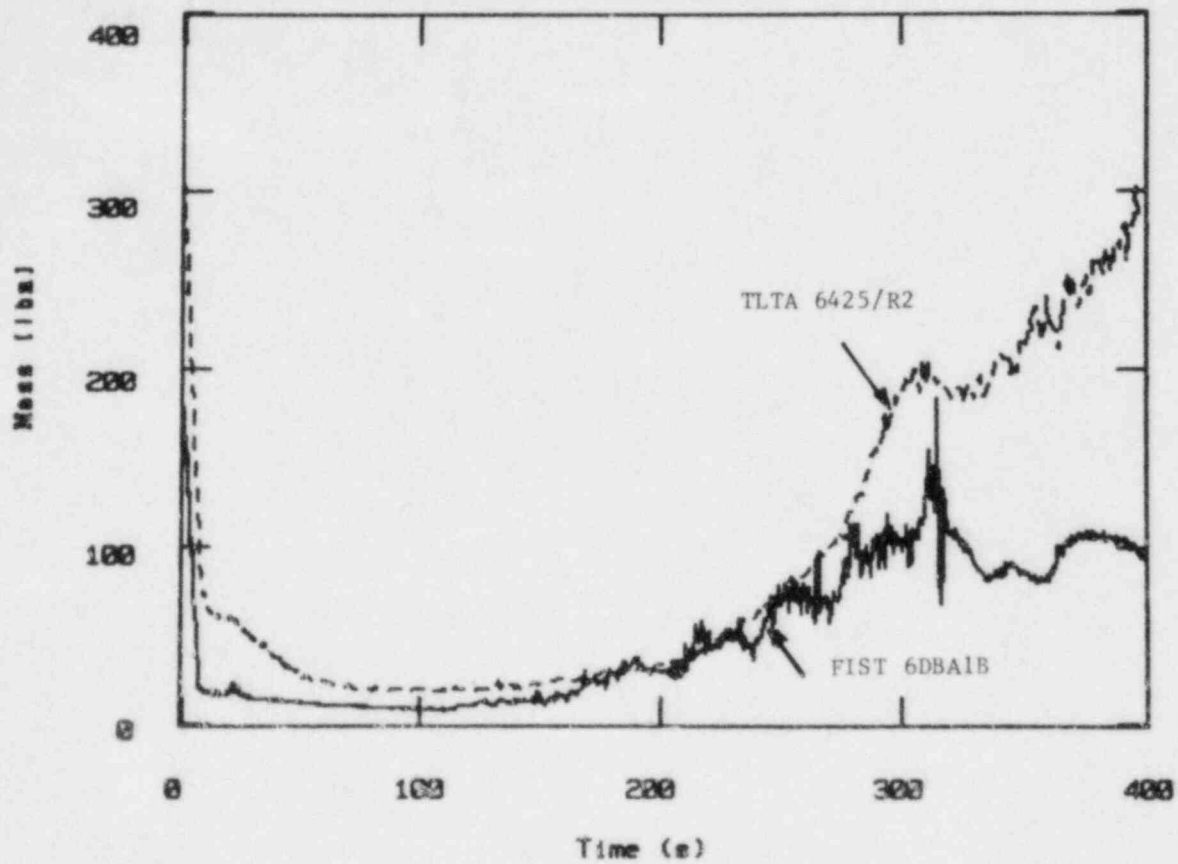

Figure 8.1-6. Downcomer Mass

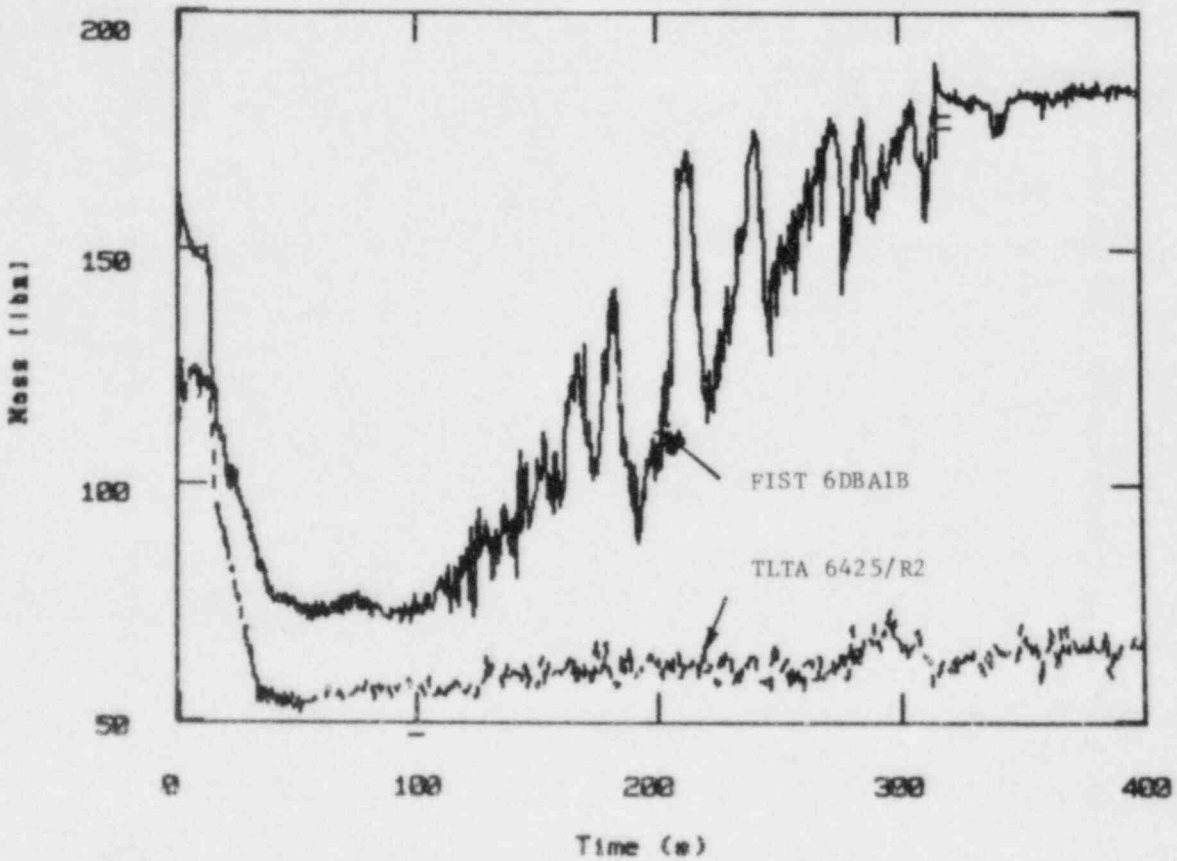

Figure 8.1-7. Lower Plenum Mass

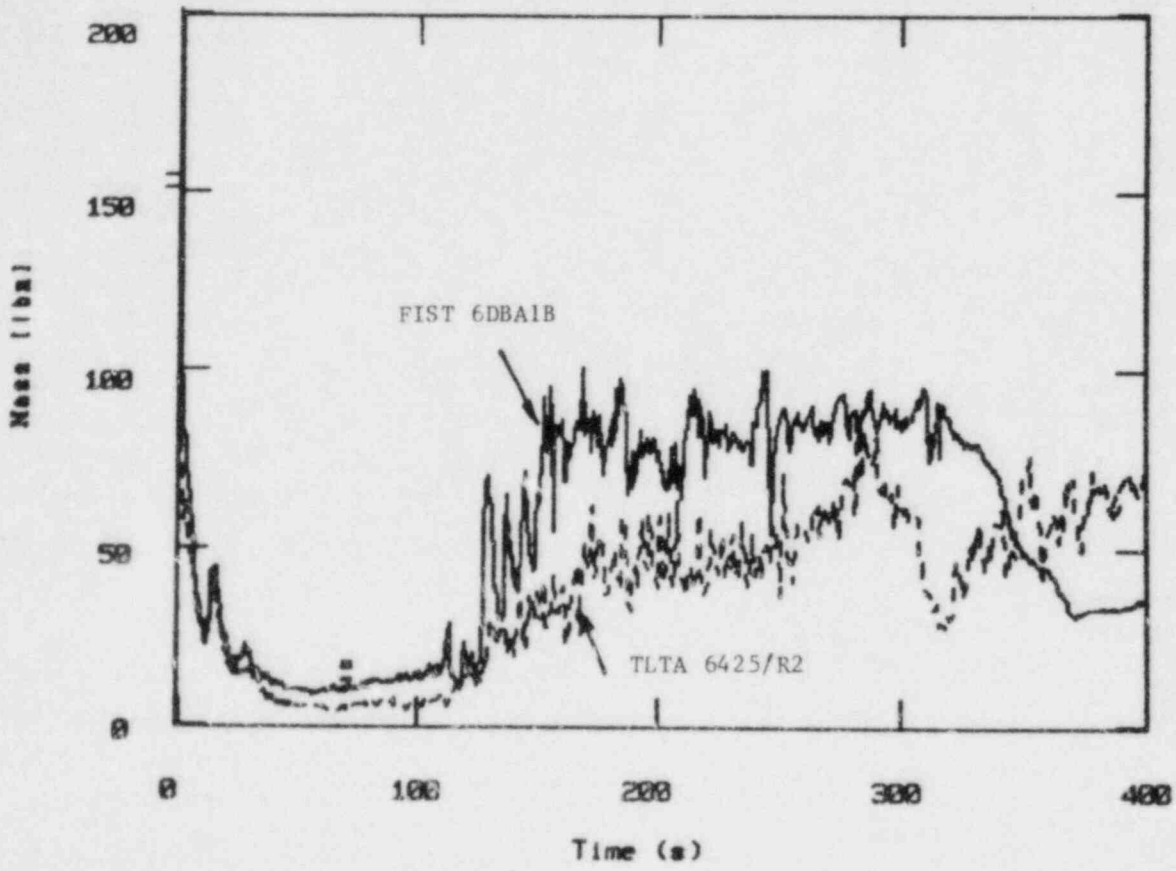

Figure 8.1-8. Bundle Mass

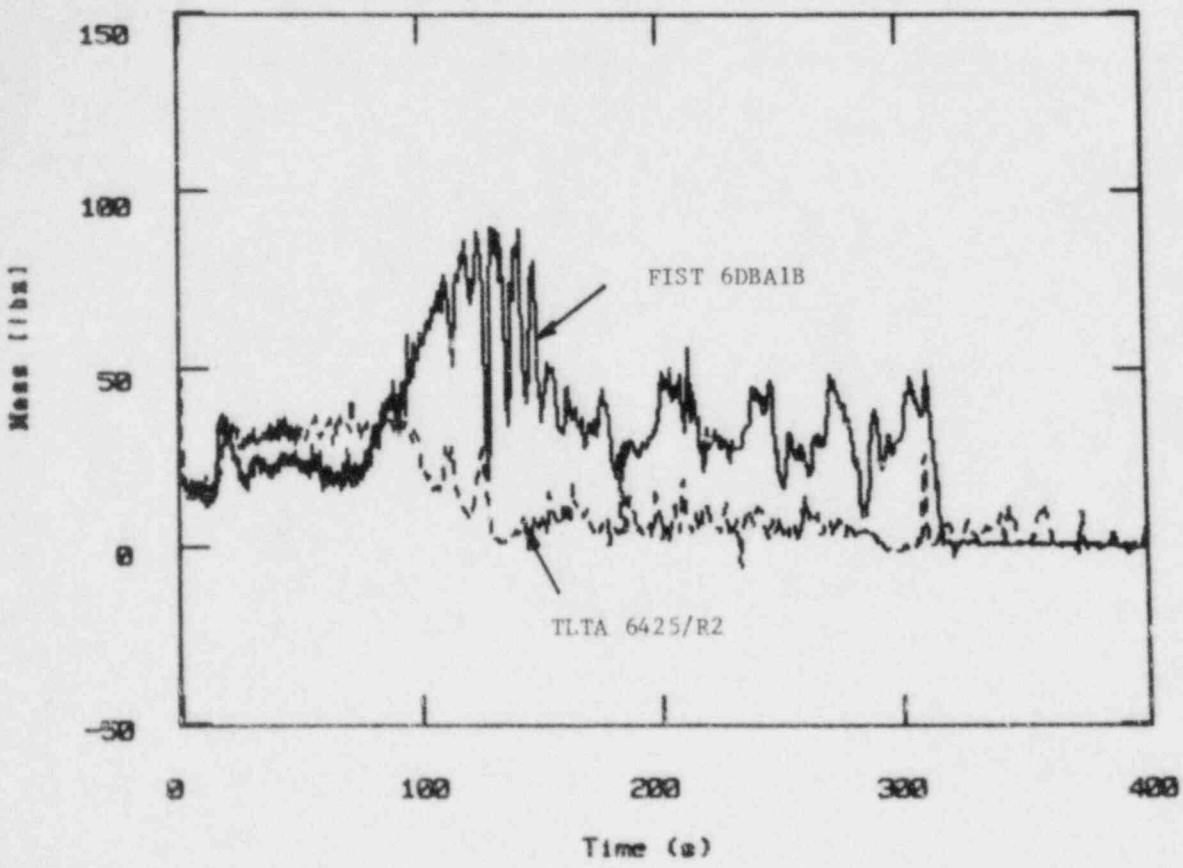

Figure 8.1-9. Upper Plenum Mass

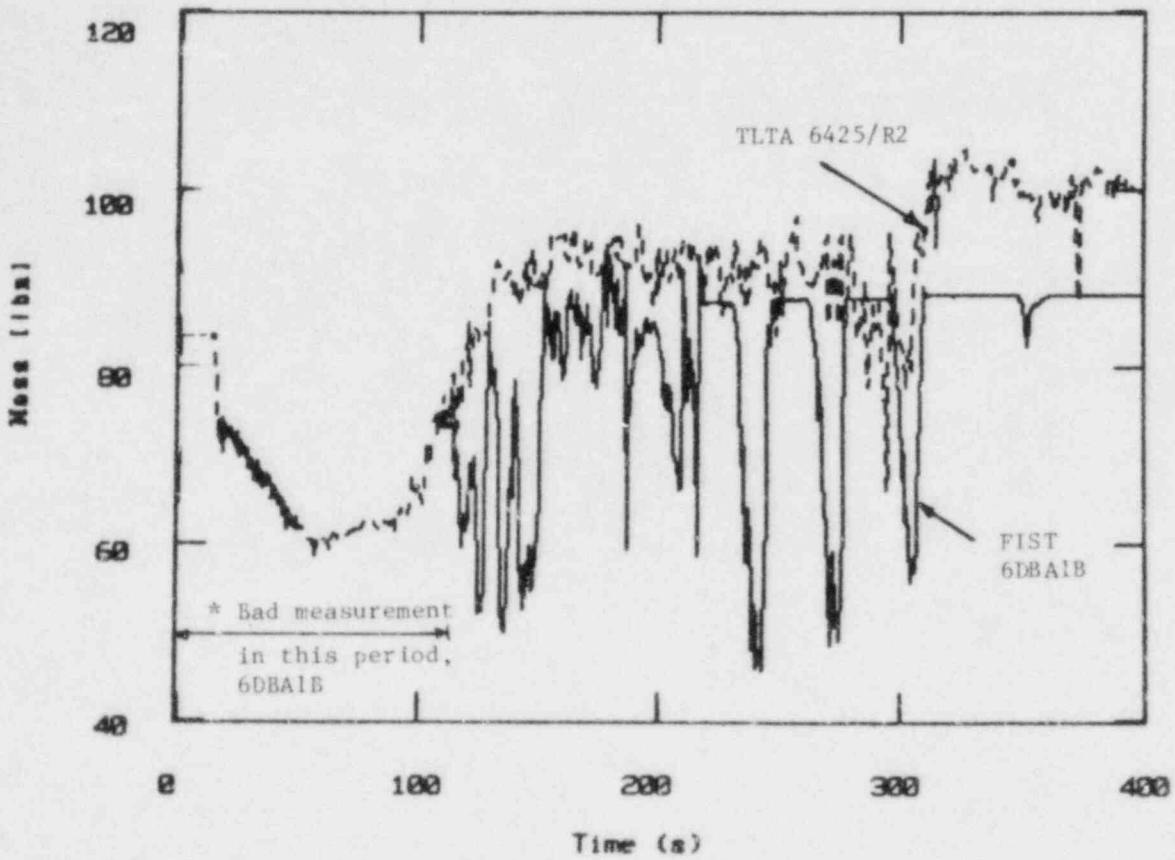

Figure 8.1-10. Guide Tube Mass

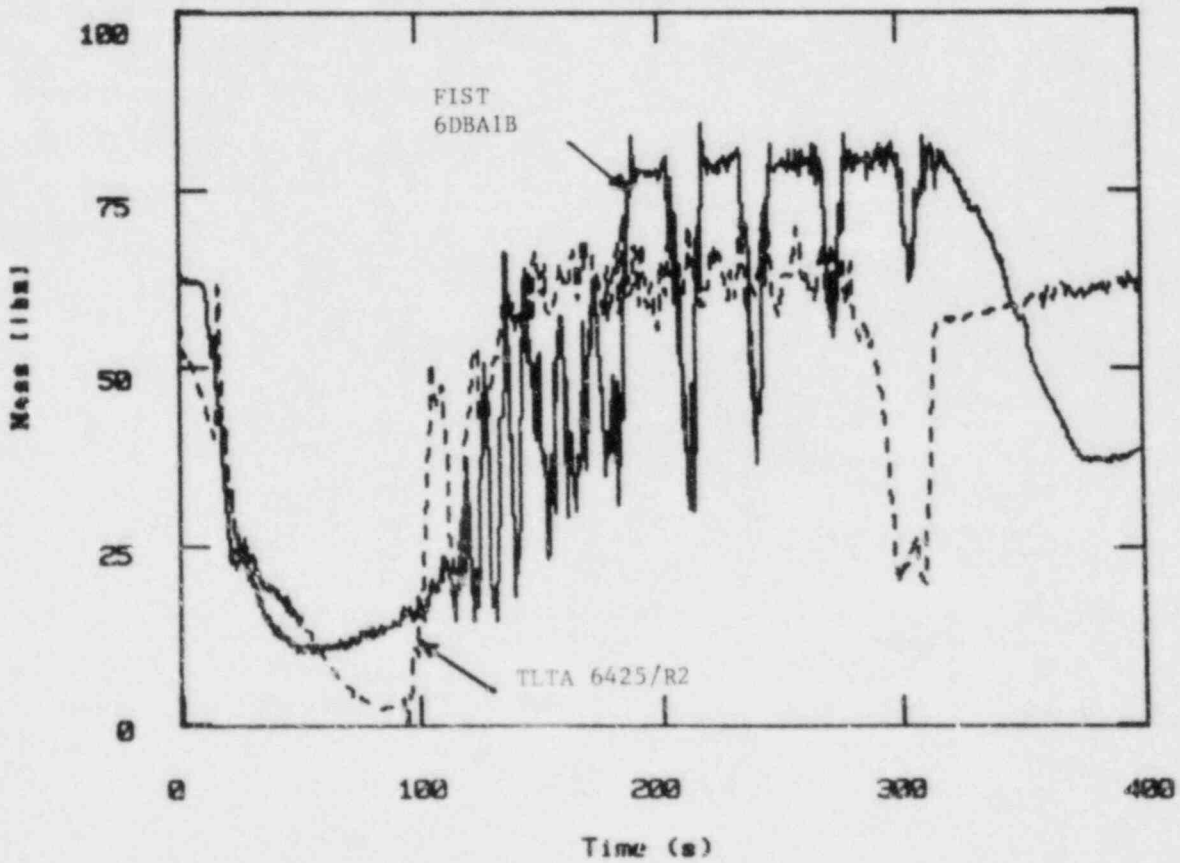

Figure 8.1-11. Bypass Mass

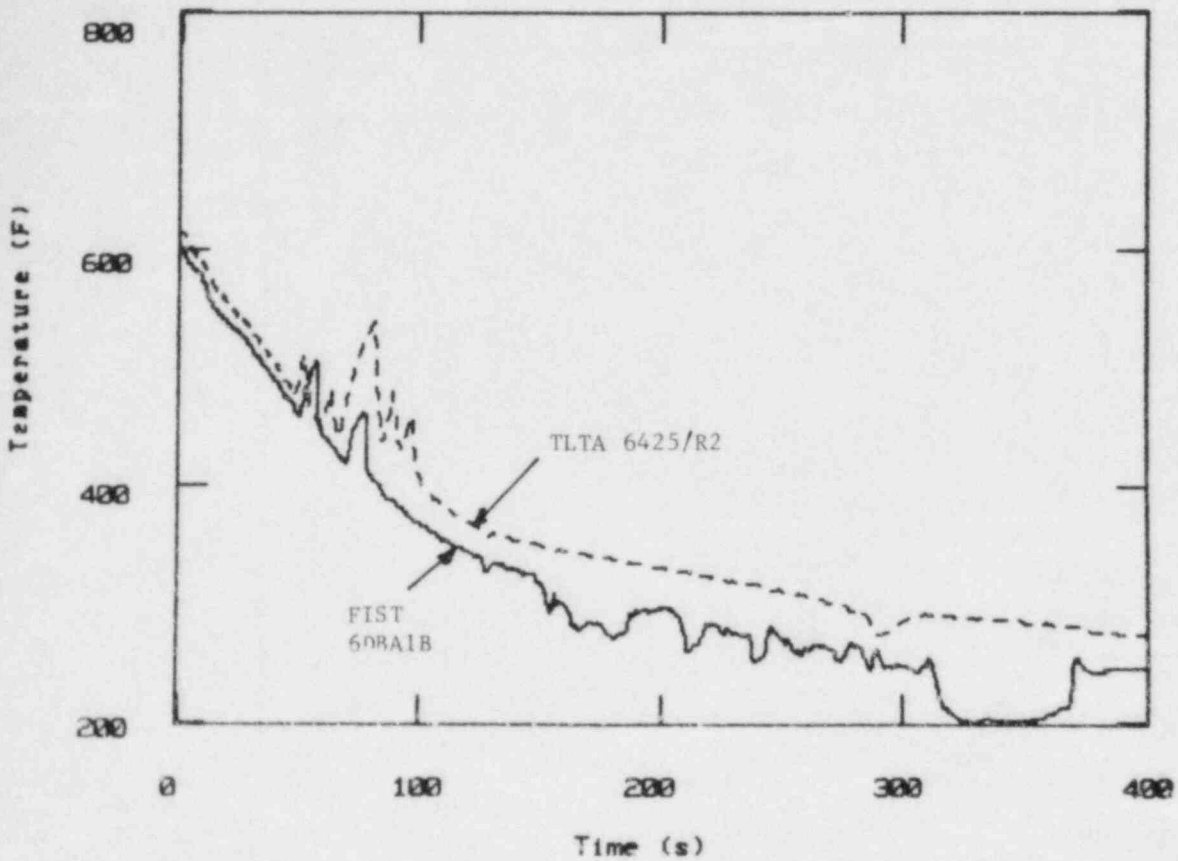

Figure 8.1-12. Rod Temperature, Elev. 61"

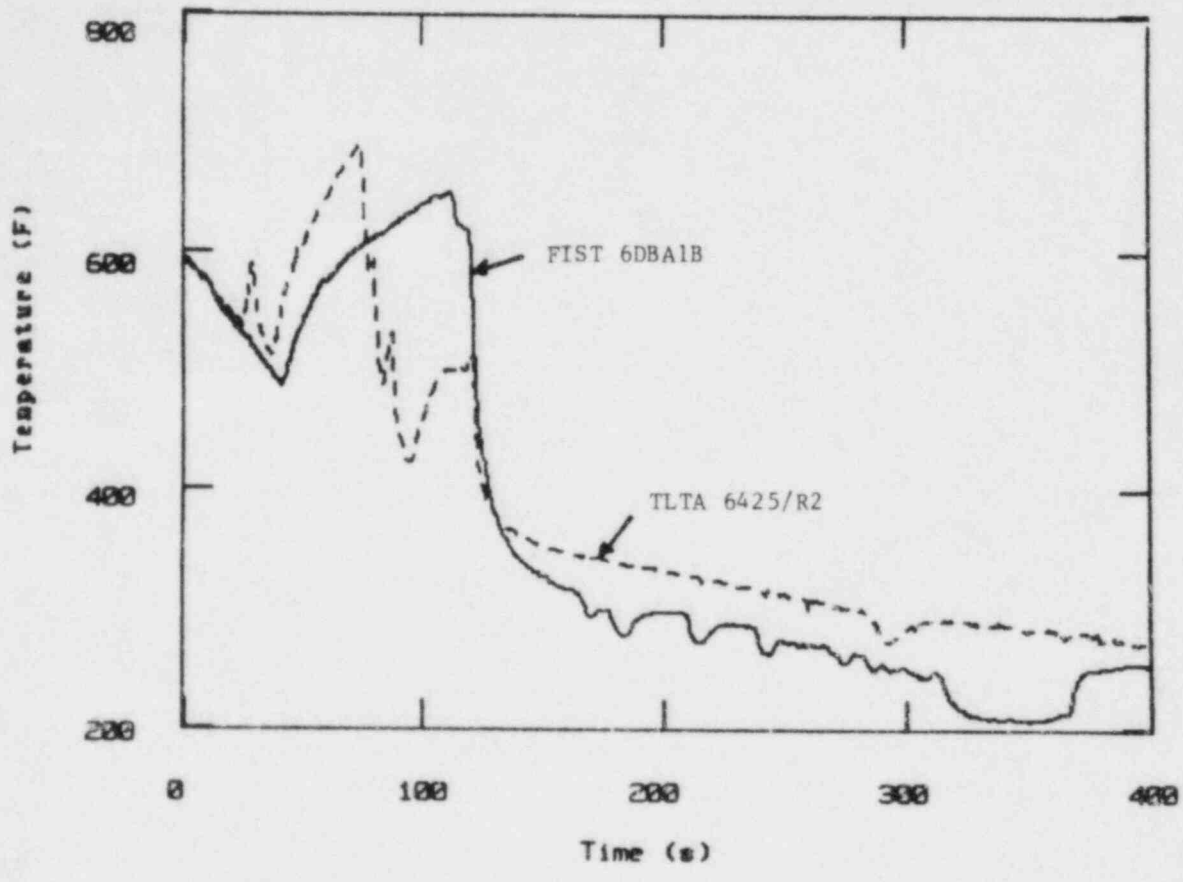

Figure 8.1-13. Rod Temperature, Elev. 69"

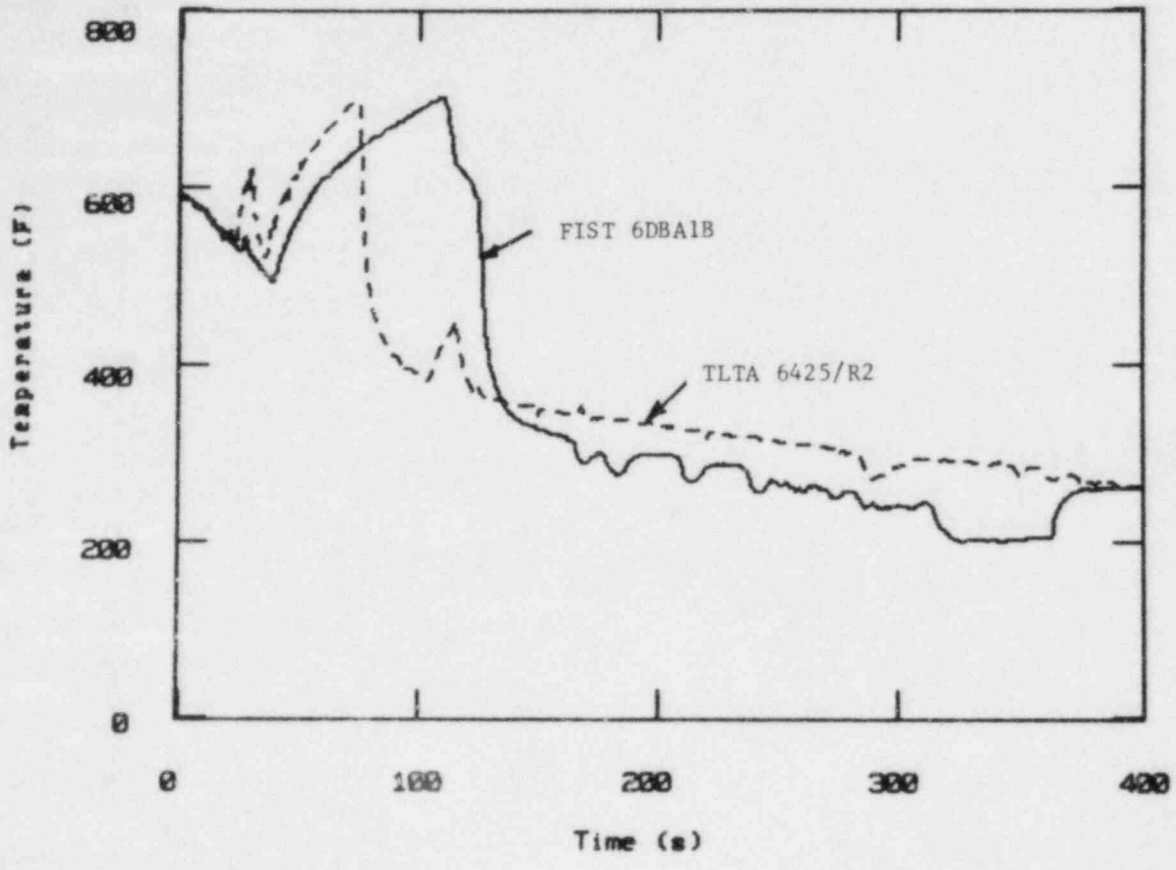

Figure 8.1-14. Rod Temperature, Elev. 77"

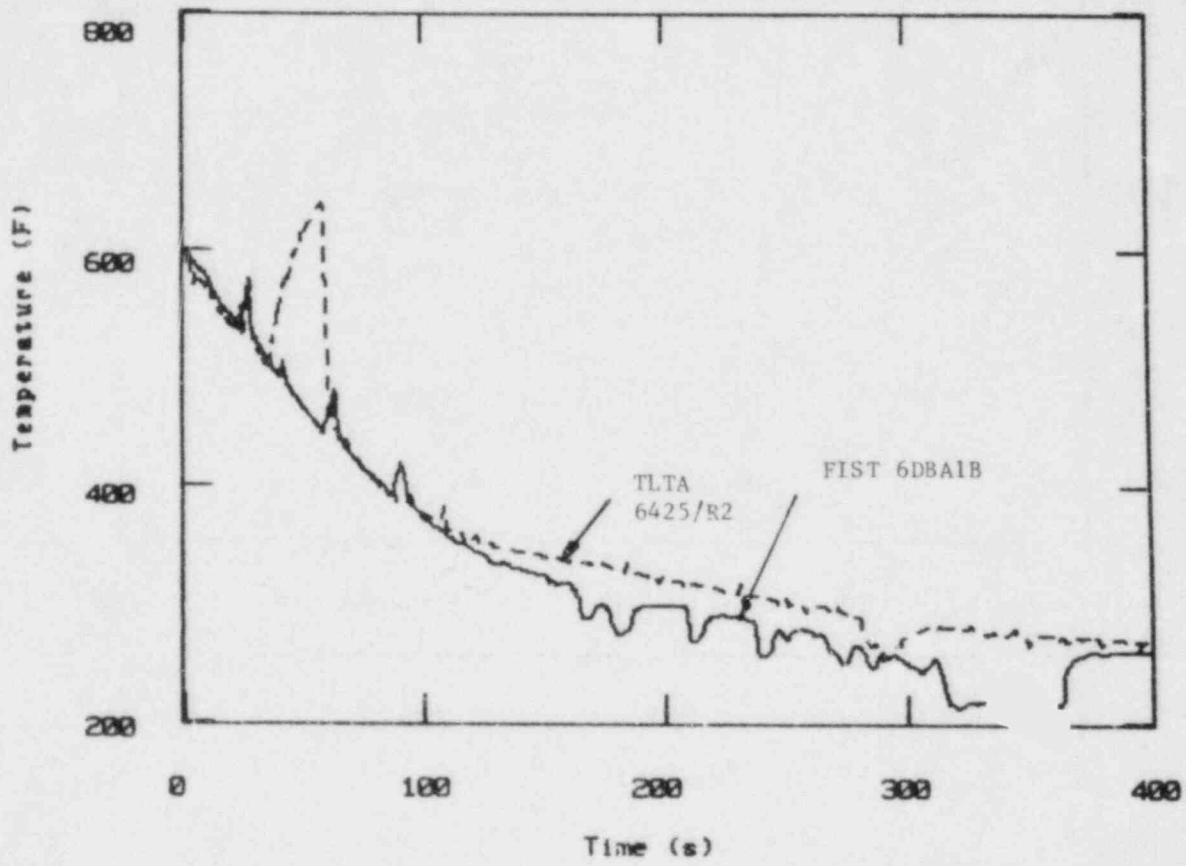

Figure 8.1-15. Rod Temperature, Elev. 77"

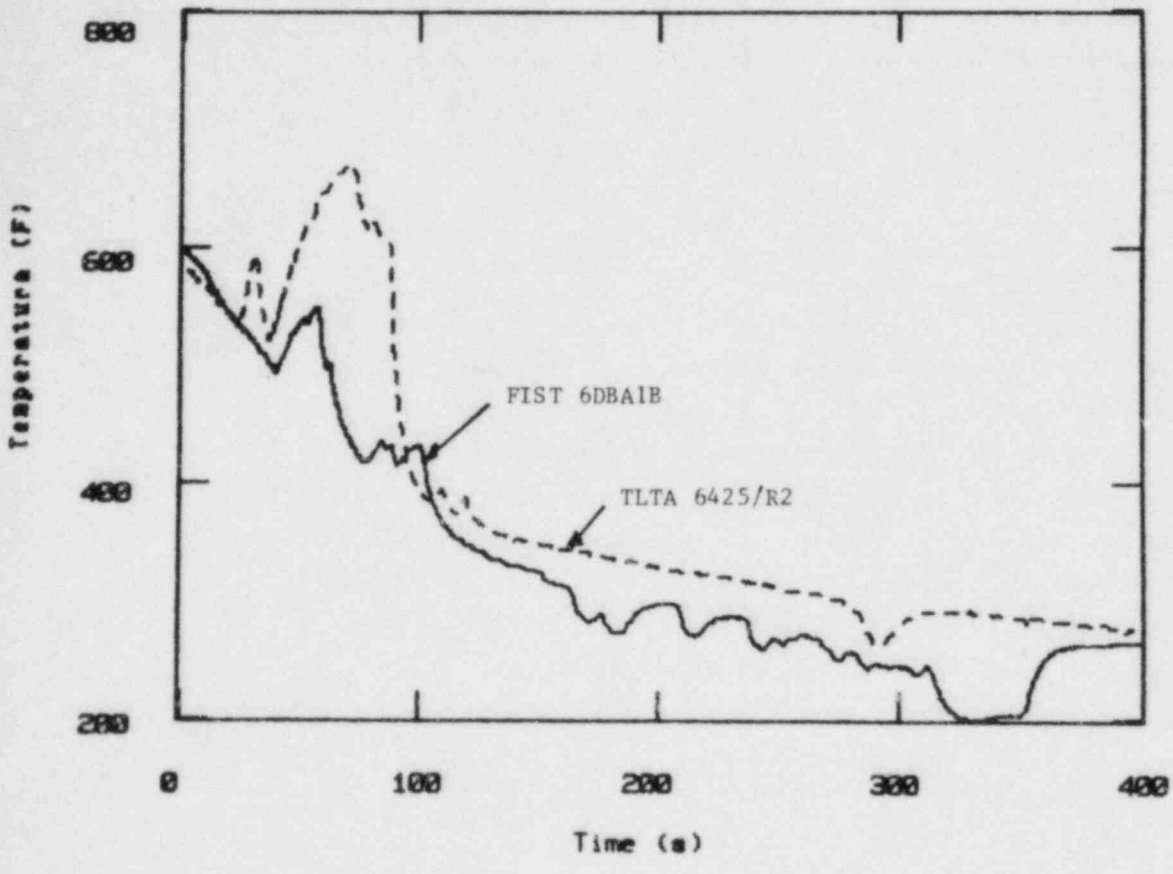

Figure 8.1-16. Rod Temperature, Elev. 88"

8.2 SMALL BREAK TESTS, FIST 6SB2C VS TLTA 6432/R1

8.2.1 General Description

The FIST small break test, 6SB2C, is a counterpart of the TLTA test, 6432/R1. Both tests simulate a BWR/6-218 recirculation line small break of 0.05 ft^2 with HPCS assumed unavailable. However, the test simulation approaches employed in these two tests are different, in order to overcome scaling compromises in the facilities. The FIST small break test is discussed in Section 7.2. To help in understanding the comparisons, the TLTA test simulation, detailed in reference 4, is briefly discussed here.

8.2.2 TLTA Test Simulation

TLTA was designed mainly to conduct large break LOCA tests. There are many scaling compromises in the TLTA for performing a small break test. Table 8.2-1 lists the key compromises identified in this facility and Figure 8.2-1 shows an elevation comparison of TLTA with a BWR. In order to overcome these scaling compromises, and perform a meaningful test, it was necessary to modify the test facility and test operation. It was decided to simulate the TLTA small break test based on the calculated BWR/6 response. Simulations of the downcomer water level and system pressure required for different periods of the transient dictated modifications made to the test facility and test operation (Table 8.2-2).

Prior to the ADS activation, the system performance is strongly affected by the inside/outside water interaction. Thus, the test simulated the calculated BWR/6 water level transient. The MSIV closure and ADS activation were controlled with a timer, based on calculation, rather than by the level 1 signal as in the FIST test.

The system depressurizes very rapidly upon ADS activation, which leads to system flashing and mass redistribution. It is necessary to simulate the system pressure response beyond ADS actuation. Because of excess fluid mass and overscaled stored heat, the steam generation in

TLTA during this period is overscaled. An oversized ADS was used so that the system depressurization would match that expected in a BWR/6 response (Figure 4.2-1). The correct pressure simulation also leads to the correct initiations of LPCS and LPCI. However, fluid mass in the downcomer at ADS was still significantly overscaled, and affected the system performance.

8.2.3 Comparison of Test Results

8.2.3.1 Pressure and Mass

Comparisons of the measured system pressure and total mass between the FIST and TLTA small break tests are shown in Figures 8.2-2 and -3. It can be seen that TLTA contains a significantly overscaled fluid mass from the beginning of the transient. Also the ADS in TLTA is activated later than in FIST. The FIST ADS was activated with water level signal, while the TLTA used a timer to trip the ADS with the timing based on a calculation. Differences in the ADS activation timing leads to different timings of LPCS and LPCI injections between two tests.

8.2.3.2 Key Events and Phenomena

Table 8.2-3 is a summary of key events and system responses observed in these two tests. Major differences in the system responses include uncoveries of the bundle, bypass, and jet pump, CCFL at the top of the jet pump and rod heatup.

8.2.3.3 Post-ADS Responses

Major interest in a small break test is the system response following ADS depressurization and the refill/reflood in the later transient. Therefore for comparisons, all FIST results are shifted to match the ADS timings between two tests for the post-ADS comparisons.

Figure 8.2-4 shows good agreement in the ADS depressurization which leads to similar LPCS (Figure 8.2-5) and LPCI (Figure 8.2-6) performance.

The total mass and region mass comparisons are given in Figures 8.2-7 through 13. At the ADS activation, TLTA contains almost twice the amount of fluid mass in FIST (Figure 8.2-7). This excess mass is mainly contributed by the overscaled downcomer flow area (Figure 8.2.8).

Regional mass plots indicate that a strong inventory redistribution takes place at ADS due to the flashing surge caused by the rapid depressurization. The inventory redistributions among various regions appear to be very similar between the TLTA and FIST tests. Mass differences shown in the guide tube and bypass between TLTA and FIST (Figures 8.2-12 and 13) during the early transient are due to the bypass/guide tube interface location being defined differently in these two facilities.

Shortly after the ADS flashing surge, the lower plenum, bundle, and bypass (Figure 8.2-9, 10 and 12) in FIST indicates a mass recovery or termination of mass depletion in these regions. In TLTA, water level in the downcomer remained relatively high due to large excess fluid mass and covers the jet pump throughout the transient. The jet pump is relatively short and full of water. This liquid continuum in the lower plenum-to-downcomer flow path had a relatively high hydrostatic head which held more inventory in the core as compared with FIST. Therefore, the bundle was full of two phase mixture and there was no rod heatup in TLTA. Upon ECCS initiation, both tests show inventory recovery in various regions until the ends of the tests.

8.2.4 Summary

Comparisons of the FIST and TLTA small break tests are summarized as follows:

(1) Timings of level 1 signal, MSIV closure and ADS actuation between the two tests are different. These differences are due to the test simulation approaches required in the tests.

(2) Several similar responses are seen during the ADS depressurization. These include the pressure transient, inventory redistribution at the ADS flashing surge and CCFL at various locations.

(3) The TLTA scaling compromises of overscaled mass and jet pump height affect the post-ADS level response. This, in turn, affects the core hydraulic performance and the associated rod temperature response. No rod heatup is observed in the TLTA test, while a PCT of 720^{o}F is seen in the FIST test.

Table 8.2-1

TLTA MAJOR SCALING COMPROMISES

- Underscaled height in regions above and below the core
- Overscaled flow areas in Lower Plenum, Downcomer, Upper Plenum and Steam Dome
- Short Jet Pumps
- Overscaled Metal Mass
- No Level Trip

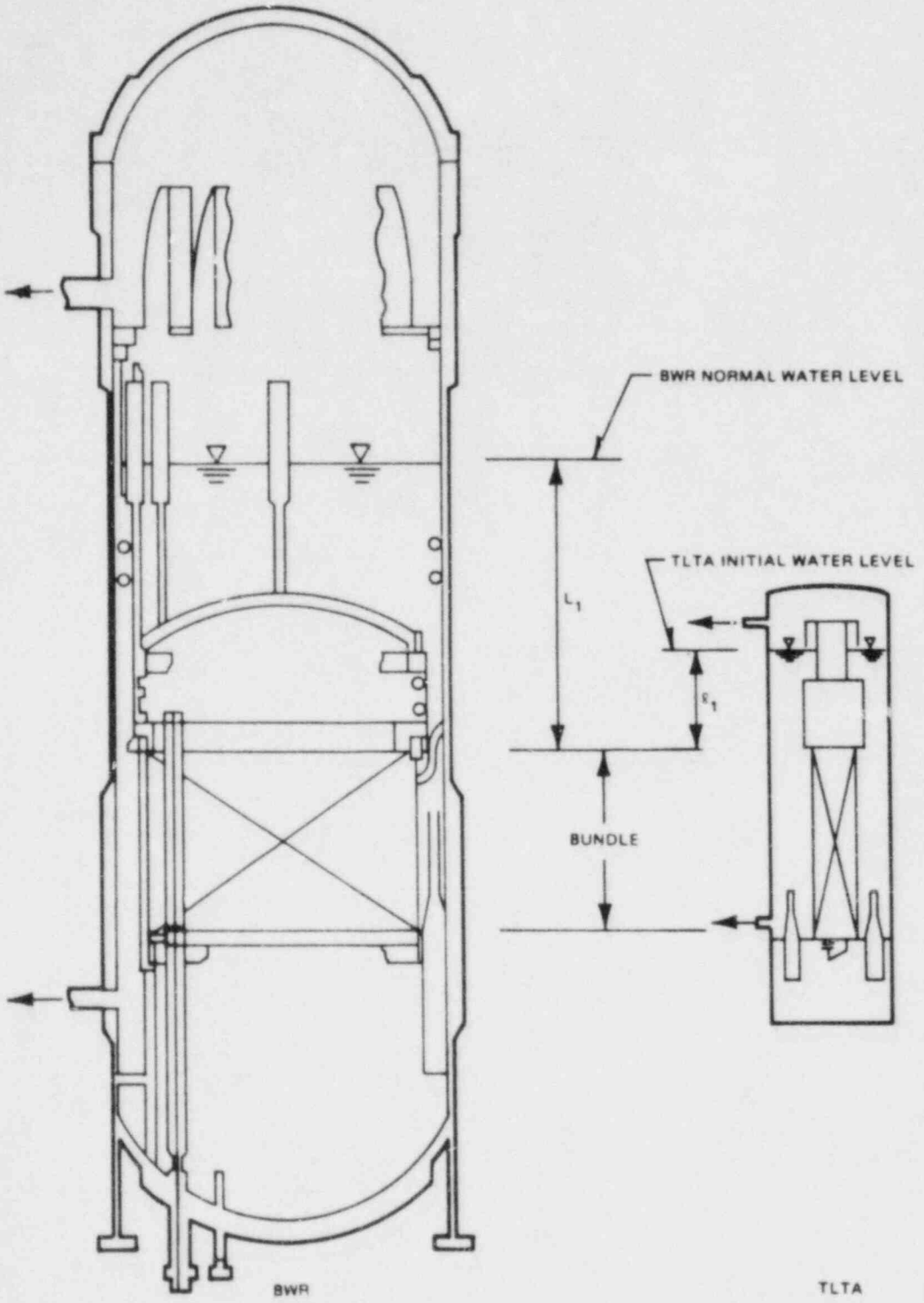

Figure 8.2-1. Relative Elevation Comparison Between BWR and TLTA

Table 8.2-2

KEY SIMULATIONS IN TLTA SMALL BREAK

- o Pressure controlled by a pressure regulator before MSIV
- o MSIV and ADS Timings
  - Activated with a Timer (166 Sec ard 286 Sec)
- o Level Transient before ADS
  - Delay (140 Sec) in Break Initiation
  - Two Breaks (0.125" ¢ + 0.153" ¢) before ADS
  - One Break (0.125" ¢) after ADS
- o Pressure Response after ADS
  - Oversized ADS (0.677" ¢)

Table 8.2-3

SUMMARY (FIST 6SB2C VS TLTA 6432/R1)

- Timings of LI, MSIV and ADS
- Similar Pressure Response After ADS
- Similar CCFL Characteristics
- Similar Response of Regional Mass Redistribution at ADS Activation
- TLTA Scaling Compromises of Overscaled Mass and Jet Pump Height Affect the Post-ADS Level Responses and Rod Temperature

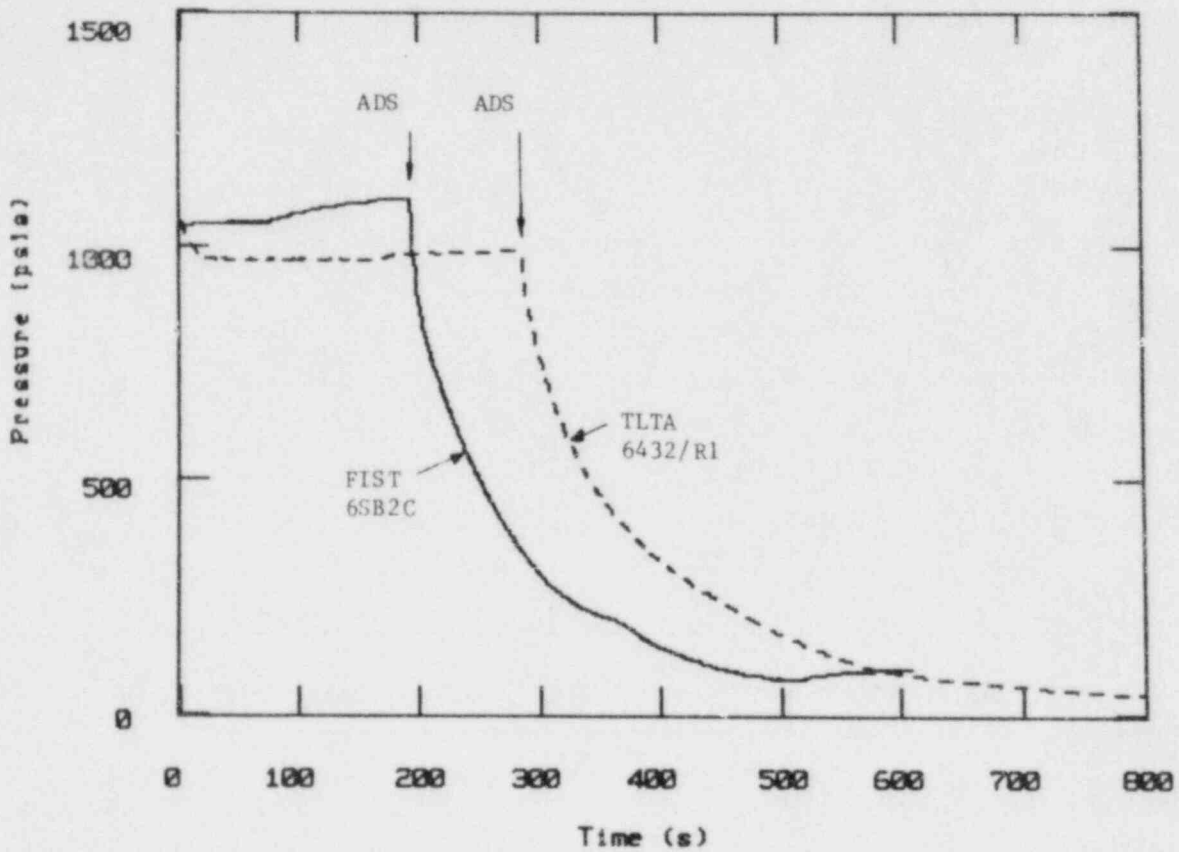

Figure 8.2-2. System Pressure

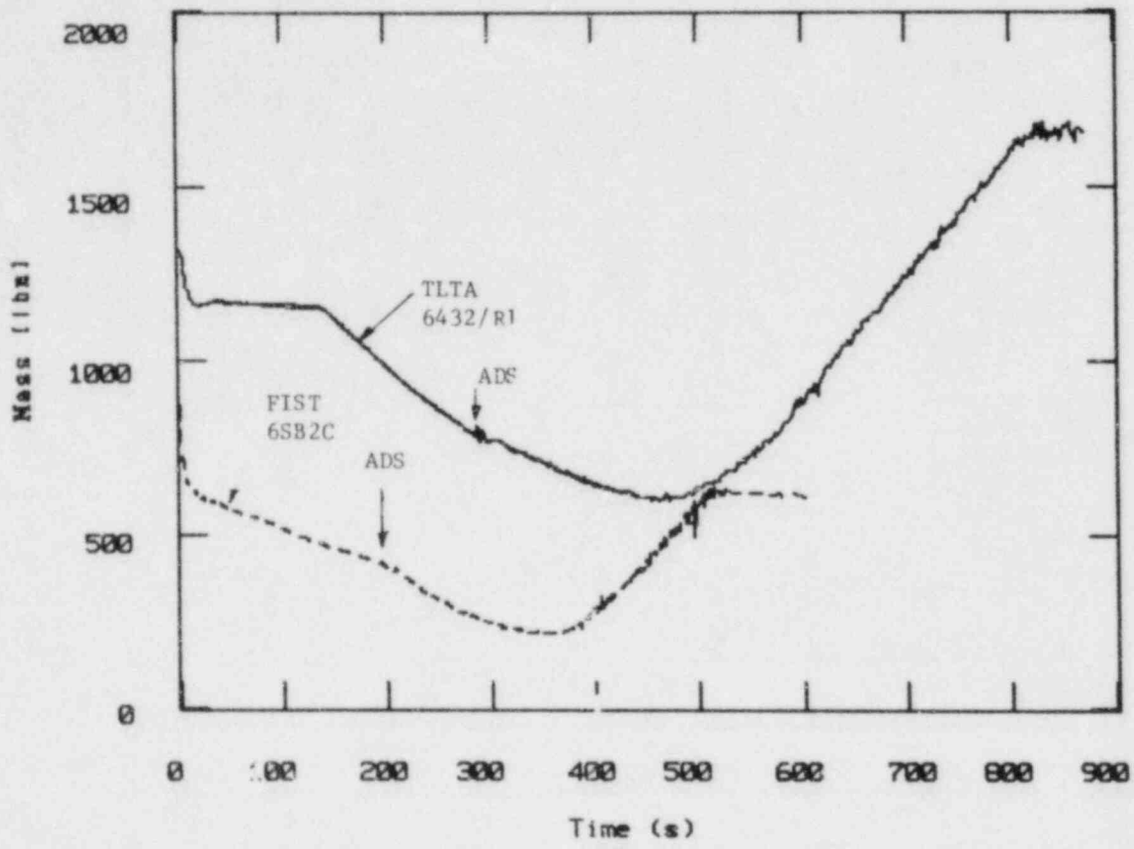

Figure 8.2-3. System Total Mass

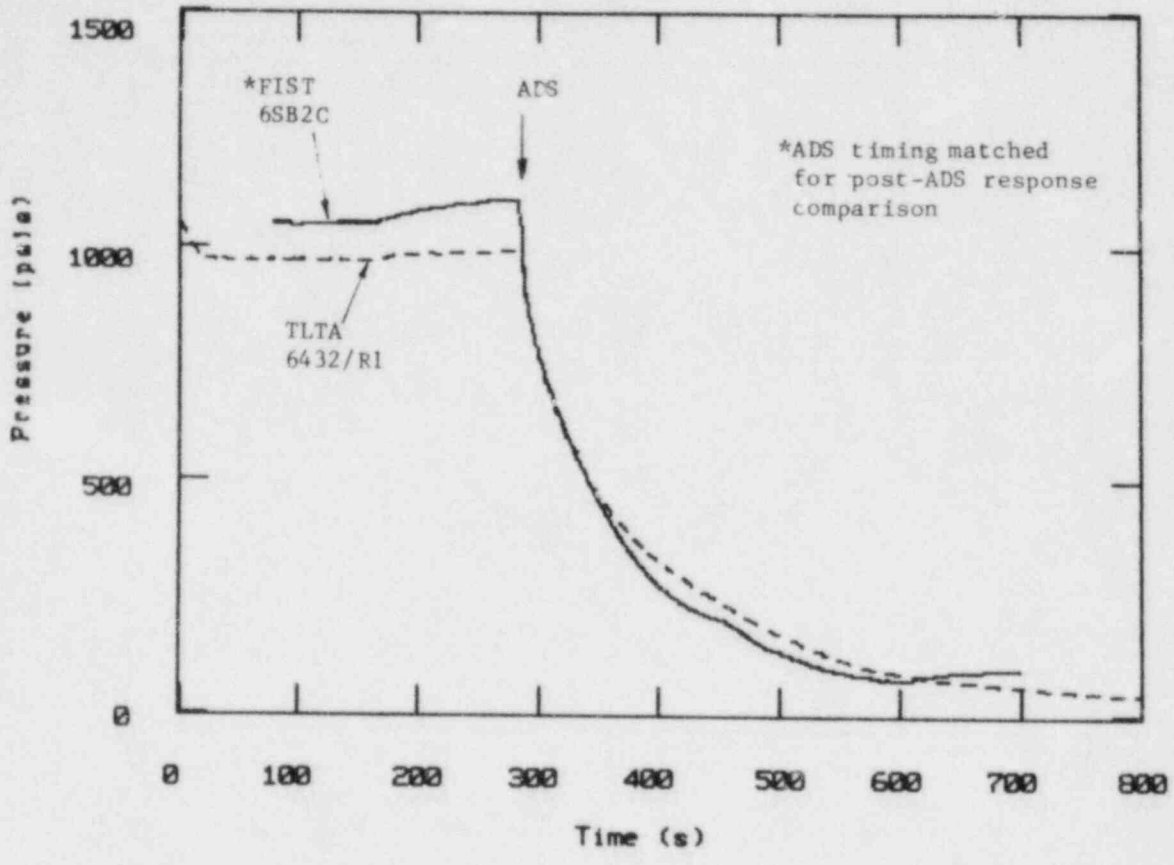

Figure 8.2-4. Post-ADS System Pressure Comparison

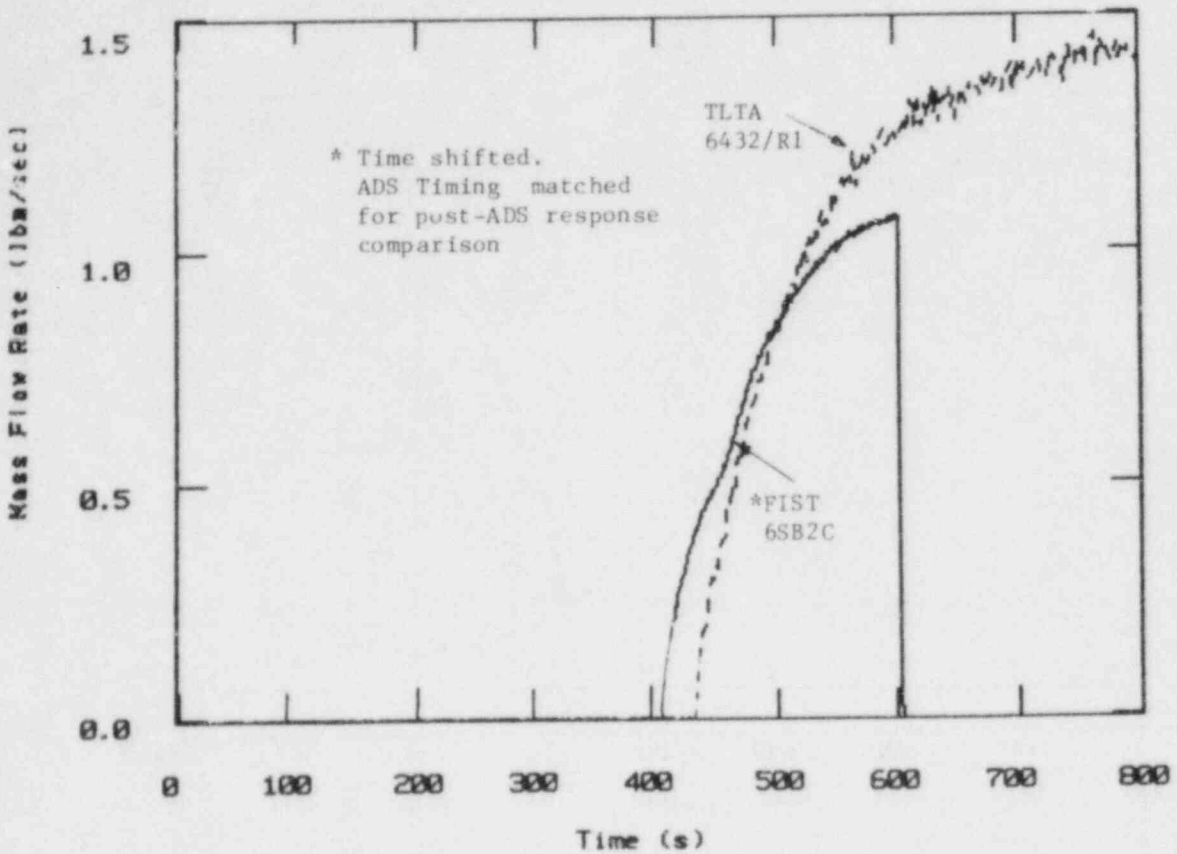

Figure 8.2-5. LPCS Flow

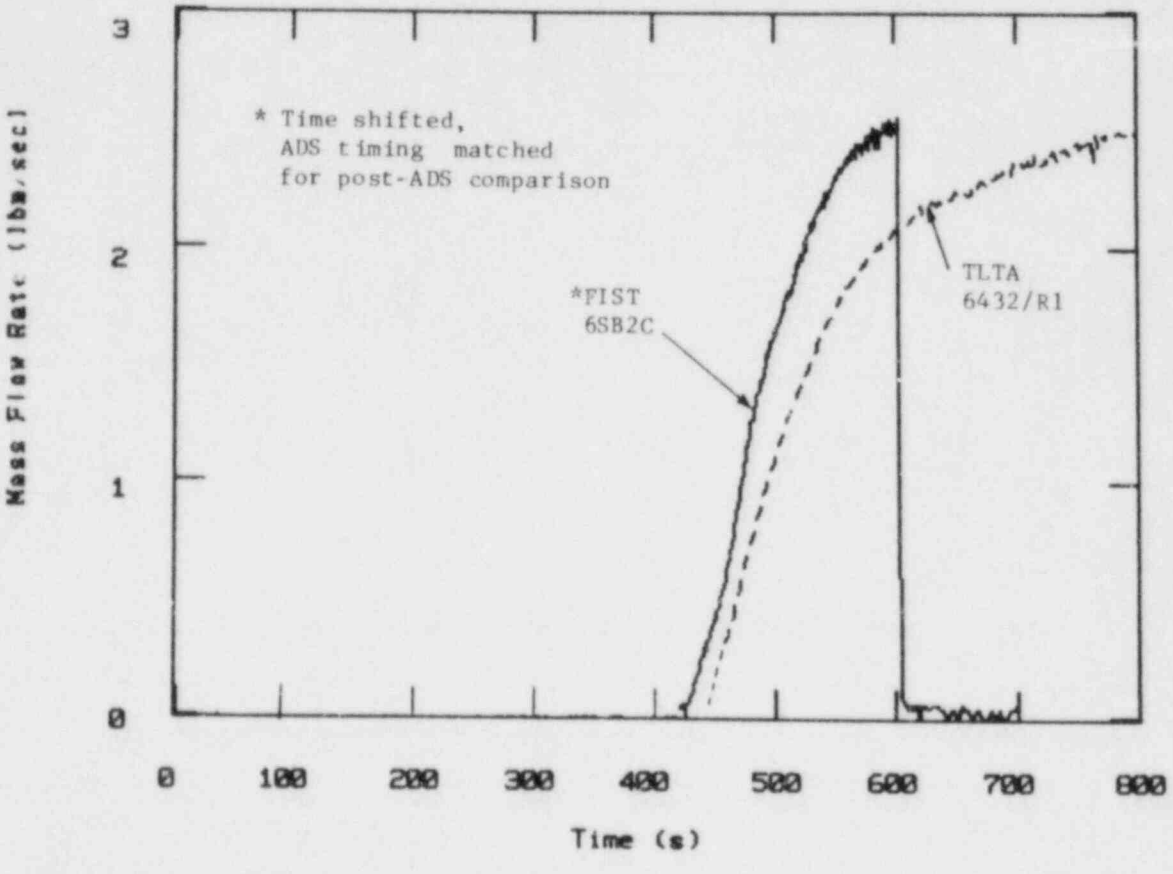

Figure 8.2-6. LPCI Flow

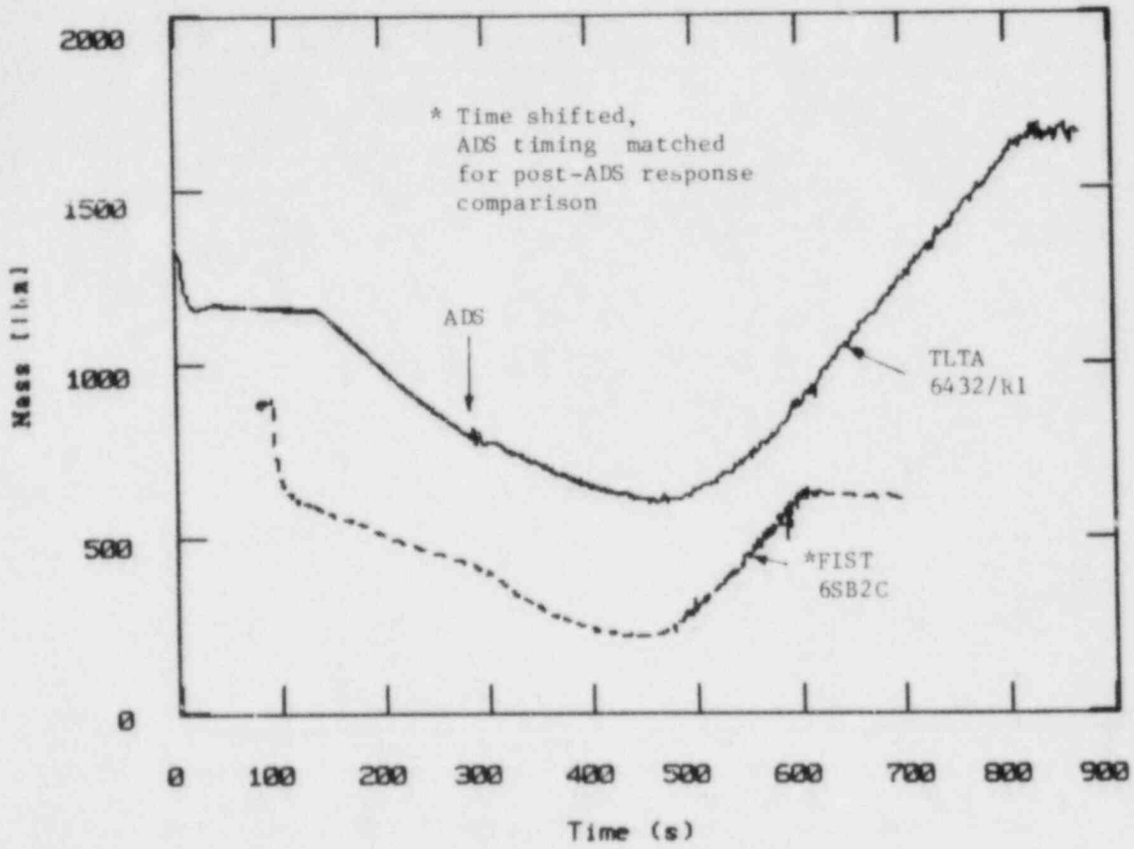

Figure 8.2-7. Post-ADS System Total Mass Comparison

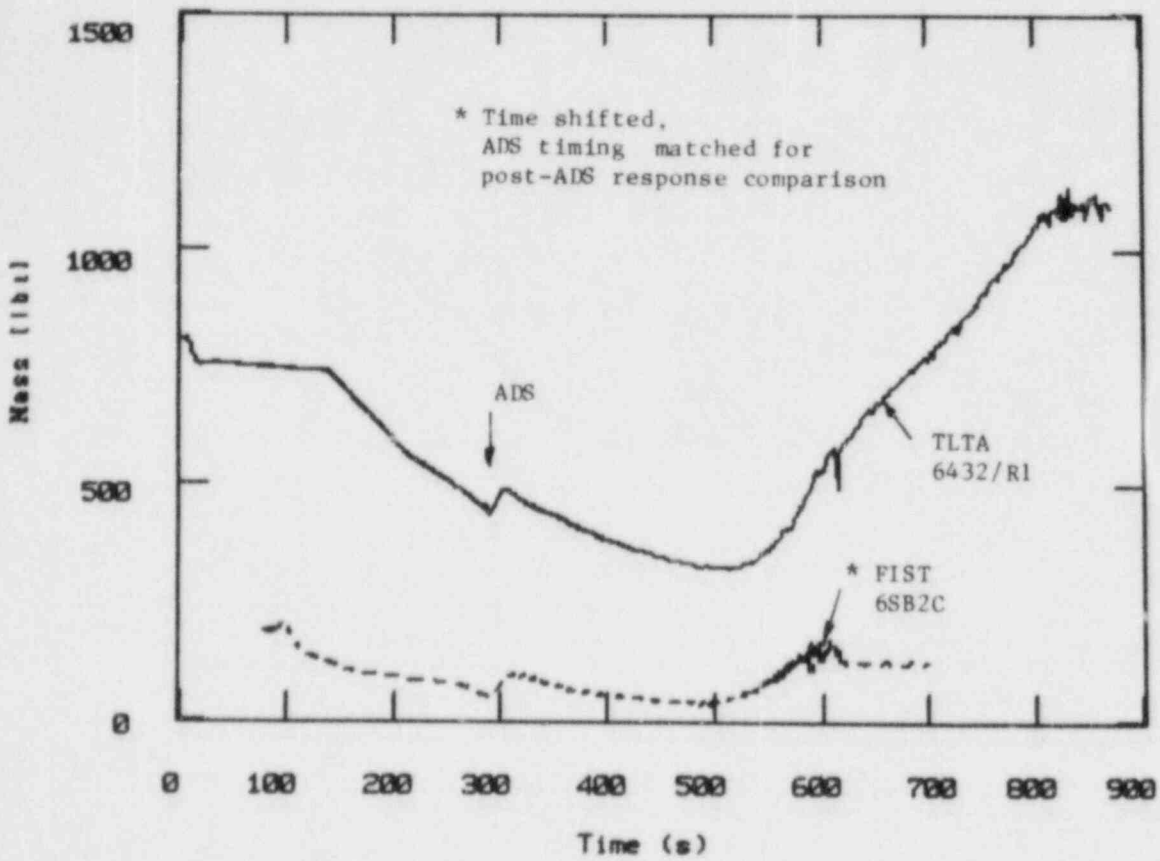

Figure 8.2-8. Post-ADS Downcomer Mass Comparison

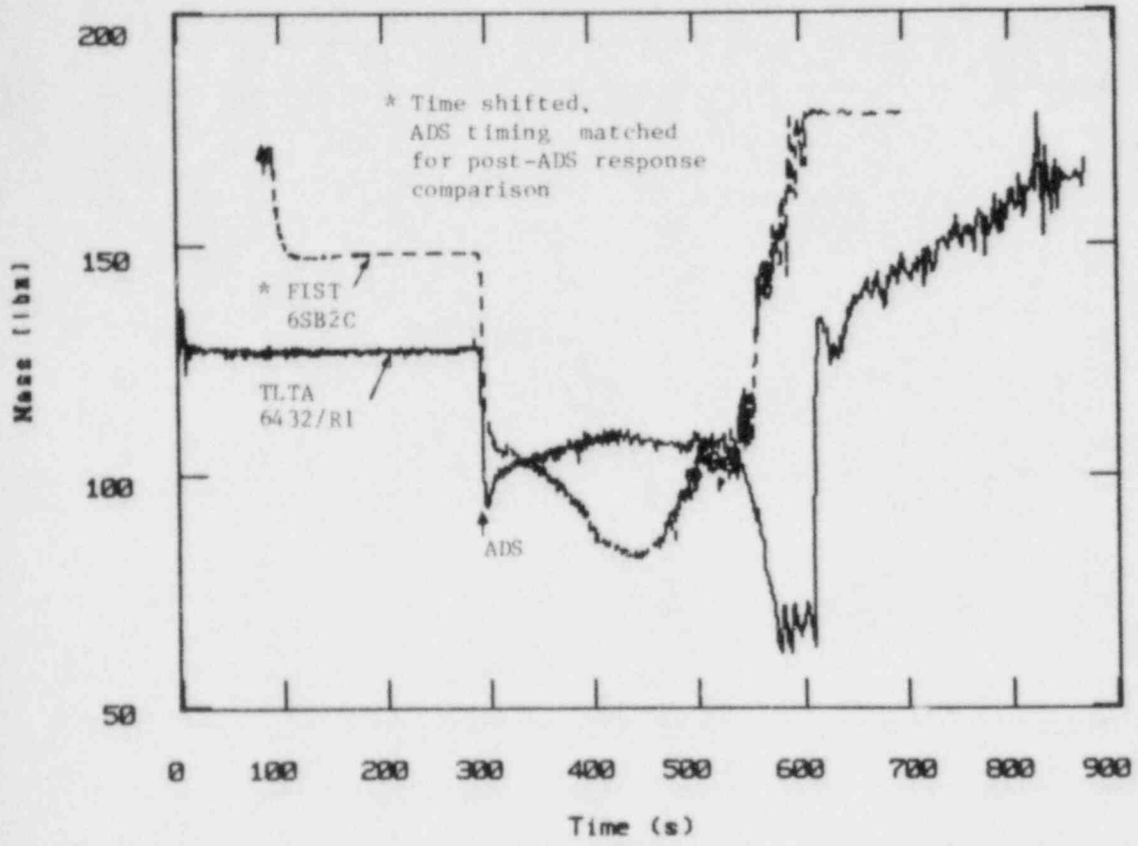

Figure 8.2-9. Post-ADS Lower Plenum Mass Comparison

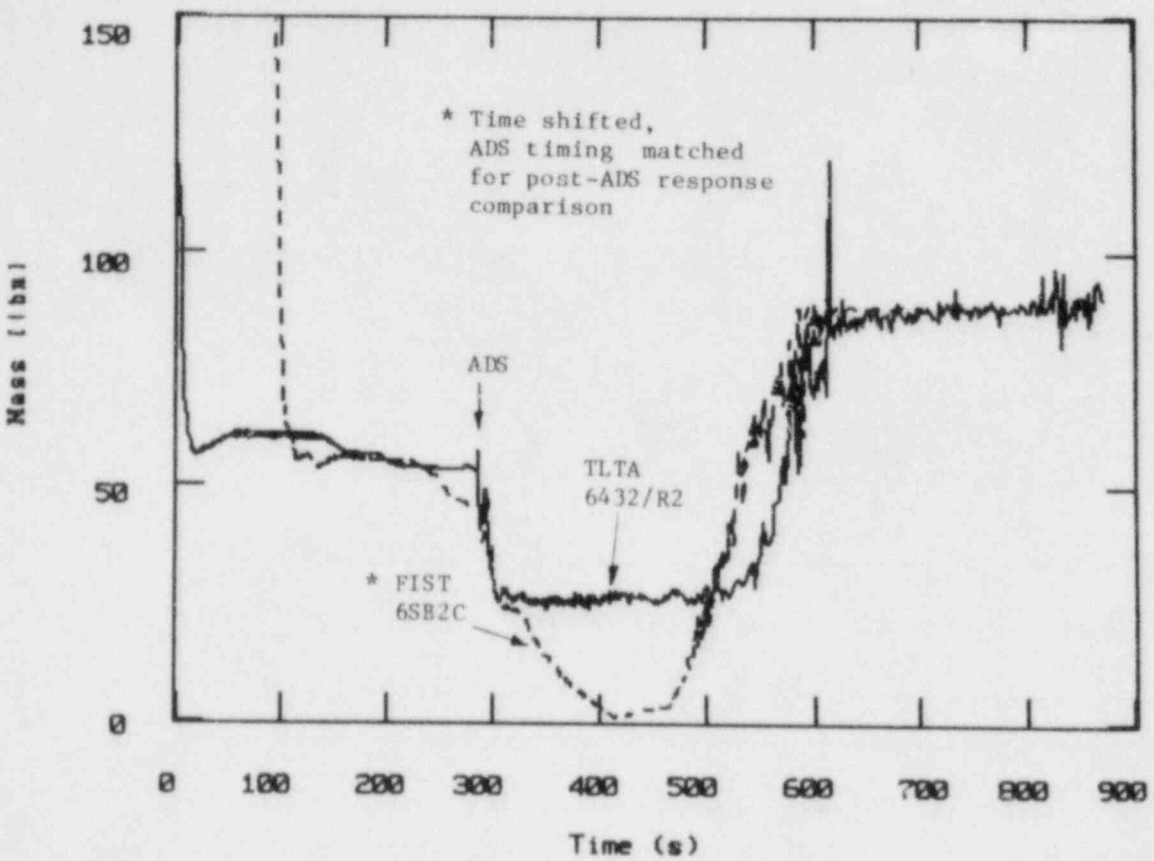

Figure 8.2-10. Post-ADS Bundle Mass Comparison

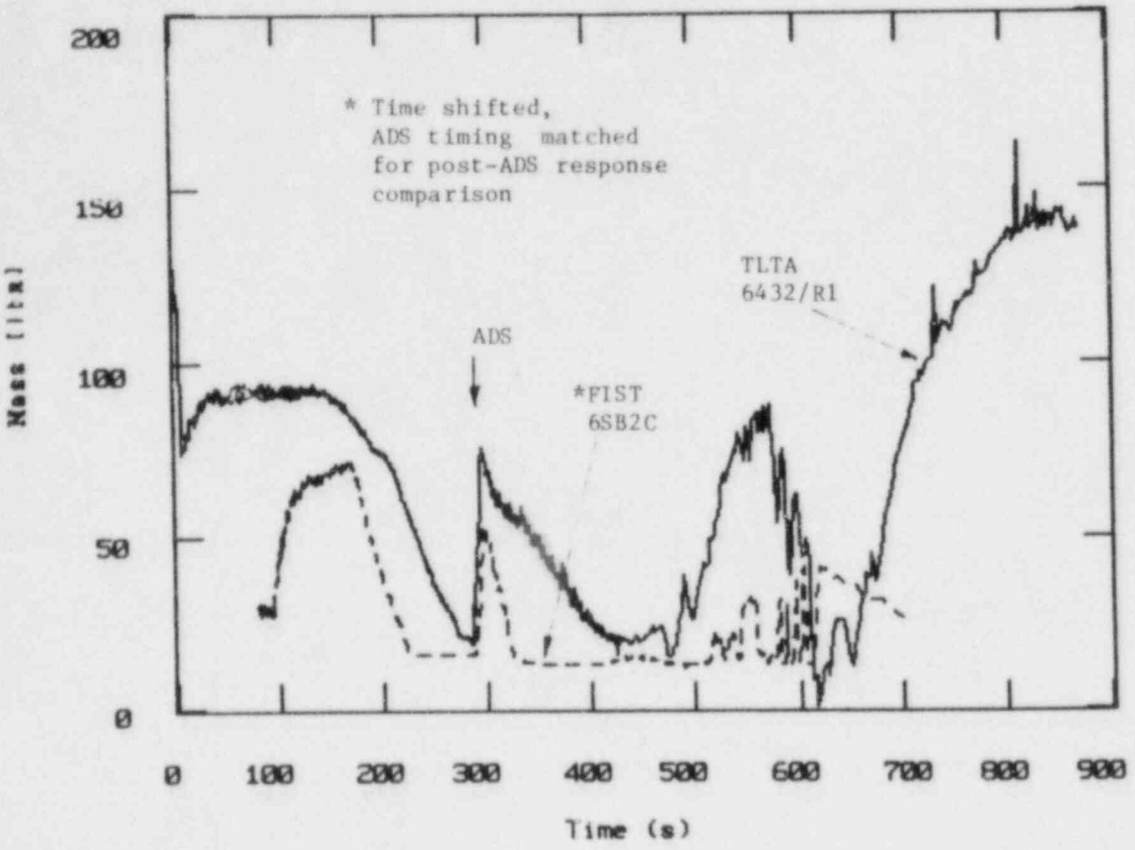

Figure 8.2-11. Post-ADS Upper Plenum Mass Comparison

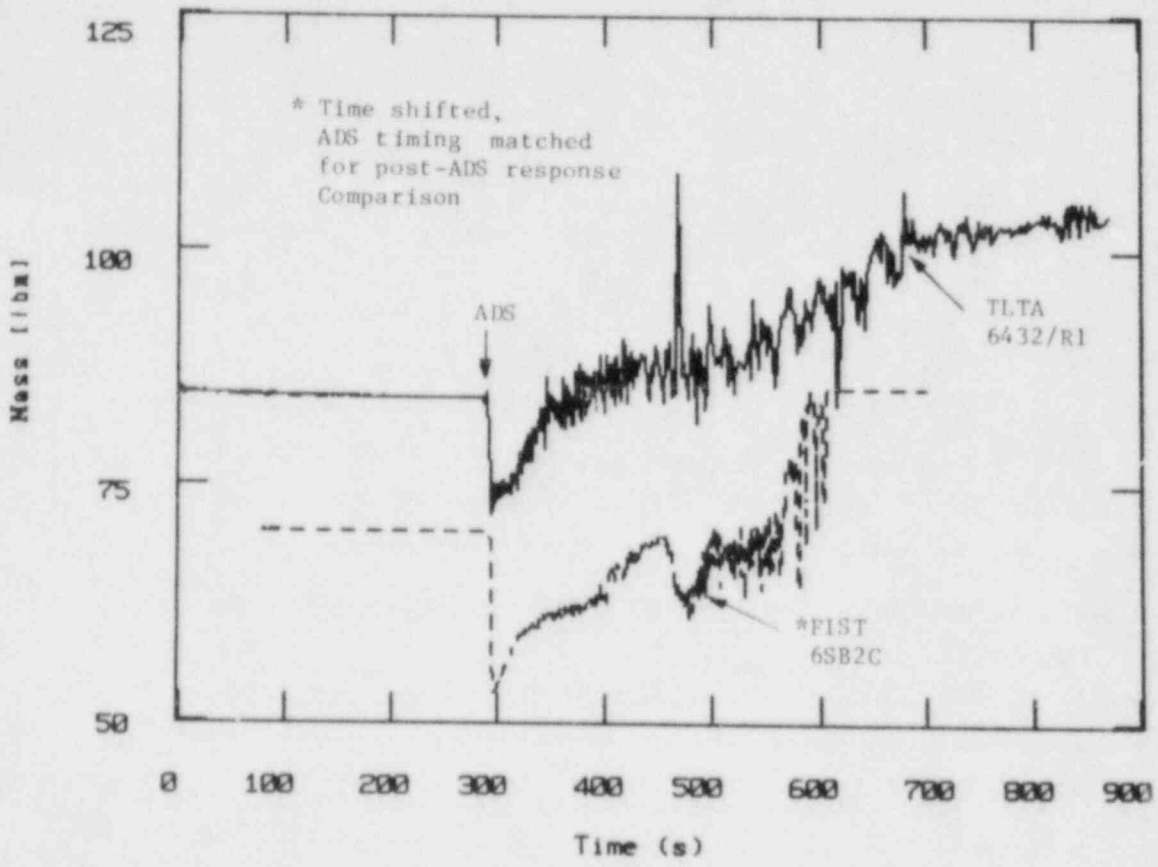

Figure 8.2-12. Post-ADS Guide Tube Mass Comparison

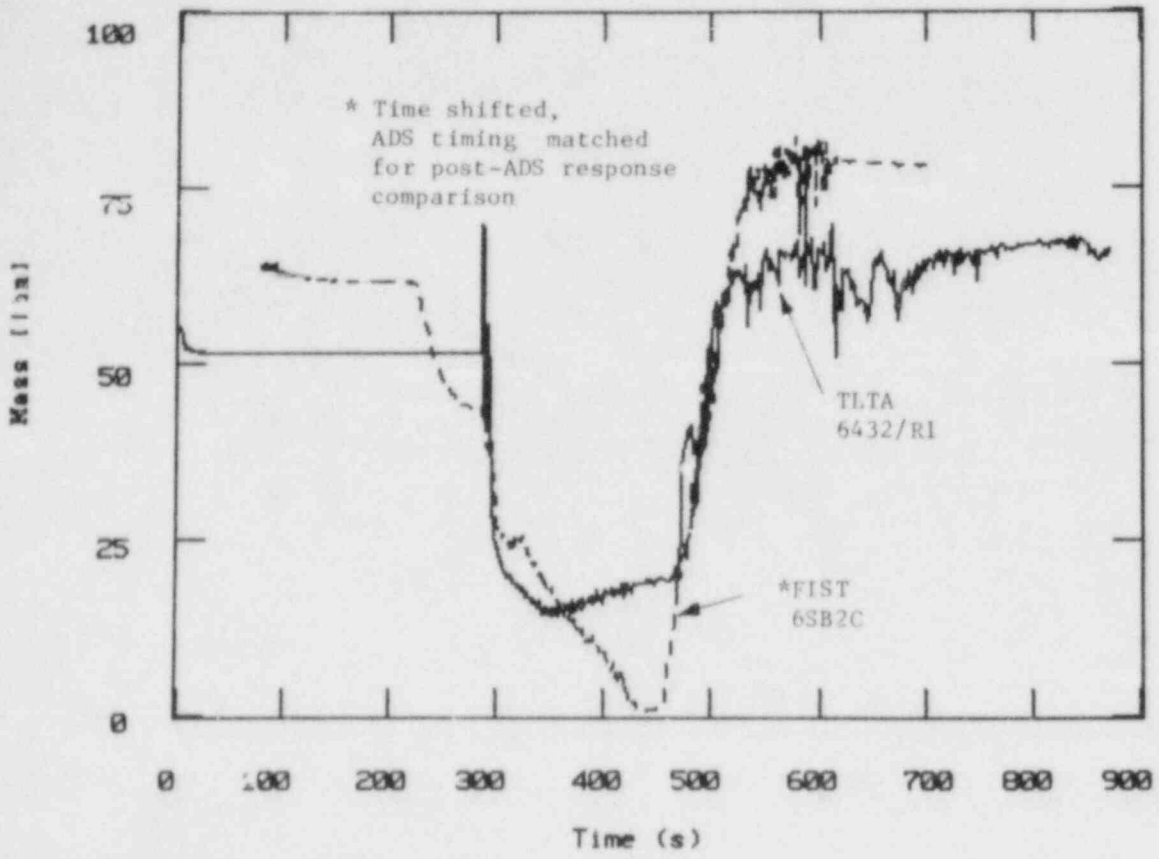

Figure 8.2-13. Post-ADS Bypass Mass Comparison

9. PRETEST PREDICTIONS

(Md. Alamgir and W. A. Sutherland)

9.1 GENERAL DESCRIPTION

One of the FIST program objectives is to assess the TRAC code with test data. This task has been carried out by performing pretest predictions of two LOCA tests, the large break 6DBA1B and the small break 6SB2C, in FIST phase I. The BWR-TRACB02 version was used to make these pretest predictions. Results of the calculations were issued to the PMG before conducting these tests (References 7 and 8) and most of the following discussions have been published in Reference 9.

9.2 SYSTEM DEFINITION INPUT MODELING

The one ring FIST vessel model used in TRAC (Figure 9.2-1) has two theta sections, one to represent the region inside the core shroud and the other for the downcomer. The vessel is divided into 23 axial vessel levels to provide geometric definition of the six principal regions in the system (e.g. lower plenum), correspondence with measurement locations, flow modeling detail (e.g., jet pump exit), and nodalization consistency (e.g. vessel cell to component junction locations). Component models represent the channel, steam separator, jet pumps and tail pipes, guide tube, and recirculation loops and pumps. Additional components model the connecting pipes, such as the ECC systems.

Vessel wall stored heat is modeled with double sided heat slab components between the principal regions and the environment, augmented by lumped heat capacity slabs to model heavy section flanges. In the calculation, the heat loss to the environment was specified using an outside surface heat transfer coefficient determined from system characterization tests by measuring the steady state regional heat losses. System characterization tests at full power steady state conditions also quantified the as-built single-phase flow loss coefficients throughout the system.

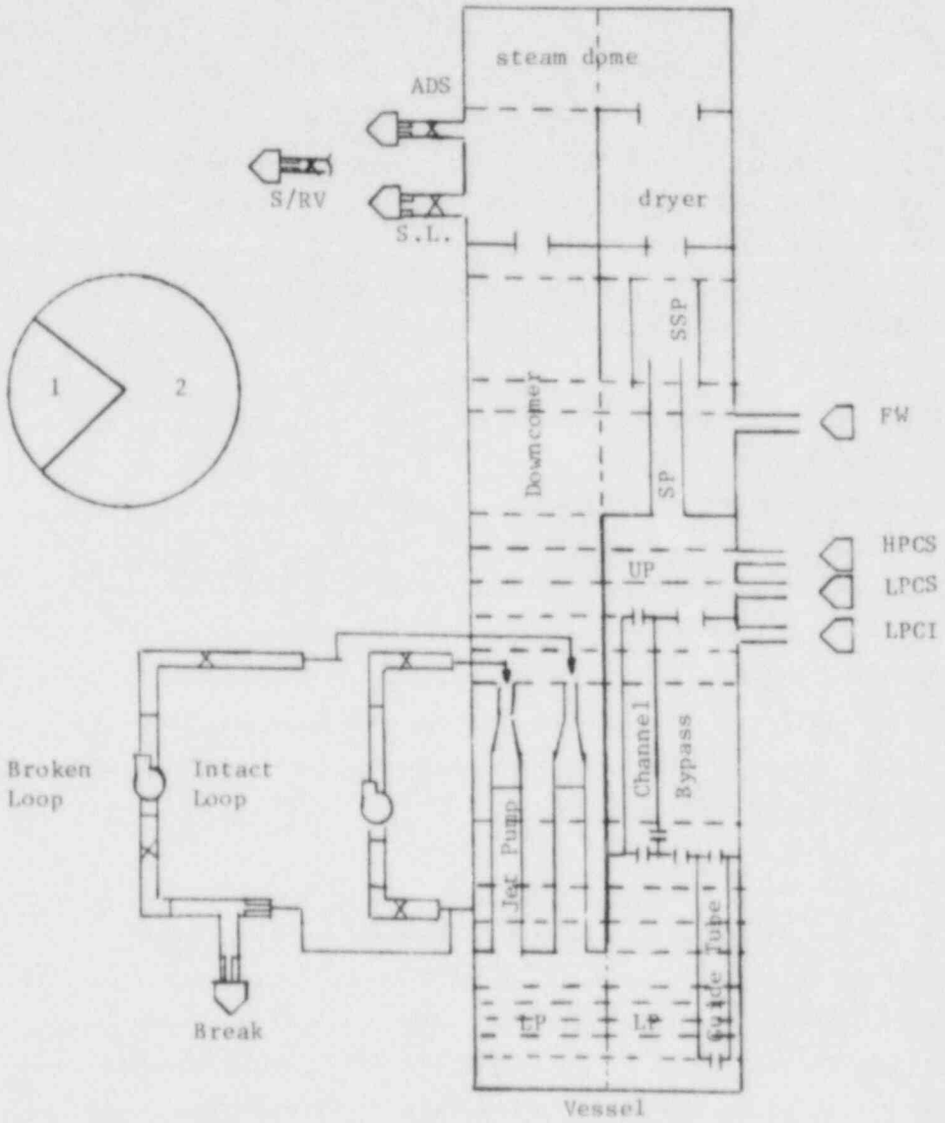

Figure 9.2-1. TRAC Model for FIST Pretest Predictions

Particular attention is given in system definition modeling to the jet pump exit region, the vessel stored heat, and the break location geometry. In cases where the two-phase level in the lower plenum is expected to drop to the jet pump exit plane, flow modeling detail is needed to capture the exit uncovery and subsequent flow split of steam between the jet pump and core regions. The level tracking option, which determines two-phase level location within a vessel cell, is used throughout the system and is particularly needed in the jet pump exit region. Vessel wall and flanges absorb energy from the fluid following a pressurization by an isolation and add energy to the fluid following a depressurization, thus attenuating system pressure response. Heat slab modeling detail is needed to capture this effect in small systems such as the FIST facility.

9.3 CALCULATION RESULTS OF LARGE BREAK TEST, 6DBA1B

System response following the break initiation is characterized by the sudden reversal of the broken loop jet pump and the corresponding decrease in core inlet flow. Pressure is maintained by the pressure control system for about eight seconds as core power decreases, and the core flow decreases to natural circulation rates. TRACB02 predicts the system thermal-hydraulic response during this period very well, as shown in Figure 9.3-1 for the broken loop jet pump flow and Figure 9.3-2 for the intact jet pump flow.

The downcomer level decreases, due to inventory loss, until the break is uncovered and the system depressurizes. As shown in Figure 9.3-3, the level uncovery time and initial depressurization are well predicted. The predicted pressure response after about 40 seconds is lower than measured, which is attributed to underprediction of liquid drops entrained in the steam flow up the jet pumps and out the break. ECCS injection occurs when system pressure decreases below the pump shut-off head. The test facility head-flow characteristic is found to be slightly higher than used in the calculation, which offsets the lower calculated system pressure. The start of injection by the ECC systems in the test and in the calculation are about the same. The satisfactory prediction of the pressure response following break uncovery, which is

dependent on predicting the critical steam flow as well as the energy input to the fluid from the core and vessel walls, leads to a satisfactory prediction of ECCS injection time.

The lower plenum remains essentially full during the first few seconds of the transient, and is then partially voided due to flashing as a result of system depressurization. As seen in Figure 9.3-4, the resulting lower plenum two-phase level is well predicted. This leads to correct calculation of the fraction of mass discharged to the downcomer and to the bundle.

The bundle inventory, shown in Figure 9.3-5, is well predicted throughout the inventory loss and initial system refill sequence. The later oscillations in the calculation are due to shortcomings in "water packing" detection logic in the code. The liquid inventory in the bundle is seen to be depleted at 40 to 50 seconds, and refill by the ECC system shows a positive effect at about 100 seconds. TRAC also predicts very well the inventory depletion and refilling in the bypass (Figure 9.3-6).

Figure 9.3-7 shows the calculated average rod surface temperature at the bundle mid-plane compared with the average of the ten measurements at that elevation. The temperature remains essentially at saturation throughout the transient. The bundle uncovery results in a mid-plane dryout at 40 seconds. The average measured rod heatup, about $50^{o}F$ above saturation, is on the same order as calculated by TRACB02. ECCS injection into the upper plenum region is predicted, and observed, to attenuate the rod heat-up. The individual temperature measurements at the bundle mid-plane are compared with the calculated average temperature in Figure 9.3-8. One thermocouple indicates a peak temperature of about $700^{o}F$. The remaining nine measurements, similar to the calculated average, show little or no heat up. The individual rod temperatures exhibit a variability in local rod surface rewet, apparently from non-uniform planar fluid conditions in the bundle, until the bundle is reflooded. The analysis satisfactorily predicts the bundle dryout. Although the bundle heat transfer model is not expected

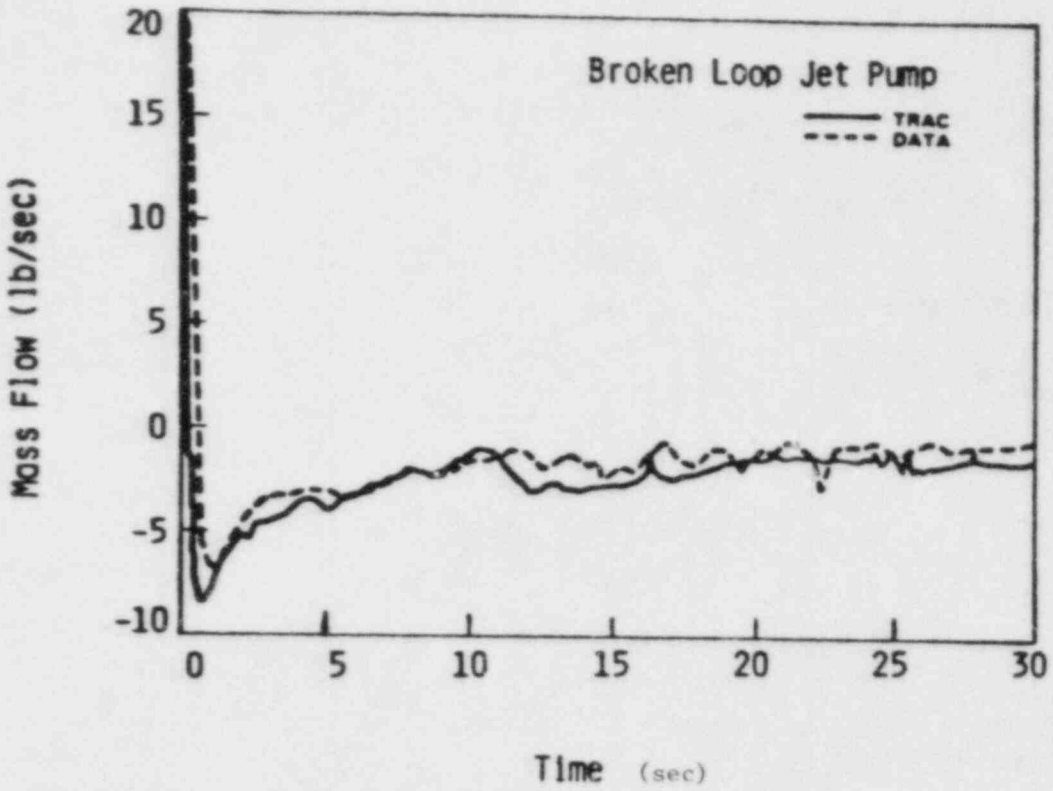

Figure 9.3-1. Comparison of Broken Loop Jet Pump Flows

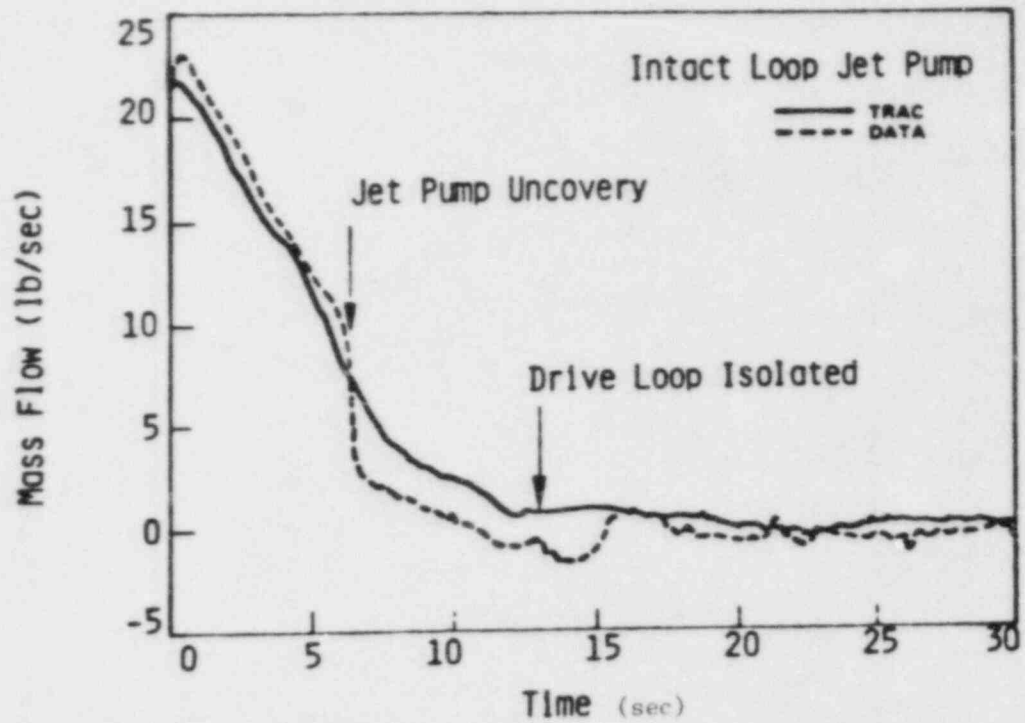

Figure 9.3-2. Comparison of Intact Loop Jet Pump Flows

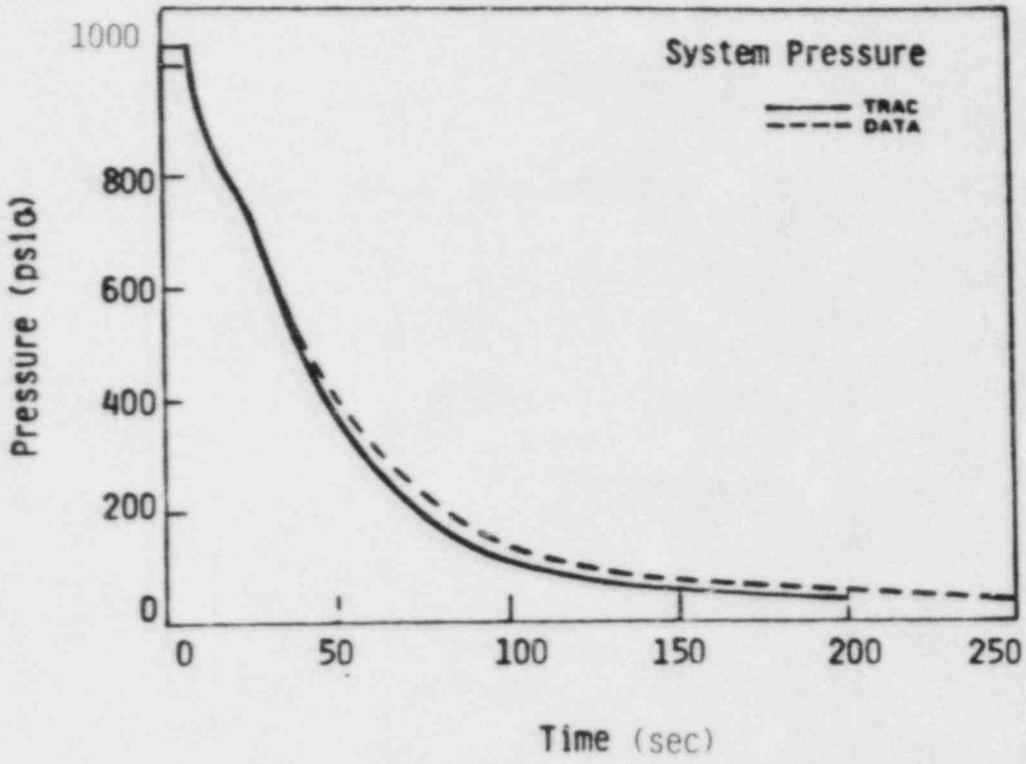

Figure 9.3-3. Comparison of System Pressures

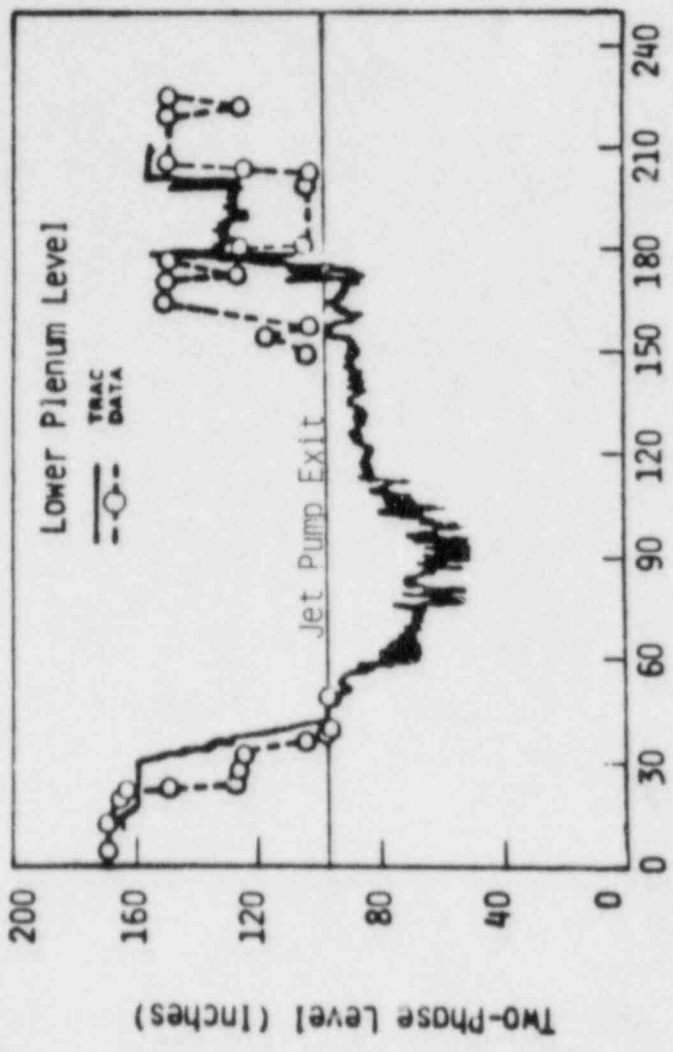

Figure 9.3-4. Comparison of Lower Plenum Water Levels

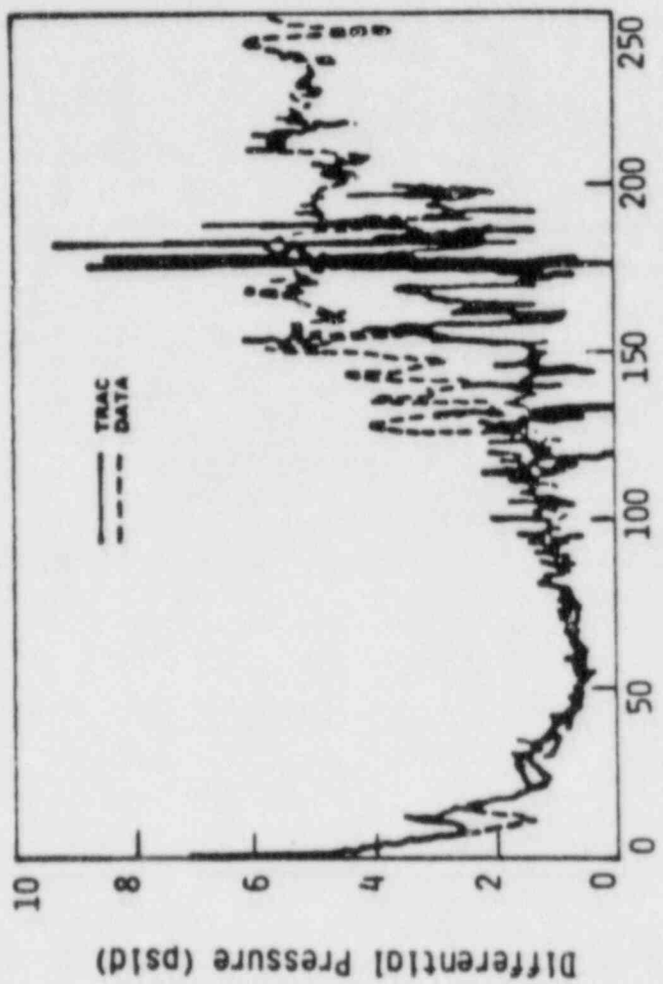

Figure 9.3-5. Comparison of Bundle Pressure Drops

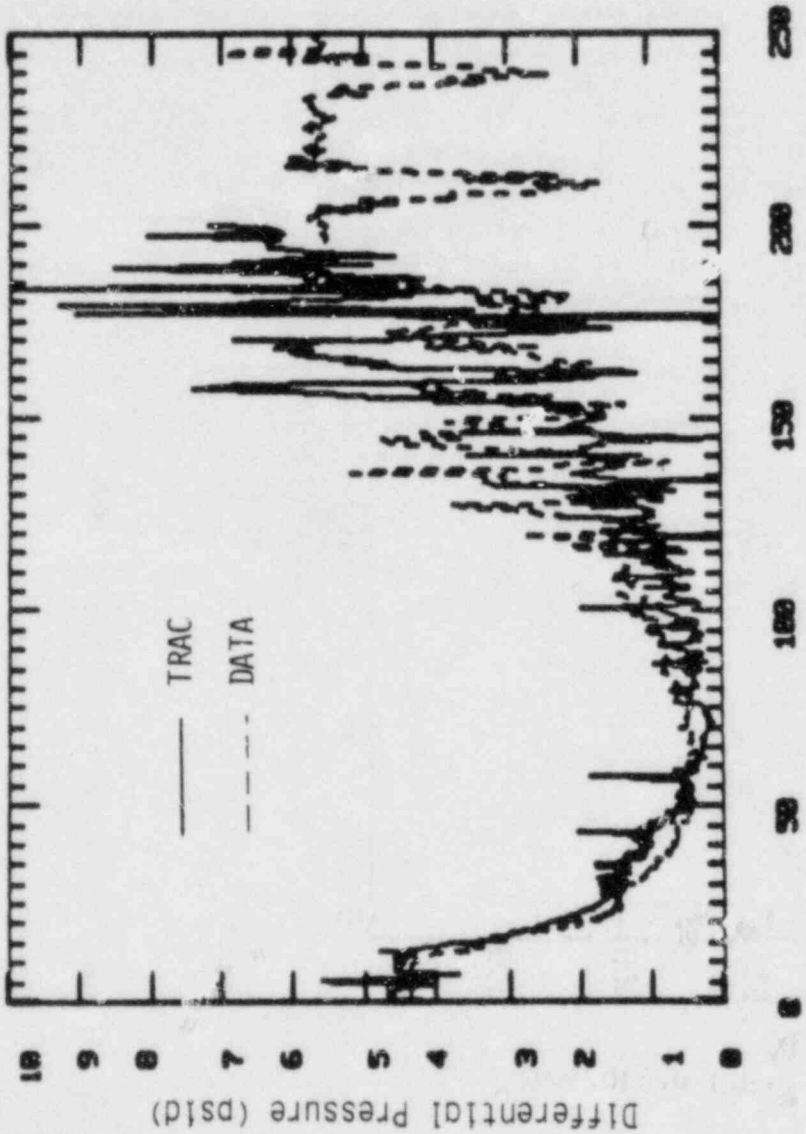

Figure 9.3-6. Comparison of Bypass Pressure Drops

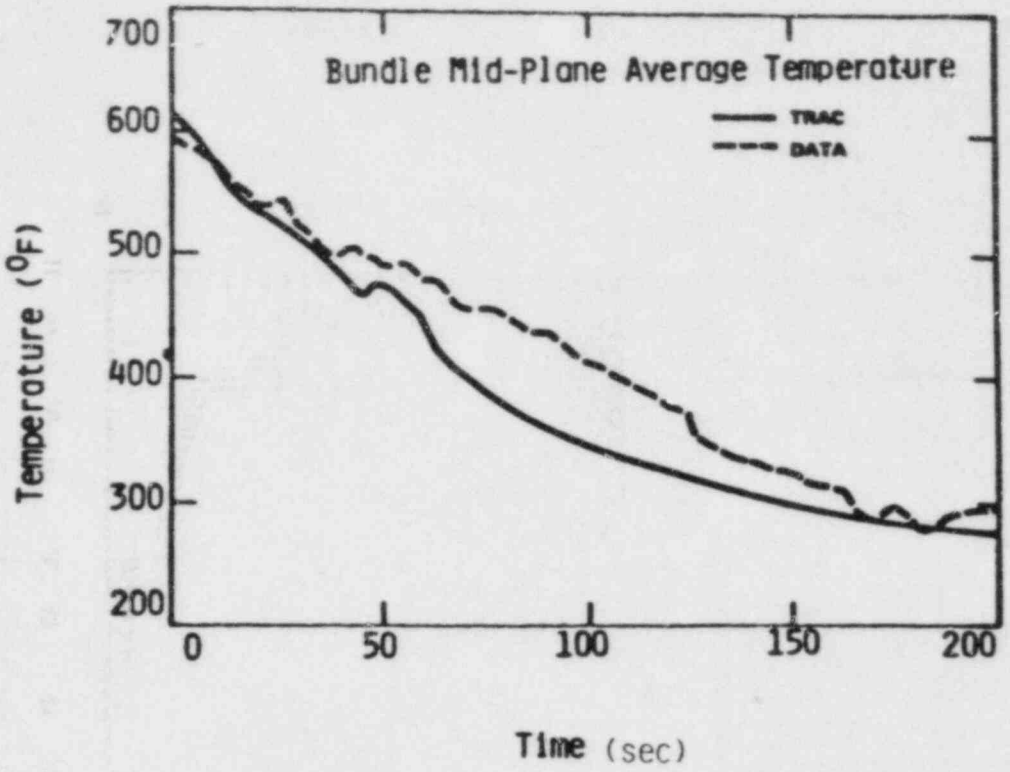

Figure 913-7. Comparison of Bundle Mid-Plane Average Temperatures

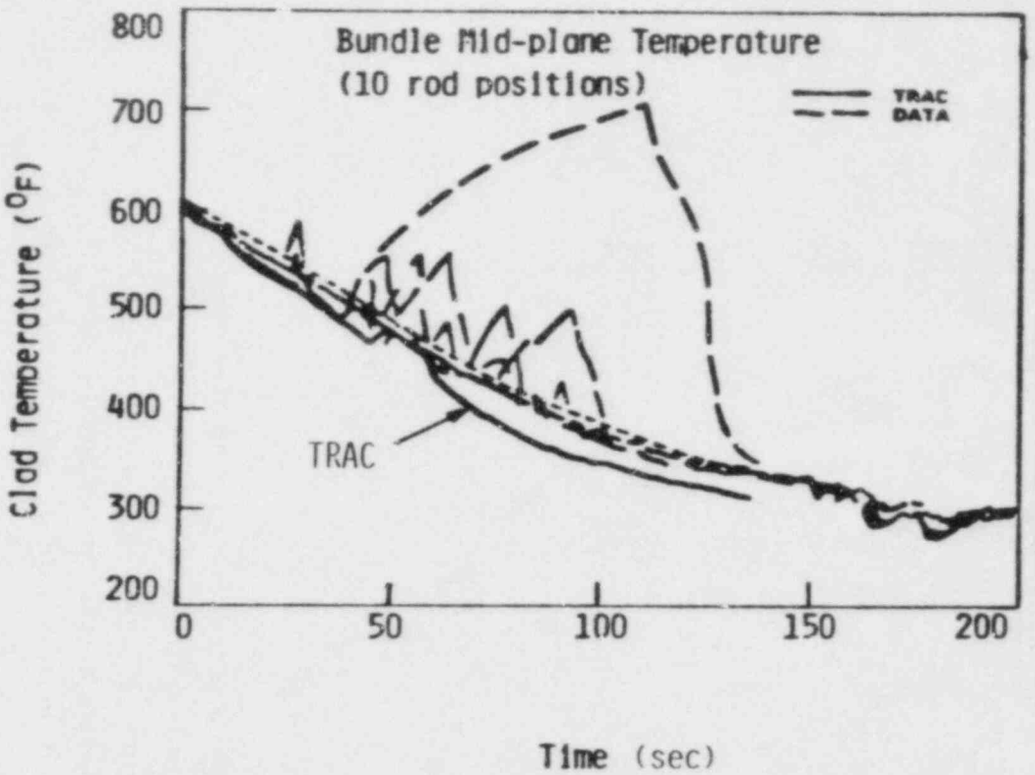

Figure 9.3-8. Comparison of Bundle Mid-Plane Individual Temperatures

to predict individual rod rewet behavior, the reflood inventory response in the bundle adequately bounds the quenching period. The calculated temperature represents the average response based on planar average fluid conditions.

9.4 CALCULATION RESULTS OF SMALL BREAK TEST, 6SB2C

System pressure following the break initiation is maintained by the pressure control system as core power decreases to decay power level and the core flow decreases due to the pump coastdown. The downcomer level begins to decrease due to inventory loss through the break. As would be expected, TRACB02 adequately predicts the system thermal-hydraulic response during this period, which lasts about three minutes.

The downcomer level is calculated to reach the level 1 trip point at 60 seconds, which closes the MSIV and starts the 120 second time delay for the ADS system. As indicated in Figure 9.4-1, the measured time for level 1 trip is 75 seconds; this difference is attributed to a 20% over prediction of subcooled critical flow mass flux during this period. The calculated system pressurization following the main steam line isolation is slightly greater than measured, which may be due to heat slab modeling or potential incomplete isolation of the facility steam line. After the 120 second delay, the ADS system is activated (Figure 9.4-2), pressurizing the system. The difference between calculated time and measured time for ADS activation corresponds to the difference in times for reaching Level 1. ECCS injection begins when system pressure decreases below the pump shut-off head. The test facility head-flow characteristics are found to be slightly higher than that used in the calculation. The satisfactory prediction of the pressure response following ADS, which is dependent on predicting the critical steam flow as well as the energy input to the fluid from the core and vessel walls, leads to satisfactory prediction of ECCS injection time.

The downcomer inventory, shown in Figure 9.4-3 by the equivalent density head measured in the test facility, shows very good correspondence. The difference in the rate of decrease is due to the

prediction of higher subcooled critical flow mass flux discussed above. It is seen that the calculated level reaches the top of the jet pumps at 130 seconds and the measured level at 165 seconds. The change in level decrease rate beyond that time is due to the reduced flow area below this elevation. The apparent stepwise response in the calculation is due to a numerical modeling limitation. The downcomer inventory comparison shows satisfactory agreement during the post ADS flashing surge period (flow surge up the jet pumps) and post ECC injection period (liquid spill over from the jet pumps).

The bypass remains essentially full during the first 100 seconds of the transient (Figure 9.4-4). When the downcomer level falls below the top of the core region, the bypass inventory has a corresponding decrease. The difference shown in Figure 9.4-4 for the starting time for bypass level decrease corresponds to the difference in downcomer level decrease. The subsequent bypass inventory and refill is well predicted. The noticeable oscillations in the predicted trace is due to a limitation in the "water packing" detection logic.

The lower plenum remains essentially full during the transient before the ADS actuation, and is then partially voided due to flashing as a result of system depressurization. The offset is again due to the difference in ADS actuation time. As seen in Figure 9.4-5, the resulting lower plenum mass inventory is well predicted, as is the fraction of mass discharged to the downcomer, Figure 9.4.3, and to the bundle, Figure 9.4-6.

The bundle inventory, shown in Figure 9.4-6, is well predicted throughout the entire inventory loss and system refill sequence. The offset during the 80 second to 180 second period is again due to the downcomer inventory difference discussed above, and the later oscillations are due to shortcomings in "water packing" detection logic in the code.

Figures 9.4-7 to 9 show the calculated rod surface temperatures at various locations compared with the average of measured temperatures at the corresponding elevations. TRAC predicts these temperature responses

very well. A small rod heatup is seen in the upper bundle, just before ADS, due to the bundle partially uncovering. All rods, however, are rewetted by the ADS flashing surge. After this flashing surge, the bundle subsequently returns to the draining mode, which results in uncovery and bulk dryout at about 250 seconds.

ECCS injection into the bypass and upper plenum regions is well predicted (Figure 9.4-1). ECC cooling attenuates the planar average heatup and results in rod rewets shortly after initiation. Final rod quenching is completed as the bundle is reflooded. (Figure 9.4-6). TRAC predicts this ECC cooling effect and planar average rod rewetting responses very well.

Figures 9.4-10 through 27 show the measured individual rod temperatures from which the above average rod temperatures are obtained. These plots indicate a variability in local rod surface rewet during the refill period.

The analysis satisfactorily predicts the bundle dryout and heatup. Although TRAC is not expected to predict individual rod rewet behavior, the reflood inventory response in the bundle adequately bounds the quenching period.

9.5 TRACB02 ASSESSMENT

The TRAC analysis quantifies a number of important BWR thermal-hydraulic phenomena, many of which occur after system depressurization. System pressure response, bulk flashing, the corresponding void distribution and two phase levels are well predicted. Counter-current flow limiting (CCFL) is predicted and observed at key areas, such as the bundle inlet and outlet. Two-phase levels are also found in various vessel regions. The TRAC/data comparisons are quite good overall. Numerical model limitations that had a small effect on the downcomer level response and "water packing" during the reflood period have been improved in a later version of the code.

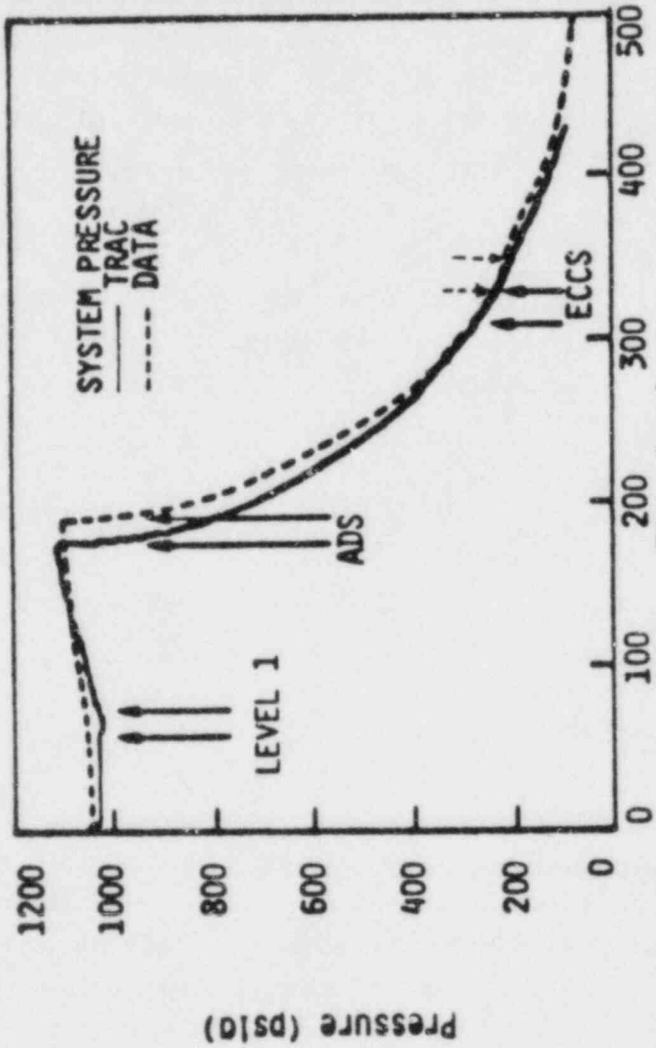

Figure 9.4-1. Comparison of System Pressures

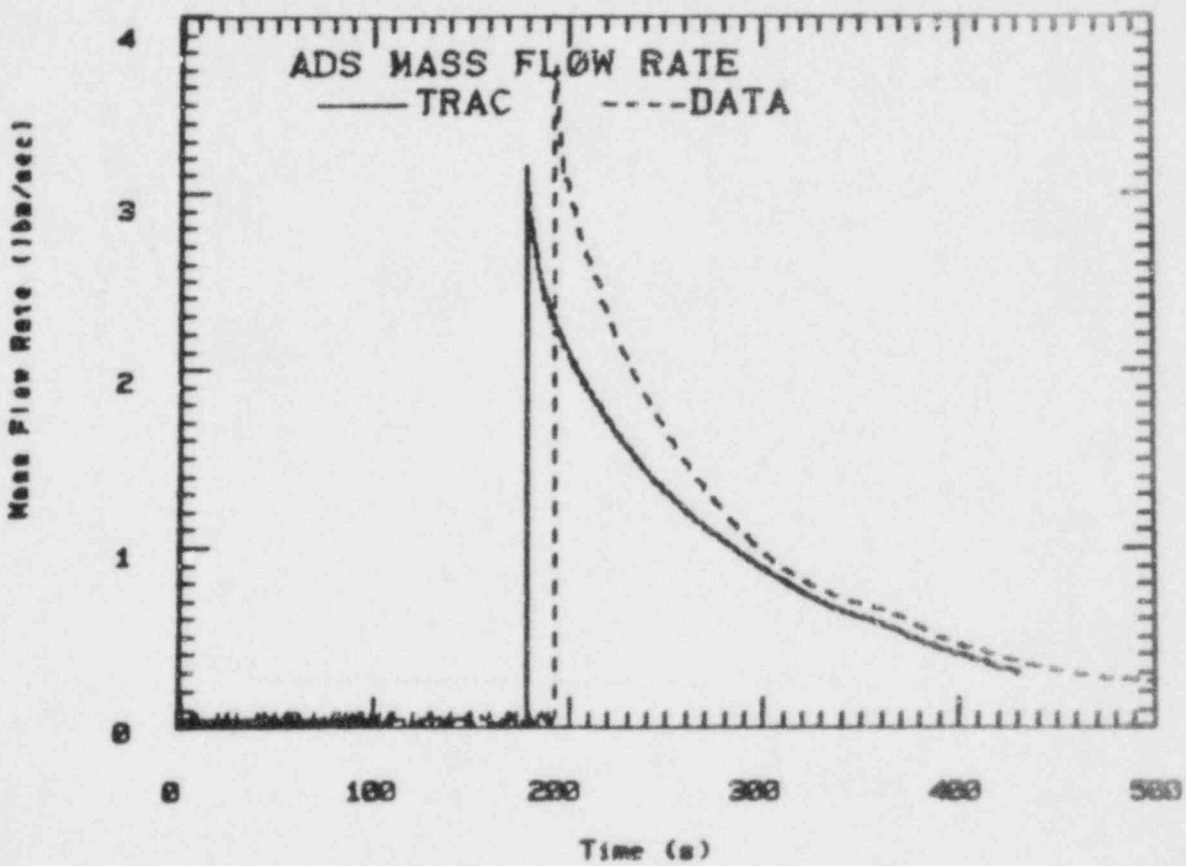

Figure 9.4-2. Comparison of ADS Flows

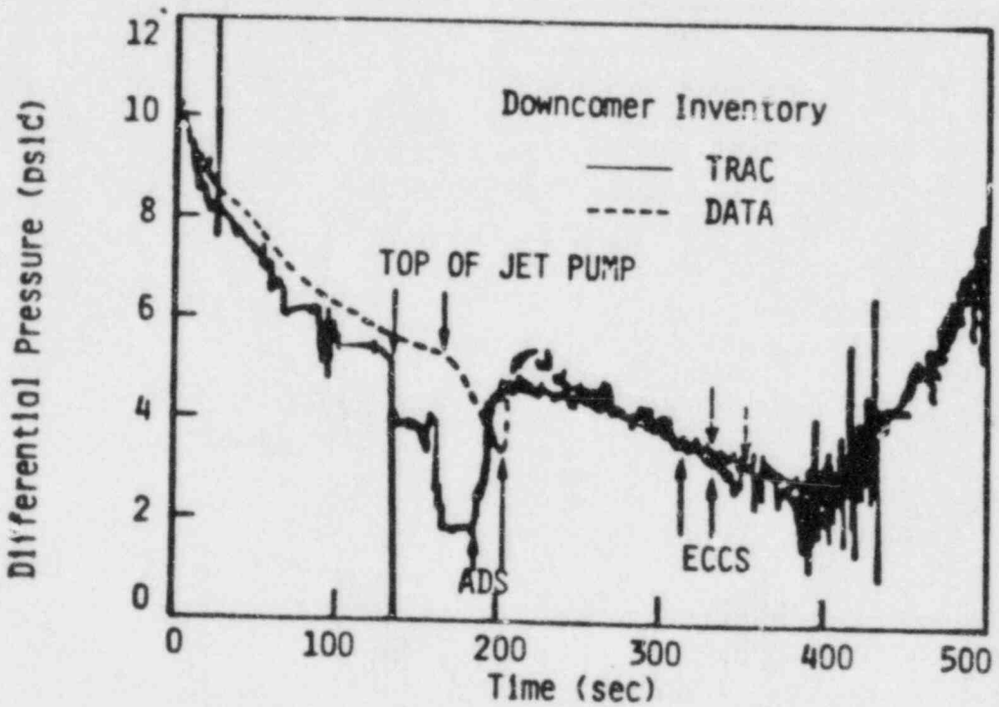

Figure 9.4-3. Comparison of Downcomer Inventories

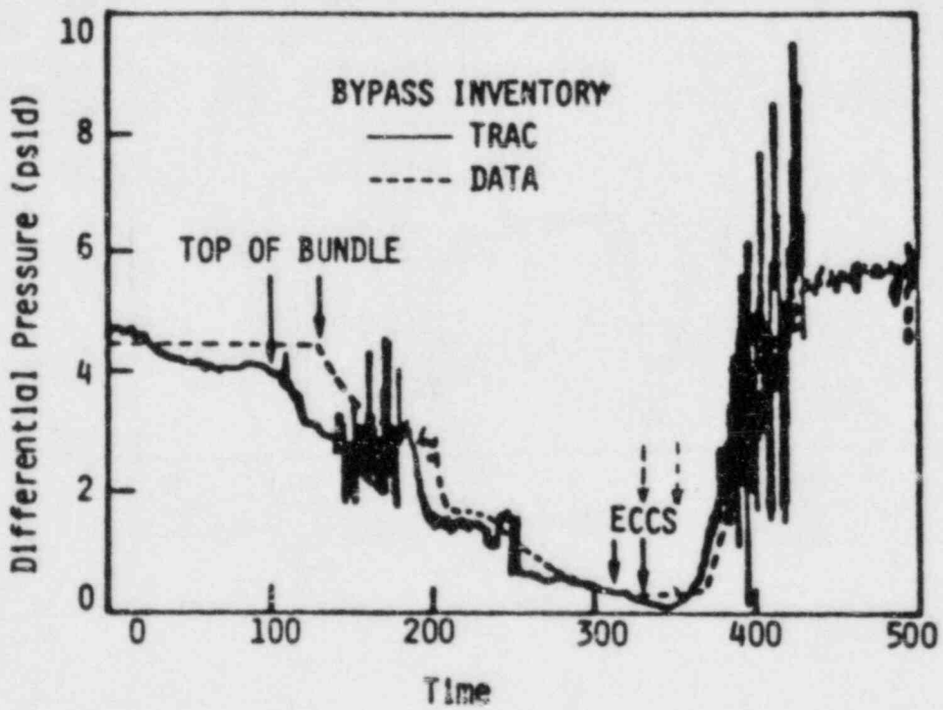

Figure 9.4-4. Comparison of Bypass Inventories

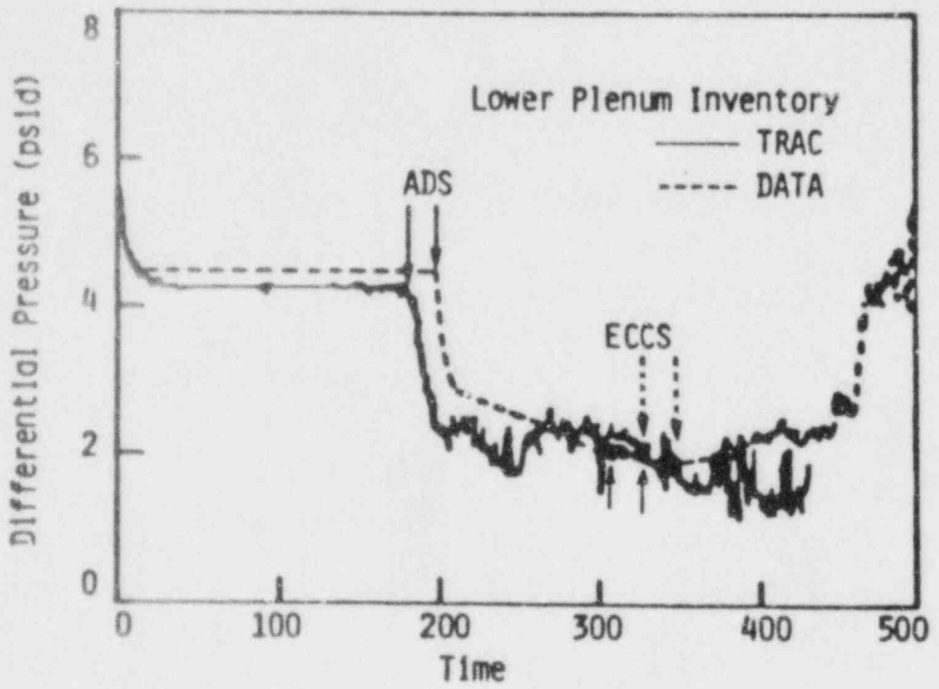

Figure 9.4-5. Comparison of Lower Plenum Inventories

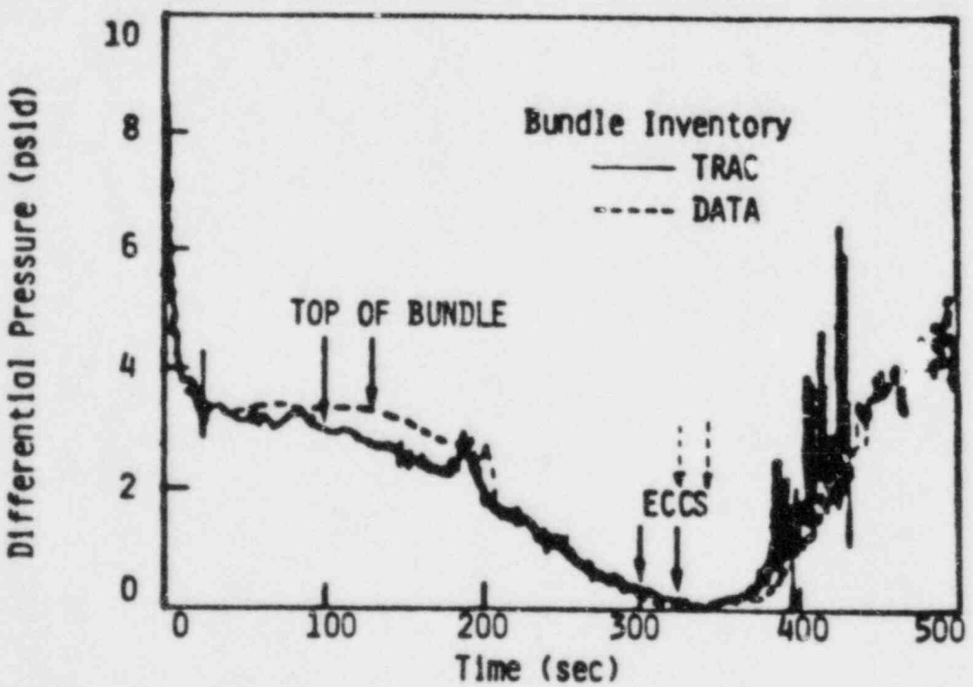

Figure 9.4-6. Comparison of Bundle Inventories

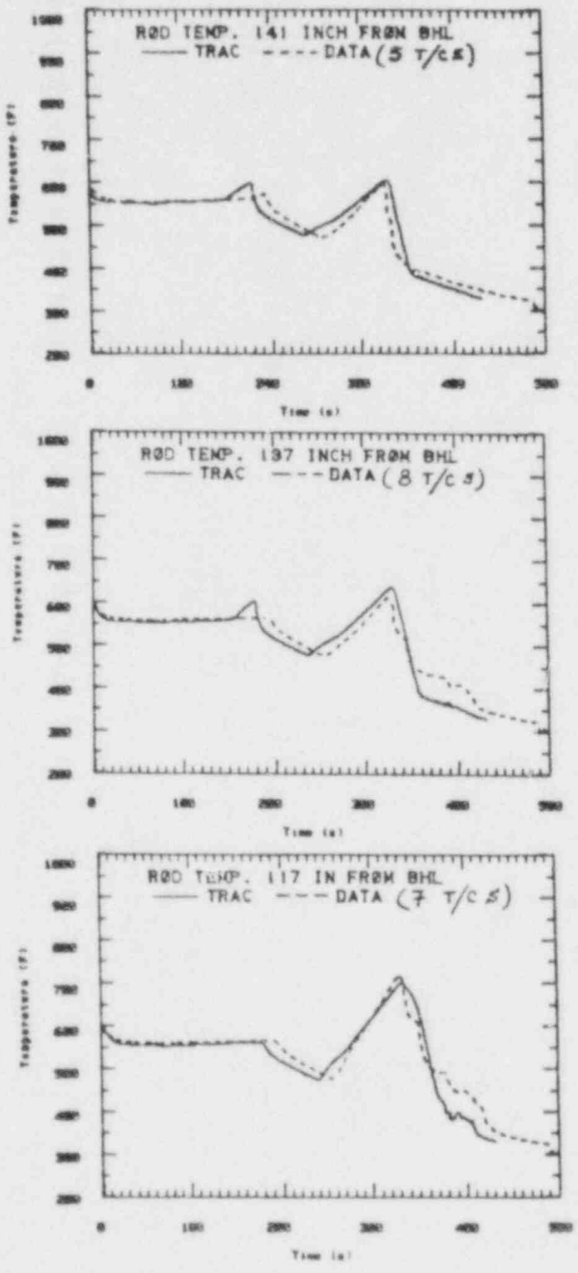

Figure 9.4-7. Comparisons of Bundle Average Temperatures Above Elev 117"

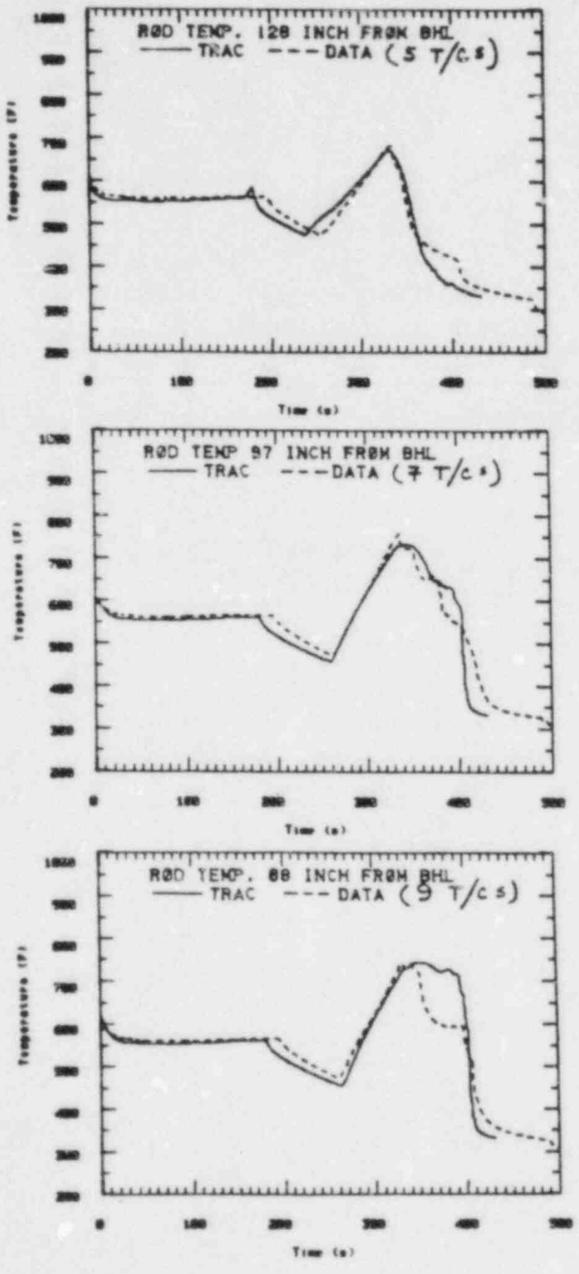

Figure 9.4-8. Comparisons of Bundle Average Temperatures Between Elev. 88" and 128"

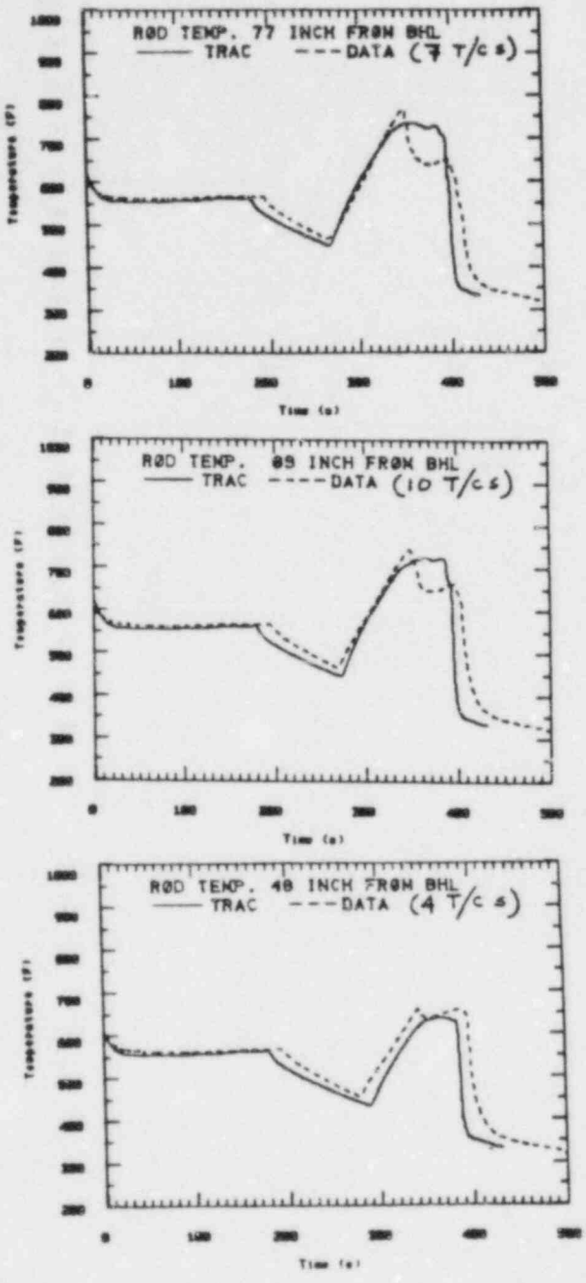

Figure 9.4-9. Comparisons of Bundle Average Temperatures Between Elev 48" and 77"

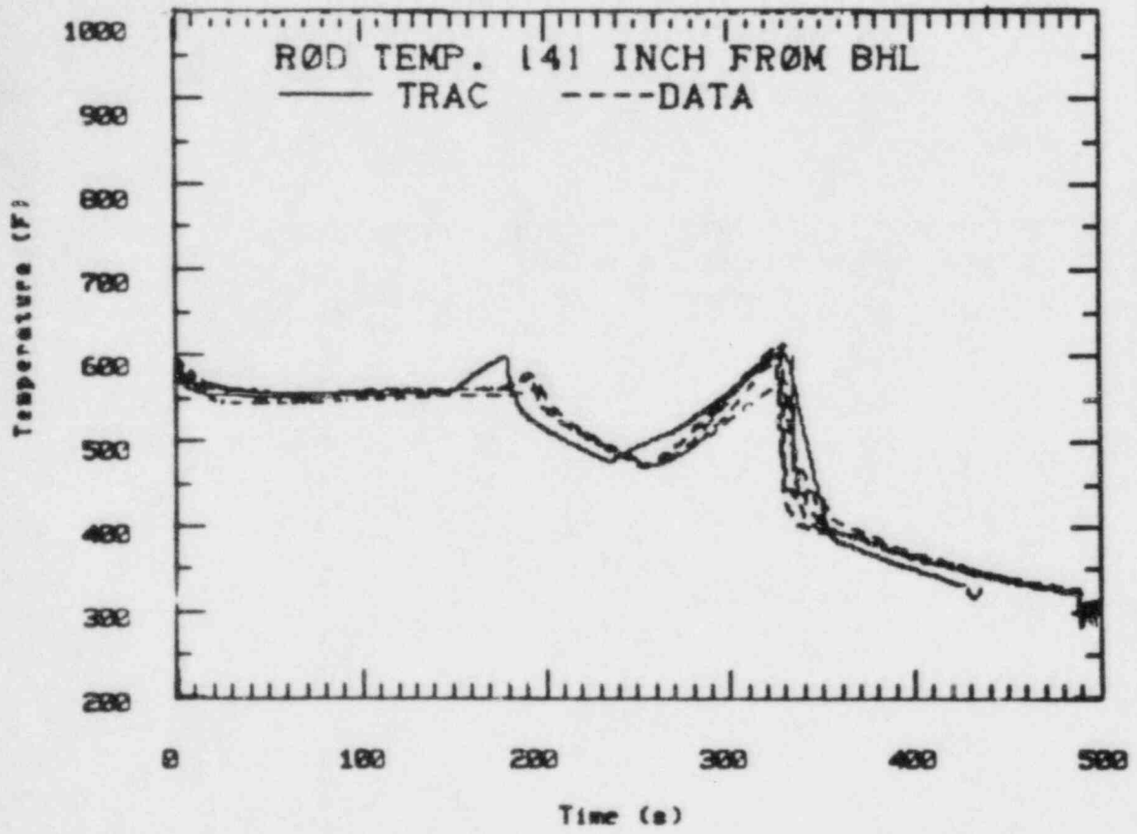

Figure 9.4-10. Comparisons with Individual Rod Temperatures at Elev. 141"

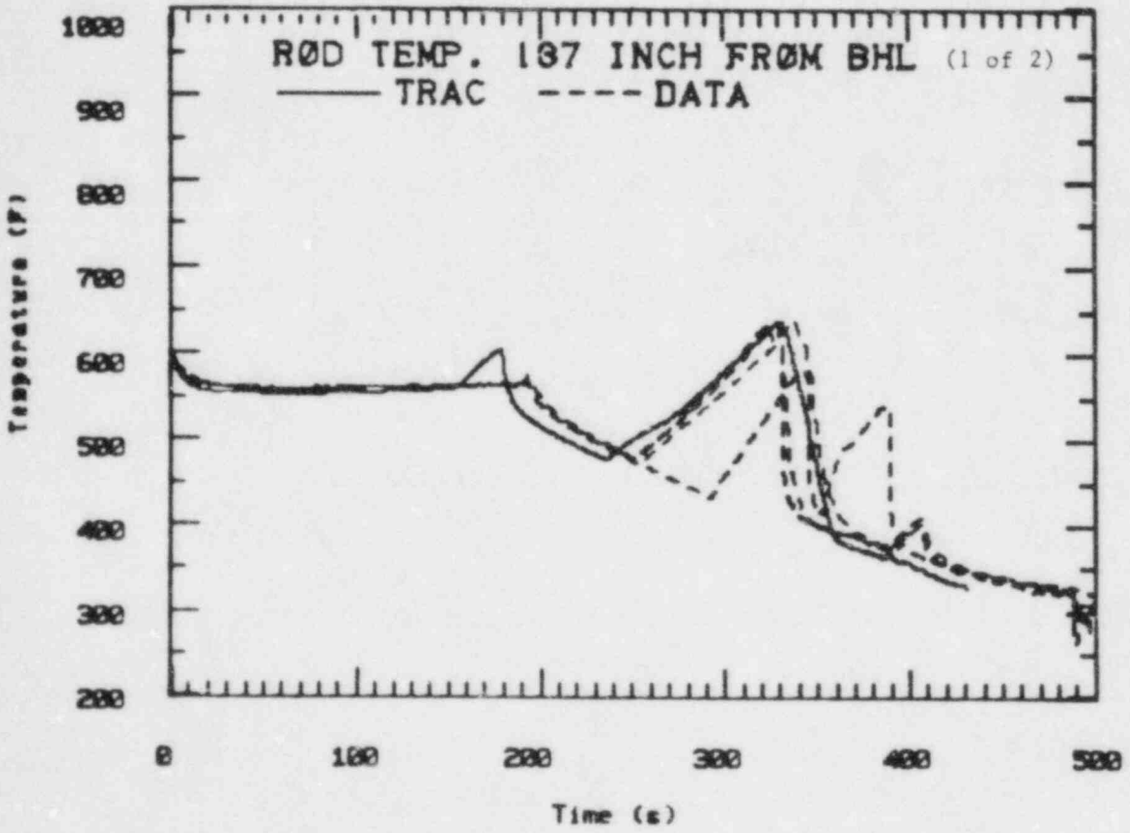

Figure 9.4-11. Comparisons with Individual Rod Temperatures at Elev 137"

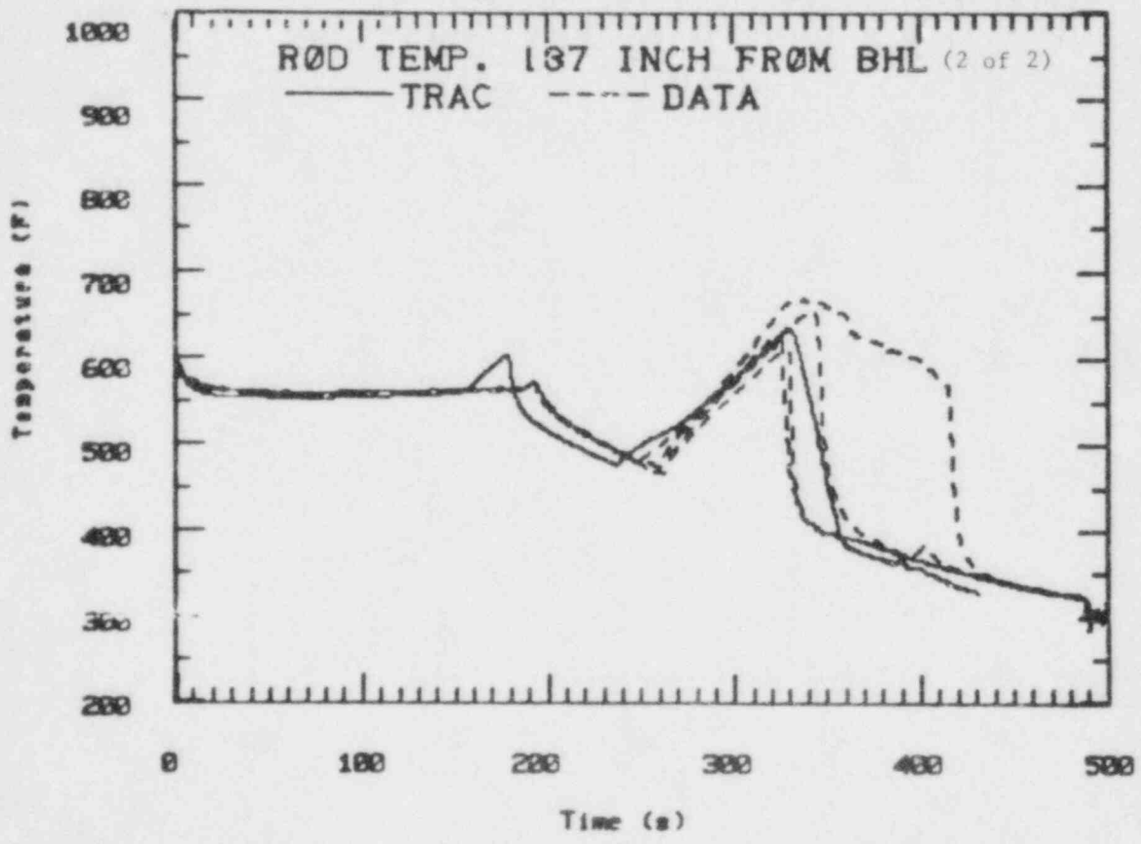

Figure 9.4-12. Comparisons with Individual Rod Temperatures at Elev 137"

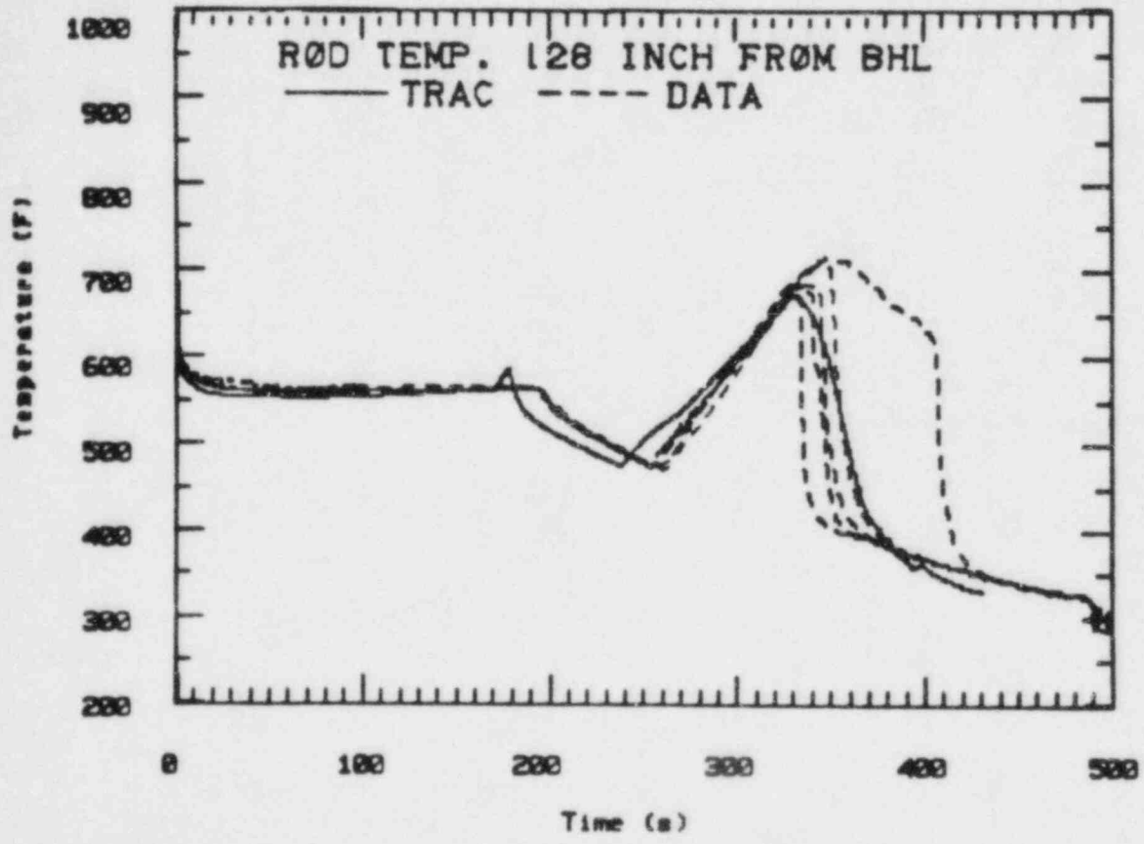

Figure 9.4-13. Comparisons with Individual Rod Temperatures at Elev 128"

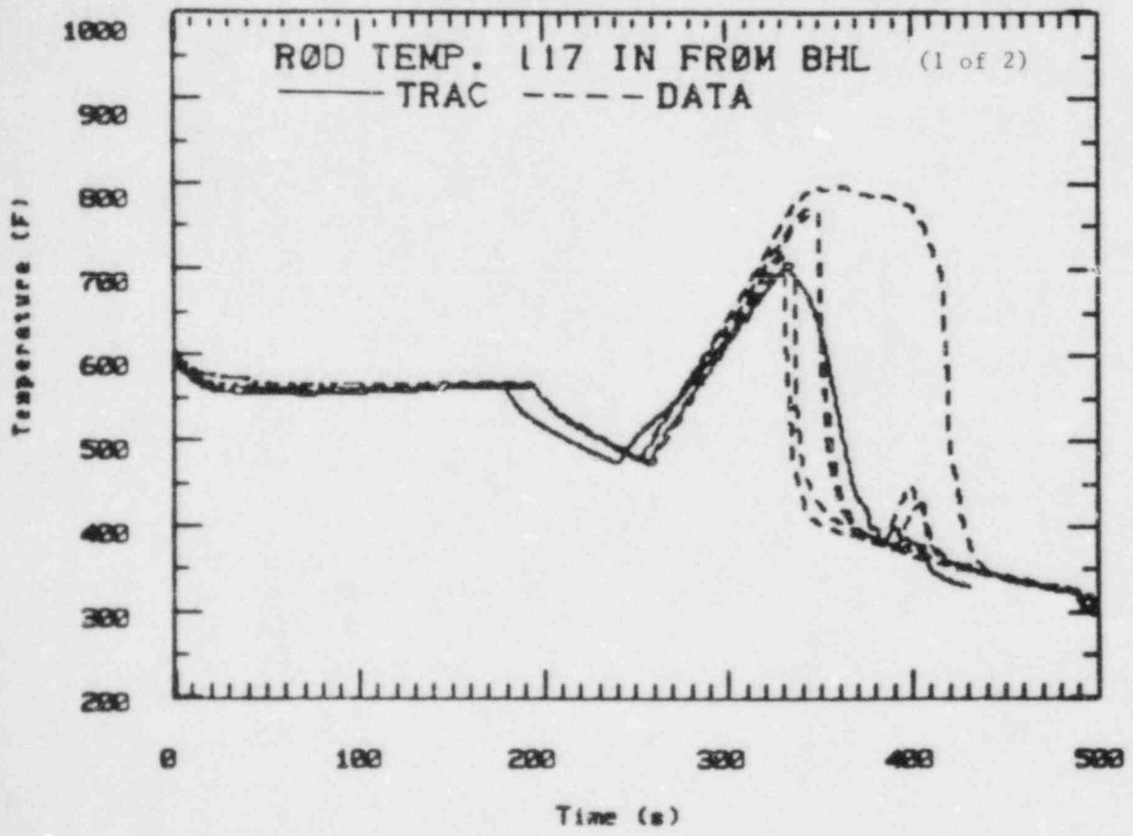

Figure 9.4-14. Comparisons with Individual Rod Temperatures at Elev 117"

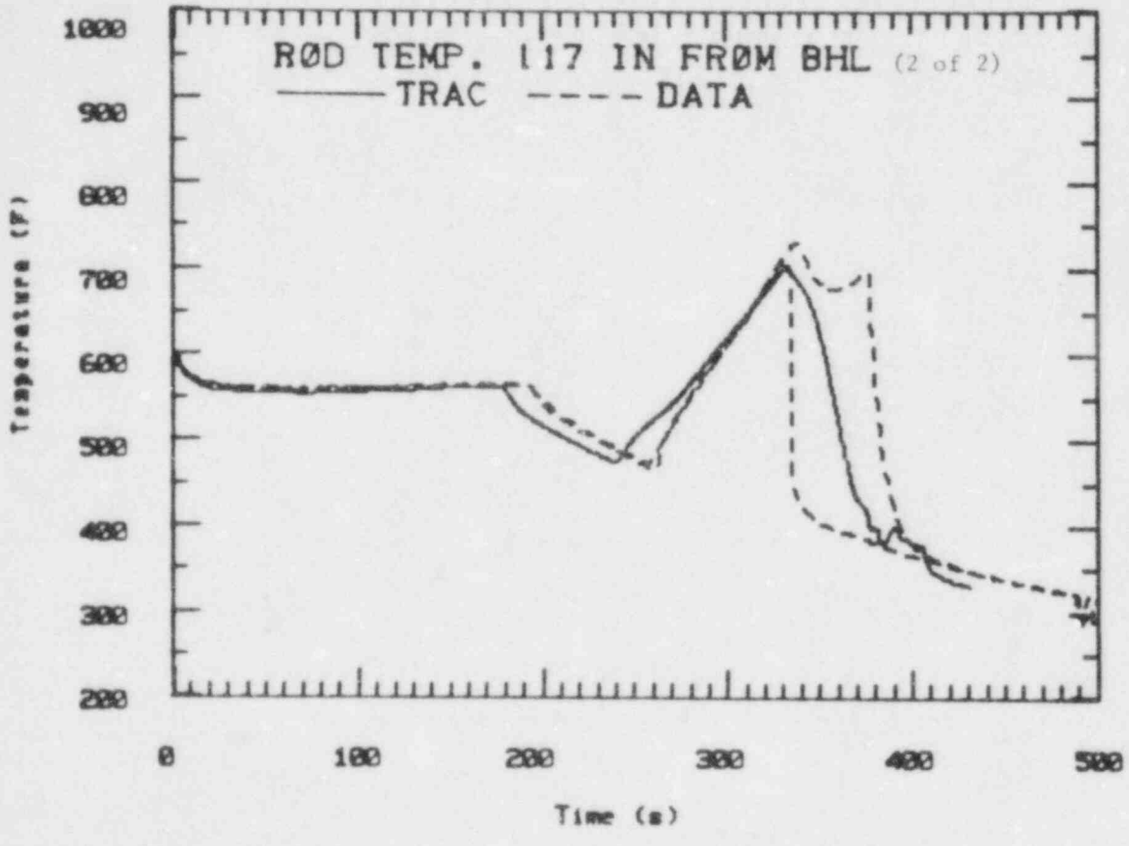

Figure 9.4-15. Comparisons with Individual Rod Temperatures at Elev 117"

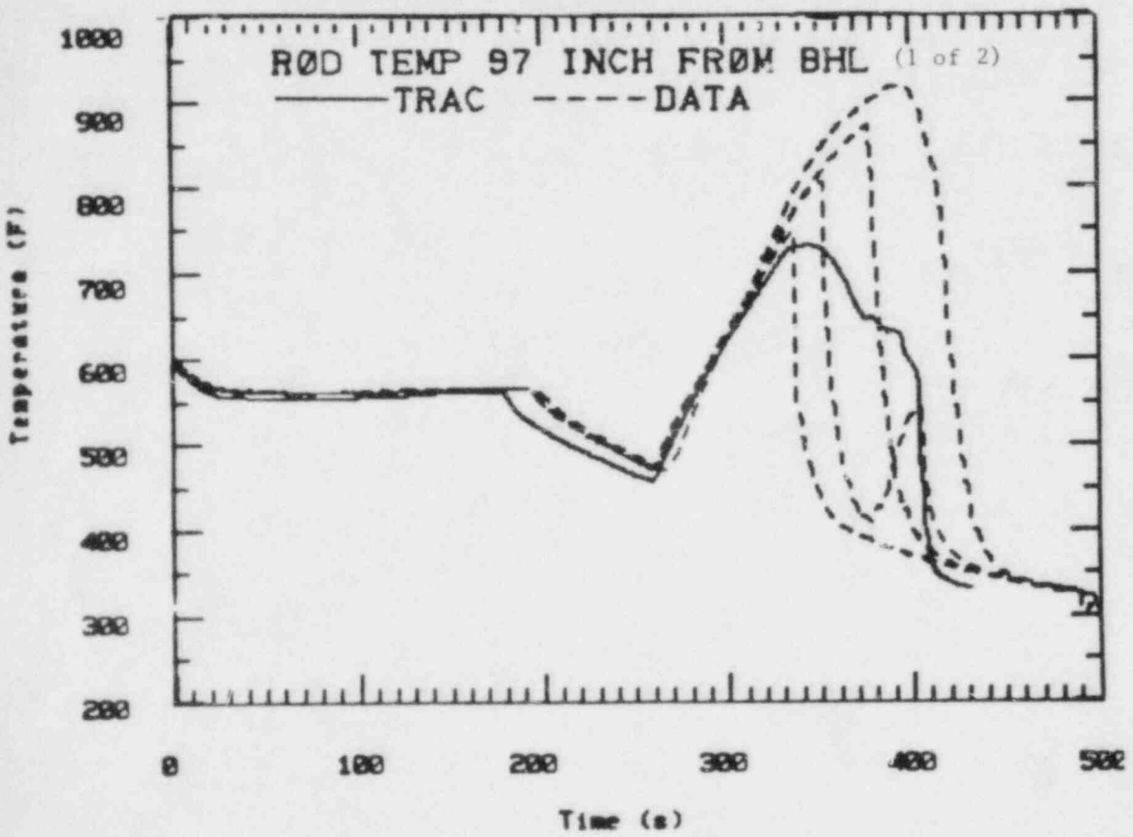

Figure 9.4-16. Comparisons with Individual Rod Temperatures at Elev 97"

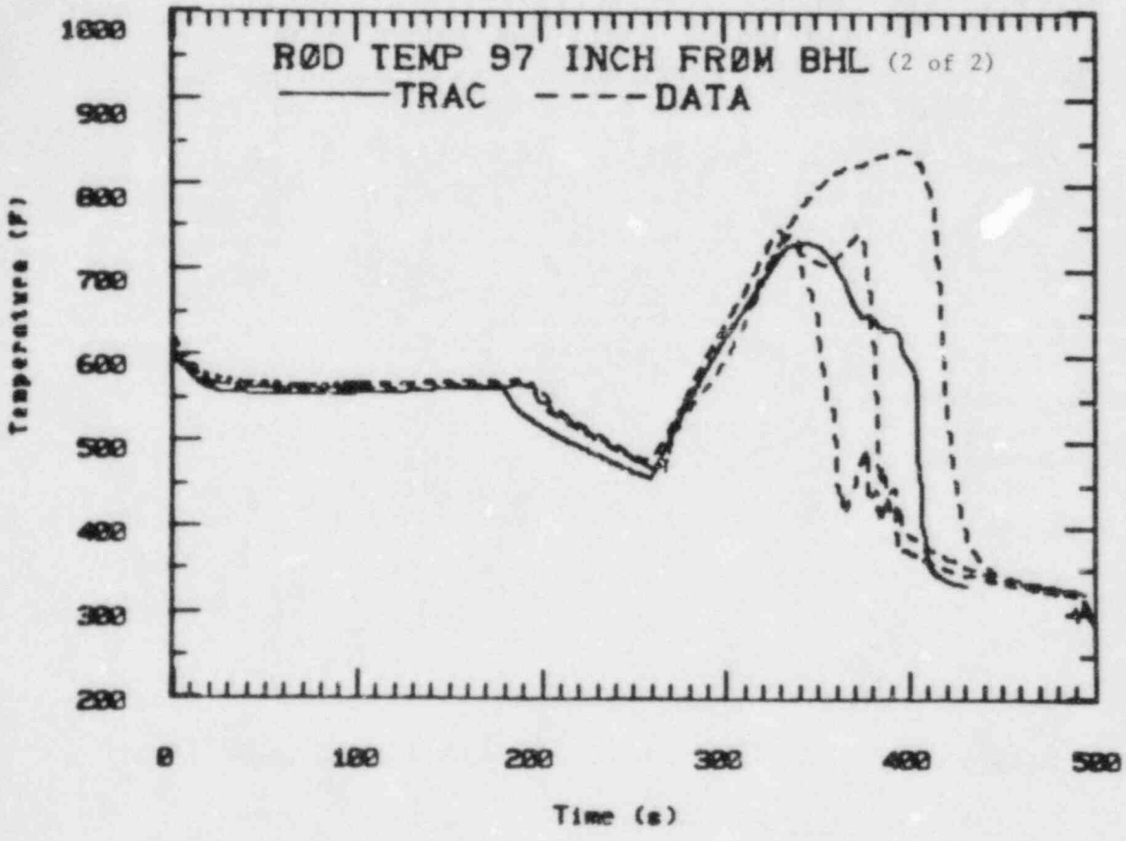

Figure 9.4-17. Comparisons with Individual Rod Temperatures at Elev 97"

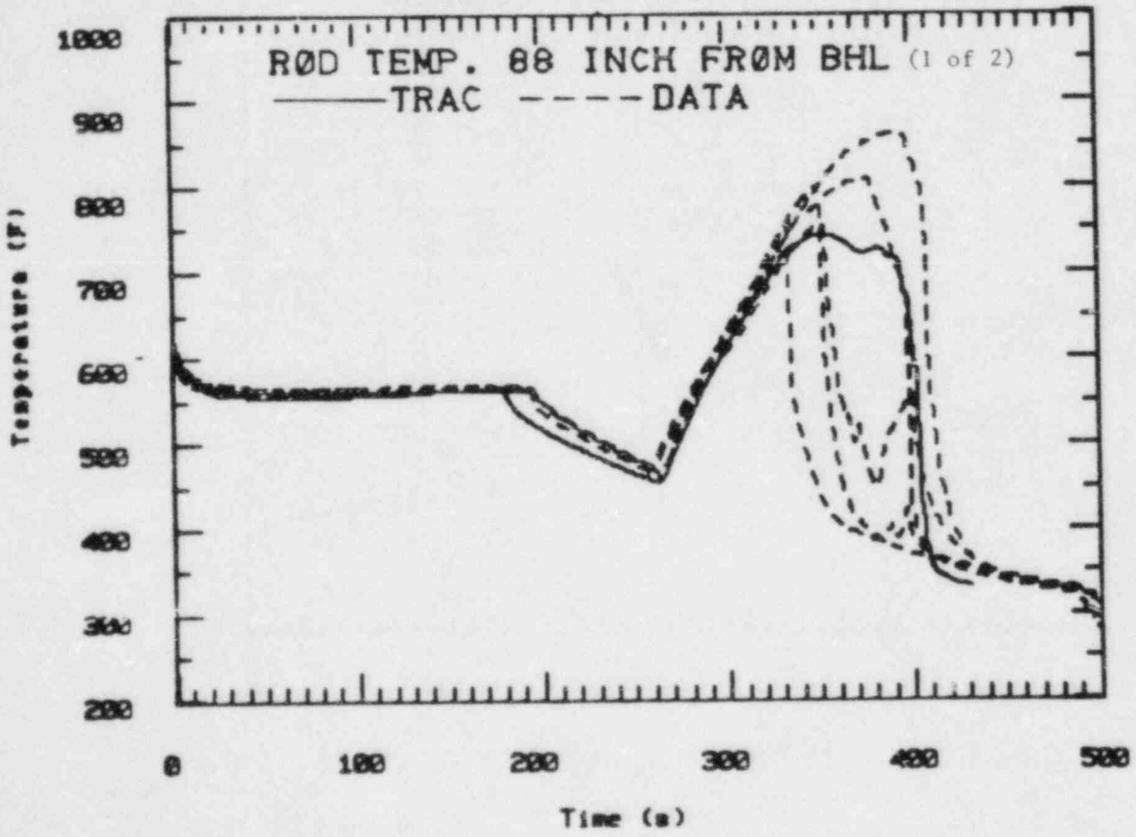

Figure 9.4-18. Comparisons with Individual Rod Temperatures at Elev 88"

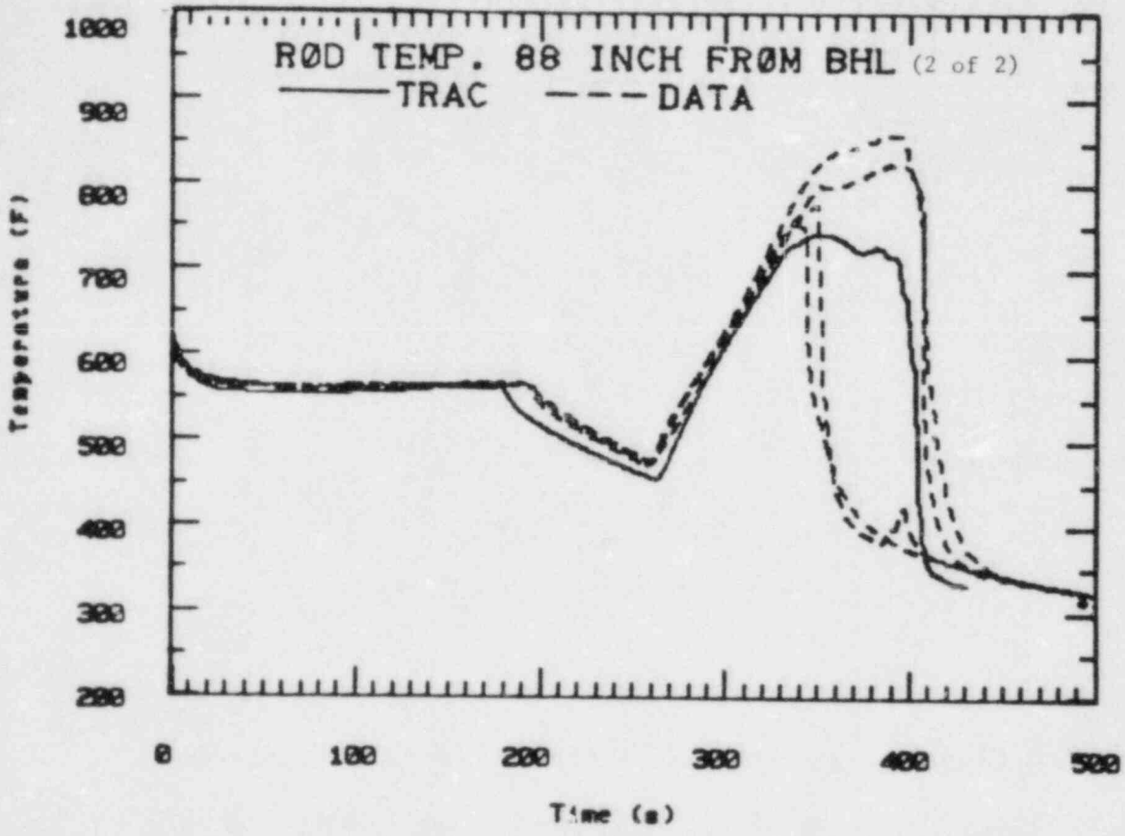

Figure 9.4-19. Comparisons with Individual Rod Temperatures at Elev 88"

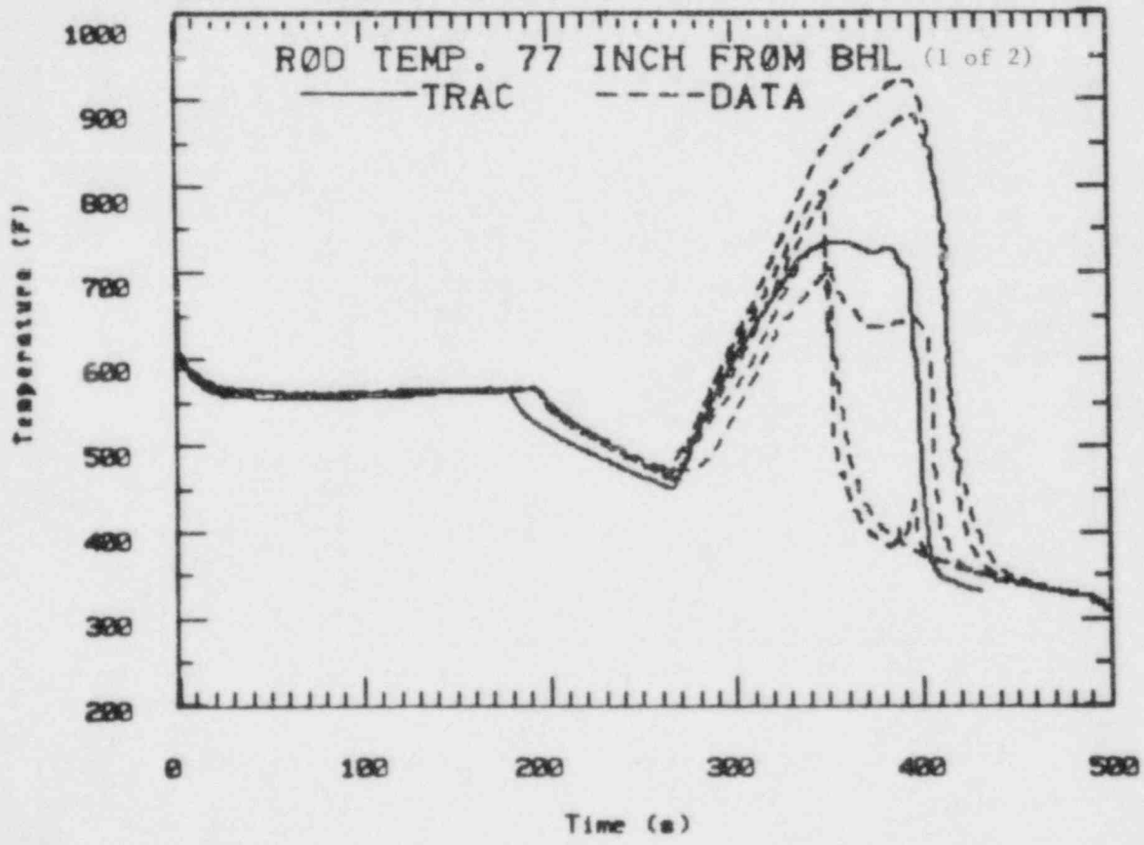

Figure 9.4-20. Comparisons with Individual Rod Temperatures at Elev 77"

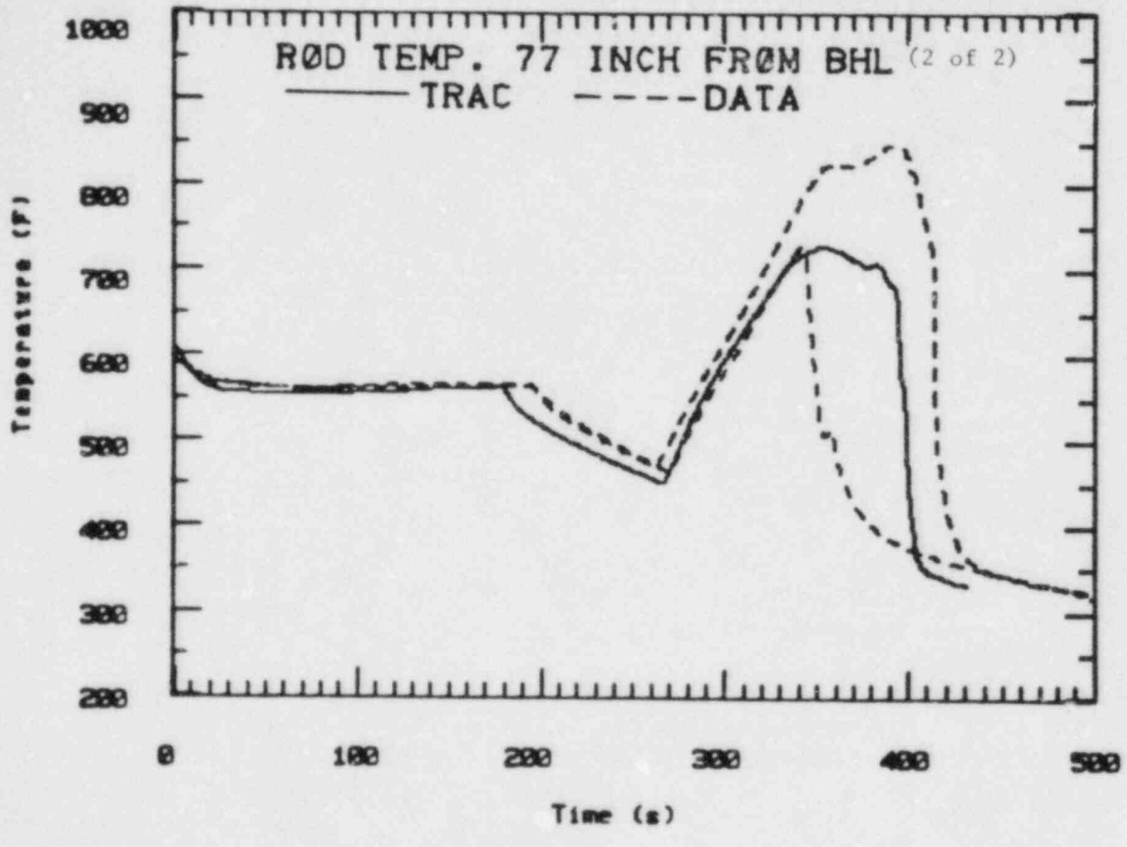

Figure 9.4-21. Comparisons with Individual Rod Temperatures at Elev 77"

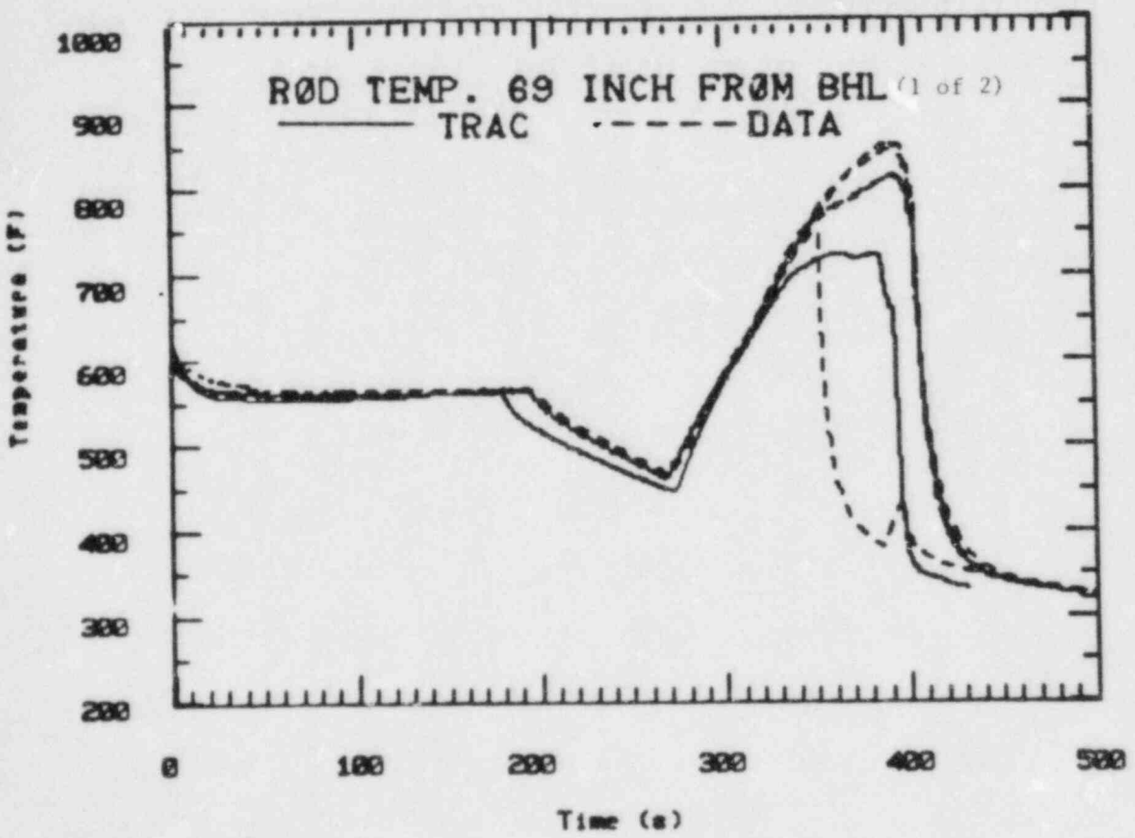

Figure 9.4-22. Comparisons with Individual Rod Temperatures at Elev 69"

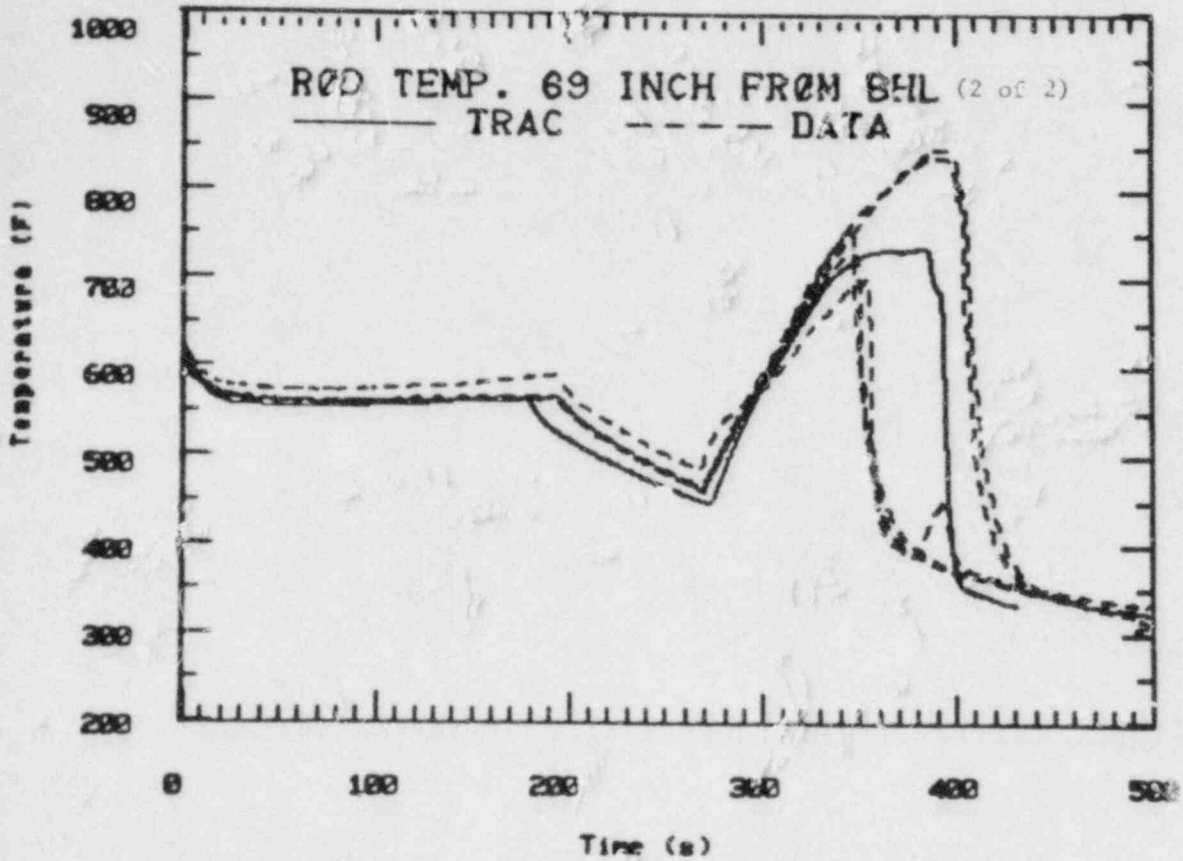

Figure 9.4-23. Comparisons with Individual Rod Temperatures at Elev 69"

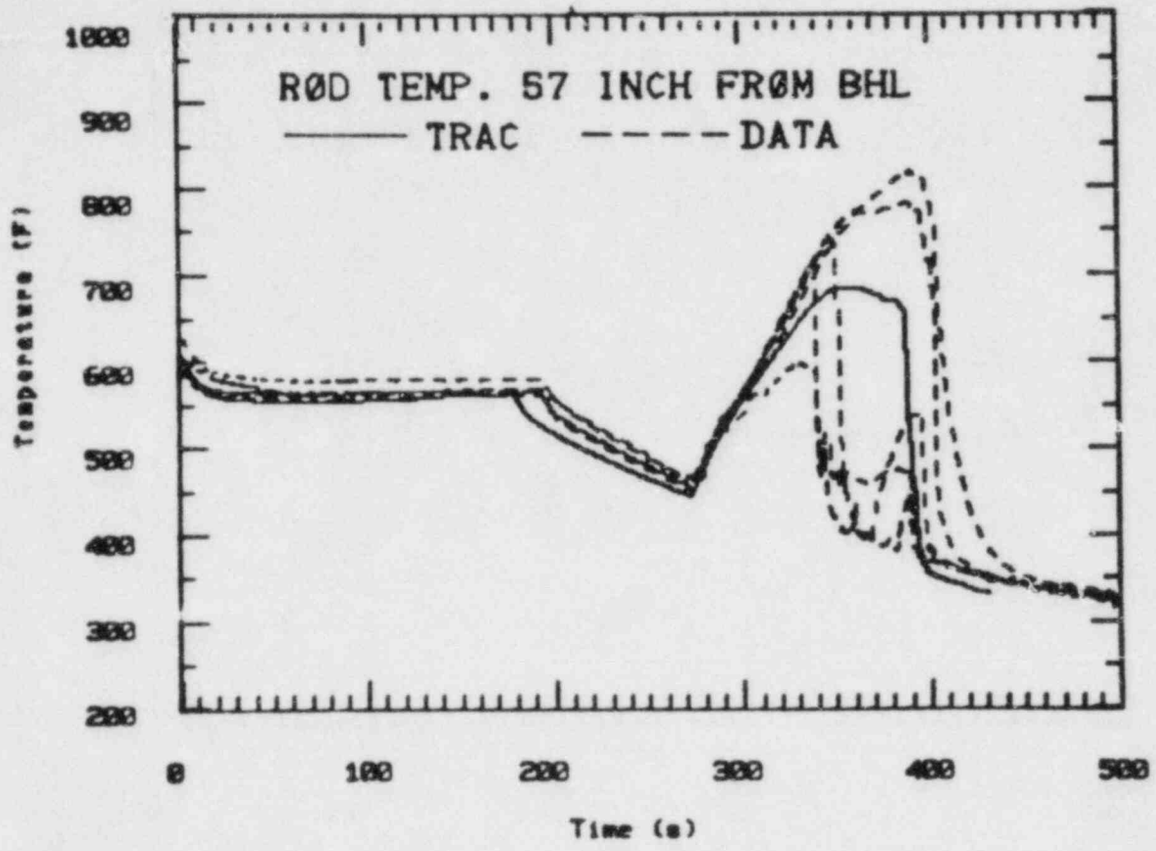

Figure 9.4-24. Comparisons with Individual Rod Temperatures at Elev 57"

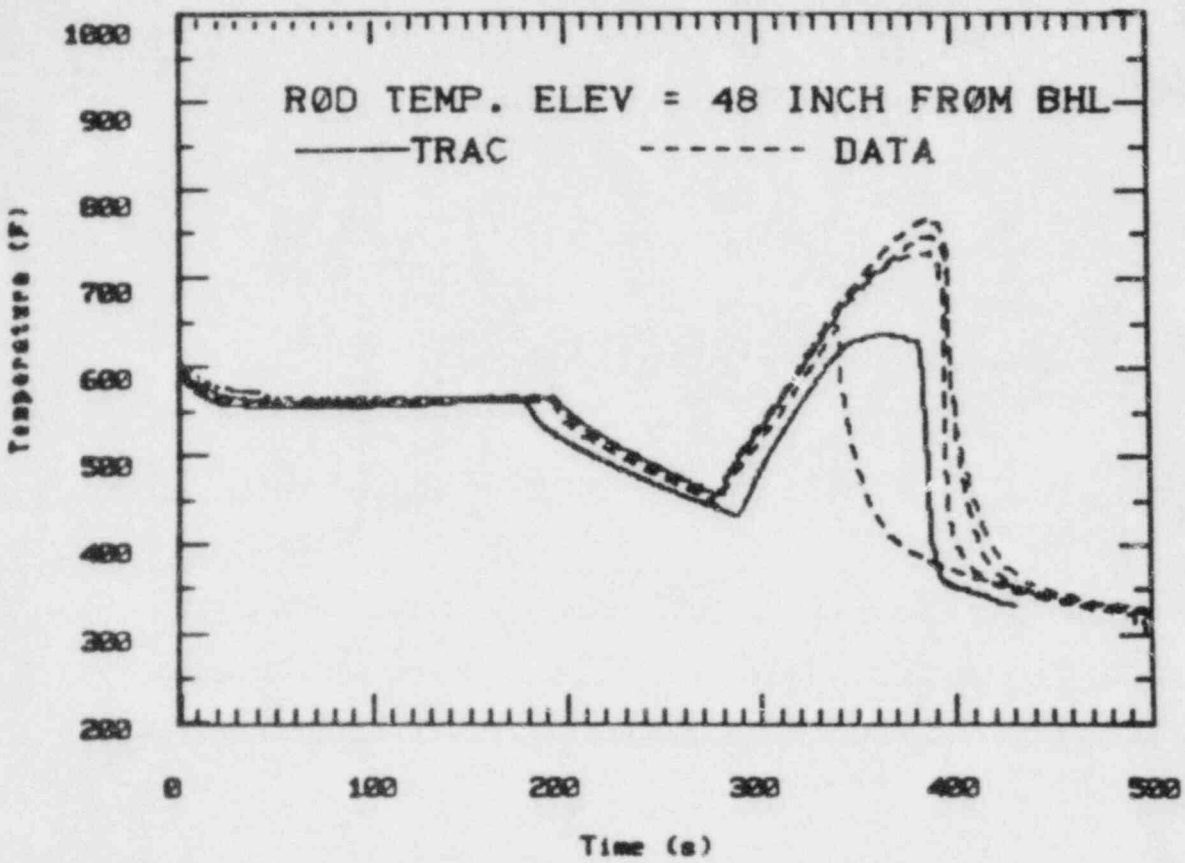

Figure 9.4-25. Comparisons with Individual Rod Temperatures at Elev 48"

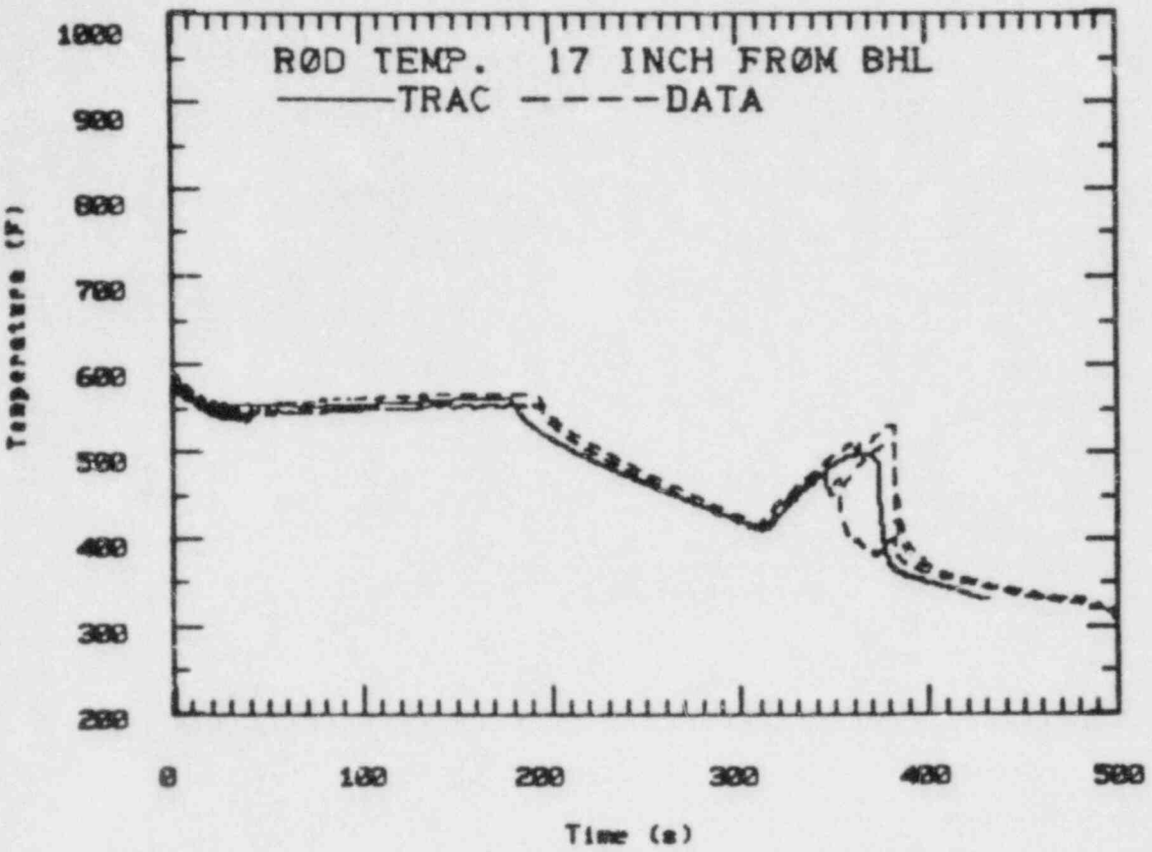

Figure 9.4-26. Comparisons with Individual Rod Temperatures at Elev 17"

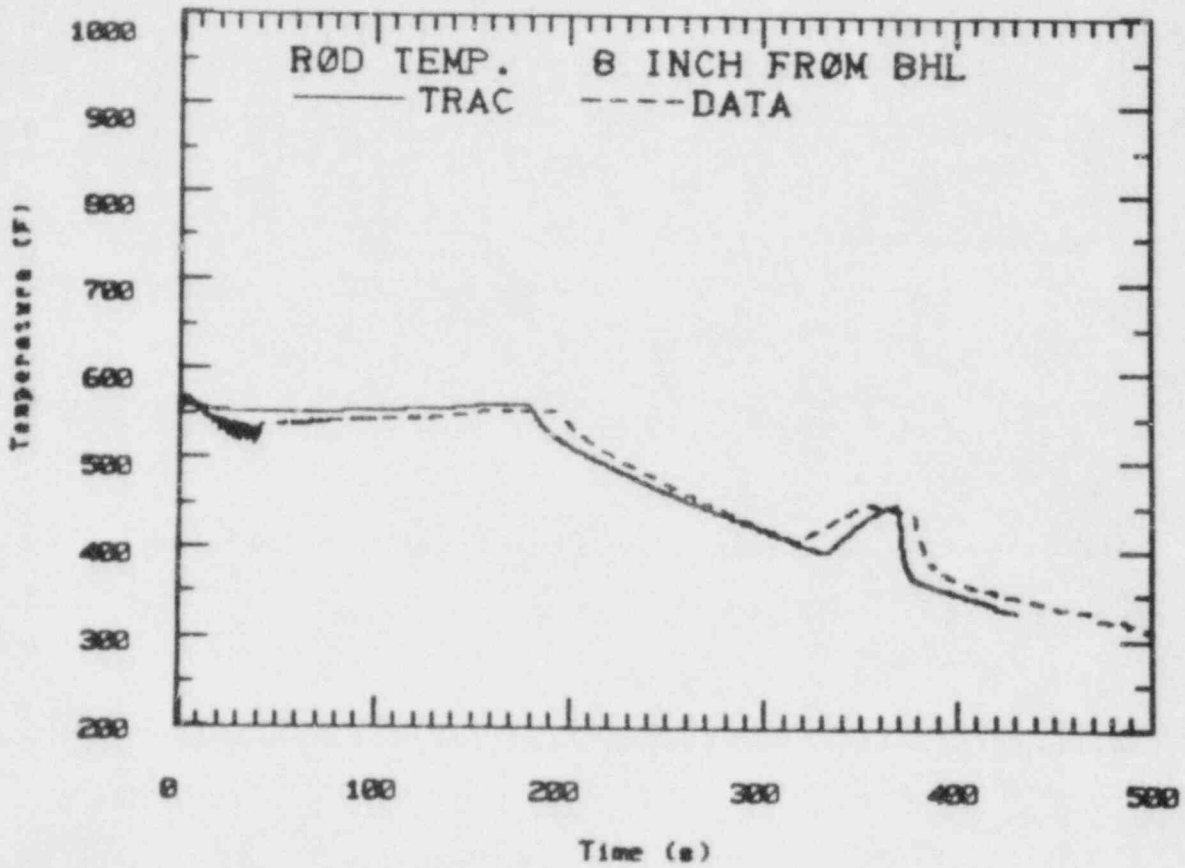

Figure 9.4-27. Comparisons with Individual Rod Temperatures at Elev 8"

9.6 SIGNIFICANCE FOR BWR APPLICATION

TRACB02 application to a BWR system follows the same approach to system definition input modeling used in these analyses of the FIST facility. The principal thermal-hydraulic characteristics difference is the reduced significance of vessel stored heat in BWR systems and the presence of parallel channel flow during system refill. These will lead to a more effective refill/reflood process than observed in FIST. The sensitivity of the small break case timing to subcooled critical flow mass flux input modeling is noticeable when making one-to-one comparisons for well-defined break size and location. This sensitivity is less significant for BWR system response evaluations. Since there is an uncertainty in the exact break size, and location, the BWR evaluation is carried out over a range of break sizes to determine the most limiting break flow value.

9.7 SUMMARY

The pre-test analysis of the large break and small break tests in the FIST facility was carried out with particular attention paid to system definition input modeling. The subsequent post-test comparisons demonstrate that TRACB02 thermal-hydraulic models capture the controlling phenomena very well. The system definition modeling leads to correct handling of level/invencory performance. The bundle and core inventory models capture bundle heat-up and quench very well.

10.0 CONCLUSIONS

Eight matrix tests were conducted in the FIST Phase I series. These tests have investigated the system responses for various BWR transients, including large break, small break, and steamline break LOCA's, as well as natural circulation and power transients.

Each of these tests has been evaluated and analyzed. System responses, highlights and governing phenomena observed in the tests have been discussed and presented in detail in this report. Through this data evaluation study, it is concluded that all FIST phase I tests have been successfully conducted and valuable data have been obtained.

Comparisons of the FIST and TLTA tests have identified similarities and differences between the counterpart tests. Effects of the facility scaling compromises on the test results have been discussed. This study has greatly improved understanding of the test results.

One of the FIST program objectives is to assess the TRAC code with test data. Two pretest predictions made with TRACB02 are presented and compared with test data in this report. These predictions agree with the test results very well. TRAC's capability to correctly predict the system responses during transients has been clearly demonstrated from this effort.

In summary, the FIST phase I program has been successfully carried out. Test data obtained in these tests have provided very valuable information and have extended the data base for further applications such as evaluating and assessing assumptions and models used in BWR analysis.

11. REFERENCES

1. A. G. Stephens, "FIST Facility Description Report" NUREG/CR2576, EPRI NP2314, GEAP 22054, December 1982.

2. J. F. Thompson, "BWR Fuel Integral Simulation Test (FIST) Program Test Plan", NUREG/CR-2575, EPRI NP-1313, GEAP 22053, April 1982.

3. L. S. Lee, G. L. Sozzi and S. A. Allison," BWR Large Break Simulation Tests - BWR Blowdown/Emergency Core Cooling Program, Volume 1 and 2", NUREG/CR-2229 EPRI-NP-1793, GEAP-24962, March 1981.

4. W. S. Hwang, "BWR Small Break Simulation Tests with and without Degraded ECC Systems - BWR Blowdown/Emergency Core Cooling Program" NUREG/CR-2230, EPRI-NP-1782, GEAP-24963, March 1981.

5. S. K. Widener, "Design Analysis and SAR Inputs for ATWS performance and Standby Liquid Control System - Coferentes plant", NEDE-22174 Class II, August 1982.

6. W. M. Chen, "Design Analysis and SAR Inputs for ATWS performance and Standby Liquid Control System - Susquehanna 1 and 2 plant", NEDE-25458 Class II, Rev. 1, April 1982.

7. Letter - "FIST Test 6DBA1-A pretest Prediction", W. A. Sutherland to W. D. Beckner and S. P. Kalra, May 5, 1983.

8. Letter - "FIST Test 6SB2-C pretest prediction", W. A. Sutherland to W. D. Beckner and S. P. Kalra, June 17, 1983.

9. W. A. Sutherland and Md. Alamgir, "BWR Full-Integral Simulation Test (FIST), Pretest Predictions with TRACB02", NRC Light Water Reactor Safety Meeting, Washington D.C., October 1983.

NRC FORM 335 (2-84) NRCM 1102, 3201, 3202

U.S. NUCLEAR REGULATORY COMMISSION

BIBLIOGRAPHIC DATA SHEET

SEE INSTRUCTIONS ON THE REVERSE

1. REPORT NUMBER (Assigned by TIDC, add Vol. No., if any)
NUREG/CR-3711
EPRI NP-3602
GEAP-30496

2. TITLE AND SUBTITLE
BWR Full Integral Simulation Test (FIST)
Phase I Test Results

3. LEAVE BLANK

4. DATE REPORT COMPLETED
MONTH: November
YEAR: 1983

5. AUTHOR(S)
W.S. Hwang, Md. Alamgir, W.A. Sutherland

6. DATE REPORT ISSUED
MONTH: September
YEAR: 1984

7. PERFORMING ORGANIZATION NAME AND MAILING ADDRESS (Include Zip Code)
General Electric Co.
175 Curtner Avenue
San Jose, CA 95125

Electric Power Research Inst.
3412 Hillview Avenue
Palo Alto, CA 94303

8. PROJECT/TASK/WORK UNIT NUMBER

9. FIN OR GRANT NUMBER
B3014

10. SPONSORING ORGANIZATION NAME AND MAILING ADDRESS (Include Zip Code)
Division of Accident Evaluation
Office of Nuclear Regulatory Research
U.S. Nuclear Regulatory Commission
Washington, D.C. 20555

11a. TYPE OF REPORT
Technical

b. PERIOD COVERED (Inclusive dates)

12. SUPPLEMENTARY NOTES

13. ABSTRACT (200 words or less)

A new full height BWR system simulator has been built under the Full Integral Simulation Test (FIST) program to investigate the system responses to various transients. The test program consists of two test phases. This report provides a summary, discussions, highlights and conclusions of the FIST Phase I Tests. Eight matrix tests were conducted in the FIST Phase I. These tests have investigated the large break, small break and steamline break LOCAs, as well as natural circulation and power transients. Results and government phenomena of each test have been evaluated and discussed in detail in this report. Two of these tests tie back to tests in the earlier TLTA facility. Comparisons between the FIST and TLTA tests have been made. The similarities and differences between counterpart tests are identified. Effects of the facility scaling compromises on the test results are identified. One of the FIST program objectives is to assess the TRAC code by comparisons with test data. Two pretest predictions made with TRACB02 are presented and compared with test data in this report. These predictions agree very well with the test results. TRAC's capability to correctly predict the system responses during the transient is demonstrated.

14. DOCUMENT ANALYSIS - a. KEYWORDS/DESCRIPTORS
boiling water reactor (BWR)
loss-of-coolant accident (LOCA)

b. IDENTIFIERS/OPEN ENDED TERMS

15. AVAILABILITY STATEMENT
Unlimited

16. SECURITY CLASSIFICATION
(This page)
Unclassified
(This report)
Unclassified

17. NUMBER OF PAGES

18. PRICE

*U.S. GOVERNMENT PRINTING OFFICE : 1984 0-421-297/4148

UNITED STATES
NUCLEAR REGULATORY COMMISSION
WASHINGTON, D.C. 20555

OFFICIAL BUSINESS
PENALTY FOR PRIVATE USE, $300

FOURTH-CLASS MAIL
POSTAGE & FEES PAID
USNRC
WASH. D.C.
PERMIT No. G-67